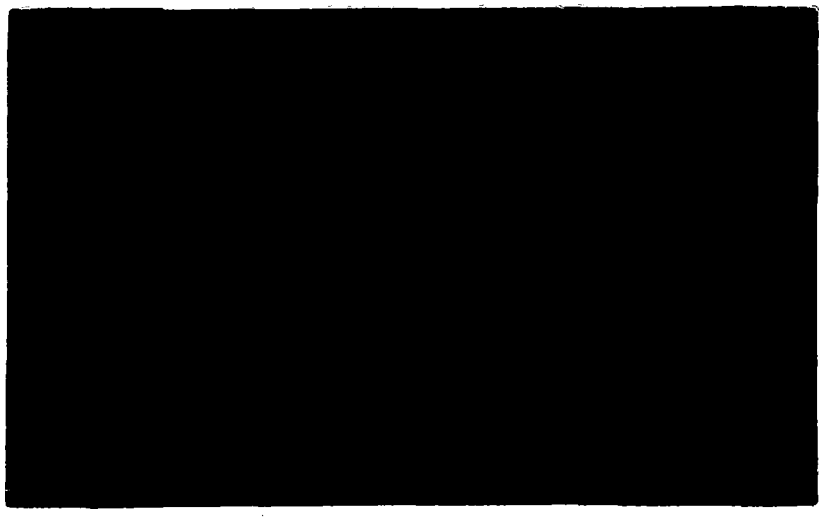

Babcock & Wilcox
a McDermott company
Contract Research Division

GUIDEWAY STRUCTURAL DESIGN AND POWER/PROPULSION/BRAKING IN RELATION TO GUIDEWAYS

INTERIM STUDY REPORT

FEBRUARY 1992

INTERIM STUDY REPORT

GUIDEWAY STRUCTURAL DESIGN AND POWER/PROPULSION/BRAKING IN RELATION TO GUIDEWAYS

PREPARED BY:

The Maglev 2000 Team

SUBMITTED BY:

Babcock & Wilcox
Contract Research Division
Lynchburg, VA

PREPARED FOR:

Department of Transportation
Federal Railroad Administration
Washington, DC
FRA Contract No. DTFR53-91-C-00065
B&W Contract No. CRD 1277

REPORT LEGAL NOTICE

INTERIM STUDY REPORT

Table of Contents

SECTION		PAGE NO.
BACKGROUND		1
CONTRACT TECHNICAL OBJECTIVE		1
EXECUTIVE SUMMARY		2-8
1.0	POWER, PROPULSION, AND BREAKING INVESTIGATION	1-1
1.1	Electrodynamic Design Summary	1-1
1.2	Propulsion System, Design	1-2
1.3	Null-Flux Guidance System	1-6
1.4	Levitation System Design	1-8
1.5	Summary of Guideway Electrodynamics Design	1-11
	TABLES 1-1 TO 1-11	1-13
	FIGURES 1-1 TO 1-8	1-25
2.0	SUPERCONDUCTOR SELECTION	2-1
2.1	Magnetic Field Calculations	2-1
2.2	Emergency Forces and Fields	2-2
2.3	Conductor and Coil Design	2-6
2.3.1	Near Term Capabilities of High Critical Temperature Superconductor Magnets and Transmission Lines	2-13
2.3.2	High Temperature Superconductors (HTSCs) with Potential Operating Temperatures of 20 TO 77 K for Use in Magnetically Levitated Vehicles	2-16
2.3.3	Refrigeration Requirements for Low and High Temperature Superconductor Devices Used in Magnetically Levitated Vehicles	2-31
2.4	Refrigeration and Heat Loads	2-39
2.5	Magnetic Shielding	2-50
	FIGURES 2-1 TO 2-26	2-56

Table of Contents
(Continued)

SECTION		PAGE NO.
3.0	GUIDEWAY EVALUATION	3-1
3.1	Existing Systems Integration	3-1
3.1.1	Description of Guideway Configurations	3-1
	Type I	3-3
	Type II	3-4
	Type III	3-5
	Type IV	3-6
	Type V	3-6
3.1.2	Guideway Design Criteria/Parameters	3-8
3.1.3	Guideway Conceptual Designs	3-11
3.1.4	Cost Criteria	3-12
3.1.5	Guideway Cost Summary	3-12
3.1.6	Guideway Construction Problems	3-13
3.2	Cost Relationships	3-13
	FIGURES 3-1 TO 3-16	3-15
	CHARTS 3-1 TO 3-10	3-32
	TABLES 3-1 TO 3-22	3-33

INTERIM STUDY REPORT

BACKGROUND:

One of the primary goals of the National Maglev Initiative is to develop an innovative system whereby the United States can benefit from existing Maglev systems and technology. In order to make improvements on current Maglev technology, present systems should first be researched, and their strengths and weaknesses identified. Once defined, strategies can be devised for improving the present designs without sacrificing their individual strengths. In addition, careful evaluation of the various systems should provide the basis for the development of an advanced, innovative Maglev system.

This Interim Study Report presents the results to date for the three primary tasks for the Babcock & Wilcox / Federal Railroad Administration contract DTFR53-91-C-00065 - GUIDEWAY STRUCTURAL DESIGN AND POWER/PROPULSION/BRAKING IN RELATION TO GUIDEWAYS. The lead subcontractors for each task - PSM Technologies Inc. for Task 4.1, Intermagnetics General Corporation for Task 4.2, and Hudson Engineering Corporation for Task 4.3 were supported by the remainder of the Maglev 2000 Team. Remaining Team members include American Superconductor Corporation, Babcock & Wilcox Co., Council on Superconductivity for American Competitiveness, Madison Madison International, and the Prairie View A&M Research Foundation.

CONTRACT TECHNICAL OBJECTIVE:

The objective of this contract is to investigate the power, propulsion, and braking systems for five (5) different existing Maglev configurations. Following this investigation, system requirements and recommendations, including a cost analysis, will be determined for each configuration. Possible multiple uses for the guideway structure will also be identified and investigated. In addition, three superconductors will be evaluated for use on Maglev systems.

Guideway?

Through this research, it is planned that improvements can be identified which will contribute towards a technically advanced economically viable U.S. Maglev system.

EXECUTIVE SUMMARY:

This report has analyzed electromagnetic and mechanical designs for a magnetically levitated train system with nominal specifications:

- maximum speed: 500 km/hr (300 mph);
- passenger capacity/car: 50-200;
- vehicle weight: 42 metric tonnes (92,600 lbs);
- guideway width: 3.65 m (12 ft.)

The analysis considers variations in vehicle length, acceleration/deceleration criteria, air-gap clearance, and maximum propulsion thrust. Five different guideway configurations have been considered, each of which is based on an air-core magnets made from low-temperature superconductors (NbTi, Nb_3Sn) or the newer high-T_c ceramic superconductors (HTSCs).

In this first phase of the project, the materials requirements and cost of the guideway electrical components were studied as a function of the energy conversion efficiency, the stator block length, required current density, expected temperature rise, and other parameters. The propulsion design focused on a dual-parallel, linear synchronous motor (LSM) with thrust modulation achieved by applying a variable frequency voltage along the guideway. Critical design parameters were estimated using a three-dimensional computer model for the inductances, magnetic fields, and electromagnetic forces. Peak field strength in the passenger compartment at various heights has been plotted for the baseline magnet design.

The main activity addressed during this reporting period concerns the conceptual design of the magnet, cryostat, and refrigeration sub-systems. Although the magnetic fields, forces, AC losses, superconductor stability, heat loading, and refrigeration demands were analyzed, and

adiabatic - a reversible thermodynamic process executed at constant entropy
~ occurring without gain or loss of heat

preliminary work on the magnetic shielding was carried out, it will not be possible to reach firm conclusions until the Phase 2 work is completed. The Phase 2 study will assess the Maglev concept as a total, integrated system. The analysis logic developed so far is shown in flow charts, and tables of formulae and data are included in this report.

Superconductor Selection

One of the most important areas to be considered in a Maglev transportation system is the choice of superconductor for the magnetic levitation and propulsion. Hence, two types of conventional low-temperature superconducting wire were assessed:

- NbTi
- Nb_3Sn,

both of which must be operated under liquid helium. In addition, four types of the new high-temperature superconductors (HTSCs) were considered using the latest performance data:

- YBCO ($Y_1Ba_2Cu_3O_7$)
- Bismuth-based, silver-sheathed, BSCCO-2223, $[(Bi,Pb)_2Sr_2Ca_2Cu_3O_x]$
- BSCCO-2212 ($Bi_2Sr_2Ca_1Cu_2O_{8+x}$)
- TBCCO ($TlBa_2Ca_2Cu_3O_y$)

The LTSC magnets were assumed to operate in the persistent mode with negligible AC losses. Both cryostable and adiabatic coil designs were considered for each conductor type. Realistic designs for a propulsion coil having a peak field of 5.3 T in the windings at a current of 600 kA have been analyzed. However, optimal design of the conductor and coil must await full assessment of shielding and AC losses.

HTSC wires appear to offer significant advantages as well as considerable promise of even further improved properties within the next year of two. These include:

- Stability under very high magnetic fields, i.e., high J_c in fields;
- A range of possible operating temperatures from 20-77 K, with optimal performance probably in the 20-50 K range;
- Easier, more efficient cooling; and
- Superior stability in presence of AC losses, due to the higher temperature.

Metal micro-composite ceramic HTSC wire in long lengths is presently available with good windability and current-densities adequate for magnet coils. As a material with a longer history and experience, NbTi appears to offer higher current densities, lower cost, and higher reliability at present. Issues of HTSC wire strength need further development; HTSC magnets at 20-50 K probably will not operate in persistent mode. And trade-offs of shielding costs vs. superimposed AC need further analysis in choosing between LTSCs and HTSCs.

Since HTSC wire development began in 1988, the performance achieved has been increasing 100 to 1000-fold per year. Although conventional NbTi LTSC conductors will provide acceptable performance, serious consideration of HTSC-wire in Maglev applications is warranted. The optimal choice of conductor type must await the overall integrated system review.

A preliminary analysis of the system's heat load and refrigeration has been completed, both for low-temperature, helium-cooled systems and for intermediate temperature BSCCO-based systems. The latter can be cooled with Gifford-McMahon or Stirling cycle refrigerators with high efficiency and reliability. The heat load was found to be surprisingly low, particularly when larger cryostats are employed, because the surface-to-volume ratio is lower and radiation losses are thus reduced.

Refrigeration is required on the vehicles, consuming between 2 and 16 kW of electric power, depending on whether HTSCs or LTSCs are used. Additional cooling for the compressors in the range of 3-25 kW would be required, but this will be accomplished by heat rejection to the atmosphere. Z which means that 3-25 kW will not be needed? On that less power - not specified - will be needed?

Baseline Requirements

Figure 2-1 summarizes the baseline requirements for refrigeration and the vehicle superconducting magnets. A value of 5.3 T as the peak field in the magnets for the LSM was obtained from a consideration of the effects of neighboring magnets and materials of the guideway. This value will be refined in the final analysis.

Figure 2-2 summarizes some requirements for the propulsion magnets; only LTSCs in persistent mode have been analyzed to date.

An aluminum eddy current shield on the floor of the vehicle is proposed to contain changing flux from the guideway magnets. A further analysis for the HTSC wires operating non-persistently at 20-50 K will be carried out in the next phase.

Design Process

Flow charts describing the design process were used for the LSM conceptual design, as well as designs for the refrigeration, active shielding, and passive shielding systems. These are shown in Figures 2-3 to 2-5.

Future Work

The next phase of the project will address mechanical design of the support and cryostat systems, further analysis of the AC losses, and the magnetic shielding. Also, the consequences of a component failure, e.g., a single magnet or refrigerator, will be considered.

Guideway Evaluation

The five guideway configurations chosen for this evaluation are described in detail in Section 3 and shown in Figures 3-1 through 3-15. The five configurations are:

- Type I Flat-top Guideway
- Type II Wrap around or clamp Type Guideway
- Type III Magnaplane Guideway
- Type IV Inverted "T" Guideway
- Type V U-shaped or Channel Guideway

The dimensions of each guideway have been developed based on the requirements of the levitation and propulsion systems that have been designed for each individual configuration. Although each configuration offers a unique solution for a magnetically levitated transportation system, the basic structural support system is similar for all guideways.

The five guideways have similar materials of construction, construction technology, installation techniques, and support systems. The base structural element for all five guideways is a shop fabricated, pre-assembled, precast, prestressed concrete girder shipped to the site as a complete assembly ready for installation. Each girder is shop tested to ensure continuity and prepared for field connection to the next girder. The precise field installation of the girder and the continued level orientation of the girder over the operational life of the structure is a critical concern. To accomplish this the girders are designed to rest on two mechanically adjustable supports. Each of these items may be adjusted vertically to level the girder during installation and to maintain the girders level during operation. A sensor system, to alert operators that the guideway supports are not within level tolerances, will be utilized to aide the maintenance operations for the life of the guideway system. The sensors will also continuously monitor the girder to alert operators to the possibility that the girders are responding differently to the loads imposed during operation.

The use of superconducting magnets requires the use of new and innovative construction materials. The potential interaction between the superconducting levitation and propulsion systems and any ferrous metals requires the use non-magnetic materials such as fiber-reinforced plastics for reinforcing and/or anchor bolts. Additional research is underway to determine the potential uses of other composite materials that may enhance the design of the guideway.

The guideway configurations described above and shown in Figures 3-1 through 3-15 provide a general summary of the current research efforts for Maglev guideway support systems. However, no one has provided a complete design/construction estimate utilizing the same design criteria and parameters for all five configurations. The primary effort of this study is to design each of the configurations using the same design criteria and prepare a construction cost estimate for each. This will enable a rigorous comparison of each system and the advantages and limitations they present.

The development of the cost criteria for estimating the construction cost of each guideway configuration includes the following items:

- Engineering/Geotechnical Support
- Temporary Construction Facilities
- Site Preparation and Finishing
- Cast-in-place Foundation
- Cast-in-place Columns and T-beams
- Precast Concrete Girder (including Aluminum Levitation Ladders and LSM)
- Shop Installation of Levitation Strips, LSM, Sensor System, Cables and Wiring
- Precast Concrete Girder Installation and Hoop-up Hook?
- Contractor contingency, overhead and profit

The lowest estimated cost of the base case for each of the guideway configurations is provided below. The base case was developed using the following criteria/parameters:

Column Spacing	30-meters (100')
Ground Clearance	10.7-meters (35')
Girder Vertical Deflection Limit	Span/1500
Column Lateral Deflection Limit	Height/500

T-beam Cantilever Vertical Deflection Limit	Width/500
Foundation Gross Allowable Base Pressure	2.0-kg/cm^2 (4000-psf)

Guideway Cost Summary

Type I	$11,200,000/mile	$6,960,000/km
Type II	$14,190,000/mile	$8.820,000/km
Type III	$12,330,000/mile	$7,660,000/km
Type IV	$11,850,000/mile	$7,360,000/km
Type V	$15,700,000/mile	$9,760,000/km

The cost provided above reflect an estimate of the engineering, fabrication and construction costs associated with a large civil project. Only an order of magnitude cost for the levitation, propulsion, and sensor systems has been included. The guideway cross-section has not been studied to determine if a more economical shape can be used. This effort will be made after the Interim Report. The use of these numbers must be limited to only a comparison of the total cost between the different guideway configurations. The design of the guideways and the assimilation of cost data is an ongoing part of this study and the final assessment of each guideway and the associated cost will be presented in the Final Report. For example a review of the data presented above indicates that Type I has an overall constructed cost less than Type V and does not indicate an actual cost for the all in construction of the guideway.

The construction cost of the guideway is dependent on many variables including site location, congestion of other facilities, terrain, accessibility of construction materials, type of soils supporting the structure, material strengths, length of span, number of supporting columns, height of structure, and the vehicle supported. The cost impacts of the following variables have been estimated and their associated cost impact assessed. These variables are: span length, column lateral deflection criteria, girder vertical deflection criteria, and height of the structure.

POWER, PROPULSION, AND BRAKING INVESTIGATION

1.1 Electrodynamic Design Summary

The first segment of the propulsion, levitation and guidance system concentrated on detailed design of the superconducting linear synchronous motor (LSM) for the 5 guideway types. The guideways all differ in structural layout, overall width, height, configuration of electrical components, etc. but do retain for the LSM a common electrical layout with minor differences adaptable to all 5 guideways. The LSM stator windings are cast in a non magnetic prefabricated tray for rapid and modular assembly at the job site. It is important to note that in all configurations, an "air-core" (i.e. non-ferromagnetic) stator is designed with the study limiting the electromagnetic airgap to a range of 0.19 m to 0.23 m, yielding a nominal 0.10 m mechanical clearance between vehicle and guideway surface. Figure 1 shows a cross section of the Type II system using the dual-parallel propulsion system and dual lift. 1-1

Table 1-1 summarizes the overall dimensions for the 5 guideway types and baseline system parameters. The point design is chosen at the higher speed of 500 km/hr. for presentation of performance data, magnetic field plots and design tradeoffs in block length as generally the high speed condition represents the greatest electrical stress on the LSM. Table 1-2 details the LSM design sequence and particularly addresses the critical mutual and self-inductance calculations for the baseline LSM design. Terminal quantities for invertor output voltage, current, MVA, power factor, efficiency and optimum load angle are given for a 60 kN cruising thrust rating. This 60 kN is used as the base modular thrust value per row of 50 superconducting vehicle field magnets, realizing a mechanical output power of 8.33 MW at high speed cruise. As the overall vehicle design evolves and aerodynamic/electrodynamic drag losses are better defined, the total LSM output thrust will be tailored by a combination of addition of field magnets or slight boost in the stator phase current rating. It is important to note, that this study has assumed that design variations in working airgap about a 0.21 m nominal gap are accommodated by alteration of the specification of field magnet MMF. The range of 500-600 8.27 in

kAT/pole (for largest gap) is used versus alternate thrust modulation techniques such as increasing magnet width.

The wavelength chosen for the baseline design is 1.14 m which fundamentally establishes the 500 km/hr. top speed at an excitation frequency of 122 Hz. The efficiency of the motor and field-stator mutual coupling is largely based on the ratio of wavelength:airgap. The base design has optimally chosen a ratio of 5.43:1. The field coil wavelength also establishes the main spatial attenuation of magnetic field in the passenger compartment. One of the early conclusions of the LSM design study is that the use of a dual LSM with individual field coils limited to one-half of a conventional LSM magnet width (and arranged in alternating N-S polarity across the vehicle width) results in a reduced passenger magnet field exposure without compromise of the magnetic field distribution at the LSM stator conductors. For this reason and the introduction of automatic roll and heave control with the dual system, all five guideway designs proceeded with dual stators of 800 mm active width for each winding.

The levitation system is "superdynamic" (also referred to as electrodynamic repulsive) with the vehicle containing separate superconducting lift magnets operating at 320-385 kAT/pole and a mean width of 0.48 m across the Niobium-titanium helium cooled superconductor.

1.2 Propulsion System Design

The electrical dimensioning of the base propulsion system design has been initiated for a reference design applicable to the five linear synchronous motor windings and interacts with a dual array of superconducting N6-Ti field magnets located on the vehicle undercarriage to produce a nominal 60 kN thrust continuous output at 500 km/hr. Once the dynamics study is performed for calculating vehicle oscillations, based on eddy current intensity in the magnet wire, then a final specification on wire type will be made. The propulsions magnets operate in a persistent-current mode with a preferred transport current of 100 A. The baseline MMF will vary between kAT and 400 kAT in all parametric studies; the exact excitation dependent on the electromagnetic airgap (19-23 cm range) and the level of braking force required.

Three-dimensional field calculations for a full width LSM magnet of 0.53 m overall length to fit a 0.57 m pole-pitch and a 0.80 m overall width have resulted in an internal self inductance/magnet of 0.409 H. This uses a specific overall conductor cross section of 40 mm x 40 mm square and with exactly 500 turns/coil. One alternate design uses a coil cross-section of 69 x 69 mm square with overall current density of 12,265 A/sq.cm. The stored energy per coil for 600 kAT excitation is 294 kJ, or for a dual 50 magnet system the total vehicle field magnet stored energy is 29.4 Mega-joules.

The specific result of incorporating 50 LSM magnet pairs at 500 kAT is a net propulsion force of 60 kN for a total magnet active surface area of 45.6 sq. m. The specific force density loading in the base design is force density loading in the base design is consequently 1,316 Newtons/sq. m. at a base airgap of 22 cm, for the maximum overall LSM efficiency point of 95.9%.

As vehicle passenger configurations evolve and weights for on-board equipment are apt to increase beyond baseline designs, it may become necessary later to increase propulsive thrust capacity beyond 60 kN. The 50 magnet array results in an overall active magnet length of 28.5 m which is near maximum to consider for a 39 m long vehicle, which has been used by MagLev 2000 for the small 200 passenger vehicle of minimum length. Provisions may also be made in the preliminary design for increase of propulsion cruise thrust to 83 kN for a large 200 passenger vehicle with a 50-55 m overall length. The aerodynamic drag at 500 km/hr. for system configuration Type V or Type II may attain 60-63 kN and the residual components such as electromagnetic drag up to 15 kN. To produce 83 kN forward thrust requires the full 600 kAT excitation and a magnet array of 77 magnets or 43.9 m active length covering 80% of the vehicle undercarriage.

In the reference design, Maglev 2000 has chosen a maximum magnetic field density at the guideway surface of 0.74 Tesla for a mean SC magnet conductor to guideway stator conductor separation of 22 cm. These numbers are specific to the Type II guideway and for a dual (parallel layout) LSM. The advantage to increasing the field density beyond 0.74 T is a reduction in number of SC magnets or surface area of the vehicle magnet array. The

disadvantage to a higher field is that the shielding becomes progressively heavier, there are higher internal stresses in the magnet and there will be higher LSM stator eddy losses in the copper or aluminum 6-phase winding. The reference design now is based on a Z-directed (vertical) peak steady-state magnetic field density of 0.62 Tesla for a 500 kAT excitation, raising up to 0.74 Tesla in overload, high acceleration or high regenerative braking which require 600 kAT excitation per magnet.

The inherent (unshielded) magnetic field in the passenger compartment peaks at 24 milli-Tesla (mT) for a 600 kAT excitation strength or at 20 mT for a 500 kAT MMF, located at a distance at exactly 1.00 m above the plane of the SC magnet center, representing the floor of the vehicle. With ferromagnetic undercarriage shielding, the 24 mT will be reduced to 5 mT with at 9mm thick steel plate. The advantage of the dual LSM over the single width LSM is a reduction in the inherent passenger magnetic field plot in the passenger compartment for the 500 kAT baseline excitation, dual LSM versus single LSM field, positioned over the transition from a north to south pole magnet.

With the particular LSM design presented, especially in a dual array not to exceed 0.80 m active magnet width, there appears little need for active magnetic shielding. Passive shielding is sufficient and offers the additional feature of structural support for the passenger floor. Thermal calculations and cryostat force distribution are being assessed for this type of geometry.

The nominal acceleration is established at 0.1 G for a 42 metric tonne vehicle which fundamentally calls for a 41,160 Newton accelerating thrust. As the vehicle approaches the cruise speed of 500 km/hr, the aerodynamic drag (with the baseline vehicle body design) builds up to 37 kN. The electrodynamic drag remains nearly constant in the range of 400-500 km/hr and peaks at 15 kN. The linear generator power pickup attributes an additional 3.5 kN of drag to provide for on-board electrical auxiliaries including HVAC and SC magnet excitation. The total calculated drag losses on the LSM are thus 55.5 kN.

To accommodate a 0.1G acceleration at high speed with a 55.5 kN total drag losses, requires a total LSM output rating of 96.6 kN or a 60% overload above base. The LSM stator

can accommodate this in acceleration sections due to the short-time duration required for boost in stator current. For example, in a 2.0 km stator guideway block section (worst-case condition) at 400 km/hr., the overload time is only 16 seconds and about equal to the thermal time constant of the winding. The major limitation on availability of overload thrust rating is at the invertor substation due to the commutation rating of the thyristor electronic switches for the 0- 122 Hz variable-frequency supply. Maglev 2000 group recommends a tapering off of the 0.1 G acceleration to 0.05 G for speeds above 400 km/hr so as to hold the maximum LSM output to 55.5 kN (drag) + 20.5 kN (accelerating) or 76 kN total. That is, in the interests of economic capital installations or substation power demand, a limit must be placed on maximum kVA demand or utility power input.

Consequently, the recommended invertor overload output rating (which is calculated for 1.0 minute) is 12.9 MVA at the substation output, with a dual 6-phase output current of 1071 Amps r.m.s./phase. The nominal or continuous rating of the invertor output is 10.5 MVA, 846 Amps/phase, at 4,170 Volts r.m.s. line to neutral. This current level can be maintained on a 24-hour basis for the invertor thyristor devises and substation step-down transformer, and protective 34.5 kV, 69 kV, or 138 kV utility switchgear. The invertor in producing variable-voltage, variable frequency (VVVF) power generates 5th, 7th, 11th, and 13th harmonics and consequently has a poor input power factor (or "displacement factor"). The estimated input utility apparent power to each invertor station will need to be 12.5 MVA continuously rated. In an overload acceleration or medium brake mode, the substation input power is calculated at 15 MVA for the high speed condition, a 42 metric tonne vehicle, and a total LSM output of 76 kN.

The overall electrical characteristics are dictated by the brake mode deceleration spec rather than acceleration mode. Maglev 2000 has designed the dual-LSM system with a 0.25 G deceleration rate from 500 km/hr, the LSM inherent braking force reaches a fadeout speed, whereby and auxiliary (mechanical) brake is required so as to avoid very low frequency (1-4 Hz) in the stator winding. The 0.25 G brake rate at high speed requires 82 kN for which 55 kN is provided by combined aero drag and electrodynamic lift system drag for which the LSM regenerates at a retarding thrust level of 27 kN or 3.75 MW peak power at the 500 km/hr. point.

Braking control of the LSM is afforded by rapidly changing invertor load (in a 25 ms period) from B = 112° to B = 280° - 290°. The 3.75 MW of available braking power is fed back into the line minus 0.70 MW for stator I^2R and invertor losses, thus injecting approximately 3.05 MW effective into the 60 H_z utility grid for a utility "power credit." Figure 1-2 shows a top-view of the Type I guideway layout showing all major electrical components for propulsion, suspension and guidance in a dual-LSM configuration.

Table 1-3 describes cost and conductor weights for two different diameters of copper conductor for Type I LSM system indicating 16,320 kg and 19,307 kg per kilometer of guideway. The addition of the null-flex guidance loops (aluminum) with the LSM conductor brings the total to 22,535 kg/km for a 12.7 mm diameter LSM stator option.

Table 1-4 describes the electrical losses for Types I-V dual LSM guideway conductors operating at nominal current of 423 Amps/conductor or 846 A/phase for 3 parametric block lengths: 0.5, 1.0 and 2.0 km, and using a specific current density of 3.36 A/mm^2. Longer blocks than 2.0 km were not considered in this study due to the drop in basic LSM conversion efficiency below 90%. Table 1-5 describes the weight and cost of 3-phase copper transmission cable from invertor station to LSM stator feed point which needs to be installed to feed multiple (2-4) stator blocks from a common invertor.

1.3 Null-flux Guidance System

The particular type of null-flux loop guidance is specially-matched to the dimensions of the LSM field magnets. In the dual LSM system, laterally adjacent field magnets are of opposite polarity and when a spatial unbalance in the normally symmetrically centered vehicle LSM field magnets occurs, a large differential EMF is induced in the null-flux loop. The resultant induced current can attain typically 7,550 Amps for a 5 cm lateral sway at the cruise speed of 150 m/s. Each, aluminum-conductor N.F. loop of 30 cm width and 50 cm length has an inductance of 0.98 uH and a resistance (20°C) of 104 u-Ohm, produces a restoring force of 4.2 kN or 210 kN for the whole vehicle. The guidance stiffness is thus 210 kN/5 cm or 4.2 x 10^6 N/m; this is

considered a stiff system. The null-flux principal is applied in Type I and II systems with nearly identical component design and cost of materials. The "magneplane" concept is modified from earlier patents (Ref. U.S. Patent 3,768,417) to include a dual LSM array and a center-located null-flux guidance ladder.

In the Type II system using the approach of a guideway underhung LSM stator and dual outriggers attached to each vehicle, lateral guidance is accomplished by electrodynamic repulsive-inductive action against side-wall mounted aluminum strips on the concrete guideway. This is substantially different from conventional null-flux techniques and is effective in being inherently stable but has a higher steady-state dissipation loss due to the continuous repulsion (y-directed) force. A second disadvantage is that the lateral stiffness of the Type III guidance falls off (at 40 km/hr of lower speeds) at a faster rate than the null-flux center loop system. A major advantage is the inherent simplicity of construction and installation of the repulsive guidance strips.

Both Type IV and Type V systems do not require either null-flux or EDS inductive-repulsive ladder strips due to the continuous use of the LSM stator, mounted in a vertical orientation. Lateral vehicle guidance is maintained strictly by B-angle control of the LSM to modulate the "normal" force to the LSM surface. The magnitude of this force is limited to approximately 1.10 per unit of the peak propulsion force for a given field MMF and stator MMF. Therefore, the peak available lateral restoring force under invertor-feedback control is 2 X 76 kN = 152 kN for a 600 kAT, 50 magnet pair excitation. This system does not have a limitation on low or high speed guidance fadeout, but does require active, high speed monitoring of vehicle yaw or sway motions to command a change in invertor B-angle. Both Types IV and V avoid any additional guideway materials/installation cost for null-flux or inductive- repulsive ladder strip materials. The LSMs for providing lateral guidance are of the same physical construction as the Type I or II and only minor special provisions (in the master control system) are necessary to use the LSMs for repetitive lateral guidance. As with all schemes in Type I, III, IV and V, failure of the LSM field magnet array to produce sufficient flux due, for example to a cryostat failure, would result in loss of lateral guidance performance. The Type II system uses a separate set of miniature, dedicated guidance SC magnets mounted on the vehicle

outrigger inner support leg. The active width of these field magnets are sized at a minimum 15 cm with a limit of 20 cm width and a field strength of 90 kAT/magnet. Each vehicle would carry 8 guidance magnets/side over a span of 27 m. Table 1-6 summarizes the guidance material weights and Table 1-10 summarizes the materials cost on guideway. The guidance material generally costs 57% of the LSM stator materials. The costing does not include exact number of cost of installation, but for initial costing purposes, guideway installation, grouting and alignment would be approximately $85,000/km of guideway.

1.4 Levitation System Design

The baseline vehicle weight is 42 metric tonnes with a nominal overall width of 3.55 - 3.65m. The heavy vehicle (freight/passenger mix) limit is 50 tonnes with the described design. The levitation parameters are as such; a total number of superconducting magnets with a minimum of five (and of seven for redundancy) per side of vehicle of length 1.50 meters at a width of about 0.48 meters. The MMF of each magnet is in the range of 320,000-385,000 ampere turns depending mainly on cornering characteristics at high speed. The field conductor is a conventional, multifilament niobium titanium, superconductor, in a 5.7:1 copper: superconductor of matrix. The levitation ladder strips on either side of the guideway are 60 centimeters wide. For high speed these have to be optimized at approximately 1.7-1.9 centimeter thick, whereas at low speed these may be thicker, approximately 2.3-2.5 centimeters. The levitation lift off force in the Type 1 system is in the range of 48 km/hr to 50 km/hr. With this type of system using 6101-T64 aluminum the mass of guideway aluminum dedicated to levitation system is 31.5-38.7 metric tones per kilometer. We have assumed the worst case conditions at 500 km/hr and that the main suspension height may be as large as 22 cm in the plane of the guideway aluminum to the plane of the superconducting magnets, leaving a track clearance of 10 to 12 cm. The provisional suspension stiffness is 3×10^6 N/M with a natural frequency of approximately 2 Hertz, and as stated, the magnetic drag in such a system at high speed is approximately 12-15 kN.

Overall dimensions for the five reference guideway's levitation conductors were fixed for incorporation in overall guideway mechanical dimensioning. A ladder levitation strip with a skewed cross member was chosen for all 5 designs over a solid strip levitation conductor. Figure 1-2 shows cross section and plan views. The electromagnetic calculations show a reduced electromagnetic drag at high speed conditions (400-500 km/hr) with a skewed ladder versus simpler arrangements, and consequently a higher L/D ratio. The ladder yields the highest lift force per ton of conductor material for the range of design considered. A rung pitch of 51 cm and a 15° skew angle were chosen. The optimum material chosen was high-conductivity "busbar" aluminum ASTM Type 6101-T64 which has 64% of the conductivity of IACS copper. Standard aluminum Type 6061-T6, the most common in general use in the U.S. has a lower conductivity of 47% of IACS and is not preferred. Further the chosen Type 6101-T64 has an ideal layout composition with no copper content and a superior resistance to weathering and pitting in comparison with lower grade aluminum. Copper was not considered for the levitation ladder due to the high capital cost.

The base design has two parallel conductor rails of cross section 10 cm wide by 1.9 cm thick and cut in maximum section lengths of 12.2 m. The two base conductors per side of guideway together have a cross section of 38 sq. cm. With a specific density of 2664 kg/cu. m, the two main side rails weigh 10.1 kg per meter guideway length. The transverse separation between outer rail dimensions varies from 60 cm. in the Type I, II & IV designs to 800 cm. in the Type III design. The smallest inner dimensions is 40 cm. and is spanned by a welded, skewed cross member, (rung) also of Type 6101-T64 aluminum and cross section 1.9 cm. x 10 cm. The rungs are of length as shown in Table 1-8 according to guideway type. The "magneplane" Type III has the longest span for rungs due to the larger than average transverse (roll) motion allowable on both straight and curved guideways. The per side conductor weight for the levitation ladder runs between 15.7 tonnes/km and 19.3 tonnes/km exclusive of the grouting fill material and stainless steel securing bolts. If a solid aluminum flat-strip were used instead, the specific weight would be considerably higher at 30.3 tonnes/km for Types I, II, IV and 34.3 tonnes/km for Type V and 40.4 T for Type III per side. The ladder levitation thus represents a savings of 29.2 tonnes/km to 42.1 tonnes/km for Type III, for two ladders/guideway. The conclusion of the electromagnetic field study is that it is not sufficient

to simply reduce the thickness of the simpler flat-strip levitation strip to attain the equivalent per unit mass as the ladder unit. The ladder configuration has a specific inductance:resistance (L/R) ratio which controls the electro-magnetic drag and this L/R ratio cannot be readily duplicated with the solid strip. The specified rung pitch is dependent on the choice of the vehicle levitation magnet longitudinal dimension and chosen to be a maximum of 52% of the recommended superconducting coil axial length. Maglev 2000 team has chosen a robust fabricated aluminum ladder with the rung cross-member welded underneath the side bars in a pre-fabricated supply unit. The overlap of rung under side bar is to be 5 cm. per side and a total weld track of 20 cm. The calculated peak induced current per rung or side-bar is 290,000 Amps at a 134 m/s linear speed. The projected side-bar current density is consequently about J=15,260 A/sq. cm. for a thermal period of t=3.8 ms. The expected temperature rise T is insignificant and calculated as:

$$T = \frac{J^2 t}{2} \text{ for J in kA/sq. cm.}$$

$$T = \frac{(15.26)^2 (.0038)}{1.45} = 0.61^{\circ}K$$

The maximum number of levitation magnets per side of vehicle is to be seven and the total temperature rise per 50 tonne vehicle passing at 134 m/s is 4.3°k. For the baseline 42 tonne vehicle, a minimum of 5 S.C. magnets per vehicle side are required.

In 1992 dollars, the cost of Aluminum 6101-T64 is $2.20 kg. which indicates a raw material cost of $69,366/km for dual Type I, II or IV levitation ladder configuration. The Type III costs $85,150/km for raw materials.

The width of the levitation ladder is based on optimizing the following parameters:

1. Ratio of ladder overall width to mean width of vehicle S.C. levitation magnet.

2. Nominal levitation height. The larger the levitation height the larger is the optimum ladder overall width. The above calculations are based on a 19-23 cm levitation height, electromagnetic and a 10 cm mechanical clearance gap.

3. The ladder reflected L/R time constant. The phase angle of the induced current w.r.s.t. the induced voltage should be in the range of 60-70° to yield a low magnetic drag and highest lift.

Figures 1-2 shows the layout of the guideway electrical conductors for linear synchronous motor, null-flux guidance loops and levitation ladder strips. The range of levitation magnet MMF per coil is 320-385 kAT and summarized in Table 1-7. It is essential to hold the levitation magnet pitch about three-times the rung pitch to minimize the space harmonic of the suspension forces. Thus if the magnet length can be sized to 1.5 m long with a rung pitch of 51 cm, the pulsations of the EDS levitation force can be held to 1% of the average force. The L/D ratio of the existing configuration is 21.0:1 when calculated at the upper speed of 150 m/s. The installation pole pitch of the lift magnets should be held to 2.04 m representing a chording ratio of 0.735:1.

1.5 Summary of Guideway Electrodynamics Design

Table 1-9 describes the total guideway electrical conductor weight for combined propulsion, levitation and guidance systems in all five type classifications. Both copper LSM stator and aluminum LSM stator options are shown. The lightest weight system are the Type IV and V due to the absence of the null-flux guidance materials. However, these systems have a much heavier concrete structure which more than offsets the reduction in conductor weight.

Types I and II are both moderately light at 50,091 - 50,830 kg/km for conductors and retain efficient lightweight concrete structures. The heaviest guideway for conductor was the Type III at 57,665 kg/km for a modified "Magneplane" design with dual LSM propulsion. The corresponding cost of materials analysis for all five types is given in Table 1-10. The Type IV & V are the lowest cost of electrical materials at $96,000 - $107,000 per km at guideway. The Type I & II are in the range of $112,000 - $118,000/km and Type III at $129,000/km, assuming 100% aluminum conductor and strip. The cost of installation of guideway electrical components remains to be exactly determined, but in general this study uses 4.0 times the cost of materials for the cost of labor to custom fabricate, install and delivery the guideway components to the job site. Thus the range of installation costs may be provisionally set at $386,000 to $517,000 /km. The LSM stator winding is modular in all designs and installed in replaceable troughs along each span. Modularity of design and installation remain a key features of the described electrodynamic systems.

Table 1-1

Operational Characteristics of the Reference Maglev Vehicle

Capacity range	50-200 passengers
Overall length	15-39 m
Width (nominal)	3.65 m
Height (nominal)	3.2 m
Aerodynamic drag coefficient	0.26
Nominal laden weight (200 poss.)	42 tonnes
Acceleration	1.0 m/sec^2 (0.1$_g$)
Deceleration - normal	2.5 m/sec^2 (0.25$_g$)
Deceleration - emergency	10 m/sec^2 (1.0$_g$)
Propulsion	LSM - Dual Stator
Upper speed range	400-500 km/hr.
Propulsion Magnet Refrigeration Load	41-50 kW

At Cruising Speed of 500 km/hr.

Max. continuous thrust	60 kN
Ground clearance	0.125-0.15 m
Magnetic drag (est.)	12-15 kN
Aerodynamic drag (est.)	35-37 kN
Side wind loading (100 km/hr. cross wind)	70 kN
Noise, at 15 m sideline	89 d BA
Guideway aluminum for lev. strips	42 metric tons/km
Superelevation limit	15°
Minimum radius at max. speed	1.6 km
Guidance stiffness - nominal-lateral	4.2 x 10^6 N/m
Suspension stiffness - nominal-vertical	3 x 10^6 N/m
Levitation system - nat. freq.	2 Hz
Guidance natural frequency	0.85-1.0 Hz
Levitation lift off speed range	48-60 km/hr.
Substation Electrical Output	12.9 MVA at 122 Hz
LSM Mechanical Output	8.33 MW
Linear Power Generator Output	475 kW

Table 1-2

Reference Design Parameters for Superconducting Dual LSM Systems

Common Design Characteristics

Thrust *	60 kN
Max. Cruising Speed, V_s	500 km/h
Mechanical Power *	8.33 MW
Field-stator Winding Separation, z_o	22 cm
On-board Power Linear Generator Drag	3.5 kN
Vehicle Aerodynamic Drag	37 kN
Electrodynamic Drag	12-15 kN
Stator Section Length, L_b (range)	0.5 - 2.0 km
Field MMF of Full-length magnets, i_f	500 kAT/600 kAT
Total Magnetic Moment of Superconducting Coils, M *	21.2 x 10^6 A-m

Conductor Material

Field Winding

Nb-Ti Superconducting Magnets		
No. of Superconducting Magnets	50	50
Mean Length, L(m)	0.53	0.53
Mean Width (round-ended), W_f(m)	0.80	0.80
Wavelength, (m)	1.14	1.14
Self Inductance, (H)	0.409	0.409

Stator Winding Cable Materials	Copper	Aluminum
No. of Parallel Conductors/phase	2	2
Active Width, W_s(m)	0.625	0.625
Conductor Diameter, d (mm)	12.7	14.6
Longitudinal Conductor Spacing	30°	30°
Conductor Length per Phase per Unit guideway length *	7.99	8.01
Winding Resistance, R_s(/km)	0.166	0.175
Mutual Inductance, M (mH/km)	0.95	0.95
Self Inductance, L_s (mH/km)	2.11	2.04
Leakage Inductance, L_L (mH/km)	1.16	1.09
Reactance for 1 km block section, $W_s L_L L_b$ ( )	0.889	0.836

Table 1-2
(Continued)

Stator Winding Cable Materials	Copper	Aluminum
Mass of Winding, (tonnes/km)	19.3	11.3
Lateral Offset of Field Array w.r.t. stator axis, y	-0.10	-0.10
Operating Parameters		
Field-stator Total Mutual Inductance, $N_{mag} M_{fsi}$ (uH)	6.70	6.70
Inverter Frequency, w_s (Hz)	122	122
Inverter Voltage, L-N (kV)	4.17	4.20
Phase Current, rms (A)	846	846
Current Density (A/mm^2)	3.36	2.53
Control Angle, B	112°	112°
Inverter Complex Power, S (MVA) *	10.5	10.6
Power Factor	0.85	0.85
Power Dissipation in 1 km block (kW)	356	375
LSM Electrical Conversion Efficiency	95.9	95.8

Table 1-3

Cost and Weight for Type 1 Dual LSM Stator Winding
6-Phase/Guideway Side with 212,000 or 250,000 CM Copper Conductor

Cond. dia-mm	Length/ phase/km	12 x Conductors	R/km of Guideway	Cost/km of Guideway	Weight kg
11.7	1332 m	15,992 m	2.65	$162,554	16,320
12.7	1332 m	15,992 m	2.25	$199,392	19,307

Null-flux and LSM-dual total conductor weight = 19,307 kg + 3,228 kg = 22,535 kg/km.

Null Flux Loops

MLT = 1.542 m

Thickness = 0.011 m

Total Vol = 0.025 x .011 x 1.542 = .000424 cu. m. x 2690 kg/m
= 1.14 kg per loop

Total loops in 1 km = 2832 loops @ pitch (avg.) of 0.343 m. including overlap
2832 x 1.14 = 3228 kg

Table 1-4

Electrical Losses for Representative LSM Propulsion Guideway Windings for Dual Stator Systems, at High Speed Condition of 500 km/hr. and Propulsion Thrust = 60 kN

Conditions: Copper Conductors, 250 MCM, 6-phase Winding per Side,
I = 423 Amps per Conductor.

Guideway Block Length	Resistance/ Conductor (Ohm)	Stator I^2 R Loss (kW)					
		Type I	Type II	Type III	Type IV	Type V	Efficiency %
0.5 km	0.083	185	178	181	178	178	97.8
1.0 km	0.166	370	356	363	356	356	95.9
2.0 km	0.332	740*	712	726	712	712	92.1

Conductor diameter = 12.7 mm
Conductor current density = 3.36 A/mm^2
Base Mechanical Output = 8.33 MW
Base Stator Power Dissipation (423 A) = 712 kW (2.0 km block)
Net Power Input = 9.04 MW (2.0 km block)
Basic Efficiency = 92.1% (2.0 km block)

* Higher than base loss due to stray induction into parallel levitation ladder in close proximity to LSM.

Resistance calculated at 20 C condition.

Table 1-5

Weight and Costing of Guideway Transmission Cable
Strands = 19, 7 kV Insulation Type EP, Copper Conductor
Calculated per 1 km Basis

Cost/km	Cable Size (dia.)	Resistance R/km	Reactance X/km *	Impedance Z/km	Weight/km
$10,166	11.7 mm	0.166	0.358	0.422	972 kg
$12,462	12.7 mm	0.141	0.313	0.343	1150 kg

* Ohms at 20 Hz.

Cable O.D. is minimum of 7 mm over indicated inner cable size for 7 kV insulation.

Table 1-6

Cost and Weight for Type I Null-flux Guidance Loops
Mean Length of Turn = 1.542 m, Field MMF = 2 x 600 kAT per Pole
Length/side = 0.471 m Loop Width (mean) = 0.30 m
Conductor Thickness = 11 mm Conductor Width = 25 mm
Total Volume = .000424 cu. m. per Null Flux Loop

Individual Loop Weight	Repetitive Layout Pitch	Loops per 1 km Guideway	Weight (kg) per km	Cost of Materials per 1 km
1.14 kg	0.353 m	2832	3228	$ 7,102
1.14 kg	0.157 m	6370 *	7261	$15,974

* Recommended base design for field magnets of pitch 0.51 - 0.59 m.

Table 1-7

Characteristics of Reference Levitation Magnet for Vehicle with Limit of 7 Magnets per Side

Maximum Lift Force/magnet	12.4 Tonnes
Mean Width	0.48 m
Mean Length	1.50 m
Nominal Levitation Height	21 - 22 cm
Amp-turns MMF	320 kAT - 385 kAT
Maximum Design Speed	150 m/s
Magnetic Moment/Coil	230,400 - 277,200 A.T.-m^2
No. of Turns	1000
Current	320 - 385 A
Conductor Active Cross Section	38 x 48 mm
Superconductor Type	Nb-Ti
Operating Temperature	4.2°k
Coil Self - Inductance	2.5517 Henries
Coil Stored Energy @ 385 A	189 KJ
Separation Mean Coil Height to Bottom of Cryostat	70 mm
Vehicle Undercarriage Aluminum Thickness*	9 mm
Thermal Insulation Distance Between Skin and Cryostat	11 mm
Total Separation Mean Conductor to Undercarriage Surface	90 mm
Estimated Electromagnetic drag/vehicle (gap dependent)	12 - 15 kN

* For damper shield and mechanical structure

Table 1-8

Weight Calculation for Ladder-type (rung pitch = 51 cm)
EDS Levitation Conductors for All Guideway Configurations

Guideway Type	Width Overall	Rungs in 1 km	Rung Length	Rung Weight	Side-bar Weight	Total Alum. Weight (kg/km)
I	60	1960	51.7	2.88	10,120	15,765 x 2
II	60	1960	51.7	2.88	10,120	15,765 x 2
III	80	1960	93.3	4.71	10,120	19,352 x 2
IV	60	1960	51.7	2.88	10,120	15,765 x 2
V	68	1960	80.8	4.08	10,120	18,126 x 2

All weights in kg, dimensions in cm unless otherwise stated.

Table 1-9

Summary of Total Guideway Electrical Conductors Weight for Combined Propulsion, Levitation and Null-flux Guidance with Aluminum and Aluminum/Copper Conductor Options Conductor Weight in kg per km of Guideway

	Type I	Type II	Type III	Type IV	Type V
LSM Stator (Copper LSM Stator (Alum.)	19,307 11,300	19,307 11,300	19,700 11,700	19,307 11,300	19,307 11,300
Levitation Strips	31,530	31,530	38,704	31,530	36,252
Null-flux Guidance ED Repulsion Guidance	7,261	N/A** 8,000	7,261	N/A *	N/A *
Total Weight (Al/Cu) Total Weight (Al only)	58,100 50,091	58,837 50,830	65,665 57,665	50,837 42,830	55,559 47,552

Type I = Flat-top guideway, all systems on top surface.
Type II = Flat-top guideway with LSMs mounted underneath structure.
Type III = Semi-circular "Magneplane" with dual LSM.
Type IV = Inverted T (Japan Railways style) with vertical dual LSM.
Type V = U-channel with separated dual LSMs, vertical.

* Incorporates LSM B-angle control for repulsive transverse guidance force.
** Uses side-wall mounted induction-repulsion transverse guidance.

N/A = Non-applicable

Table 1-10

Summary of Cost for Electric Materials for Propulsion, Levitation and Guidance Systems (per kilometer)

Values in U.S. Dollars, 1992 Base
Materials: Aluminum Type 6101-T64 for Bar, Plate for Levitation and Guidance Components

	Type I	Type II	Type III	Type IV	Type V
Dual LSM Stator (Cu)	162,554	162,554	165,862	162,554	162,554
Dual LSM Stator (Al)	27,120	27,120	28,100	27,120	27,120
Levitation Strip *	69,336	69,366	85,148	69,366	79,754
Null-flux Guidance	15,974	22,000	15,974	0	0
Cost in Copper/Al.	$247,894	$253,920	$266,984	$231,920	$242,308
Cost in All Al.	$112,430	$118,486	$129,222	$96,486	$106,874

Aluminum costed at specific price of $2.20/kg for bar and plate.

Aluminum costed at specific price of $2.40/kg for LSM conductor.

* Dual Ladder Type.

Table 1-11

Magnitude and Location of Peak Lift and Drag Forces for 1.5 m. Long Lift Magnet at 22 cm. Height

Upper Speed Case V - 150 m/s
Values per Magnet, MMF - 320 kAT

Magnet Width	Max. Lift Force (Tonnes)	At Guideway Width (m)	Max. Drag Force	At Guideway Width (m)	L/D Ratio
0.2 m	3.63	0.35	0.11	0.51	33.0
0.3	6.31	0.39	0.24	0.70	26.3
0.4	9.90	0.46	0.38	0.72	26.1
0.5	12.40	0.51	0.59	0.75	21.0
0.6	14.50	0.60	0.82	0.88	17.7

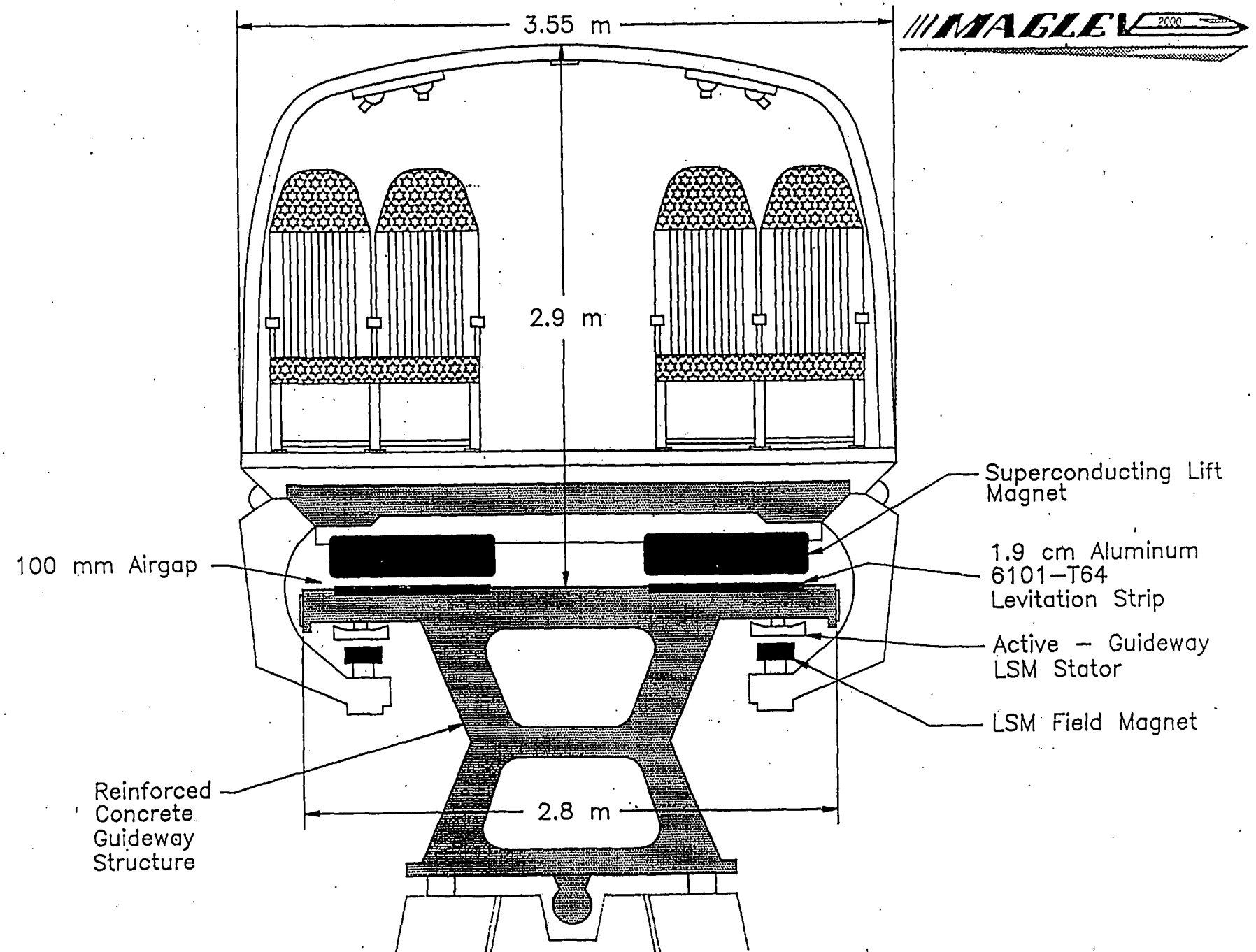

Fig. 1-1 General view of EDS Lift and Propulsion System Type II System

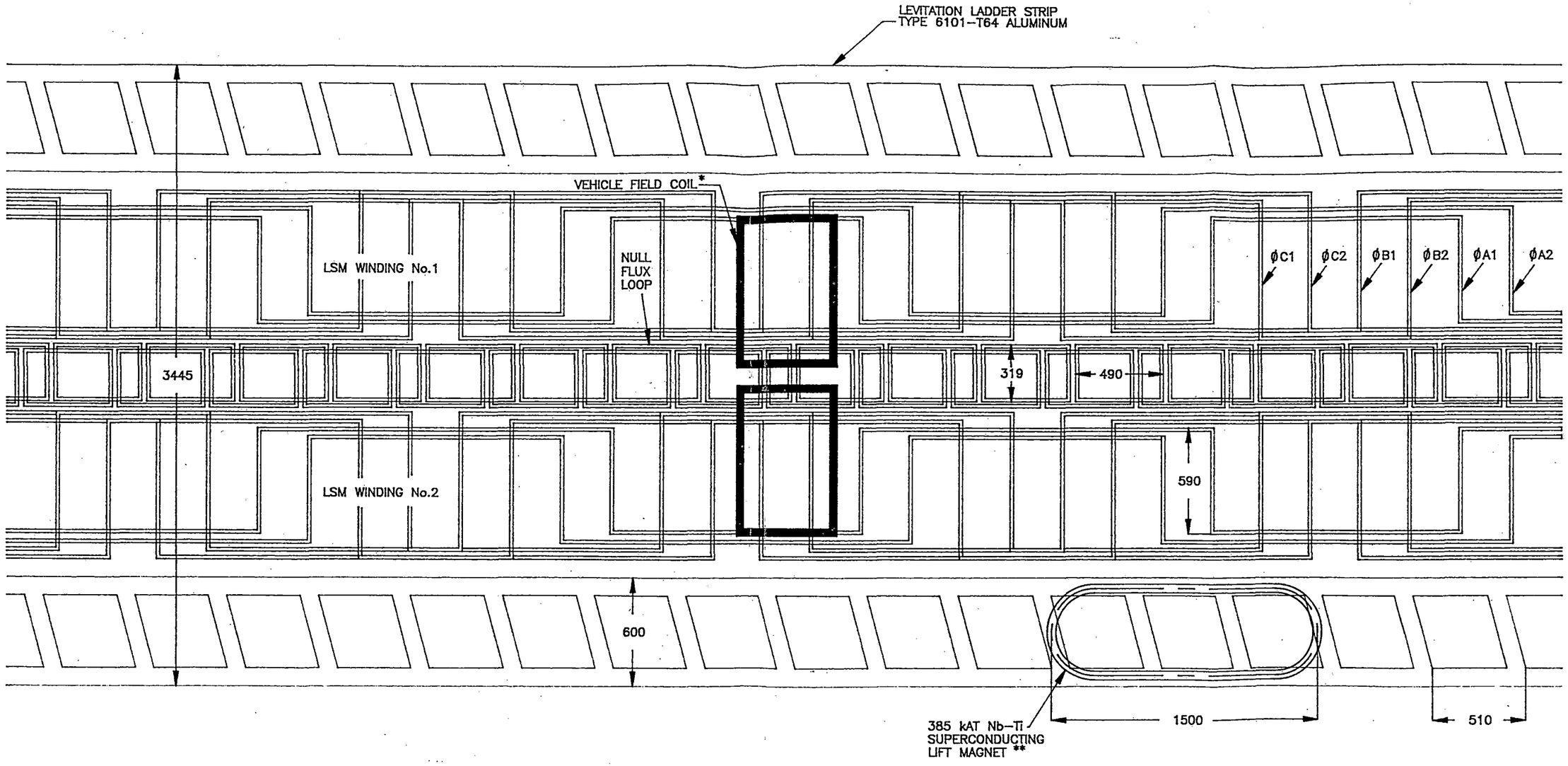

Figure 1-2 TYPE I FLAT–TOP MAGLEV GUIDEWAY WITH DUAL LINEAR SYNCHRONOUS MOTOR AND NULL–FLUX GUIDANCE LOOPS FOR 50 TONNE VEHICLE

NOTES:
*ONLY ONE VEHICLE LSM FIELD COIL SHOWN IN ARRAY OF 40 – 50 PER SIDE
**ONLY ONE LIFT MAGNET SHOWN IN ARRAY OF 5 – 7 PER SIDE OF VEHICLE

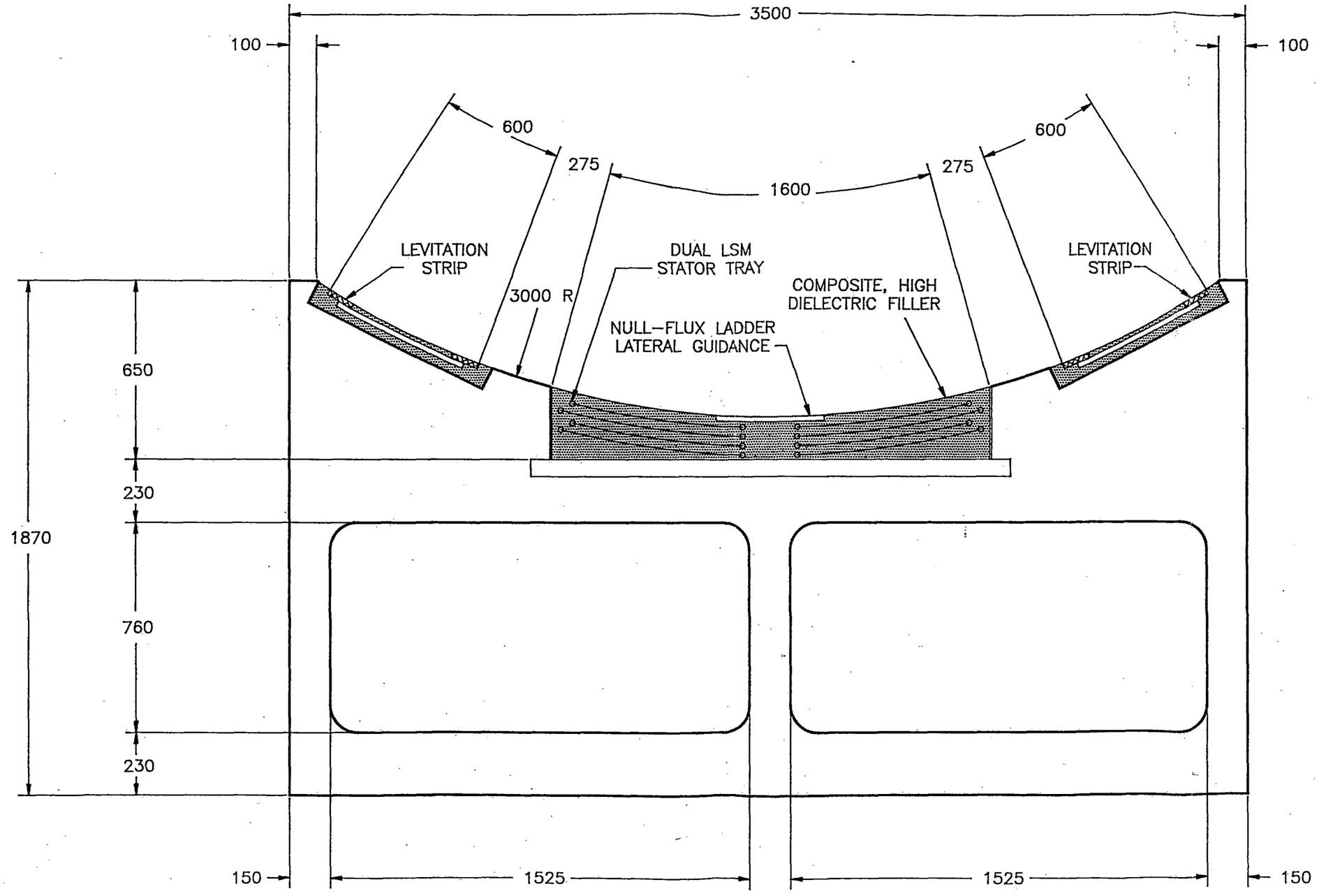

Figure 1-3 Type III Maglev Guideway

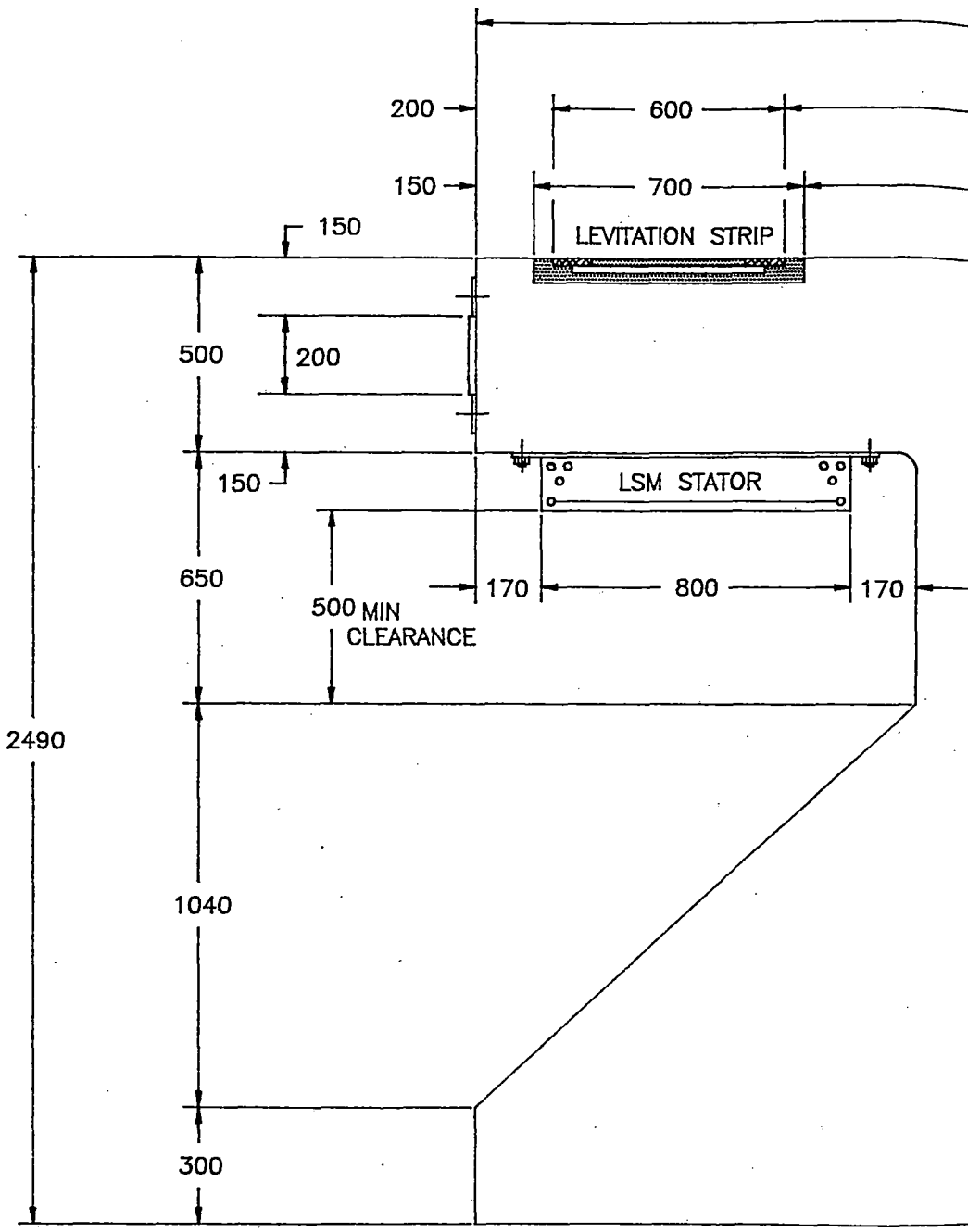

Figure 1-4 Type II Maglev Guideway

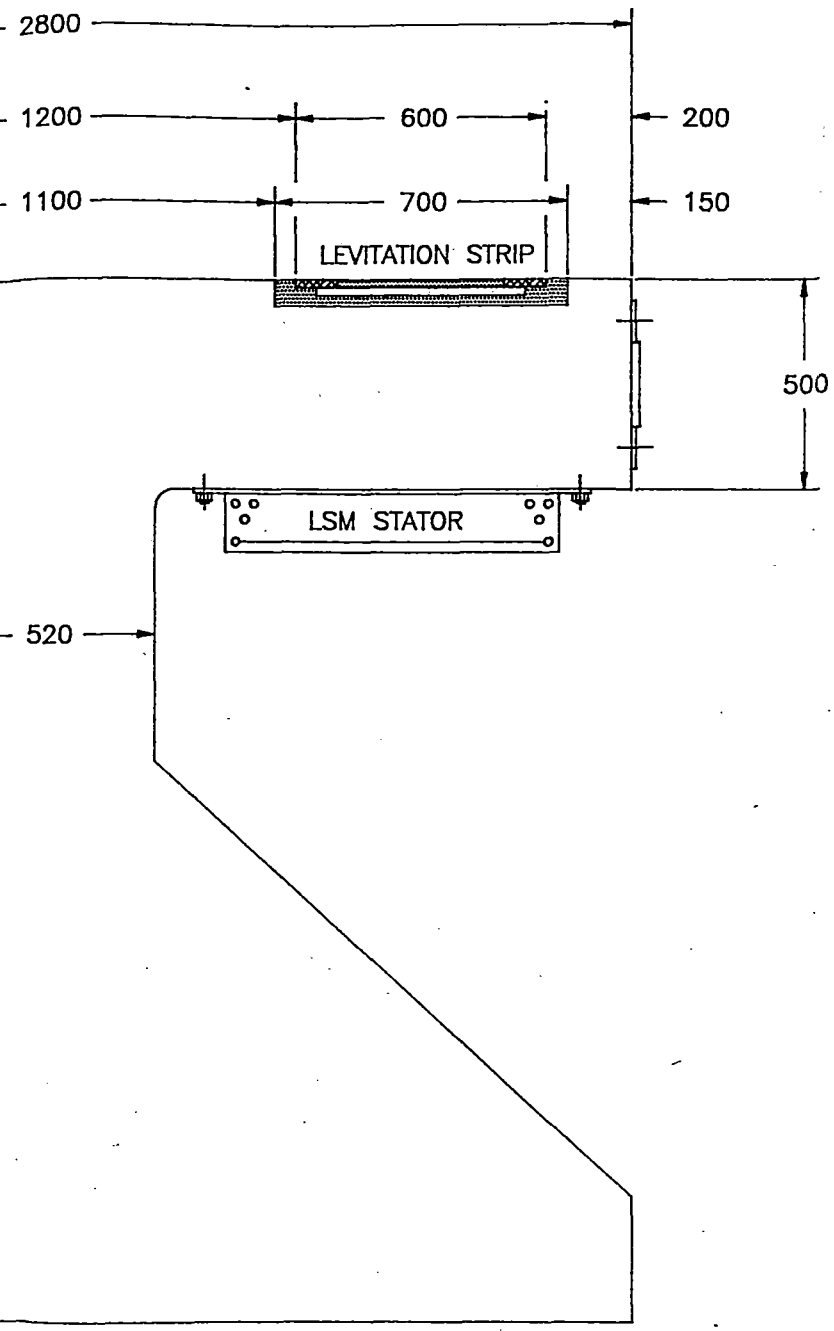
2800
1200
600
200
1100
700
150
LEVITATION STRIP
500
LSM STATOR
520

$$C = 1.0 + .5\,wR + (db(A) - 65)/10 + 17\,aT + 17\,aV$$

wR - roll rate (RMS) = .9 deg/sec
aT - transverse accel (RMS) = .06 g
aV - vertical accel (RMS) = .05 g
$db(A)$ - noise limit = 62 db (A)

$C_D = ?$

$$C = 1.0 + .5(.9) + \left(\frac{62-65}{10}\right) + 17(.06) + 17(.05)$$

$$= 1.0 + .45 + (-.3) + 1.02 + .85$$

$$C = 3.02$$

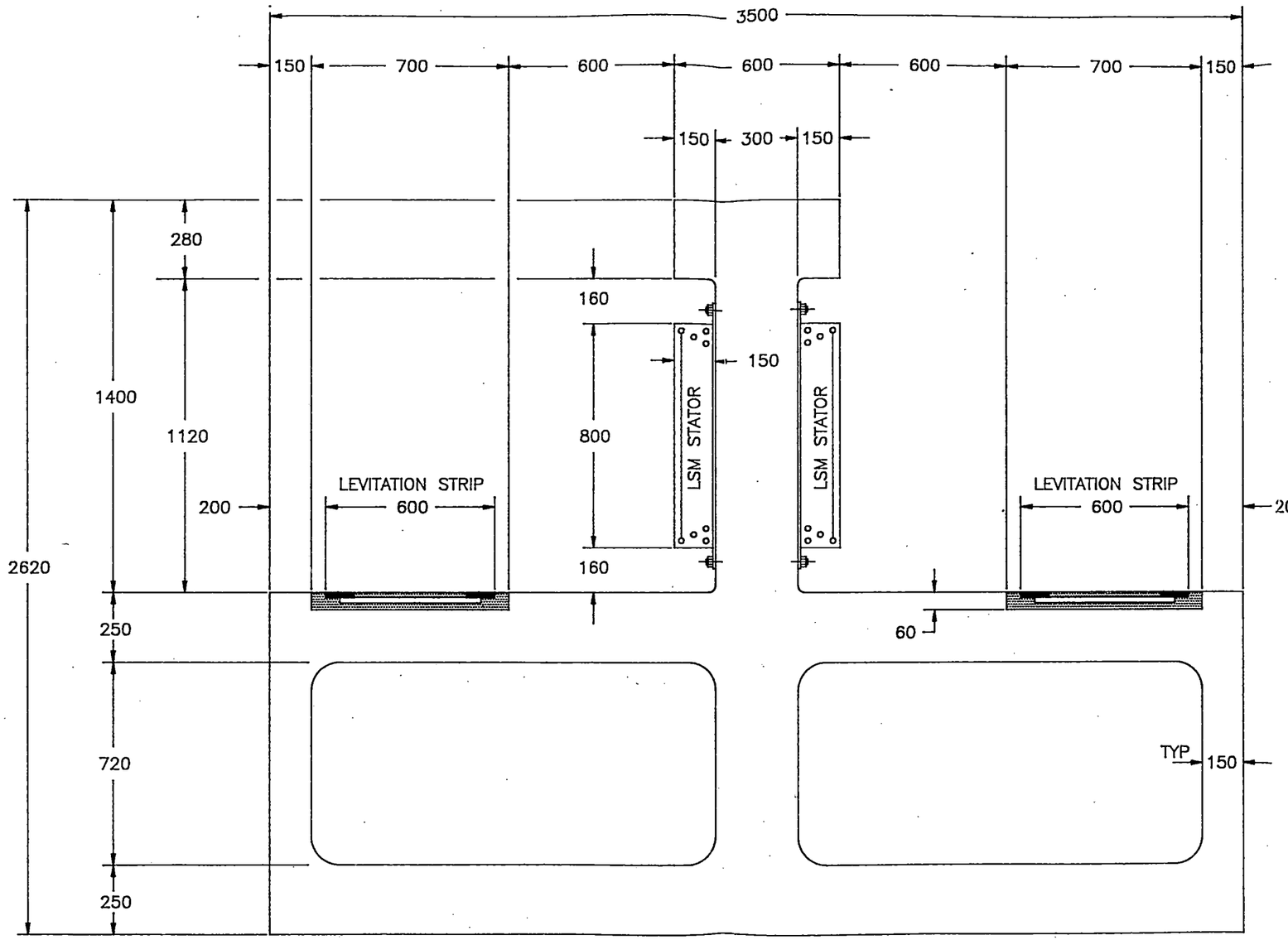

Figure 1-5 TYPE IV GUIDEWAY CROSS SECTION
INVERTED T CONFIGURATION – DUAL LSM

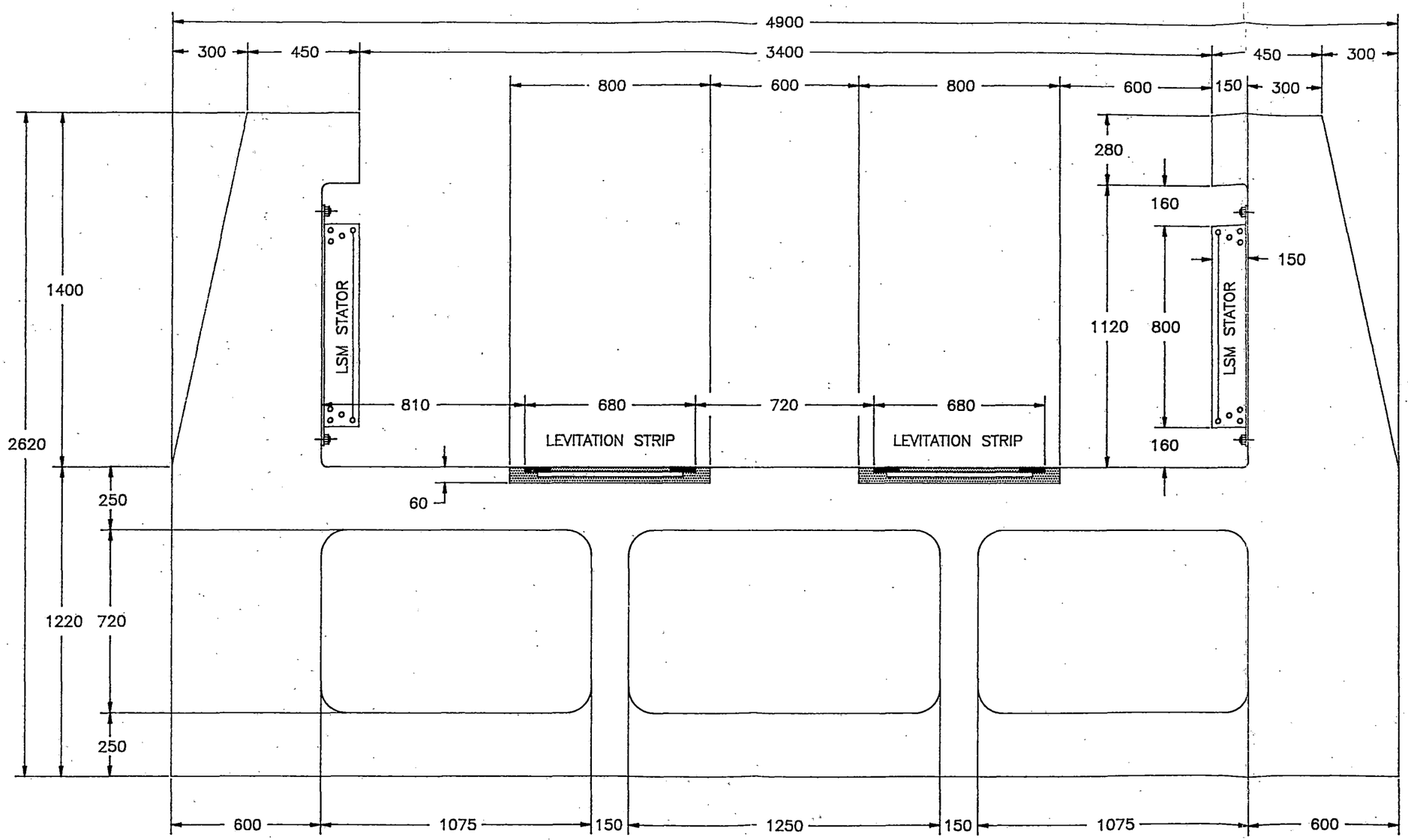

Figure 1-6 TYPE V GUIDEWAY CROSS SECTION U CONFIGURATION – DUAL LSM

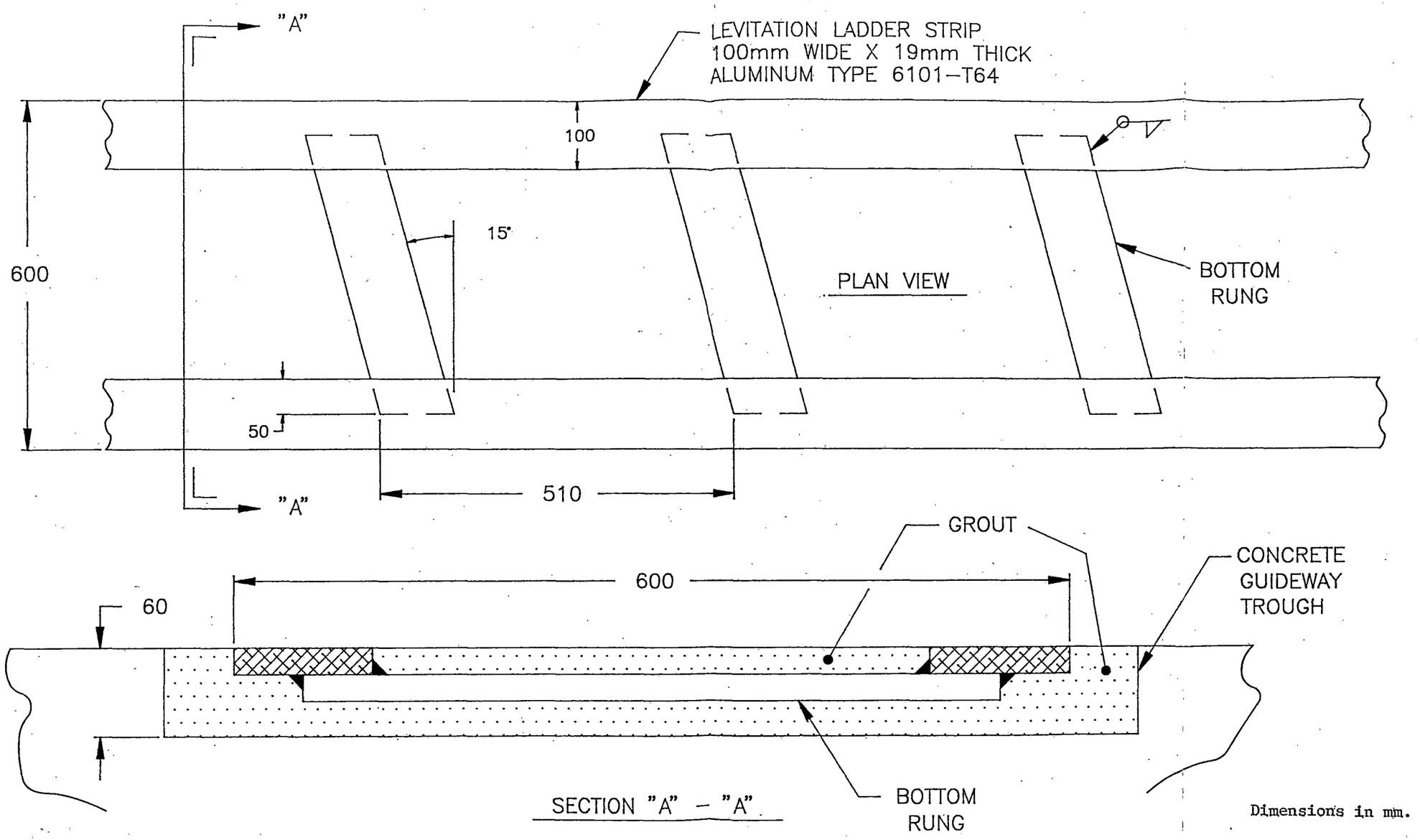

Dimensions in mm.

Figure 1-7 Cross section of levitation ladder strips and rungs.

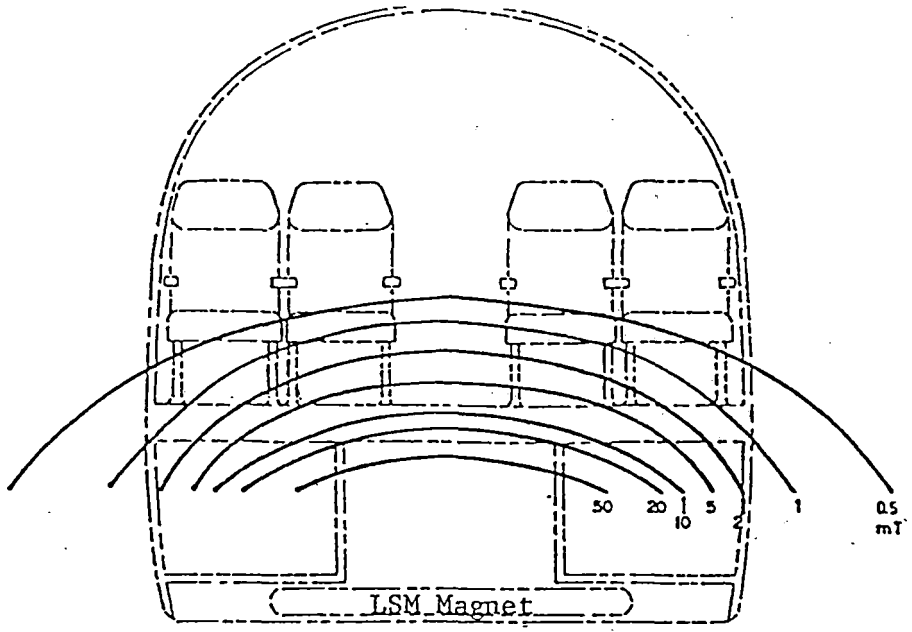

Single LSM Array Inherent Field

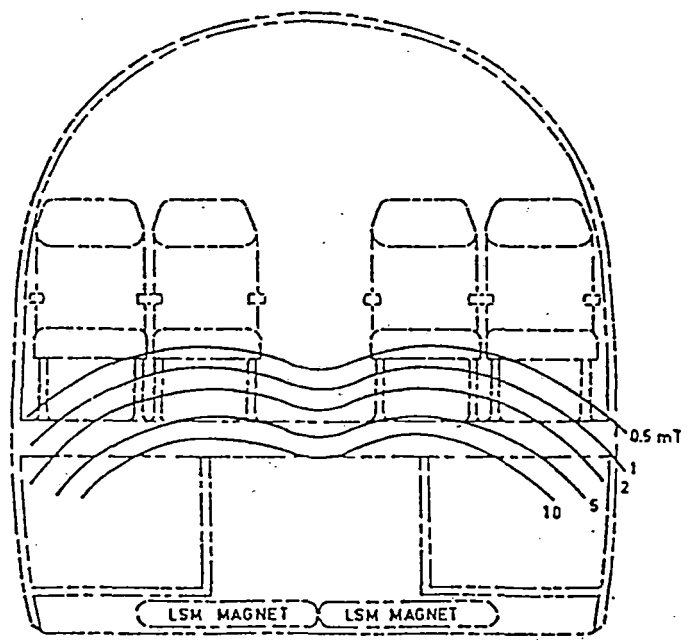

Dual LSM Array Inherent Field

Figure 1-8 Peak magnetic field densities in passenger compartment with single and dual LSM superconducting magnets at 500 kAT excitation and no ferromagnetic shielding.

SUPERCONDUCTOR SELECTION

2.1 Magnetic Field Calculations

The starting point of the conceptual design is magnetic field analysis. Computer codes were written for racetrack coil shapes from rectangular to purely circular. The magnetic field calculations are used for evaluating propulsion and lifting forces as well as magnetic shielding and are shown in Figures 2-8-1 through 2-8-5.

Field plots were generated for a typical propulsion racetrack coil. Figure 2-9 shows the Bz component of the magnetic field, and Figure 2-10 shows a field map in the x-y plane.

Propulsion Force Analysis

A set of analytical formulae based on the Biot-Savart law has been developed for computing the propulsion forces on the vehicle's LSM coil. The formulae describe the interaction between the three phase AC windings in the guideway and the superconducting coil on the vehicle.

The formulae consist of a finite series of terms representing the force from each segment of guideway. The series can be truncated at any number of segments. It is expected that not more than 10 terms are required.

Analytical formulae for the propulsion coil are shown in Figures 2-11-1 through 2-11-5. Simplified formulae for the rectangular coil that is a first approximation of the racetrack coil are shown in Figures 2-12-1 through 2-12-4.

Field Accuracy Study

The magnetic field for the superconducting coil was previously calculated using a thin single wire as an approximation to the finite wire bundle. We have verified the accuracy of the

thin wire approximation as compared to a coil with finite cross section. The accuracy of the thin wire approximation was found to be within 1%.

Finite Element Study of the Racetrack Coil

The forces and fields on the superconductors in the propulsion coil have also been calculated using a commercial finite element software package sold by Vector Fields. The program used in this work is Tosca, which is useful for computing static or slowly varying AC fields.

The finite element calculation agrees well with previous magnetic field calculations using analytic methods. This confirmation is valuable since we can use either method with confidence in future analyses. It is particularly valuable to have an independent confirmation of the finite element method.

Fields and self forces were calculated at the circumference of the racetrack coil. Calculations were done for 400 kAT and 600 kAT. Coil dimensions were supplied by the principal investigator. Fields and self forces are shown in Tables 2-1 and 2-2.

2.2 Emergency Forces and Fields

All the formulae used to calculate forces and fields will be used to calculate emergency forces and fields. This will be done in the detailed design phase of the project.

Table 2-1

Peak Field in a 600 kAT Propulsion Coil Using TOSCA

Coil Data

Coil Shape:	Racetrack Reinforcement Thickness (in.): 0.005
Jc (A/mm^2 @5.3T):	2900 Current Density (A/cm^2): 12265.41
Transport Current (A):	100 Total Ampereturns (Aturns): 603000
Conductor Dimension (mm^2):	0.232324 Coil Cross-Section S (cm): 6.9 x 6.9
Coil Size (cm^2):	47.61 Width (cm): 6.9
Layers:	90 Height (cm): 6.9
Turns (turns/layer):	67 Racetrack Width (cm): 57
Packing Factor:	0.587 Racetrack Length (cm): 80
Interlayer Thickness (in.):	0.003 Cu:Sc: 5.75:1
Insulation Thickness (in.):	0.0015

Peak Field in Gauss on XZ plane (excluding coil neighbors and guideway fields)

Field along arc 0 0 33.1 21.6 0 11.5 arc radius = 21.6 cm

Coordinates		A/m^2		Gauss		
X	Z	Jx	Jz	Hy	Bm	Point
0	33.1	-12665.4	0	-39514.5	39514.5	0
3.378984	32.83407	-12509.5	1981.306	-39508.4	39508.4	1
6.674767	32.04282	-12045.5	3913.826	-39490.5	39490.5	2
9.806195	30.74574	-11285	5749.974	-39458.5	39458.5	3
12.69616	28.97477	-10246.5	7444.539	-39408.5	39408.5	4
15.27351	26.77351	-8955.79	8955.795	-39333.7	39333.7	5
17.47477	24.19616	-7444.54	10246.53	-39221.8	39221.8	6
19.24574	21.30619	-5749.97	11284.96	-39049.1	39049.1	7
20.54282	18.17477	-3913.83	12045.52	-38765.6	38765.6	8
21.22407	14.87898	-1981.31	12509.47	-38245.9	38245.93	9
21.6	11.5	4.28^{-11}	12665.41	-37121.4	37121.4	10

Table 2-1
(Continued)

Peak Field in a 600 kAT Propulsion Coil Using TOSCA

Field along line 21.6 0 11.5 21.6 0 0

Coordinates		A/m²		Gauss		
X	Z	Jx	Jz	Hy	Bm	Point
21.6	11.5	0	12665.41	-37121.4	37121.4	10
21.6	10.35	0	12665.41	-36632.9	36632.9	11
21.6	9.2	0	12665.41	-36272.1	36272.1	12
21.6	8.05	0	12665.41	-36004.5	36004.5	13
21.6	6.9	0	12665.41	-35803.4	35803.4	14
21.6	5.75	0	12665.41	-35651.9	35651.9	15
21.6	4.6	0	12665.41	-35538.7	35538.7	16
21.6	3.45	0	12665.41	-35456.7	35456.7	17
21.6	2.3	0	12665.41	-35401	35401	18
21.6	1.15	0	12665.41	-35368.7	35368.7	19
21.6	0	0	12665.41	-35358.1	35358.1	20

Table 2-2

Self Forces on 600 kAT Propulsion Coil

Coordinates		Newton/m^3		Newton/cm		Lb/in	
X	Z	Fx	Fz	Fxu	Fzu	Fxu	Fzu
0	33.1	0	5.00^{8}	0	23827.24	0	13601.06
3.37894	32.83407	78278233	4.94^{8}	3726.827	23530.26	2127.346	13431.54
6.674767	32.04282	1.55^{8}	4.76^{8}	7358.551	22647.29	4200.406	12927.52
9.806195	30.74574	2.27^{8}	4.45^{8}	10802.01	21200.14	6166.001	12101.46
12.69616	28.97477	2.93^{8}	4.04^{8}	13967.73	19224.93	7973.057	10973.97
15.27351	26.77351	3.52^{8}	3.52^{8}	16771.31	16771.31	9573.397	9573.397
17.47477	24.19616	4.02^{8}	2.92^{8}	19133.85	13901.56	10921.98	7935.284
19.24574	21.30619	4.41^{8}	2.25^{8}	20980.18	10689.94	11975.9	6102.026
20.54282	18.17477	4.67^{8}	1.52^{8}	22231.57	7223.475	12690.22	4123.302
21.33407	14.87898	4.78^{8}	75776894	22778.36	3607.738	13002.34	2059.368
21.6	11.5	4.70^{8}	-1.6^{-6}	22384.2	-7.6^{-11}	12777.35	-4.3^{-11}
21.6	10.35	4.64^{8}	0	22089.64	0	12609.2	0
21.6	9.2	4.59^{8}	0	21872.08	0	12485.01	0
21.6	8.05	4.56^{8}	0	21710.71	0	12392.9	0
21.6	6.9	4.53^{8}	0	21589.45	0	12323.68	0
21.6	5.75	4.52^{8}	0	21498.1	0	12271.54	0
21.6	4.6	4.50^{8}	0	21429.84	0	12232.57	0
21.6	3.45	4.49^{8}	0	21380.39	0	12204.35	0
21.6	2.3	4.48^{8}	0	21346.8	0	12185.18	0
21.6	1.15	4.48^{8}	0	21327.33	0	12174.06	0
21.6	0	4.48^{8}	0	21320.93	0	12170.41	0

2.3 Conductor and Coil Design

Conductor designs have been completed for propulsion coils with Nb_3Sn, NbTi, and high T_c compounds. Two stability criteria were used in the designs: cryostability and adiabatic stability. Cryostability criteria are usually most conservative and expensive in terms of space and material utilization, but usually produce coils with the highest operating margin. Adiabatically stabilized conductors usually produce a more efficient magnet design but are prone to training quenches.

The requirements which drive the conductor design include:

- the peak field at the winding
- the number of amp turns
- the normal operating current
- the coil size and geometry
- the insulation requirements
- the superconductor and its properties
- the matrix selection
- the coolant selection
- the reinforcement requirements from the self forces

The design outputs include:

- the conductor to current density
- the matrix to superconductor ratio
- the conductor dimensions
- the conductor mass and length

From this information one forms a coil design which has as its output:

- the coil cross section

- the number of turns
- the number of turns/layer
- the number of layers
- the inductance
- the coil energy

The reference data for the critical current densities of the superconductors used in the conceptual design are listed below:

- for NbTi, Figure 2-13-1
- for Nb_3Sn, Figure 2-13-2
- for YBCO, Figure 2-13-3
- for Bismuth 2223, Figure 2-13-4
- for TBCCO, Figure 2-13-5

There are filament diameter limitations to satisfy cryostability conditions. They are shown for NbTi and Nb_3Sn in Figure 2-14. Data on the copper magneto resistivity effect are shown on Figure 2-15, which is typical of a matrix material.

The conductor and coil designs for 600 kAT propulsion coils are presented in Figures 2-16-1 through 2-16-10. Each figure describes coil dimensions, bundle cross section, conductor cross section, and all input and output data for different superconducting materials and different design models chosen. A summary of coil design is shown in Table 2-3.

NbTi

Conceptual magnet designs using commercially available NbTi conductor are shown in Figures 2-16-1 and 2-16-2. The conductor properties used in the study are the SSC type whose properties are listed in Figure 2-13-1. Note from Table 2-3 that the adiabatic coil is one of the smallest and most efficient in terms of weight and coil cross section. The adiabatic coils are usually potted in epoxy for added strength and reliability which is an additional advantage.

Nb_3Sn

The advantage of using Nb_3Sn for Maglev is that the critical temperature is higher so the coil should be more stable than for NbTi coils. We examined two types of coils in our studies, one adiabatic and one cryostable. Cryostable Nb_3Sn coils are usually encased forced flow conductors, but for the purposes of analysis we assumed an ideal fully cryostable coil which may not be easily realized in practice, but gives us a baseline with which to make a comparison with other designs.

The coils are shown in Figure 2-16-3 and 2-16-4. Both coils are similar in size with their NbTi counterparts in Figures 2-16-1 and 2-16-2 because the current densities at low fields for Nb_3Sn are about the same as for NbTi. There is no advantage to Nb_3Sn in these configurations since Nb_3Sn conductor is more expensive and the coils are more expensive to fabricate using wind and react technologies.

A forced flow Nb_3Sn system has not been considered in this phase of the program. There may be some savings in refrigeration since the coil could be operated at a higher temperature using cooled He gas.

High T_c

Three high T_c superconductors were analyzed for Maglev propulsion and levitation coil applications. Some promising high T_c compounds operating at 77 K were examined in this analysis including thick film thallium compounds (TBCCO) which have current densities shown in Figure 2-13-5. A more practical compound is the bismuth compound BSCCO fabricated as a silver tape. This compound works best at 4.2 K as shown in Figure 2-13-4. The most ideal conductor would be a YBCO tape operating close to thin film values at 4.2 K, and a concept for comparison is shown in Figure 2-13-3.

The magnet designs summarized in Table 2-3 show that high T_c compounds at 77 K are not particularly attractive. Even the BSCCO compounds require a 4.2 K operation to achieve

a practical current density. In addition BSCCO is expensive in that it requires silver. In comparison to NbTi conductors, the high T_c compounds do not seem attractive. If an order of magnitude higher current density could be achieved at 77 K, the savings resulting from refrigeration could be significant and the added cost of rare earth material or expensive silver stabilizers could be offset.

AC Losses

The DC coil is under the influence of the AC current in the track windings. This creates AC losses in the coil. The losses were evaluated and are shown in Tables 2-4 and 2-5.

AC Losses Studies

Although in the conceptual design it is assumed that the AC losses in the superconductive magnet are negligible, a study was undertaken to assess the magnitude of these losses. At first we looked at low field effects. For this study the assumptions concerning the nature of the eddy current source and coil were as follows:

- The magnetic field is self field only.
- Continuous $\pm 20\%$ variation of the control current about steady state at 10 Hz.
- The actual operating spectrum is required to estimate average loss over time.
- Winding current density is 25% of critical (15,000 A/cm^2).
- Extrapolation from loss data at 50 Hz and $\pm 100\%$ variation of magnetic field variation.

To extrapolate the data, we made further assumptions:

- AC losses per cycle are linear at low fields.
- AC losses per cycle are independent of frequency.

Note:

- These assumptions are valid at fields less than 0.5T.
- These assumptions are linear approximations of the Bean model and agree with data taken for typical superconductors.

The calculation proceeds as follows:

From attached figure, the AC loss per cycle at 50 Hz and 0.5T is 10 kW/m³. The energy loss per cycle is:

$$E_0 = (10 \text{ kW/m}^3) / (50 \text{ Hz}) = 200 \text{ J/m}^3$$

The total power loss at any frequency scales with frequency and field and is given by:

$$P_0 = E_0 (f/f_0) (B/B_0)$$

where $E_0 = 200$ J

$f_0 = 50$ Hz

$B_0 = 0.5$T

Simplifying:

$P = 400\ B \cdot f$ W/m³, where B is in Tesla and f is in Hz

Table 2-3

Summary of 600 kA Propulsion Coil Designs

Superconductor	Coil Temp. (K)	Matrix	Stability	Matrix to Superconductor	Critical Current Density (A/cm^2)	Average Current Density (A/cm^2)	Cross Section (cm^2)	Mass (kg)
NbTi	4.2	Cu	cryostable	7.2:1	290,000	10,615	56.07	130
NbTi	4.2	Cu	adiabatic	4.9:1	290,000	19,438	29.89	70
Nb_3Sn	4.2	Cu	cryostable	12.2:1	290,000	10,615	56.07	130
Nb_3Sn	4.2	Cu	adiabatic	4.6:1	290,000	20,153	29.40	68
YBCO	4.2	Cu	cryostable	21.7:1	800,000	10,615	56.07	130
YBCO	4.2	Cu	adiabatic	12.9:1	800,000	21,987	26.79	73
BSCCO	4.2	Ag	cryostable	3.7:1	110,000	2,807	212.52	578
BSCCO	4.2	Ag	adiabatic	1.1:1	110,000	6,467	92.56	250
TBCCO	4.2	Cu	cryostable	2.4:1	100,000	9,175	64.99	176
TBCCO	4.2	Cu	adiabatic	1.0:1	100,000	19,242	31.00	84
TBCCO	77	Cu	cryostable	0.0:1	10,000	3,180	186.56	510
TBCCO	77	Cu	adiabatic	0.0:1	10,000	5,561	107.07	291

Table 2-4

AC Loss Conditions

Ampere Turns	B_{max} (Tesla) Bundle Dia.		AC Field (Tesla) Bundle Dia.	Conductor Bundle Cross Section	Conductor Volume	
kA	10 cm	20 cm	10 cm	20 cm	(cm^2)	(m_3)
100	.4	.2	.08	.04	6.67	6.67×10^{-4}
200	.8	.4	.16	.08	13.3	1.33×10^{-3}
300	1.2	.6	.24	.12	20	2×10^{-3}
400	1.6	.8	.32	.16	26.7	2.67×10^{-3}
500	2	1	.40	.20	33.3	3.33×10^{-3}

- B_{max} is the peak DC field at the winding.
- AC Field is the peak AC field at the winding. AC Field is 20% of B_{max}.
- Turn length = 1 m.
- Conductor current density = 15,000 A/cm^2 (25% of J_c).

Table 2-5

AC Losses

Ampere Turns	AC Loss/Volume (kW/m^3) Bundle Diameter		AC Loss (W) Bundle Diameter	
kA	10 cm	20 cm	10 cm	20 cm
100	.320	.16	.21	.105
200	.64	.32	.85	.425
300	.96	.48	1.92	.96
400	1.28	.64	3.42	1.71
500	1.6	.8	5.33	2.66

- Data is extrapolated from known losses at 50 Hz, 0.5T.
- Losses assume DC field in the magnet is zero.

2.3.1 Near Term Capabilities of High Critical Temperature Superconductor Magnets and Transmission Lines

For power applications only two classes of the new oxide materials appear to have promise when large quantities of material are required. These families based on rare earth and bismuth perovskites have as their most common members $YBa_2Cu_3O_{7-x}$(YBCO) and $Bi_2Sr_2Ca_1Cu_2O_{8+x}$ or $Bi_2Sr_2Ca_2Cu_3O_{10+x}$(BSCCO). The thallium-based oxides are not considered here largely because of the scarcity of thallium and their near universal use in thin film applications.

The great challenge in using oxide superconductors has been to improve their critical currents in high magnetic fields, electrical contact characteristics, and mechanical characteristics. Without adequate electrical and mechanical properties, bulk-processed, oxide superconductors cannot be used in practical power applications.

Most of these challenges have been met by using microcomposite structures that mix a normal metal like silver with the superconducting oxide. Below is a description of how conventionally processed oxide-superconductor and metal-oxide-superconductor microcomposites are being developed by the oxide superconductor community.

The Present State of Conductor Development - BSCCO

The issues involved in wire, magnet, and cable development and manufacture (e.g., oxide powder production, wire shaping, wire annealing treatments and microstructure development, wire bundling techniques, etc.) are being solved.

BSCCO - Recent Results

The bismuth family of superconductors has shown the most promise to date for high-field power applications like Maglev. Most BSCCO work is oxide- or metal-precursor powder-in-silver-tube with subsequent deformation and heat treating.[1] Since this is a relatively inexpensive

manufacturing technique which may be readily scaled to production quantities, this approach shows promise for high-field, high current density applications at low temperatures (10-40 K).

Silver is one of few metals that do not seriously degrade the electrical properties of copperoxide-based superconductors. Because oxygen diffusion through silver is relatively fast compared with oxygen diffusion through the superconducting oxides, silver may also aid in achieving the proper oxygen stoichiometry in copperoxide-based superconductors.[2,3] Thus, silver is a desirable metal for use in a superconducting oxide/metal composite.

Heine et al, and a variety of Japanese workers have demonstrated exciting results for BSCCO materials at 4 K. Recent results by Carter and Sandhage[4] shown in Figure 2-24, have shown similar results at 20 K. The advent of a superconductor material which can handle currents higher than 10,000 A-cm^{-2} in fields higher than 20 Tesla leads to exciting prospects for the production of very high field magnets. From the viewpoint of Maglev, performance in the 10-40 K range at fields of 5-8 Tesla appears practical with the materials under development. Similar curves have been demonstrated for the other BSCCO compound $Bi_2Sr_2Ca_2Cu_3O_{8-x}$. It is anticipated that an additional order of magnitude in current density at high fields will be available in polycrystalline, bulk conductors within a few years. These current densities will service the Maglev industry.

Polycrystalline BSCCO materials show limited current densities in magnetic field for temperatures above 20-30 K. When adequate pinning mechanisms are found, then high critical current operation at higher temperatures in high field will be possible.

In Figure 2-24 typical data[4] for 2212 material shows the effects of temperature on current density in magnetic field for material where no effort has been made to improve pinning or texture. Since T_c for 2212 is only 85 K, the critical current in magnetic field is characteristically poor at 66 and 77 Silver-sheathed $(Bi,Pb)_2Sr_2Ca_2Cu_3O_x$(Pb BSCCO, 2223) wires have attained Jc (77K, B=0) values[5] of 17,400 A/cm^2 with recent improvements to 57,300 A-cm^{-2}.[6] Subsequent work on $Bi_2Sr_2Ca_1Cu_2O_{8+x}$(BSCCO, 2212) have shown current densities approaching 320,000 A-cm^{-2} at 4.2 K.[7]

BSCCO(2223) materials have sufficient properties for operation in low fields even at 77 K. The low fields associated with most AC applications allow the oxide ceramics to operate with good J_c's at temperatures in the 50-80 K range. The low stored energy and low magneto-mechanical stresses in low-field AC applications have removed several wire fabrication and coil design challenges apparent in high field applications. These challenges include cryostability and burnout protection.

The Case of AC Losses

Any cryocooled current-carrying application must consider the AC losses in the conductor itself and in the surrounding structure which makes up part of the cold mass of the magnet. Usually, it is the eddy current losses in the normal metal components in the cold mass which set the refrigeration requirements of the system. If eddy current losses dominate the engineering of a low-field, AC system, such as a transmission line, then the overall need for large amounts of cooling power indicate operation at the highest temperature consistent with the superconductor selected.

For example, if cryocooled copper is the stabilizer chosen for the transmission line, the AC losses in the superconductor can probably be ignored if

$$\rho 77^{HTc}(AC) < 1/10\rho 77^{Cu}(AC)$$

These low AC losses in the superconductor have been demonstrated, and the results show that high energy-density AC applications are practical at low temperatures. In fact, AC losses are so low as to be insignificant compared to other losses in the system.

The ability to operate at relatively high temperatures in low to moderate AC fields is a unique advantage for HTSC materials. Utilizing this advantage will be achieved by assuring that the HTSC remains stable under internal resistive heating and for the heat to be efficiently removed by a 50-80 K cryocooler.

Since there are losses in all superconductors operating in an alternating current environment, the higher operating temperature makes heat removal and thermal stability in the presence of AC losses easier to control. AC induced eddy current losses in the cryogenically cooled structural components will often dominate the cooling power requirements. Since cooling is less expensive at higher temperatures, AC applications which require relatively low magnetic fields will run at the highest temperature possible. At preset, AC losses in unoptimized materials are approximately an order of magnitude better than high purity copper operating at the same temperature.

Materials properties are good enough now to produce 0.1 T coils with the best of the 2223 materials at 77 K. As materials properties improve, higher field coils willl be produced. However, the rapid improvement in J_c performance at lower temperatures means that higher field coils will always be produced at 20-30 K compared to 77 K. Higher fields also require a burnout protection scheme be developed for 77 K which willl require considerable innovation compared to the techniques presently available at lower temperatures.

Currently, J xL > 10^8 A-cm^{-1-8} is achievable at 77 K in low magnetic fields with AC loss substantially better than copper operating at the same temperature. J xL has increased a few orders of magnitude per year since 1988. If J xL is a useful predictor, then low-field, commercial AC applications should have oxide superconductor wire available for first demonstrations in the 1992-93 time frame. Sumitomo has already reported on components for an AC transmission line.

2.3.2 High Temperature Superconductors (HTSCs) with Potential Operating Temperatures of 20 to 77 K for Use in Magnetically Levitated Vehicles

Applications of Superconductor - Normal Metal Composites

For a majority of power applications, including Maglev, the combination of a superconductor and a normal metal composite will give optimum results, as it does for the existing metallic superconductors operating at liquid helium temperatures.[8]

Many of the reasons for using metal composites with oxide superconductors and with metal-based superconductors are the same, e.g. cryostability, normal zone propagation, ductility, etc. A few, including thermo-mechanical properties at higher operating temperatures, are different. The extensive literature which has evolved for the use of metal-based superconductors is a useful guide for applications involving oxide superconductors.

ELECTRICAL PROPERTIES OF THE SUPERCONDUCTOR

The electrical properties of superconductors are the driving force for applications. The ability of superconductors to carry very high current densities compared to copper enable applications like high-field, air-core magnets. The basic parameters which describe a superconductor are the critical temperature, T_c, the critical current density, J_c, and the critical field, H_c. These are briefly described below, and a more detailed discussion is available in tests like Rose-Innes.[9]

T_c, J_c, and H_c

Superconductors operating below their critical temperature, T_c, are characterized by their lack of DC electrical resistivity, ρ. In the best low-T_c superconductors $\rho < 10^{-18}$ Ω-cm, which is the limit of the measurement capability by persistent current techniques. The ability of a high field magnet to operate in persistent mode with no electrical connections is important in high stability applications where very constant fields are required.

Resistivities measured in highly-oriented, polycrystalline thin films of $Tl_2CaBa_2Cu_2O_x$, and single-crystal samples of $Bi_2Sr_2Ca_1Cu_2O_{8+x}$ for $26 < T < 100$ K have been several orders of magnitude higher than those measured in low-T_c superconductors, and the resistivity has shown strong magnetic-field orientation dependence.[10] Resistivity values will need to improve if oxide superconductors are to be used in persistent mode.

The superconductor will stay superconducting up to when a critical field H_c is applied, or when a critical current is passed through the sample at a given temperature and field. Most of the discussion of superconducting properties focuses on improving the critical current.

The J_c vs. B characteristics of oxide superconductors in bulk form will be a major component in determining their usefulness. Most of the practical, large-scale manufacturing techniques produce poly-crystalline materials. Therefore, critical current properties must be adequate in these wires for the applications of interest. In general this corresponds to $J_c > 10{,}000$ A-cm^{-2} in magnetic fields characteristic of the application.

The critical current performance of the superconductor often drives a given application. The values of the critical current are based on the total cross-section of the active filaments including the normal conductor between the filaments but excluding outer sheaths and insulation. This has been normal practice in the low temperature superconductors industry.

The Importance of Wire Length

While critical current is an important operating parameter for coils, the ability to make long lengths of wire economically with high critical currents is a better measure of performance. Therefore the J_c xL criteria is usually more useful when considering applications where reasonable lengths of wire are required. While melt-textured and single-crystal materials have provided the best J_c performance to date, they are usually not of practical value for coil applications due to limitations on length which can be made.

OPERATIONAL REQUIREMENTS

Wires for Maglev coils made from oxide superconductors will have several requirements which are similar to copper and metal superconductors. These will include compatibility with processing and uniformity of electrical and mechanical properties along the entire useful length of materials.

Compatible with Processing

Compatibility with subsequent processing has been a major issue with all wire forms. In the silver and tin plated wire industry, for example, plating non-uniformities and porosity are exacerbated when the wire must be insulated with very thin high-temperature polymer insulation. This processing is done at elevated temperatures and if often sufficient to cause interdiffusion of plating and the metals, and release of trapped gases due to poor plating.

Similarly, Nb_3Sn must have all of its mechanical processing completed before conversion to superconducting form. When a wind-and-react approach is used, the wire needs an insulation technology compatible with the winding of the material into a magnet and subsequent firing at temperatures beyond the range of polymer insulations. When a react-and-wind approach is used, the mechanical properties of the superconductor must be sufficient to survive the winding process. As a result, Nb_3Sn and related compounds are only used in situations where NbTi cannot be used. The resulting Nb_3Sn magnets are substantially more expensive than NbTi magnets mostly due to process compatibility problems.

Oxide superconductors will be no different in requiring compatibility with subsequent processing. For materials which require a wind-and-react approach, mineral insulations compatible with oxide superconductors are being developed for direct contact with YBCO materials.

To date, polymer insulations do not show promise of long term lifetime when in contact with oxides containing alkali earth material like Sr, Ba, or Ca. Materials which are sheathed in silver are much less problematic in that they can be sheathed in conventional polymer insulations.

Mechanical Properties

Once the basic issues of sufficient critical current are addressed, most of the issues with coils will be related to their mechanical and thermal properties. In high field coils, the magnetic

stresses are close to the limits of high strength steels. In the simple case of solenoids, the stress is proportional to B^2r. Therefore, producing high field magnets with large bores will be an extremely difficult problem. Since the oxide superconductors do not appear to have high mechanical strength, some form of strengthening member needs to be introduced.

This strengthening member needs to have a thermal expansion match close to that of the oxide superconductor, and it must be compatible with the processing of the superconductor if wind-and-react processing is to be used. A rich literature of mechanical support of superconducting windings in epoxy based materials already exists for metal superconductors. It is expected that oxide superconductors will build on this existing expertise.

In order to use oxide superconductors effectively they must have mechanical properties which allow their fabrication and their use with thermal cycling when they are superconducting. A useful empirical method for measuring the fracture toughness of a superconducting oxide/metal composite is to measure the critical current of the superconducting oxide as a function of strain and/or applied stress.

A plot of the critical current performance of the common superconductors as a function of strain is shown in Figure 2-25. Note that the BSCCO materials already has mechanical properties better than Nb_3Sn. These BSCCO materials are mechanically robust and allow the production of react and wind coils on conventional equipment.

AC Properties

Since most of the oxide wires used in coil applications will be metal-superconducting oxides composites of one form or another, they will have loss properties in AC fields similar to metal superconductors. There is a rich literature on the AC properties and behavior of metal superconductors in the presence of magnetic fields.

When normal metal is used in small quantities for improved mechanical properties, then interconnectivity of the normal metal is avoided and eddy current losses at higher frequencies

can be reduced. Unoptimized wires have demonstrated over an order of magnitude improvement in 50-100 Hz AC losses at 77 K compared to silver operating at 77 K. Further progress is expected as AC loss issues are further addressed.

In a Maglev magnet, there is some small component of AC loss due to the imperfections of the electrical characteristics of the guideway. For 4 K systems this will require a substantial flux shield. In a HTSC system, refrigeration requirements due to AC loss can be traded against the weight of the flux shield.

Residual Resistance

There is usually some residual resistivity in superconductors. This is especially the case under AC conditions. Simple pinning models show that in a field reversal, the flux must be depinned to change direction under the influence of the alternating field. This depinning is a nonconservative event and leads to thermal losses.

The residual resistance under low field conditions is typically very low at DC and is often connected with the loses in the normal metal under AC conditions.

Cryostability

Cryostability implies the ability of a conductor to return to the superconducting state after a small to moderate perturbation. The larger the amount of normal material in intimate thermal contact with the superconductor, the better its cryostability. The addition of silver to oxide superconductors improves cryostability, especially when the material is processed by the metal precursor route. Note however, that the larger amounts of normal metal included usually reduces the available critical current in a given cross-section.

Normal Zone Propagation

As was discussed in the section above, the motion of flux in a superconductor causes energy dissipation. Motion of the conductor itself can cause similar dissipation. If the energy dissipated due to any cause cannot be removed from the superconductor rapidly enough, then the superconductor in the area where the dissipation occurs will convert to a normal zone.

If the current cannot be shunted around the normal zone, and there is a substantial amount of energy stored in the superconducting device, then the normal zone will heat until the material melts. Therefore, it is important to provide a current shunt around the superconductor to handle the current, and to provide a method for the removal of heat. This is especially the case when superconductors are in devices with large amounts of stored energy, like high field magnets.

The normal zone propagation velocity is related to the heat capacity, the thermal conductivity, and the configuration of the wire in a given device. Note that thermal conductivity and heat capacity are strongly temperature dependent below 80 K. In oxide superconductors the thermal conductivity is low and the heat capacity is comparable to the normal metal included for cryostability. Therefore, normal zone propagation is determined by the normal metal characteristics.

The operating temperature of superconducting devices with large stored energy may not be determined by the properties of the superconductor, but by the ability of the normal conductor to propagate the normal zone with sufficient velocity.

OPERATIONAL REQUIREMENTS AND CHARACTERISTICS OF HIGH TEMPERATURE SUPERCONDUCTIVITY

Current densities above 10,000 A/cm^2 have now been achieved in significant magnetic fields ($<$1T) at 77 K, the boiling point of liquid nitrogen. While the more recent results for current densities at 77 K are very encouraging, indeed, it is clear that the results currently available at lower temperatures (20 to 30 K) warrant *immediate, accelerated work on the*

demonstration of magnet technologies for application at the lower temperatures. Cooling in the latter case would be achieved by closed-cycle refrigerators. As the critical current densities at higher temperatures increase over time, the wire, cooling and magnet technologies developed now for 20-30 K operation would be directly applicable to higher temperature operations.

The operation of HTSC magnets at 20 to 30 K is also important be cause it:

1. optimizes superconducting properties per cooling cost,

2. does not require major innovation in normal zone propagation and magnet protection, and

3. highly reliable refrigeration technology exists and is relatively inexpensive compared to 4 K liquefiers.

4. Uses off-the-shelf components.

It is not appropriate to wait until higher current densities are achieved at higher temperatures in research samples to develop wire scale up, and to start development of cooling and magnet technologies. By that time, our foreign competition will have advanced so far in the down-stream technology development that American industry may never catch up.

In addition to the excellent current-carrying abilities of HTSC wires, American Superconductor Corporation has been able to demonstrate that HTSC wires can be made flexible. Long lengths of wire (50m) have been produced with strain tolerances of 0.5%, which is sufficient to allow for robust manufacturing processes for the wire, and to allow the wire to be formed into usable coils. While much remains to be accomplished to demonstrate all of the properties required for commercial superconducting coil applications, it is clear that the mechanical properties of HTSC wires will not be an insurmountable barrier to the development and commercialization of HTSC wire technology.

At this point, no additional scientific breakthroughs are required in order to commercialize HTSC technology. What is required is a very strong effort to overcome the significant engineering hurdles involved in tailoring HTSC properties for use in a final device. These hurdles include:

1. achieving long lengths of wire with the same properties as the research wire samples,

2. proving process capability in important specifications over long lengths,

3. proving useful magnets can be made with the HTSC wires

4. integrating cryocoolers with the HTSC magnets to take advantage of the promise of HTSC technology, and

5. demonstrating useful subsystems with all design considerations met.

Enough science exists now to allow commercialization of HTSC technology. The field is entering the development stage, and foreign competition is devoting very significant efforts to developing both HTSC wire technology and applications for this technology. Owing to the cost of capital in the United States, American industry has not been able to justify making significant investments in HTSC technology because the technology is not likely to enjoy widespread commercialization for at least five years from the present time. This barrier has not been an impediment in Japan, where industrial and government efforts in HTSC wire technology are moving forward at breakneck speed.

Energy-Storage Time Figure of Merit

Coils are normally used as energy converters, i.e., they convert electric current into stored magnetic energy residing in a volume V(m^3). Since Maglev requires a high energy density in the suspension and propulsion magnets, some form of actively cooled magnet is

required. These magnets could be actively cooled copper, LTSC, or HTSC. A useful energy-storage figure of merit[11] for coil based systems is the storage time, t:

$$t(\text{sec}) = \frac{\text{Stored Magnetic Energy (J)}}{\text{Power to Store Energy (W)}} \tag{1}$$

$$t(\text{sec}) \propto \frac{[B(\text{Tesla})]^2 V(\text{m}^3)}{\text{Cooling Power (Watts)} + \text{other losses}} \tag{2}$$

This time can be considered as the decay time for the stored energy in a short-circuited inductor with a finite resistance, or the time for a similarly configured resistanceless coil to lose its stored energy, if some of the stored energy is used to provide the cooling power.

Cryocooled Copper

For a resistive coil operating at current density J, with electrical resistivity $\rho(\Omega\text{-m})$ and winding volume $V_{coil}(m^3)$, resistive losses, which represent the cooling power required, can be expressed as

$$I^2R = J^2 \rho V_{coil} \tag{3}$$

Substituting eq. 3 into eq. 2 with $V \approx V_{coil}$, and using the fact that

$$B \propto JV \tag{4}$$

gives

$$t(\text{sec}) \propto \frac{V^2}{\rho} \tag{5}$$

Note that eq. 5 is independent of J and only depends on size and resistivity. If all of the I^2R losses are totally absorbed by a closed-loop cooling system, then only the cooling system power needs to be considered.

Actively cooling and operating a copper coil in liquid nitrogen or liquid hydrogen is practical only if the resistivity is low enough to support the use of coolant. For example,

$$\rho 273^{Cu} = 1.545 \times 10^{-8} (\Omega\text{-m}) \tag{6}$$

$$\rho 77^{Cu} \approx 1/5\ \rho 273^{Cu} \tag{7}$$

$$\rho 21^{Cu} \approx 1/120\ \rho 273^{Cu} \tag{8}$$

To be efficient, the cost of cooling the copper must be less than the reduction in I^2R losses. At temperatures below 77 K the resistivity depends on the purity of the material. The number given in eq. 8 assumes that the copper is moderately pure and fully annealed.

Cryocooled Aluminum

For high energy-density applications in high magnetic fields, hyperpure aluminum operating at 20 K has been used since the late 1950's[12,13] for large magnets. Aluminum is used instead of copper because of its lower magneto-resistance in high magnetic fields, which reduces the power dissipation for a given field generated. Purcell's magnet[13] with 99.9983% aluminum has

$$\rho 21^{Al} = 2 \times 10^{-11} (\Omega\text{-m}) \tag{9}$$

Even lower values of resistivity have been obtained.

Water-Cooled Copper

To water-cool copper, the minimum water flow is governed by the equation:

$$Q(kW) = m(kg\text{-}sec^{-1}) c_p(kJ\text{-}kg^{-1}\text{-}K^{-1}) \Delta T(K) \tag{10}$$

where $c_p^{water} \approx 1(kJ\text{-}Kg^{-1}\text{-}K^{-1})$. To remove 10 kW with a 30 K temperature rise requires 0.3 kg/sec or $\approx$ 181/min when friction losses are included. For a small coil, head loss will probably be 40-60 psig which consumes $\approx$ 750 W of electricity.

Refrigeration Trade Offs

Good single-stage refrigerators have total efficiencies of $\approx$ 8% at 77 K and $\approx$ 5% at 50 K; two-stage refrigerators have total efficiencies of $\approx$2% at 20 K for 300 K sink temperatures; and two-stage refrigerators operating at 20 K with a series of Joule-Thompson valves to reduce operating temperature to 4.5 K for reliquefying helium will have total efficiencies of $\approx$0.4% at 4.5 K for 300 K sink temperatures. Therefore, cryocooled copper at 77 K has approximately half the energy efficiency of air- or water-cooled copper at room temperature, and LTSCs will suffer an energy penalty in efficiency and/or refrigeration sizing of $\approx$5x compared to HTSCs operating at 20 K.

Optimizing Operating Temperature for HTSC Coils Based on Application

Optimizing the performance of the superconducting magnet and refrigeration system for HTSCs can be done at several temperatures unlike the case of LTSC magnets that must operate near 4.2 K. Figure 2-26 illustrates such an optimization as analyzed by Joshi. The refrigeration load includes heat leaks from the leads and residual conduction losses for a vacuum-jacketed coil. Note that the optimum system performance occurs in the 20-30 K range.

Normal Zone Propagation and Magnet Protection as a Function of Temperature

Two of the most important magnet design issues are: 1) stability, both mechanical and electrical; and 2) protection from a quench, i.e. the uncontrolled release of magnetic stored energy due to a portion of a superconducting magnet becoming normal.

Even moderate sized (diameter $\approx$ 0.3 m, length $\approx$ 0.5 m, B $\approx$ Tesla) superconducting magnets store $\approx$1/4 MJ of energy. An uncontrolled release of this much energy is roughly

equivalent to a stick of dynamite. Therefore, it is imperative to channel and distribute this energy release carefully. Brown and Iwasa[14] note that:

> . . .once a high performance magnet is driven normal over a winding volume greater than the minimum propagation zone (MPZ), it quenches. Protection is concerned with magnet longevity. Its chief objective is to ensure that a magnet suffers no permanent damage upon quenching. . . .Specifically, the peak temperature reached over the normal zone initially created must not exceed a level at which the conductor might suffer permanent damage nor must the temperature distribution be so steep as to cause large thermal strains within the winding pack, which might damage the structural integrity of the magnet. The post-quench temperature distribution, including the peak temperature is determined by the normal-zone evolution in the winding pack and the process is controlled principally by the so-called normal-zone propagation velocities. . .

Iwasa[15] has shown that for thermally isolated HTSC magnets the propagation velocity is too slow at temperatures above 20-30 K to distribute energy throughout the structure and prevent localized magnet burnout. This is largely due to the high specific heat of the superconductor and of the normal metal stabilizer at higher temperatures when compared to 4 K. Therefore, adiabatic magnets either 1) must be operated below 30 K for adequate protection, 2) must have active detection and protection schemes, or 3) require designs which allow forced cooling of the magnet.

Systems Issues for High Field Coils

If sufficient critical current in high field can be obtained in a superconductor, then issues of building high field coils are nearly totally thermal and mechanical in nature. The fields and the resulting forces in a high field high-T_c superconductor magnet are the same as in low-T_c superconductor material.

In the Maglev application, all of the suspension and propulsion forces must be transmitted through the cryogenic envelope with the attendant heat leak due to more substantial mechanical structure requirements. This imposes a larger refrigeration penalty for LTSC than HTSC.

Stability

If any microscopic motion of the conductors occurs at high fields, then a significant amount of energy is released. A motion of a single metal superconductor wire by 0.0001" can be sufficient to produce enough heat locally to drive the magnet normal at 4 K. Since the heat capacity rises quickly above 4 K, it is much easier to keep these small perturbations from driving the magnet unstable at elevated temperatures. Magnet stability at 4 K is more difficult than at higher temperatures, but magnet protection is more difficult at elevated temperature than at 4 K.

Protection

If a perturbation in the wire drives the magnet unstable and allows the formation of a normal zone, then the normal zone must either propagate quickly through the magnet (quench) or shrink fast enough so that the stored energy in the magnet cannot burnout the normal zone. Studies by Iwasa[16] indicated that the thermal properties of the coil winding tend to dominate normal zone propagation. Based on these findings, the optimum operating temperature for an adiabatic, oxide superconductor magnet appears to be 20-40 K.

Driven vs. Persistent Mode

Superconducting magnets which do not require frequent changes in field are often short-circuited with a superconducting connection after charging and run in persistent mode. For magnetic resonance imaging magnets at liquid helium temperature this is often done with retractable current leads so that thermal loss can be reduced. Magnets which must change field frequently keep the leads firmly connected to the magnet and sustain a higher liquid helium loss. Lead loss is usually a major source of helium boil-off in DC applications of low-T_c superconductor magnets. Lead loss is a particularly serious problem in large energy storage magnets.

Two properties of the superconductor determine if the material can be run in persistent mode. These are the index and the residual resistance. The index represents the coefficient in the equation

$$V = V_c[I/I_c]^n$$

where V is the voltage and I the current flowing through the coil. This model adequately describes the I-V characteristic of most superconductors in the transition from superconductor to normal conductor. The measurement is performed at operating magnetic field. The subscripted variables are measured at the critical current with the given criteria. The residual resistance, R = V/I, and the inductance of the coil determines the time constant for a magnet in persistent mode. If the index of the wire is low, then only a relatively small fraction of the current density can be used to keep an acceptable value of residual resistance. Values of n = 30 are desirable for magnets operating in persistent mode since nearly all of the critical current can be used before the resistance begins to rise.

The residual resistance is directly related to the index in the transition region since

$$R = V/I = [V_c/I]\ [I/I_c]^n$$

Present oxide superconductor materials have residual resistances which are too high to allow most magnets to be run in persistent mode for acceptable times. This problem will be solved as flux pinning methods are improved for oxide superconductors.

$$\mathbf{J_cV \approx BR^2}$$

The time frame for the construction of large solenoidal magnets will be related to the volume of superconductor which can be produced with a specific critical current. For a specific wire size $J_cV \approx Br^2$ is closely related to J x L. It also points out that the production of high magnetic fields over large areas requires very large quantities of material with good properties.

2.3.3 Refrigeration Requirements for Low and High Temperature Superconductor Devices Used in Magnetically Levitated Vehicles

Cooling Requirements

The discovery in 1986 of a whole new class of materials that superconduct at higher temperatures was truly a scientific breakthrough. The new materials, which are ceramics, exhibit their superconducting properties at temperatures which can be attained by efficient refrigerators, known as cryocoolers. The possibility of building superconducting, electromagnetic systems that could operate without the need for liquid helium changed the entire outlook regarding the widespread application of superconductivity, especially for smaller systems.

Metallic superconductor wire technology has been developed over the last 30 years, and has become a rather mature technology. Typically liquid helium is used for metallic (or low-temperature) superconductor (LTSC) applications. Cryocoolers used to provide liquid helium refrigeration between 4.2 and about 10 K in a closed cycle for LTSC wires have been limited to larger systems because of the high cost of providing a small, closed-cycle helium liquefier.

High temperature superconductors will operate in applications at temperatures from 4-77 K. The refrigeration issues for 4 K will be defined based on liquid helium and the possible addition of refluxers to reduce the boil off of liquid helium. However, cooling requirements for superconductor components in the 10-77 K range need to be addressed. The challenge of using this temperature range will be to find an adequate cooling method without the use of liquid cryogens.

Several refrigerator types cover this temperature range adequately. These range from Gifford McMahon machines (10-20 K), to pulse tubes, to Stirling cycle machines (40-80 K). Besides refrigeration capability, the ability to place the cooling at the proper points in a device and the ability to handle varying loads will be examined.

Smaller systems, like Magnetic Resonance Imaging (MRI) magnets, are successfully using liquid helium. However, open-cycle, cryogenic systems using condensable liquids typically have not had a large measure of success in the industrial world. For small, industrial systems, like Maglev, closed-cycle refrigeration, transparent to the end user, requiring conventional input power, and a minimum of special heat rejection equipment will be the most successful.

Cryocoolers

For machines with less than a few hundred watts of cooling in the 15-77 K temperature range, there are only two classes of cryocoolers with wide commercial availability. They are Stirling Cycle machines, which are the most efficient, and the Gifford McMahon (GM) Cycle machines, which are most widely used. Very large machines are often built with customized hybrid cycles for best efficiency.

Most cryopump manufacturers use oil-lubricated freon compressors which are manufactured in very large quantity for the refrigeration industry. Helium operation of these compressors forces them to run hotter. Hermetically sealed compressors have mean times between failure (MBTF) in helium service with proper deratings of > 100,000 hours. Larger semi-hermetic compressors can be rebuilt periodically. Compressor selection is part of the GM cryocooler manufacturers' art.

Stirling Cycle machines have higher thermal efficiency than GM machines. However, the only long commercial experience with small Stirling cryocoolers is with fractional-watt, common module refrigerators developed for military applications. These machines have MTBFs of only 4000 hours. With exceptional precautions, small Stirling machines should be capable of million hour MTBFs.

Interfaces Between Cryocoolers and Devices

There is a body of literature describing the cooling of LTSC magnets in liquid helium or supercritical helium. For small adiabatic magnets where field precision and stability are important, liquid cryogens are preferred. For large systems where mechanical support members need to be included, cable-in-conduit systems with supercritical helium are often the preferred approach.

Simple conduction cooling systems with mechanical GM refrigerators have recently been attempted with Nb_3Sn superconductors operating to keep the coil at 12 K.[17] While conduction cooling was shown to be effective, the refrigerators are operating very close to their minimum temperature ($\approx$ 9 K). Temperature stability and power output[18] also need improvement in this temperature range.

The conduction cooling approach will be much more practical using HTSC coils with a refrigerator operating at $>$ 15 K. It is likely to be practical only for DC magnets which do not generate a large amount of heat that must be removed in a short period of time; small AC or pulsed magnets may also be cooled using the conduction-cooling approach. Thermal time constants is limited by the thermal resistance between the cryocooler and the coil and by the heat capacity of the coil. Cool down times will be relatively long, and temperature stability under thermal transients will be poor compared to systems with the coil immersed in a liquid cryogen. However, the continuous operation of a Maglev vehicle, and the relatively small quantity of superimposed AC current due to guide-way inhomogeneities, make this an attractive option.

Thermal transients in the 20 K range will be minimized by the relatively high thermal conductivity in this temperature range and by the 10-fold increase in specific heat of the coil at 20 K compared to 10 K.[19] Additional heat transfer mechanisms will need to be implemented for improved stability in the presence of thermal transients due to fault situations and for AC applications.

Economic Drivers

Several systems, like MRI magnets, small Superconducting Magnetic Energy Storage (SMES) magnets, and High Gradient Magnetic Separation (HGMS), are existing products built with superconductors. The economics a Maglev system should be similar to these systems with either LTSC or HTSC. The move to actively cooled, closed cycle systems has been driven by superior performance or the value added from the use of superconductors compared to systems which use conventional conductor technology and room temperature cooling systems. Both of these reasons apply to Maglev.

Improved performance and reduced life cycle cost of superconducting vs. normal conducting systems has lead to the development of the MRI magnet market of several hundred units per year, an embryonic HGMS market, and an emerging small SMES market. For these markets to be industrially viable, the installed or fixed cost of the cryogenics and superconductor must be reduced, while the operating or variable cost and the system's reliability must be deemed acceptable by the user community. An example of these economic drivers will be given in the purchase cost section below for small SMES applications.

Life Cycle Cost

Life cycle cost is often defined as a combination of the fixed and variable costs of a system over its useful lifetime with some form of discounting of operating costs and depreciation of the fixed cost.

Fixed Costs

The typical cost of the cryogenics in small-to-moderate sized applications has been 5-10% of the system's price, $16,000 for 50 W at 50 K being typical, but 20-30% savings can be obtained in quantity purchases. Magnets with dewar have cost about 25% of the system price

in those applications where the magnet is a key component in many operations where no substitute can be found, e.g., MRI systems.

Green and Byrns give estimate[20] of the cost of refrigeration with closed cycle liquid helium refrigerators. Since the magnets in a Maglev system are relatively small, one would expect that the cost of a closed cycle refrigerator would be high compared to an open dewar arrangement in a LTSC system.

HTSC magnets, on the other hand, can use inexpensive, two-stage, Gifford-McMahon cycle refrigerators for 20 K operation, or Stirling cycle refrigerators for 77 K operation and meet the above cost targets, even for magnets as small as those used in Maglev systems.

Operating Costs

A closed cycle refrigeration system needs to be cost competitive in operation both with a conventionally cooled room temperature system as well as with cryogen-cooled systems. For large systems, liquid nitrogen costs $\approx$ 6¢/liter, liquid helium costs $\approx$ \$4/liter, and industrial electricity costs $\approx$ 6¢/kWh. The electric cost on board a Maglev vehicle may be several times higher than this number. Therefore, some estimate of on board electric cost needs to be generated.

System Reliability

Closed cycle systems have the potential for being more reliable than open cycle systems that depend on evaporation for cooling. Open systems are prone to icing, as well as valving and sensor problems. Closed cycle systems are subject to mechanical failures and electrical outages.

Single-stage, Gifford-McMahon refrigerators offer approximately half the efficiency of a comparable Stirling Cycle refrigerator. However, GMs have a much larger installed base, and are probably lighter than an equivalent Stirling machine. The two-stage GM machine is the most

common, small refrigerator used in the 20 K range. These have demonstrated reliable performance with > 70,000 hours MTBF.

CONCLUSIONS

The integration of HTSC coils and GM cryocoolers will be a practical solution for high field operation of DC magnets in the 20-30 K range. AC applications will be handled by Stirling or GM machines in the 50-80 K range. AC applications will be handled by Stirling or GM machines in the 50-80 K range. Novel integration schemes are possible which will enhance the value of the overall system. LTSC magnets will either run with liquid helium only, avoiding the weight penalty of the cryocooler, or with a high efficiency, light weight cooler yet to be developed.

SUMMARY

Operational requirements and characteristics of high temperature superconductors (HTSC) indicate that low field and AC applications will require refrigeration in the 50-77 K region and high field DC applications will require refrigeration in the 20-30 K range. Very high field magnets will require 4 K refrigeration.

A figure of merit, t, is developed which relates the stored energy in coils to the power required to cool them. HTSC materials give the highest figure of merit when compared to cooled normal metal and low temperature superconductors. Optimizing t shows that the best operating temperatures are in the 20-30 K range. This temperature range is also the best operating range to implement conventional magnet protection schemes for adiabatic magnets.

Low cost refrigeration will be essential for small systems using HTSC or LTSC to be economical. The typical first cost of cryogenics in small to moderate sized systems is usually 5-10% of systems price. A closed cycle refrigeration system also needs to be cost competitive in operation both with a conventionally cooled room temperature system, and liquid cryogen cooled systems.

REFERENCES

1. Kenneth H. Sandhage, Gilbert N. Riley, Jr., and William Carter, "Critical Issues in the OPIT Processing of High-J BSCCO Superconductors", J. of Metals, Vol. 43, No. 3, pg. 21, 1991.

2. T. A. Ramanarayanan, and R. A. Rapp, "The Diffusivity and Solubility of Oxygen in Liquid Tin and Solid Silver and the Diffusivity of Oxygen in Solid Nickel," Met. Trans., Vol. 3, No. 12, pg. 3239, 1972.

3. S. J. Rothman, J. L. Routbort, L. J. Nowicki, K. C. Goretta, L. J. Thompson, J. N. Mundy, and J. E. Baker, "Oxygen Diffusion in High-Tc Superconductors," Preprint from Argonne National Laboratory, 1989.

4. W. L. Carter and K. H. Sandhage, "Transport Properties of 300 Ampere Silver Sheathed $Bi_2Sr_2Ca_1Cu_2O_{8+x}$ Conductors", paper H10.2, Material Research Society Fall Meeting, Boston, Massachusetts, November 26 - December 1, 1990.

5. T. Hikata, T. Nishikawa, H. Mukai, K. Sato, H. Hitotsuyanagi, "Electromagnetic Properties and Morphology of Ag-Sheathed Bi-Pb-Sr-Ca-Cu-O Superconducting Wires," Jap. J. Appl. Phys., Vol. 28, No. 7, pp. L1204-6, 1989.

6. Ken-ichi Sato, Nobuhiro Shibuta, Hidehito Mukai, Takeshi Hikata, Munetsuga Ucyama and Takeshi Kato "Development of Silver-Sheathed Bismuth Superconducting Wires and Their Applications" presented at the MMM conference Pittsburgh, Pennsylvania, June, 1991.

7. Naoki Uno, Noritsuga Enomoto, Hiroyuki Kikuchi, Kaname Matsumoto, Masanao Mimura and Minoru Nakajima, "The Transport Critical Current Property of High Tc Superconducting Wires", presented at International Symposium on Superconductivity '89 at Tsukuba, Japan, November 14-17, 1989.

8. Martin N. Wilson, Superconducting Magnets, Oxford University Press, Oxford England 1983.

9. A. C. Rose-Innes and E. H. Rhoderick, Introduction to Superconductivity, 2nd ed., Pergamon Press, Oxford England, 1978.

10. D. H. Kim, K. E. Gray, R. T. Kampwirth, and D. M. McKay, "Possible Origins of Resistive Tails and Critical Currents in High Temperature Superconductors in a Magnetic Field", submitted to Phys. Rev B.

11. C. H. Joshi, unpublished.

12. H. L. Laquer and E. F. Hammel, Rev. Sci. Inst. 28, 875 (1957).

REFERENCES
(Continued)

13. J. R. Purcell, "An Aluminum Magnet Cooled with Liquid Hydrogen, High Magnetic Fields", Proceedings of the International Conference on High Magnetic Fields held at the Massachusetts Institute of Technology, Cambridge, Massachusetts, November 1-4, 1961. H. Kolm, B. Lax, F. Bitter, and R. Mills ed. MIT Press and J. Wiley and Sons 1962.

14. J. N. Brown IV and Y. Iwasa, "Temperature dependent stability and protection parameters in an adiabatic superconducting magnet", Cryogenics 31, 341 (1991).

15. Y. Iwasa, "Design and Operational Issues for 77 K Superconducting Magnets", IEEE Trans. Magn. MAG-24 (1988).

16. Y. Iawsa, "Engineering Design and Operational Issues for 77 K Superconducting Magnets: A Magnet Designer's View", presented at DARPA Workshop on Applications of High Temperature Superconductors, Houston, Texas, 1 March, 1990.

17. M. T. G. Van Der Laan, R. B. Tax, H. H. J. Ten Kate, L. J. M. Van De Kluderert, "A 12 K Superconducting Magnet System, Cooled via Thermal Conduction by Means of Cryocoolers". ICMC91 paper BE 16 (to be published).

18. R. A. Ackerman, "Cryorefrigerator Evaluation for Future Magnetic Resonant Imaging Applications". Proceeding of the Sixth International Cryocoolers conference, Plymouth, Massachusetts, October 25-26, 1990, Geoffrey Green and Margaret Knox eds., Volume 1, pg. 3.

19. C. A. Thompson, W. M. Manganaro, F. R. Fickett, "Cryogenic Properties of Copper", National Institute of Standards and Technology, Boulder, Colorado.

20. M. A. Gren and R. Byrns, "Estimating the Cost of Superconducting Magnets and the Refrigerators Need to Keep Them Cold", to be published in Advances in Cryogenic Engineering, Vol. 37, February 1992.

2.4 Refrigeration and Heat Loads

Cryostat

Three cryostat systems were considered in the conceptual design. For all systems, it was assumed that there would be a liquid nitrogen reservoir near or about the magnets. Liquid nitrogen could be eliminated by additional on-board refrigeration.

The first system, System 1, uses three separate shields (80 K, 20 K, and 4 K) to maintain a liquid helium environment for the superconducting magnet. For this configuration, shown in Figure 2-17, a refrigerator is required to maintain the 20 K shield. System 1 assumes that everything reasonable is done to lower the liquid helium boil-off and 4 K refrigeration requirement. It assumes that the required space is found for the gas cooled 20 K and 80 K radiation shields and that the primary load-bearing supports are gas cooled at 20 K and 80 K heat intercepts and that adequate room is found for these critical support members.

A second configuration, System 2, shown in Figure 2-18, also contains three shields, but no refrigerator is required. It is assumed that liquid nitrogen and liquid helium would be provided externally from a ground-based reservoir or that a liquifier would be carried on board. System 2 also assumes that all of the above care goes into the design of the cryostats. System 2 differs from System 1 in that the 40 K low temperature radiation shield and the 40 K thermal intercept on the supports are cooled strictly from the liquid helium boil-off gas (pool boiling).

The third system, System 3, shown in Figure 2-19, contains only one thermal shield, an 80 K shield. System 3 makes an obvious simplification and saves space by eliminating the 20 K and 40 K radiation shields and thermal intercepts on the supports below 80 K. This simplification increases the size of the 4 K refrigerator significantly.

Heat Loads

Typical heat load calculations have been tabulated for the three cryostat systems using the analysis in Figures 2-9 and 2-10. The major assumptions for the heat load calculations are listed below.

1. The on-board magnets are operated in persistent mode with the high current leads retracted.

2. The magnets at 4 K are shielded from heat-producing eddy currents using conductive shields at 300 K or 80 K or both.

3. The weight of a car that needs to be supported by the magnets at 4 K is assumed to be 445,000 kg.

4. The total service space available for the magnets per car is assumed to be a box which is roughly:

   - 30 m ¥ 3.4 m ¥ 0.8 m.
   - This box has volume of approximately 80,000 liters.
   - The total area of the sides of this box is approximately 250 m^2
   - It is assumed that 40% of this area (100 m^2) will radiate to the heat shields of the cryostats.
   - The heat load of the cryogenic piping is neglected. Bear in mind that the heat load of the piping for a continuous 4 K supply can be larger than the heat load of all the cryostats.

5. The heat load calculations are based on data for MRI magnets and the SSC accelerator.

6. We view these results as the "Best" one can do with each of these cryogenic systems.

- Practical considerations or adverse design choices will increase these cryogenic requirements.
- Lateral loads have been ignored, so that the total of loads to be supported from 4 K will be greater than 445,000 kg.
- Likewise when all the radiation area is taken into account, it is expected to exceed 100 m^2.
- For convenience of scaling, the heat loads are based on 445,000 kg per car and 100 m^2 of radiation per car.

7. To create some feeling for what these loads mean, we have assumed some reasonable fraction of the service volume being occupied with cryogens.

- Some storage is desirable to back up the refrigerators and provide for power failure.
- We would expect that we would want to recover and recycle all of the helium.
- The use of LN_2 looks promising in order to significantly reduce the size and power requirements of an on-board refrigerator.
- The use of open cycle liquid helium should be considered only if every possible method can be used to minimize boil-off. We view this possibility as very unlikely.

A summary of heat loads is shown in Table 2-6. The computed heat loads for the 77 K shield and 20 K shields compare well with data from MRI systems and SSC cryostats, as shown in Table 2-7.

Using the heat loads, an estimate of the storage time or pot life was made. The pot life of the helium ranges from 9-90 days depending on the shield configuration. Liquid nitrogen storage is estimated to last about 38 days independent of the shield configuration.

Refrigerator for Liquid Helium

It is difficult to size the liquid helium refrigerator without having a detailed design for the cryostats and interconnecting helium supply line. However, using the heat loads in Table 2-6 we can make some estimates of the helium refrigerator capacities required. In all these estimates we have assumed that the eddy current losses in the cryostat are negligible and that the magnets are operated in the persistent mode with power leads retracted.

A summary of the liquid helium refrigerator requirements is shown in Table 2-8. The most likely or possible refrigeration power requirement is 16 kW for the refrigerator plus 25 kW for compressor cooling. This power can be used as the basis of power for cooling requirements. Note that an important parameter in the table is the power required to cool the compressors, which can be substantial for a mobile vehicle. For land-based compressors, the cooling is usually obtained from chillers or water circulation. Some of the cooling required for the compressor may be obtained from air flow as the vehicle moves down the guideway.

An analysis of cryogen consumption per vehicle, and efficiency and refrigerator weight is shown in Tables 2-7, 2-8, 2-9, and 2-10. Some important observations can be made from this data and the overall system requirements, even without a detailed design:

- From the data it is apparent that it is most efficient to use one refrigerator per car rather than a multiple of smaller ones. The smaller units must pay a penalty in cost, weight, volume, input power, and cycle efficiency.
- The smallest or most optimistic size considered was 2 watts at 4 K. The size and power requirements are modest. This small size is unrealistic when the necessary continuous feed liquid supply line is taken into consideration.

- On the other end of the sizes considered, the 200 watt machine is not realistic either. It would require a significant fraction of the train's space and power.
- In the middle of these two extremes is a 20 watt, 4 K machine that looks feasible. It would be 5% of the weight and need 8% of the service volume. It would require 16 kW of power to be transferred to the levitated train.
- At this point one might be tempted to put a design limit of 10 watts at 4 K on both the cryostats and the liquid helium supply line.
- This 4 K supply line that needs to run the full length on each car might require as much design work as the cryostats. At a minimum, it will also require an 80 K cooled radiation shield. Just figuring out how to plumb it in will require considerable effort. Hopefully we will be able to piggy-back on previous design efforts.
- It is obvious that realistic limits need to be established for the size of the 4 K refrigerator *before* one proceeds with a detailed design of the cryostat or the superconducting coil it houses.
- It may not make sense to design a super efficient cryostat if the losses are overwhelmed by the unavoidable transfer system.
- Anything short of a "systems" approach is not likely to be effective. Care should be taken to ensure that one part of the design does not get too far ahead of the other.
- For this simple analysis we have assumed that LN_2 would be stored on board. This would reduce power requirements and help in the case of a power outage. When the system is better defined, it may well be that this is not necessary.

Figures 2-20 through 2-23 show efficiency and weight data for the proper refrigerator choice.

Table 2-6

Maglev Superconducting Magnet Cryogenic Performance

	System 1	System 2	System 3
For 50 tons $Q_{conduction}$			
Q_{4K}	1.0	3.0	8.0
Q_{shield}	7.0	5.5	–
Q_{80K}	100	100	100
For 100 m^2 $Q_{radiation}$			
Q_{4K}	0.3	0.6	5.0
Q_{shield}	4.5	4.0	–
Q_{80K}	100	100	100
Q_{total} (watts)			
Q_{4K}	1.3	3.6	13.0
Q_{shield}	11.5	9.5	–
Q_{80K}	200	200	200
Q_{total} (liter/hr)			
LHe	1.8	5.0	18.0
Shield	need 20K refr.	–	–
LN_2	4.4	4.4	4.4
Pot Life – 4,000 liters each			
LHe (days)	93	33	9
LN_2 (days)	38	38	38

Table 2-7

Magnet Cryogenic Heat Load Estimates

Conventional heat loads with 77 K shield and vapor-cooled shield at 20 K (comparison)

	SSC Dipoles	IGC MRI Systems
Radiation (300K to 77K)	0.75 W/m²	< 1.0 W/m²
Radiation (20K to 4K)	0.004 W/m²	< 0.002 W/m²
Cold Mass Support Conduction (300K to 77K) (Watts per 445 kg of supported mass)	1.12 W/1,000 kg	1.12 – 2.24 W/1,000 kg
Cold Mass Support Conduction (20K to 4K) (Watts per 445 kg of supported mass)	0.018 W/1,000 kg	0.011 – 0.022 W/1,000 kg

Table 2-8

4 K Refrigerator Requirements for Maglev Vehicle

(Assumes one refrigerator per car and that LN_2 is on-board)

	Min.	Most Likely	Max.
Capacity of 4 K refrigerator	2 watts	20 watts	200 watts
Power Required	4 kW	16 kW	80 kW
Weight of refrigerator	445 kg	2,225 kg	9,000 kg
Fraction of car weight	(445,000 kg)	1%	5%20%
Volume of refrigerator	1.5 m^3	6 m^3	20 m^3
Fraction of service volume	(80 m^3)	0.8%	8%25%
Specific work	300 kW/4 kW	2,000 to 1	800 to 1400 to 1
Carnot efficiency	4%	10%	20%
LN_2 required for refrigerator	0	5 L/hr	25 L/hr
LN_2 required for cryostats	5 L/hr	5 L/hr	5 L/hr
Total LN_2 required	5 L/hr	10 L/hr	30 L/hr
Power required for	compressor cooling	6 kW	25 kW 125 kW

Table 2-9

Cryogen Consumption per Maglev Vehicle

Assume each car weighs ~ 50 tons

	20 K – 4 K LHe Liquid Helium		300 K – 80 K LN_2 Liquid Nitrogen	
	Watt	L/hr	Watt	L/hr
Conduction				
Vert. 50 tons	1.0	1.4	100	2.2
Horiz. (Braking) 0.5g	0.5	0.7	50	1.1
Radiation 50%	0.4	0.6	130	2.9
TOTAL	1.9	2.7	280	6.2

Assume 4,000 liter of each LHe and LN_2 containers

Pot Life Hours	1,480	645
Number of Days	62	27

Total of 10% of service volume occupied with LHe and LN_2

Table 2-10

Cryogen Heat Loads per Car (Calculations)

Conduction 20 K - 4 K
To support weight of car
Assume Q = 0.022 W/1,000 kg
Assume weight of car = 445,000 kg
Qcar = 0.0225 W/kg ¥ 44,500 kg
= 1 Watt per car
= 1.4 liter/hr LHe per car

Radiation 20 K - 4 K
Area top and bottom = 2 ¥ 3.4 ¥ 30 = 204 m^2
sides = 2 ¥ 33.4 ¥ 0.8 = 53 m^2
Assume 0.003 Watt/m^2 ¥ 257 ~ 1 liter/hr per car
Assume A_{EFF} = 50%
The Q = 1/2 ¥ 1 = 0.5 liter/hr per car helium boil-off

Q Total 20 K - 4 K
$Q_T = Q_{support} + Q_{radiation}$
= 1.4 + 0.5
~ 2 liter/hr per car

Volume Service Compartment
Vol= 0.8 m ¥ 3.4 ¥ 30
≈ 80 m^3
= 80,000 liters
Assume 5% is LHe
Vol_{LHe} = 4,000 liters
Time to boil away
4,000 liters/2 liters per hour = 2,000 hours
÷ 24 = 83 days

Table 2-11

Cryogen Heat Loads per Car (Calculations)

Assume LN_2 300K – 77 K

Radiation 1 Watt/m^2

$Q = 50\% \times 257\ m^2 \times 1\ \text{Watt}/m^2$

$= 130$ Watt

Conduction 300 K – 77 K

$Q = 2.25\ \text{W}/1{,}000\ \text{kg} \times 44{,}500\ \text{kg}$

$= 100$ Watt

$Q_{TOTAL} = 130+100 = 230$ Watts 300K – 77 K

Let us also assume 4,000 liters of LN_2

Then:

$$\frac{\frac{45\ \text{Watt/hr}}{\text{liter}}}{230\ \text{Watt}} = \frac{0.2\ \text{hr}}{\text{liter}} \approx \frac{5\ \text{liter}}{\text{hr}}$$

$$\frac{4{,}000\ \text{liters}}{} = 800\ \text{hr} \div 24 = 33\ \text{days}$$

WT_{LN2} 4,000 liters x 0.40 kg/liter

$= 3.5$ turns $\div$ 50 turns $\approx$ 7% of total

2.5 Magnetic Shielding

The flow chart for the design process is shown in Figure 2-5 for active shielding and in Figure 2-6 for passive shielding. The formulae given in Figure 2-8 will be used to calculate magnetic field in the detailed design phase.

REFERENCES

Conductor Design	Source
Figure 2-13-1	ASI Manufacturing Data
Figure 2-13-2	Reed, Clark, *Advances in Cryogenic Materials*
Figure 2-13-3	DOE/EPRI Assessment of High T_c Superconductors
Figure 2-13-4	Sato, Hikata, Iwasa, *Applied Physics Letters*
Figure 2-13-5	GE Research Report, December 1991
Figure 2-14	M. Wilson, *Superconducting Magnets*
Figure 2-15	NBS Data Sheet

Refrigeration

Figures 2-20 – 2-23 T. R. Strobridge and D. B. Chelton

LITERATURE REVIEW

I. General Levitation

1. J. R. Hogan, "Comparison of Lift and Drag Forces on Vehicle Levitation by Eddy Current Repulsion for Variations and Normal Flux Magnets with One or Two Tracks," Sept. 1974.

2. John R. Reitz, "Forces on Moving Magnets Due to Eddy Currents," *Journal of Applied Physics*, Vol. 41, No. 5, Apr. 1970.

3. E. R. Laithwate, "Electromagnetic Levitation," IEEE Proceedings, Vol. 112, No. 12, Dec. 1965.

4. Richard D. Thornton, "Design Principles for Magnetic Levitation." *Proceedings of the IEEE*, Vol. 61, No. 5, May 1973.

5. Shung-Wu Lee, "Force on Current Coils Moving over a Conducting Sheet with Application to Magnetic Levitation," *Proceedings of the IEEE*, Vol. 62, No. 5, May 1974.

6. Richard D. Thornton, "Magnetic Levitation and Propulsion, 1975," *IEEE Transactions on Magnets*, Vol. Mag-11, No. 4, July 1975.

7. J. R. Reitz, "U.S. Department of Transportation Program in Magnetic Suspension (Repulsion Concept)," Toronto Intermag Conference, May 14-17, 1974.

8. J. F. Eastham, "Experiments on the Lateral Stabilisation and Levitation of Linear Induction Motors," Toronto Intermag Conference, May 14-17, 1974.

9. G. T. Danby, "Force Calculations for Hybrid (Ferro-Nullflex) Low-Drag Systems," Toronto Intermag Conference, May 14-17, 1974.

10. J. P. Howell, "Stability of Magnetically Levitated Vehicles Over a Split Guideway," *IEEE Transactions on Magnetics*, Vol. Mag-11, No. 5, Sept. 1975.

11. J. F. Eastham, "Full-Scale Testing of a High Speed Linear Synchronous Motor and Calculation on End Effects," *IEEE Transactions on Magnetics*, Vol. 24, No. 6, Nov. 1988.

12. P. E. Burke, "Dual Linear Synchronous Motor for Maglev Vehicles," *IEEE Transactions on Magnetics*, Vol. Mag-13, No. 5, Sept. 1977.

13. Sakae Yamamura, "Electromagnetic Levitation System by Means of Salient-Pole Type Magnets Coupled with Laminated Slotless Rails."

14. R. H. Borcherts, "Lift and Drag Forces for the Attractive Electromagnetic Suspension System."

15. M. Iwamoto, "Magnetic Damping Force in Electrodynamically Suspended Trains."

16. H. T. Coffey, "Dynamic Performance of the SRI Maglev Vehicle."

17. P. E. Burke, "The Calculation of Eddy Losses in Guideway Conductors and Structural Members of High-Speed Vehicles."

18. C. H. Tang, "A Review of the Magneplane Project," *IEEE Transactions on Magnetics*," Vol. Mag-11, No. 2, March 1975.

19. C. A. Guderjahn, "Magnetic Suspension and Guidance for High Speed Rockets by Superconducting Magnets," *Journal of Applied Physics*," Vol. 40, No. 5, April 1969.

20. R. G. Rhodes and B.E. Nulhall, *Magnetic Levitation for Rail Transport*, Clareton Press, 1981.

21. E. R. Laithwaite, *Linear Electric Motors*, Nills and Bosh Ltd., 1971.

22. E. R. Laithwaite, *Propulsion Without Wheels*, Tlart Publishing Company, NY, 1966.

23. J. R. Powell and G. Danby, "Magnetically Suspended Train for Very High Speed Transport," *Proceedings of the 4th IECEC Conference*, Washington, 1969.

II. Superconductivity Aspect

1. H. Tsuchishima, "Superconducting Magnet and On-Board Refrigeration System on Japanese Maglev Vehicle," *IEEE Transactions on Magnetics*, Vol. 27, No. 2, March 1991.

2. O. Tsukamoto, "Development of Superconducting Linear Induction Motor for Steel Making Processes," *IEEE Transactions on Magnetics*, Vol. 27, No. 2, March 1991.

3. Boon-Teck Ooi, "Electromechanical Dynamics in Superconducting Levitation Systems," *IEEE Transactions on Magnetics*, Vol. Mag-11, No. 5, Sept. 1975.

III. General Maglev

1. William F. Hayes, "Magnetic Field Shielding for Electrodynamic Vehicles," IEEE, 1987.

2. Gordon R. Slemon, "The Canadian Maglev Project on High-Speed Interurban Transportation," *IEEE Transactions on Magnetics*, Vol. Mag-11, No. 5, Sept. 1975.

3. Stephen Kuznetsov, "Commercialization of Maglev Technology for U.S. Baseline Interurban System: An Industrial Perspective," presented at Eighth International Convention on High Speed Rail, Anaheim, CA, May 6, 1991.

4. *Conceptual Design and Analysis of the Tracked Magnetically Levitated Vehicle Technology Program (TMLV). Repulsion Scheme. Volume I. Technical Studies.* The Philco-Ford Corporation. Prepared for Federal Railroad Administration, Feb. 1975.

5. O. Tsukamoto, "A New Magnetic Levitation System with AC Magnets," *IEEE Transactions on Magnetics*, Vol. 24, No. 2, March 1988.

6. Yoshiro Kyotani, "Recent Progress by JNR on Maglev," *IEEE Transactions on Magnetics*, Vol. 24, No. 2, March 1988.

7. A. H. Greene, "LSM Control of Maglev Vehicle Ride Quality."

8. "Magnetically Levitated High-Speed Ground Transportation System for New York State." Prepared for The New York State Energy Research and Development Authority, July 10, 1990.

9. G. R. Slemon, "A Linear Synchronous Motor for High-Speed Ground Transport," Toronto Intermag Conference, May 14-17, 1974.

10. P. C. Sen, "On Linear Synchronous Motor (LSM) for High-Speed Propulsion," *IEEE Transactions on Magnetics*, Vol. Mag-11, No. 5, Sept. 1975.

11. J. Meins, "The High Speed Maglev Transportation System Transrapid," *IEEE Transactions on Magnetics*, Vol. 24, No. 2, March 1988.

12. W. S. Brown, "The Effect of Long Magnets on Inductive Maglev Ride Quality,"*IEEE Transactions on Magnetics*, Vol. Mag-11, No. 5, Sept. 1975.

13. Y. Iwasa, "An Operational 1/25-Scale Magneplane System with Superconducting Coils," *IEEE Transactions on Magnetics*, Vol. Mag-11, No. 5, Sept. 1975.

14. K. Oberretl, "Transients and Oscillations in the Repulsive Magnetic Levitation System," *IEEE Transactions on Magnetics*, Vol. Mag-11, No. 5, Sept. 1975.

15. T. Umemori, "Study on Miniaturization of Electromagnet for DC Linear Motor," *IEEE Transactions on Magnetics*, Vol. Mag-16, No. 5, Sept. 1980.

16. David W. Jackson, "Magneplane Power Supply Costs."

17. G. Bohn, "The Magnetic Train Transrapid 06."

18. Hisashi Tanaka, "JR Group Proves Maglev Frontiers," *Railway Gazetta International*, July 1990.

19. Yoshihiro Kyotani, "Present Status of JNR Maglev Development."

20. New York State Technical and Economic Maglev Evaluation," prepared for New York State Energy Research and Development Authority, 1990.

21. L. R. Johnson, D. M. Rote, J. R. Hull, H. T. Coffey, J. G. Daley and R. F. Giese, "Maglev Vehicles and Superconductor Technology," Argonne National Laboratory, 1989.

System Characteristics	
Thrust	50 kN
Vehicle Weight	445 kN
Cruise Speed	500 km/hr (138.9 m/s)
Mechanical Power	6.945 MW
Field-Stator Winding Separation	0.21 m
Stator Block Length	2 km
LSM Configuration	Dual
Vehicle Dimensions	
length	30 m
width	3.4 m

Vehicle Field Magnets	
Number of Magnets	88–104
Mean Length (range)	0.53 – 0.85 m
Pole-pitch (range)	0.57 – 0.81 m
Mean Width	0.80 m
Field MMF (range)	400 kAT – 600 kAT
B_{peak} at Windings	5.3 T

Baseline Parameters of Linear Synchronous Motor
Figure 2-1

Propulsion Magnet Length	57–83 cm
Propulsion Magnet Width	80 cm
Field MMF	400K–600K Amp-turns
Peak Field at Winding	5.3 T
Operating Current	100 Amps
Conductor Type	Nb_3Sn or NbTi or High T_c
Conductor Stability	adiabatic or cryostable
Conductor Margin	50% cryostable
	80% adiabatic

Derived Propulsion Magnet Requirements
Figure 2-2

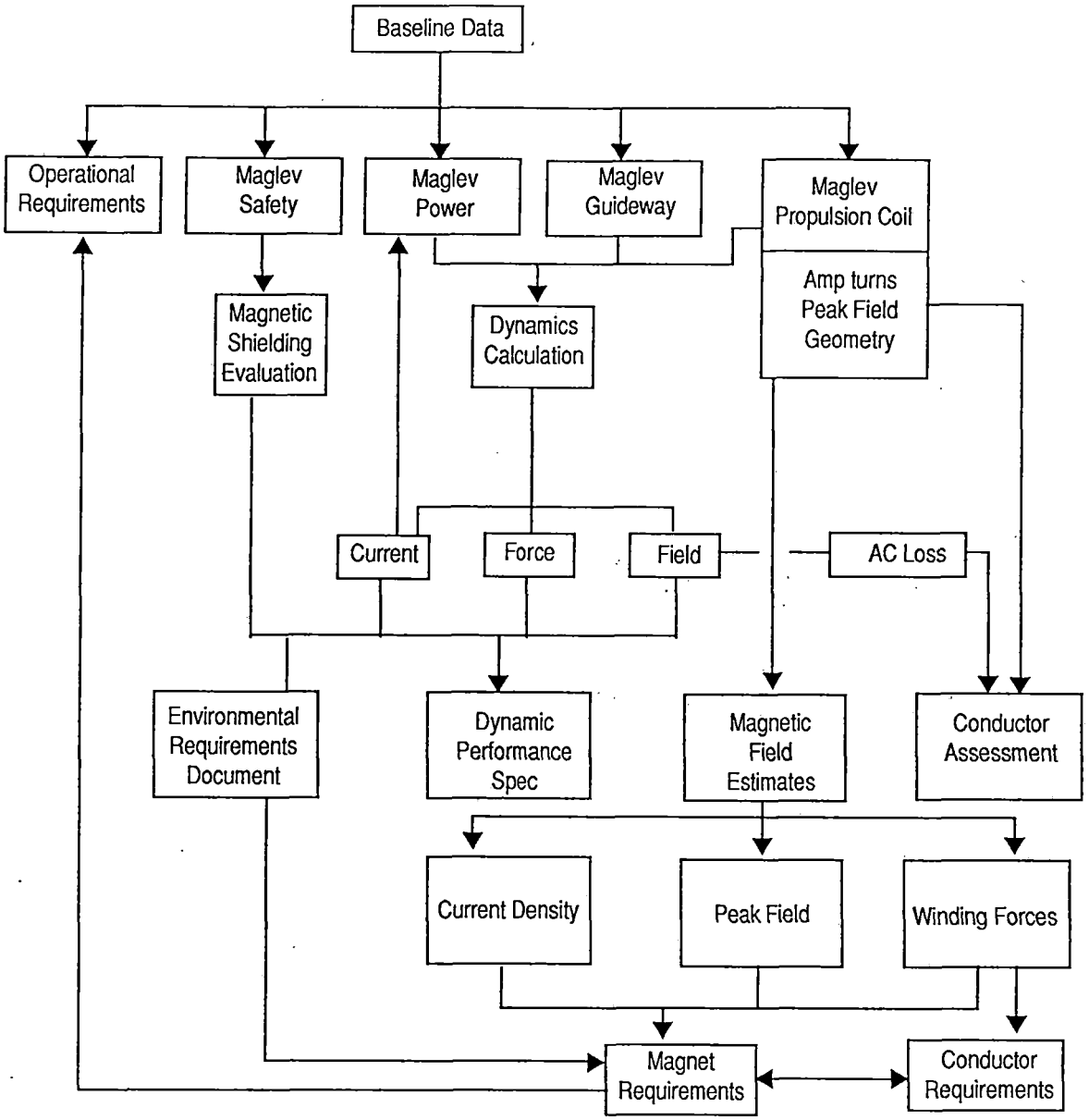

LSM Conceptual Design
Figure 2-3

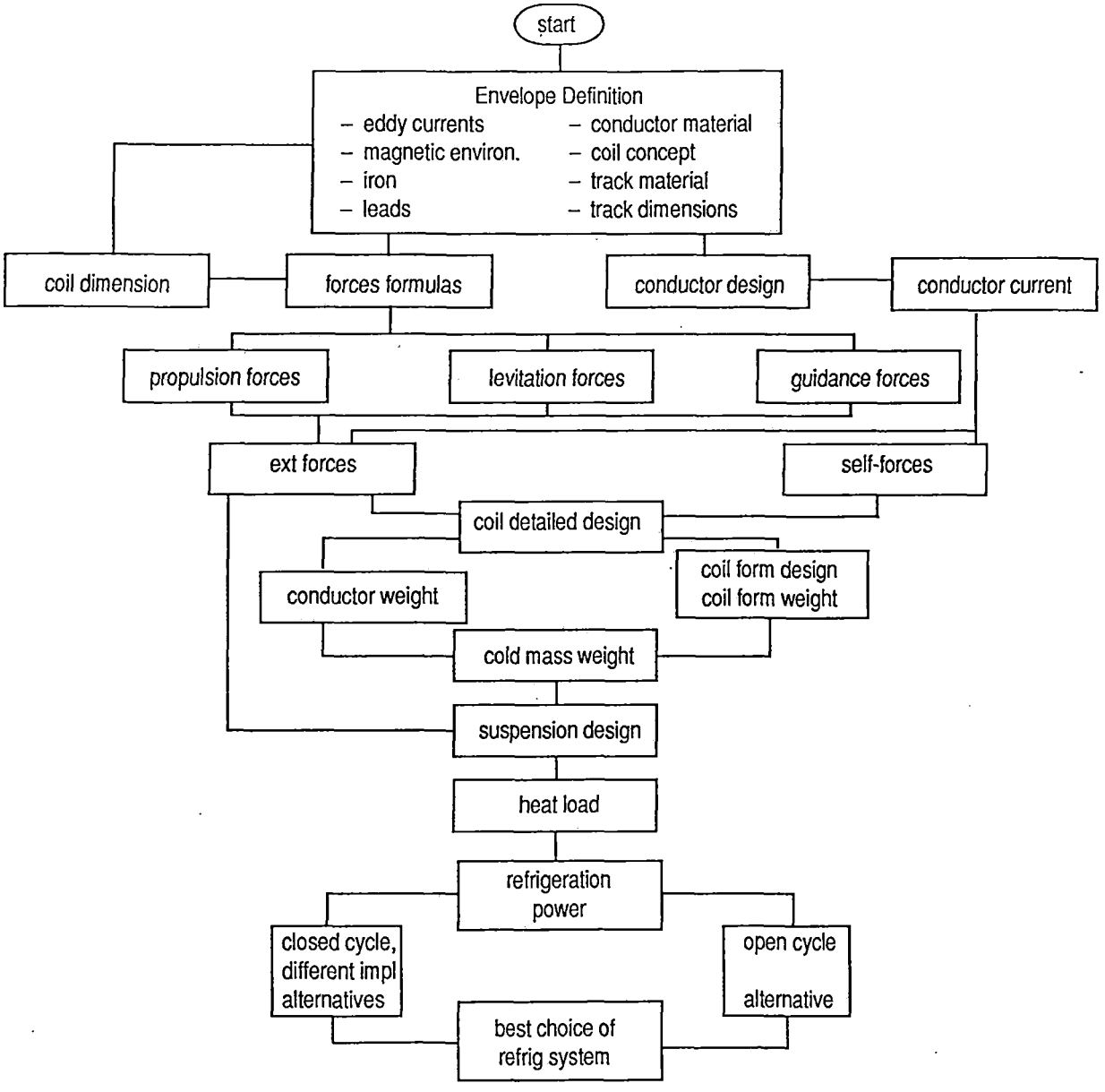

Diagram of refrigeration design process
Figure 2-4

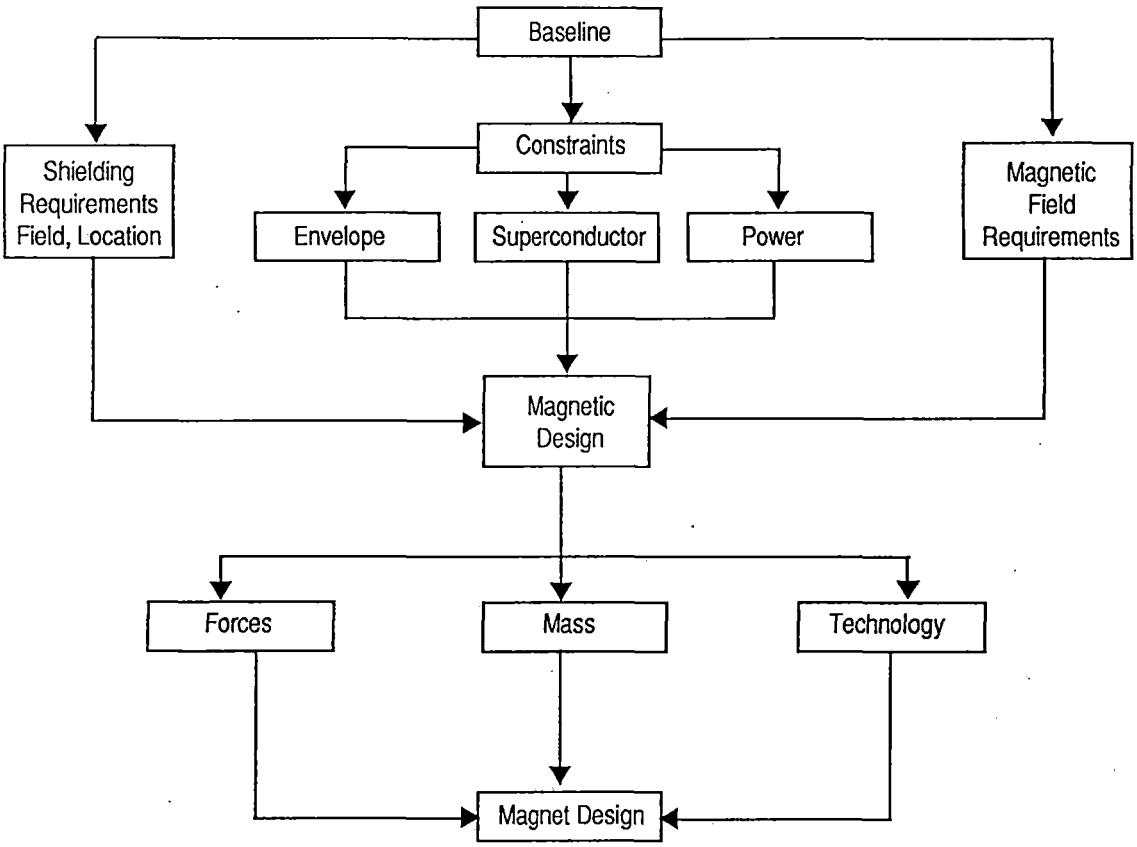

Conceptual Design Process for Active Shielding of the Magnetic Fields
Figure 2-5

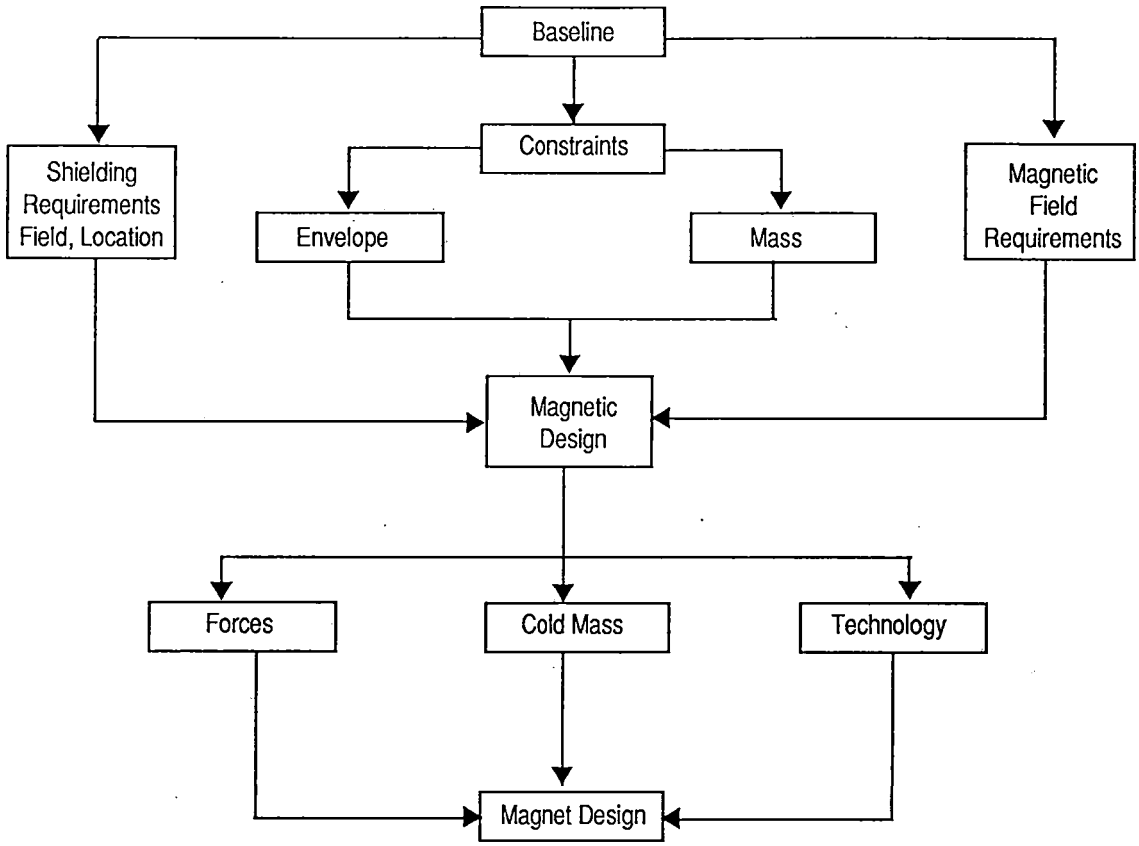

Conceptual Design Process for Passive Shielding of the Magnetic Fields
Figure 2-6

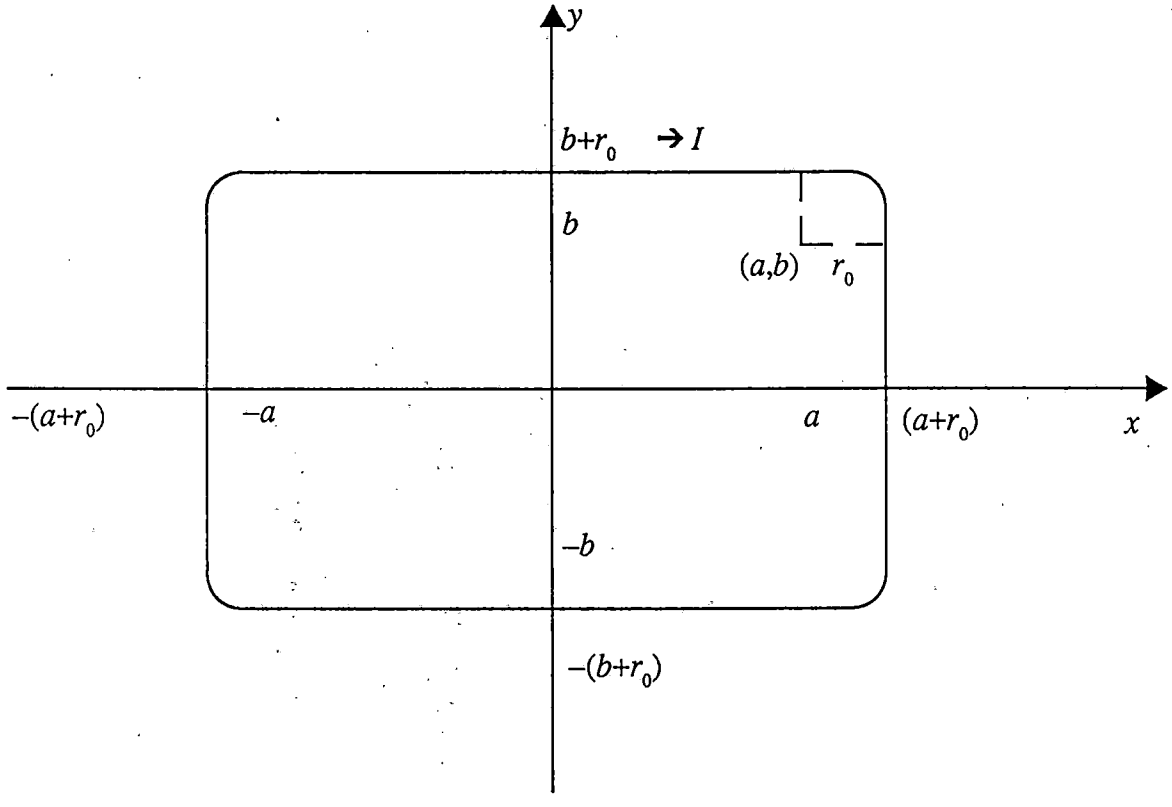

Racetrack coil (definiton)
Figure 2-7

$$\vec{B} = \frac{\mu_0 I}{4\pi}\int_l \frac{d\vec{s}\times\vec{R}}{R^3}$$

$$\xi = x_0 + r_0\cos\theta$$
$$\eta = y_0 + r\sin\theta$$
$$d\xi = -r_0\sin\theta d\theta$$
$$d\eta = T_0 + \cos\theta d\theta$$

$0 \le \theta \le 90°$

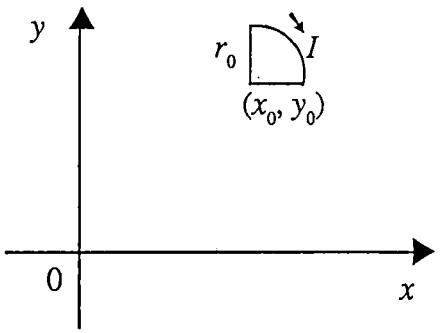

$$\vec{r} = x\vec{x} + y\vec{y} + z\vec{z}$$
$$\vec{r}_1 = \xi\vec{x} + \eta\vec{y}$$
$$\vec{R} = \vec{r} - \vec{r}_1$$
$$d\vec{s} = d\xi\vec{x} + d\eta\vec{y} \qquad d\vec{s}\times\vec{R} = zd\eta\vec{x} - zd\xi\vec{y} + \left[(yd\xi - xd\eta) + (\xi d\eta - \eta d\xi)\right]\vec{z}$$

$$B_x = -\frac{\mu_0 Iz}{4\pi}\int_0^{\pi/2} \frac{r_0\cos\theta d\theta}{\left\{\left[(x-x_0) - r_0\cos\theta\right]^2 + \left[(y-y_0) - r_0\sin\theta\right]^2 + z^2\right\}^{3/2}}$$

$$B_y = -\frac{\mu_0 Iz}{4\pi}\int_0^{\pi/2} \frac{r_0\sin\theta d\theta}{\left\{\left[(x-x_0) - r_0\cos\theta\right]^2 + \left[(y-y_0) - r_0\sin\theta\right]^2 + z^2\right\}^{3/2}}$$

$$B_z = -\frac{\mu_0 r_0}{4\pi}\int_0^{\pi/2} \frac{(x-x_0)\cos\theta d\theta + (y-y_0)\sin\theta d\theta + r_0 d\theta}{\left\{\left[(x-x_0) - r_0\cos\theta\right]^2 + \left[(y-y_0) - r_0\sin\theta\right]^2 + z^2\right\}^{3/2}}$$

Formulae for magnetic field calculations for racetrack coil defined on Figure 2-7

Figure 2-8-1

$$\vec{B} = \frac{\mu_0 I}{4\pi} \int_l \frac{d\vec{s} \times \vec{R}}{R^3}$$

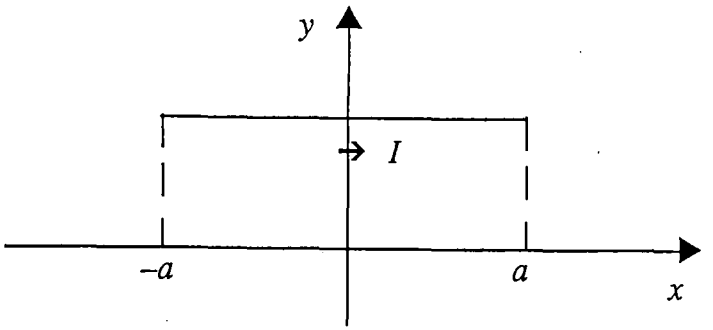

$$\vec{r}_s = t\vec{x} + b\vec{y}$$

$$\vec{r} = x\vec{x} + y\vec{y} + z\vec{z}$$

$$\vec{R} = \vec{r} - \vec{r}_s = (x-t)\vec{x} + (y-b)\vec{y} + z\vec{z}$$

$$R = \left[(x-t)^2 + (y-b)^2 + z^2\right]^{\frac{1}{2}}$$

$$d\vec{s} = dt\vec{x}, \quad d\vec{s} \times \vec{R} = -z\,dt\vec{y} + (y-b)\,dt\vec{z}$$

$$\therefore \qquad B_x = 0, \quad B_y = \frac{\mu_0 I z}{4\pi} \int_{-a}^{a} \frac{dt}{R^3}, \quad B_{z=} \frac{\mu_0 I (y-b)}{4\pi} \int_{-a}^{a} \frac{dt}{R^3}$$

$$B_x = 0$$

$$B_y = \frac{\mu_0 I z}{4\pi} \left(\frac{a-x}{A^2\left[(a-x)^2 + A^2\right]^{\frac{1}{2}}} + \frac{a+x}{A^2\left[(a-x)^2 + A^2\right]^{\frac{1}{2}}} \right) \quad A^2 = (y-b)^2 + z^2$$

$$B_z = \frac{\mu_0 I (y-b)}{4\pi} \left(\frac{a-x}{A^2\left[(a-x)^2 + A^2\right]^{\frac{1}{2}}} + \frac{a+x}{A^2\left[(a-x)^2 + A^2\right]^{\frac{1}{2}}} \right)$$

Formulae for magnetic field calculations for racetrack coil defined on Figure 2-7

Figure 2-8-2

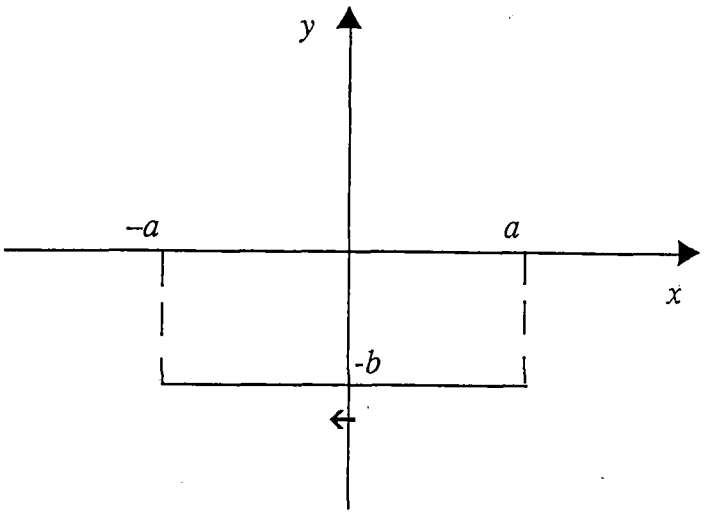

$$B_x = 0$$

$$B_y = \frac{\mu_0 I z}{4\pi} \int_{-a}^{a} \frac{dt}{\left[(x-t)^2 + (y+b)^2 + z^2\right]^{3/2}}$$

$$B_z = \frac{\mu_0 I (y+b)}{4\pi} \int_{-a}^{a} \frac{dt}{\left[(x-t)^2 + (y+b)^2 + z^2\right]^{3/2}}$$

$$B_x = 0$$

$$B_y = \frac{\mu_0 I z}{4\pi} \left(\frac{a-x}{A^2\left[(a-x)^2 + A^2\right]^{\frac{1}{2}}} + \frac{a+x}{A^2\left[(a-x)^2 + A^2\right]^{\frac{1}{2}}} \right) \qquad A^2 = (y-b)^2 + z^2$$

$$B_z = \frac{\mu_0 I (y+b)}{4\pi} \left(\frac{a-x}{A^2\left[(a-x)^2 + A^2\right]^{\frac{1}{2}}} + \frac{a+x}{A^2\left[(a-x)^2 + A^2\right]^{\frac{1}{2}}} \right)$$

Formulae for magnetic field calculations for racetrack coil defined on Figure 2-7

Figure 2-8-3

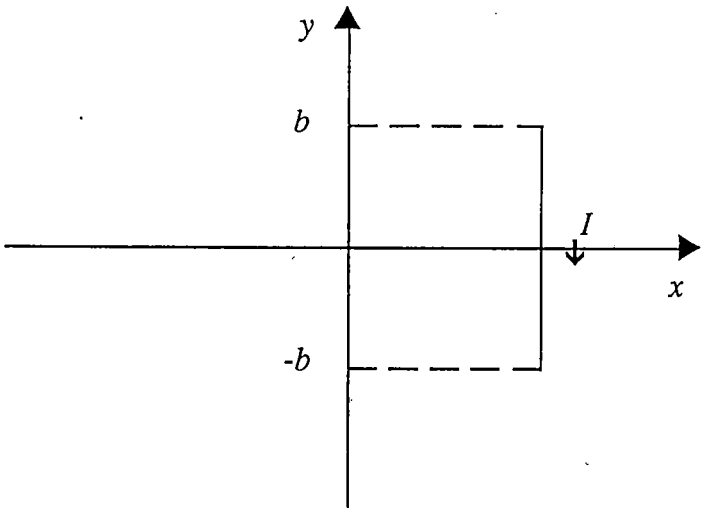

$$B_y = 0$$

$$B_x = \frac{\mu_0 I z}{4\pi} \int_{-b}^{b} \frac{dt}{\left[(x-a)^2 + (y-t)^2 + z^2\right]^{3/2}}$$

$$B_z = \frac{\mu_0 I (x-a)}{4\pi} \int_{-b}^{b} \frac{dt}{\left[(x-a)^2 + (y-t)^2 + z^2\right]^{3/2}}$$

$$B_y = 0$$

$$B_y = \frac{\mu_0 I z}{4\pi} \left(\frac{b-y}{A^2\left[(y-b)^2 + A^2\right]^{\frac{1}{2}}} + \frac{b+y}{A^2\left[(y-b)^2 + A^2\right]^{\frac{1}{2}}} \right) \qquad A^2 = (x-a)^2 + z^2$$

$$B_z = \frac{\mu_0 I (x-a)}{4\pi} \left(\frac{b-y}{A^2\left[(y-b)^2 + A^2\right]^{\frac{1}{2}}} + \frac{b+y}{A^2\left[(y-b)^2 + A^2\right]^{\frac{1}{2}}} \right)$$

Formulae for magnetic field calculations for racetrack coil defined on Figure 2-7

Figure 2-8-4

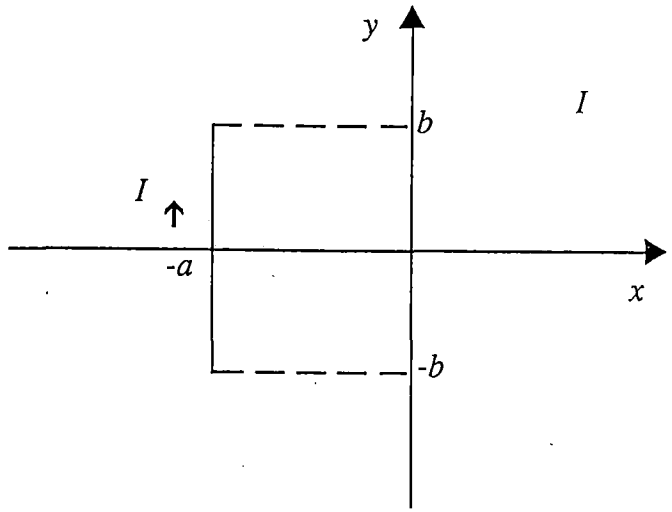

$$B_y = 0$$

$$B_x = \frac{\mu_0 I z}{4\pi} \int_{-b}^{b} \frac{dt}{\left[(x-a)^2 + (y-t)^2 + z^2\right]^{3/2}}$$

$$B_z = \frac{\mu_0 I (x+a)}{4\pi} \int_{-b}^{b} \frac{dt}{\left[(x+a)^2 + (y-t)^2 + z^2\right]^{3/2}}$$

$$B_y = 0$$

$$B_y = \frac{\mu_0 I z}{4\pi}\left(\frac{y-b}{A^2\left[(y-b)^2 + A^2\right]^{\frac{1}{2}}} + \frac{y+b}{A^2\left[(y+b)^2 + A^2\right]^{\frac{1}{2}}}\right) \qquad A^2 = (x+a)^2 + z^2$$

$$B_z = \frac{\mu_0 I (x+a)}{4\pi}\left(\frac{y-b}{A^2\left[(y-b)^2 + A^2\right]^{\frac{1}{2}}} + \frac{y+b}{A^2\left[(y+b)^2 + A^2\right]^{\frac{1}{2}}}\right)$$

Formulae for magnetic field calculations for racetrack coil defined on Figure 2-7

Figure 2-8-5

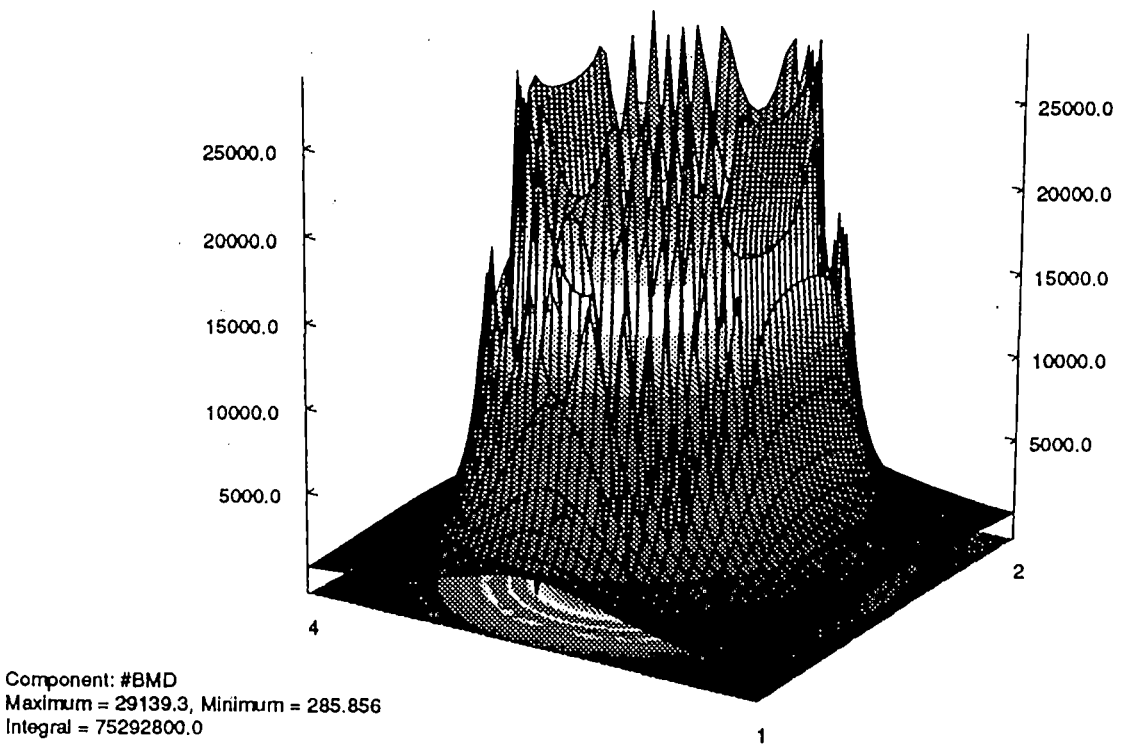

B_z component of the field of the racetrack coil

Figure 2-9

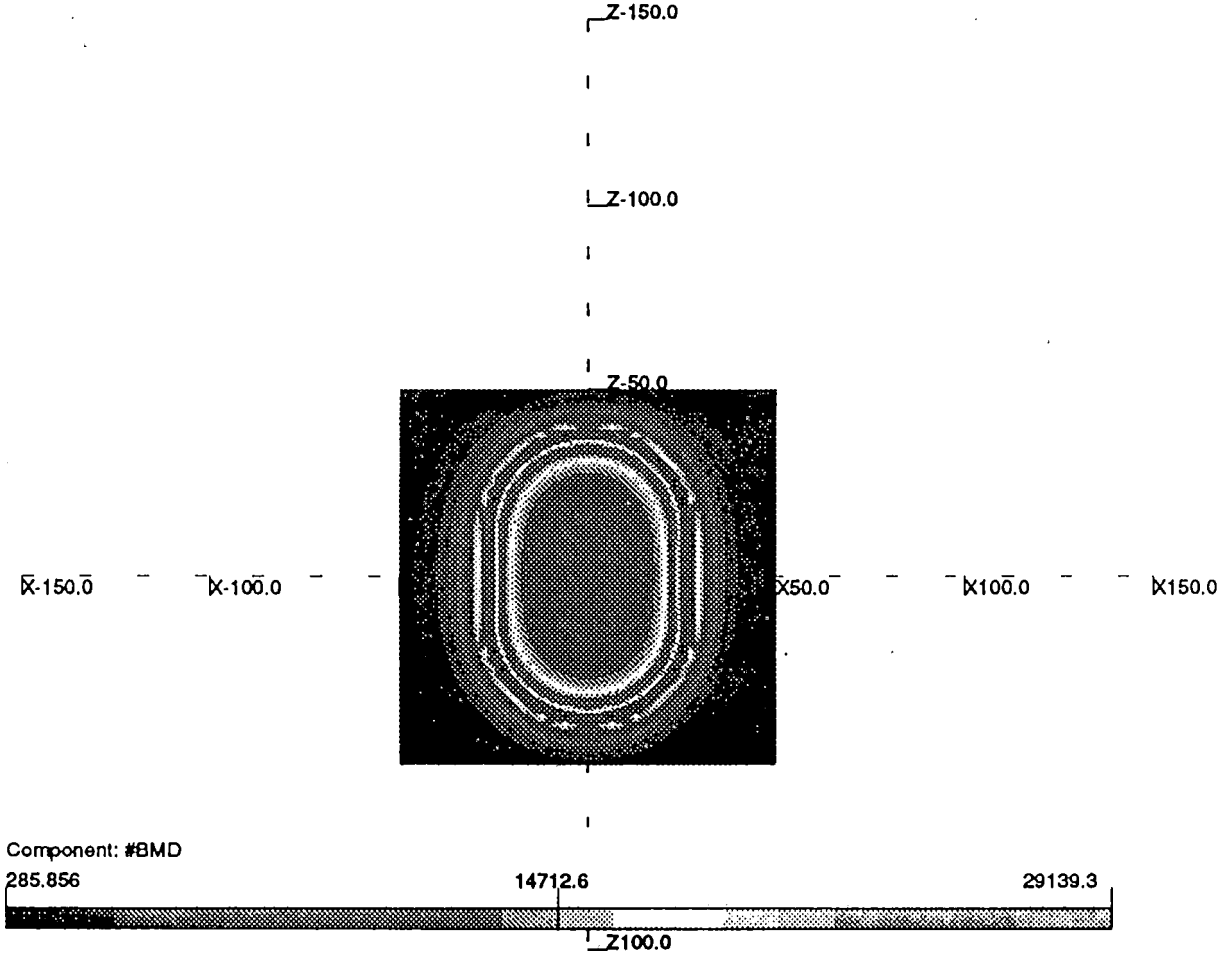

Field map in the xy plane
Figure 2-10

Basic Formula

$$\vec{F} = \frac{\mu_o I_1 I_2}{4\pi} \oint_{l_s} \oint_{l} \frac{d\vec{S}_1 \left(\vec{r} \times d\vec{S}_2 \right)}{r^3}$$

$\vec{F} = (Fx, Fy, Fz)$

Fy: the propulsion force,

Fx: the guidance force,

Fz: the levitation force.

An algorithm computing propulsion force for LSM

Figure 2-11-1

$$Pf_1(I_1,I_2)=\frac{\mu_0 I_1 I_2}{4\pi}\begin{cases}-\left[y_o+r_c-4(i+1/4-j/24)\omega\right]\int_{-l}^{l}\int_{-h}^{h}\dfrac{dx_1dx_2}{\left\{(x_1-x_2)^2+\left(y_o+r_c-4(i+1/4-j/12)\omega\right)^2+z_o^2\right\}^{3/2}}\\ \left[y_o+r_c-4(i-1/4-j/24)\omega\right]\int_{-l}^{l}\int_{-h}^{h}\dfrac{dx_1dx_2}{\left\{(x_1-x_2)^2+\left(y_o+r_c-4(i-1/4-j/12)\omega\right)^2+z_o^2\right\}^{3/2}}\\ -\int_{-l}^{l}\int_{4(i-1/4-j/12)\omega}^{4(i+1/4-j/12)\omega}\dfrac{(x_1-h)dx_1dy_2}{\left\{(x_1-h)^2+\left(y_o+r_c-y_2\right)^2+z_o^2\right\}^{3/2}}\\ -\int_{-l}^{l}\int_{4(i+1/4-j/12)\omega}^{4(i+3/4-j/12)\omega}\dfrac{(x_1+h)dx_1dy_2}{\left\{(x_1+h)^2+\left(y_o+r_c-y_2\right)^2+z_o^2\right\}^{3/2}}\end{cases}$$

An algorithm computing propulsion force for LSM

Figure 2-11-2

$$Pf_2(I_1,I_2)=\frac{\mu_0 I_1 I_2}{4\pi}\left\{\begin{array}{l}+\left[y_o+r_c-4(i+1/4-j/24)\omega\right]\int_{-l}^{l}\int_{-h}^{h}\dfrac{dx_1dx_2}{\left\{(x_1-x_2)^2+\left(y_o-r_c-4(i+1/4-j/12)\omega\right)^2+z_o^2\right\}^{3/2}}\\ -\left[y_o-r_c-4(i-1/4-j/24)\omega\right]\int_{-l}^{l}\int_{-h}^{h}\dfrac{dx_1dx_2}{\left\{(x_1-x_2)^2+\left(y_o-r_c-4(i-1/4-j/12)\omega\right)^2+z_o^2\right\}^{3/2}}\\ \int_{-l}^{l}\int_{4(i-1/4-j/12)\omega}^{4(i+1/4-j/12)\omega}\dfrac{(x_1-h)dx_1dy_2}{\left\{(x_1-h)^2+\left(y_o-r_c-y_2\right)^2+z_o^2\right\}^{3/2}}\\ -\int_{-l}^{l}\int_{4(i+1/4-j/12)\omega}^{4(i+3/4-j/12)\omega}\dfrac{(x_1+h)dx_1dy_2}{\left\{(x_1+h)^2+\left(y_o-r_c-y_2\right)^2+z_o^2\right\}^{3/2}}\end{array}\right.$$

An algorithm computing propulsion force for LSM

Figure 2-11-3

$$Pf_3(I_1,I_2)=\frac{\mu_0 I_1 I_2}{4\pi}\left\{\begin{array}{l}
-\int_{-\frac{\pi}{2}}^{\frac{\pi}{2}}\int_{-h}^{h}\dfrac{r_c\sin\alpha\left(r_c\sin\alpha+y_o-4(i+1/4-j/24)\omega\right)d\alpha dx}{\left\{\left(r_c\omega s\alpha+l-x\right)^2+\left(r_c\sin\alpha+y_o-4(i+1/4-j/12)\omega\right)^2+z_o^2\right\}^{3/2}} \\
\int_{-\frac{\pi}{2}}^{\frac{\pi}{2}}\int_{-h}^{h}\dfrac{r_c\sin\alpha\left(r_c\sin\alpha+y_o-4(i-1/4-j/24)\omega\right)d\alpha dx}{\left\{\left(r_c\omega s\alpha+l-x\right)^2+\left(r_c\sin\alpha+y_o-4(i-1/4-j/12)\omega\right)^2+z_o^2\right\}^{3/2}} \\
-\int_{-\frac{\pi}{2}}^{\pi}\int_{4(i-1/4-j/12)\omega}^{4(i+1/4-j/12)\omega}\dfrac{r_c\sin\alpha\left(r_c\cos\alpha+l-h\right)d\alpha dy}{\left\{\left(r_c\omega s\alpha+l-h\right)^2+\left(r_c\sin\alpha+y_o-y\right)^2+z_o^2\right\}^{3/2}} \\
-\int_{-\frac{\pi}{2}}^{\pi}\int_{4(i+1/4-j/12)\omega}^{4(i+3/4-j/12)\omega}\dfrac{r_c\sin\alpha\left(r_c\cos\alpha+l+h\right)d\alpha dy}{\left\{\left(r_c\omega s\alpha+l+h\right)^2+\left(r_c\sin\alpha+y_o-y\right)^2+z_o^2\right\}^{3/2}}
\end{array}\right.$$

An algorithm computing propulsion force for LSM

Figure 2-11-4

$$Pf_4(I_1,I_2)=\frac{\mu_0 I_1 I_2}{4\pi}\left\{\begin{array}{l}
-\int_{\frac{\pi}{2}}^{\frac{3\pi}{2}}\int_{-h}^{h}\dfrac{r_c\sin\alpha\left(r_c\sin\alpha+y_o-4(i+1/4-j/24)\omega\right)d\alpha dx}{\left\{\left(r_c\omega s\alpha-l-x\right)^2+\left(r_c\sin\alpha+y_o-4(i+1/4-j/12)\omega\right)^2+z_o^2\right\}^{3/2}} \\
\int_{\frac{\pi}{2}}^{\frac{3\pi}{2}}\int_{-h}^{h}\dfrac{r_c\sin\alpha\left(r_c\sin\alpha+y_o-4(i-1/4-j/24)\omega\right)d\alpha dx}{\left\{\left(r_c\omega s\alpha-l-x\right)^2+\left(r_c\sin\alpha+y_o-4(i-1/4-j/12)\omega\right)^2+z_o^2\right\}^{3/2}} \\
-\int_{\frac{\pi}{2}}^{3\pi}\int_{4(i-1/4-j/12)\omega}^{4(i+1/4-j/12)\omega}\dfrac{r_c\sin\alpha\left(r_c\cos\alpha-l-h\right)d\alpha dy}{\left\{\left(r_c\omega s\alpha-l-h\right)^2+\left(r_c\sin\alpha+y_o-y\right)^2+z_o^2\right\}^{3/2}} \\
-\int_{\frac{\pi}{2}}^{3\pi}\int_{4(i+1/4-j/12)\omega}^{4(i+3/4-j/12)\omega}\dfrac{r_c\sin\alpha\left(r_c\cos\alpha-l+h\right)d\alpha dy}{\left\{\left(r_c\omega s\alpha-l+h\right)^2+\left(r_c\sin\alpha+y_o-y\right)^2+z_o^2\right\}^{3/2}}
\end{array}\right.$$

An algorithm computing propulsion force for LSM

Figure 2-11-5

The propulsion force

$$Pf = Pf_1 + Pf_2 + Pf_3 + Pf_4$$

For the three-phase track winding, the propulsion force

$$Pf_T = Pf(I_0, I_m) + Pf\left(I_0, I_m e^{i\pi/3}\right) + Pf\left(I_0, I_m e^{2i\pi/3}\right)$$

Propulsion force calculation for the rectangular DC coil

Figure 2-12-1

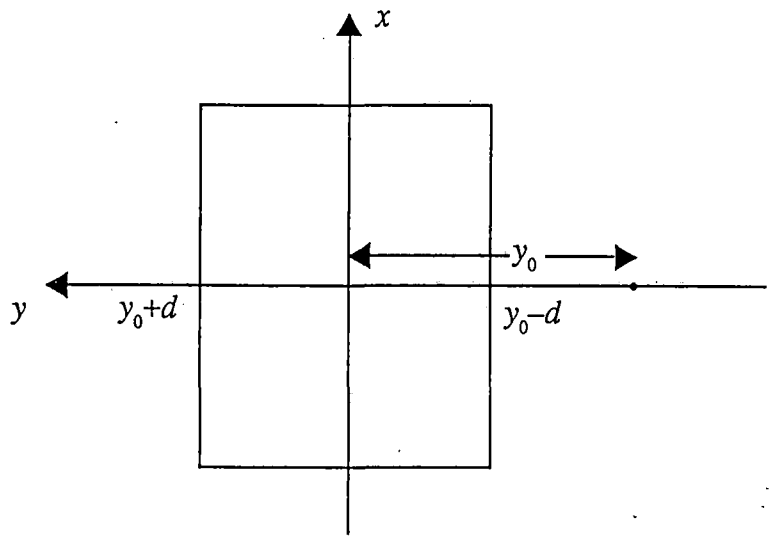

The propulsion force for a rectangular coil

$$Pf_1(I_1,I_2)=\frac{\mu_0 I_1 I_2}{4\pi}\sum_{j=-\infty}^{+\infty}\frac{y_0+d-y_j}{(y_0+d)^2+z_0^2}\left\{\left[(2h)^2+(y_0+d-y_j)^2+z_0^2\right]^{\frac{1}{2}}-\left[(y_0+d-y_j)^2+z_0^2\right]^{\frac{1}{2}}\right\}$$

$$+\sum_{j=-\infty}^{+\infty}\frac{y_0-d-y_j}{(y_0-d)^2+z_0^2}\left\{\left[(2h)^2+(y_0-d-y_j)^2+z_0^2\right]^{\frac{1}{2}}-\left[(y_0-d-y_j)^2+z_0^2\right]^{\frac{1}{2}}\right\}^{(*)}$$

$\{y_j\}$ run over the whole number ladder of the track winding.

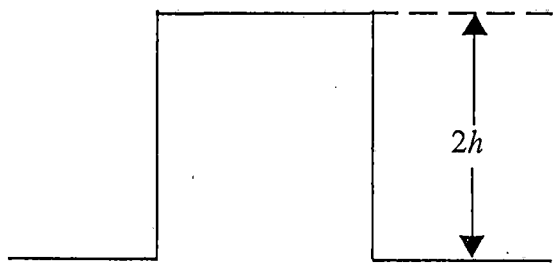

Propulsion force calculation for the rectangular DC coil

Figure 2-12-2

$$Pf_2(I_1 I_2) = \frac{\mu_o I_1 I_2}{4\pi} \sum_{j=-\infty}^{+\infty} \left\{ \begin{array}{l} \left[(2h)^2 + z_0^2\right] arcsh \dfrac{y_j - y_0 + d}{\sqrt{(2h)^2 + z_0^2}} - z_0^2 arcsh \dfrac{y_j - y_0 + d}{z_0} + \left(y_j - y_0 + d\right) \\ \left(\sqrt{\left(y_j - y_0 + d\right)^2 + (2h)^2 + z_0^2} - \sqrt{\left(y_j - y_0 + d\right)^2 + z_0^2} \right) \\ + \left[(2h)^2 + z_0^2\right] arcsh \dfrac{y_j - y_0 + d}{\sqrt{(2h)^2 + z_0^2}} - z_0^2 arcsh \dfrac{y_j - y_0 - d}{z_0} + \left(y_j - y_0 - d\right) \\ \left(\sqrt{\left(y_j - y_0 - d\right)^2 + (2h)^2 + z_0^2} - \sqrt{\left(y_j - y_0 - d\right)^2 + z_0^2} \right) \end{array} \right\}$$

Propulsion force calculation for the rectangular DC coil

Figure 2-12-3

$$Pf(I_1, I_2) = Pf_1(I_1, I_2) + Pf_2(I_1, I_2)$$

For the three-phase track winding, the propulsion force

$$Pf_T = Pf(I_0, I_m) + Pf\left(I_0, I_m e^{i\pi/3}\right) + Pf\left(I_0, I_m e^{2i\pi/3}\right)$$

Propulsion force calculation for the rectangular DC coil

Figure 2-12-4

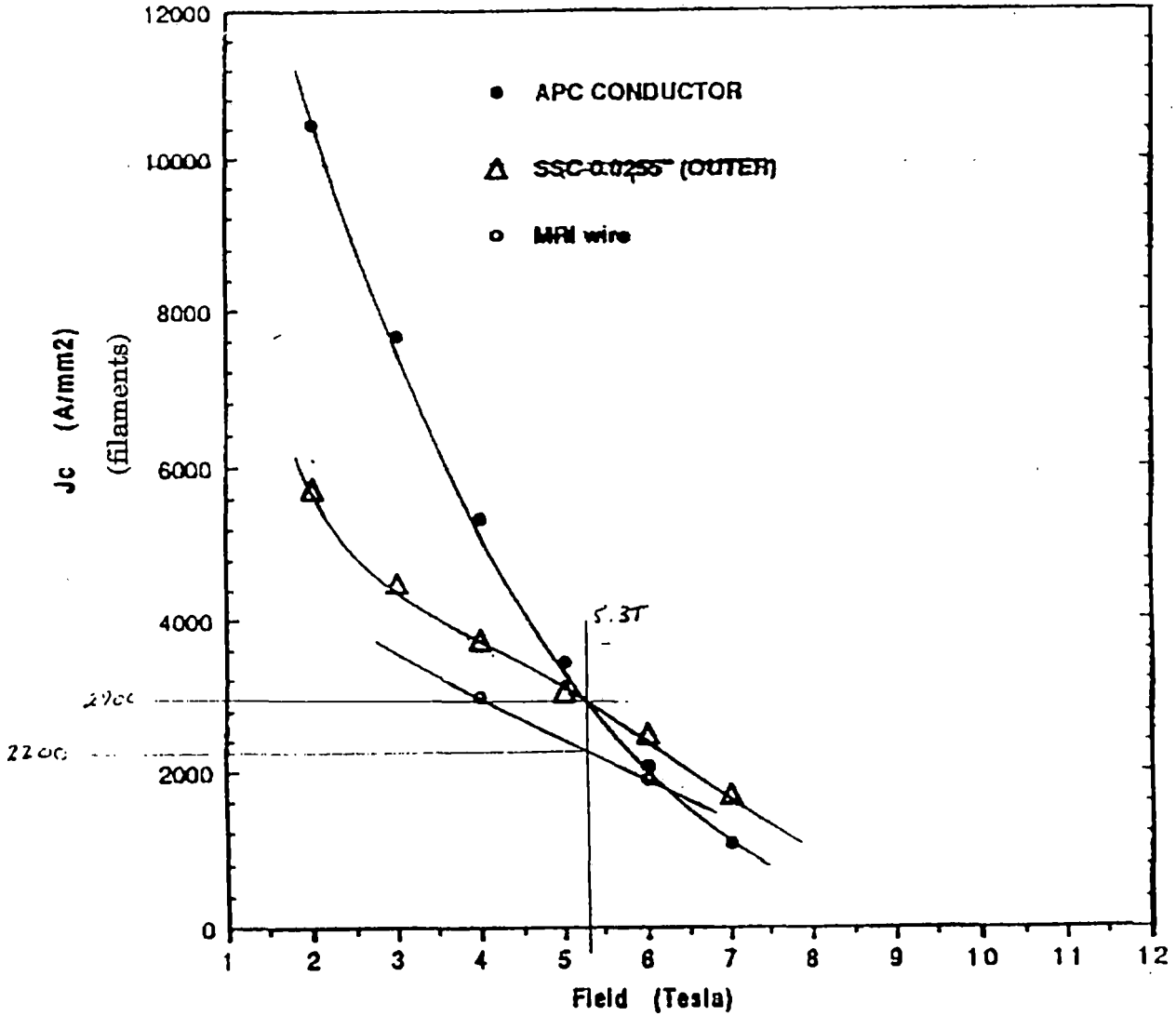

Field dependence of the critical current (NbTi)

Figure 2-13-1

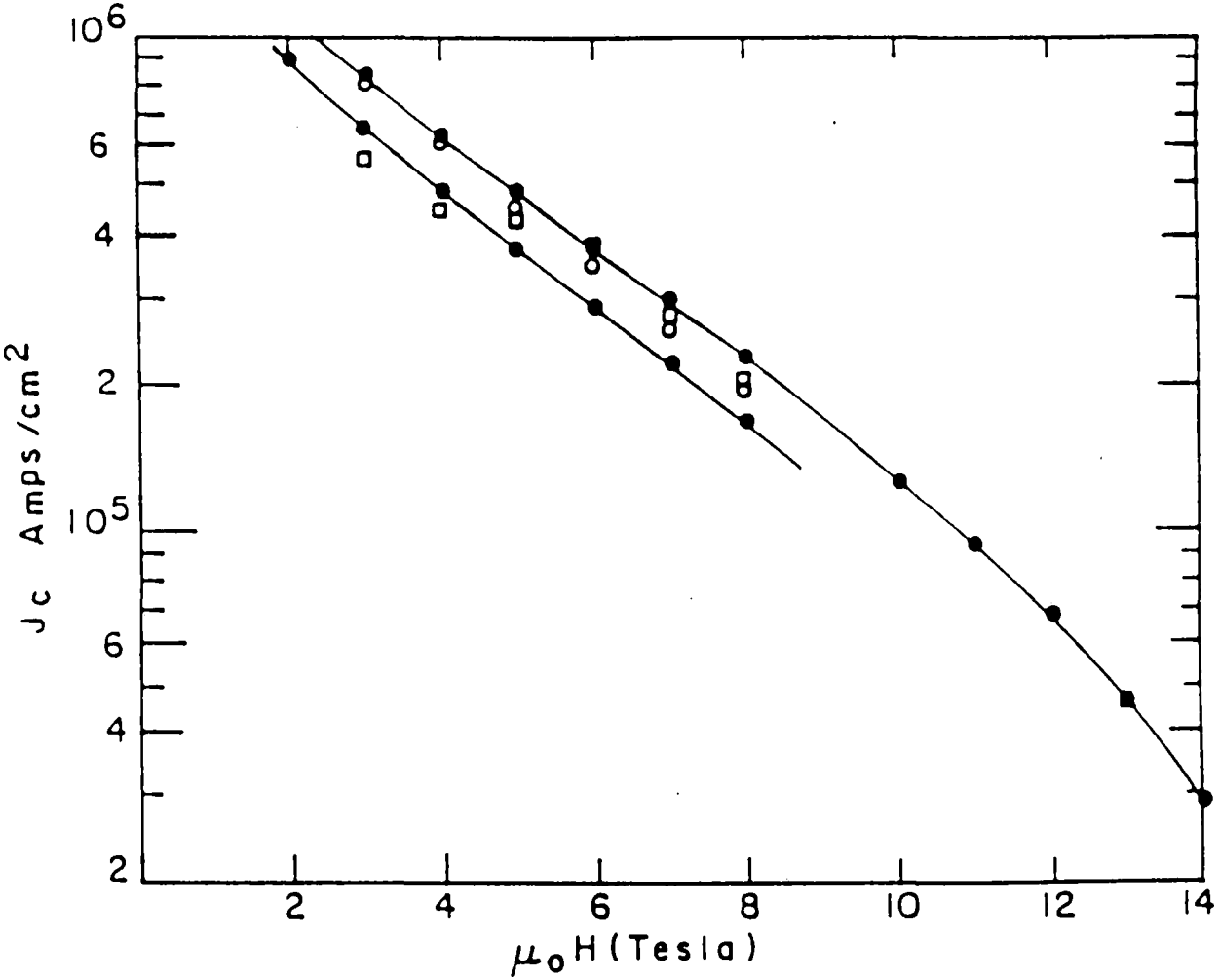

Field dependence of the critical current (Nb_3Sn)

Figure 2-13-2

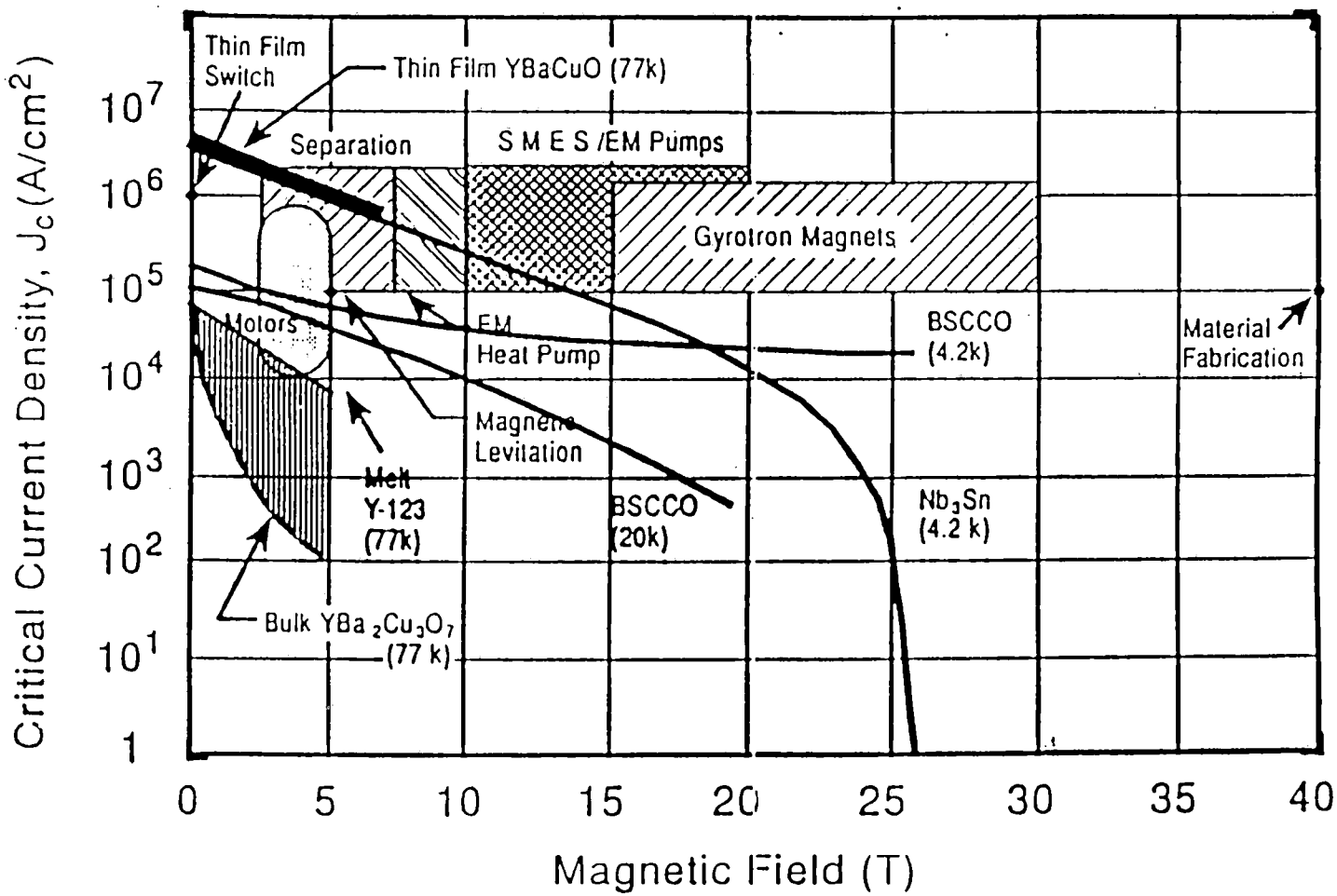

Estimated target critical current density vs. magnetic field values for various superconducting applications

Figure 2-13-3

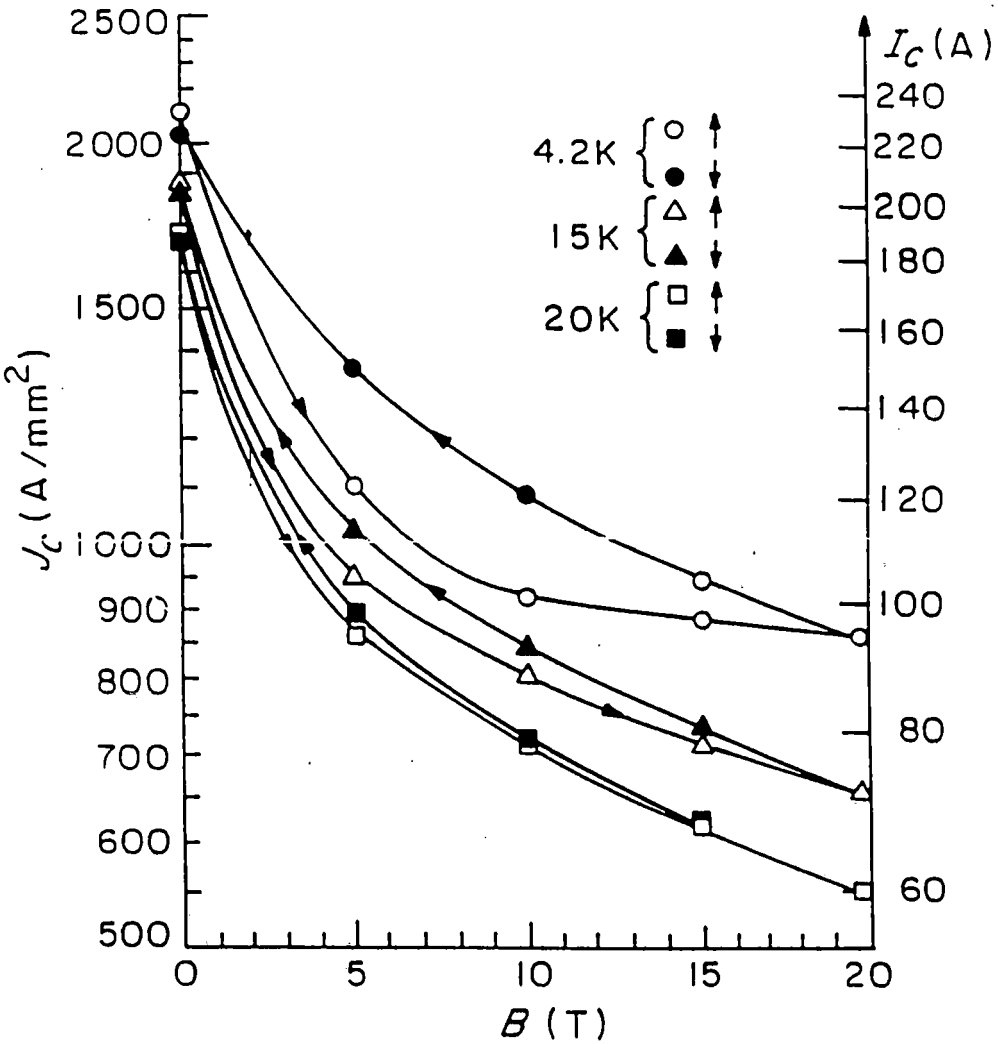

Field dependence of the critical current (Bismuth 2223)

Figure 2-13-4

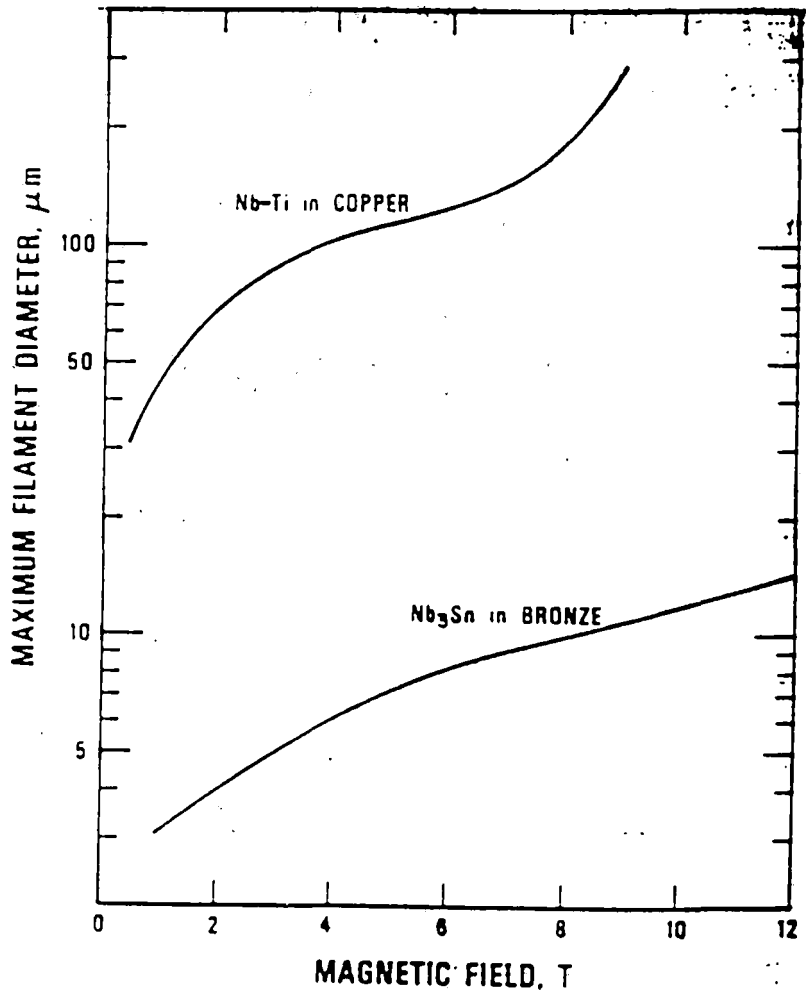

Filament diameter limits for achieving flux-jump stability in Nb-Ti and Nb_3Sn conductors, calculated using the dynamic stability criterion.

Figure 2-14

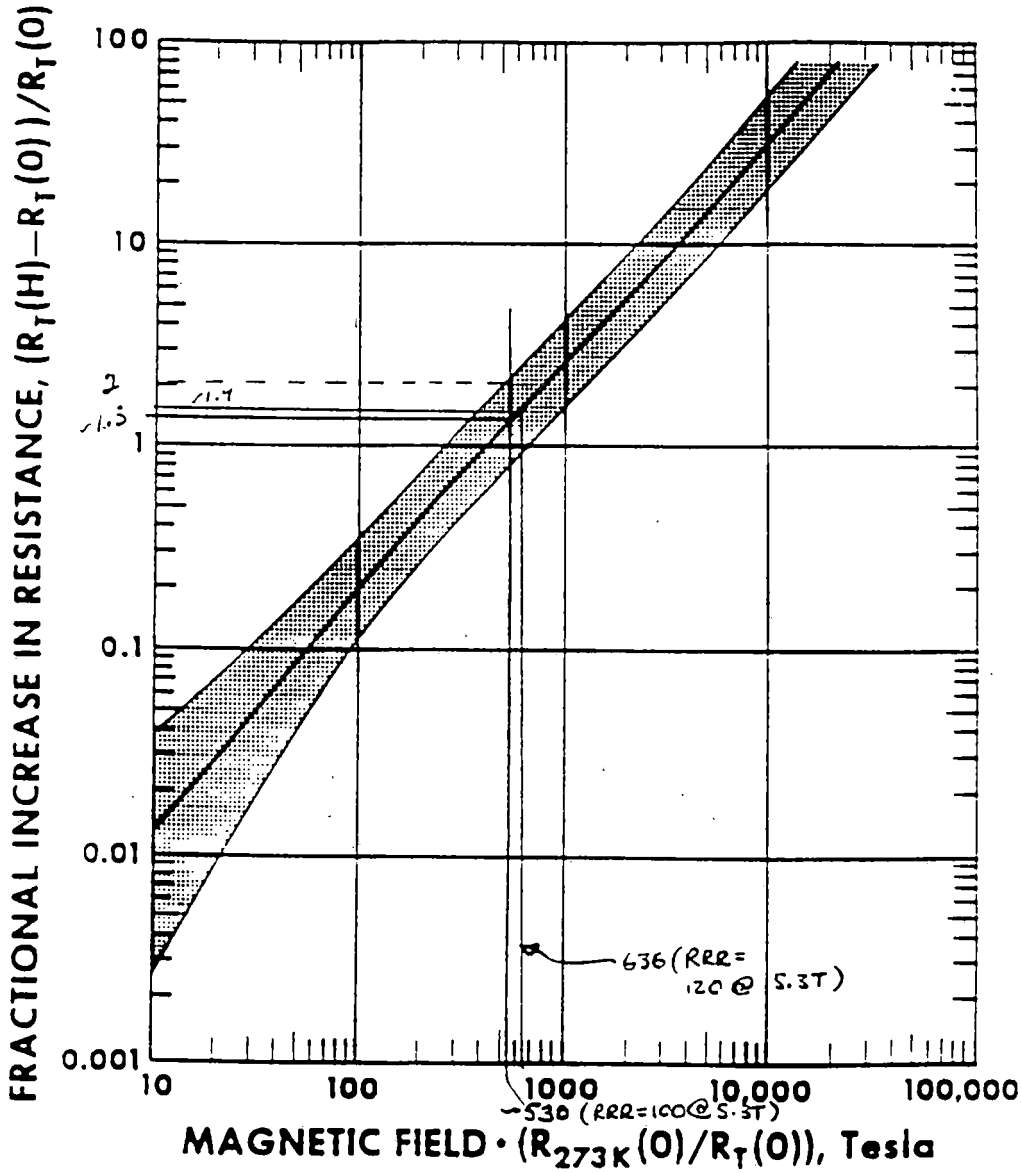

Average curve (heavy line) of the fractional change in electrical resistivity with transverse magnetic field. The uncertainty estimated from the variance of the data is shown by the shaded band.

Figure 2-15

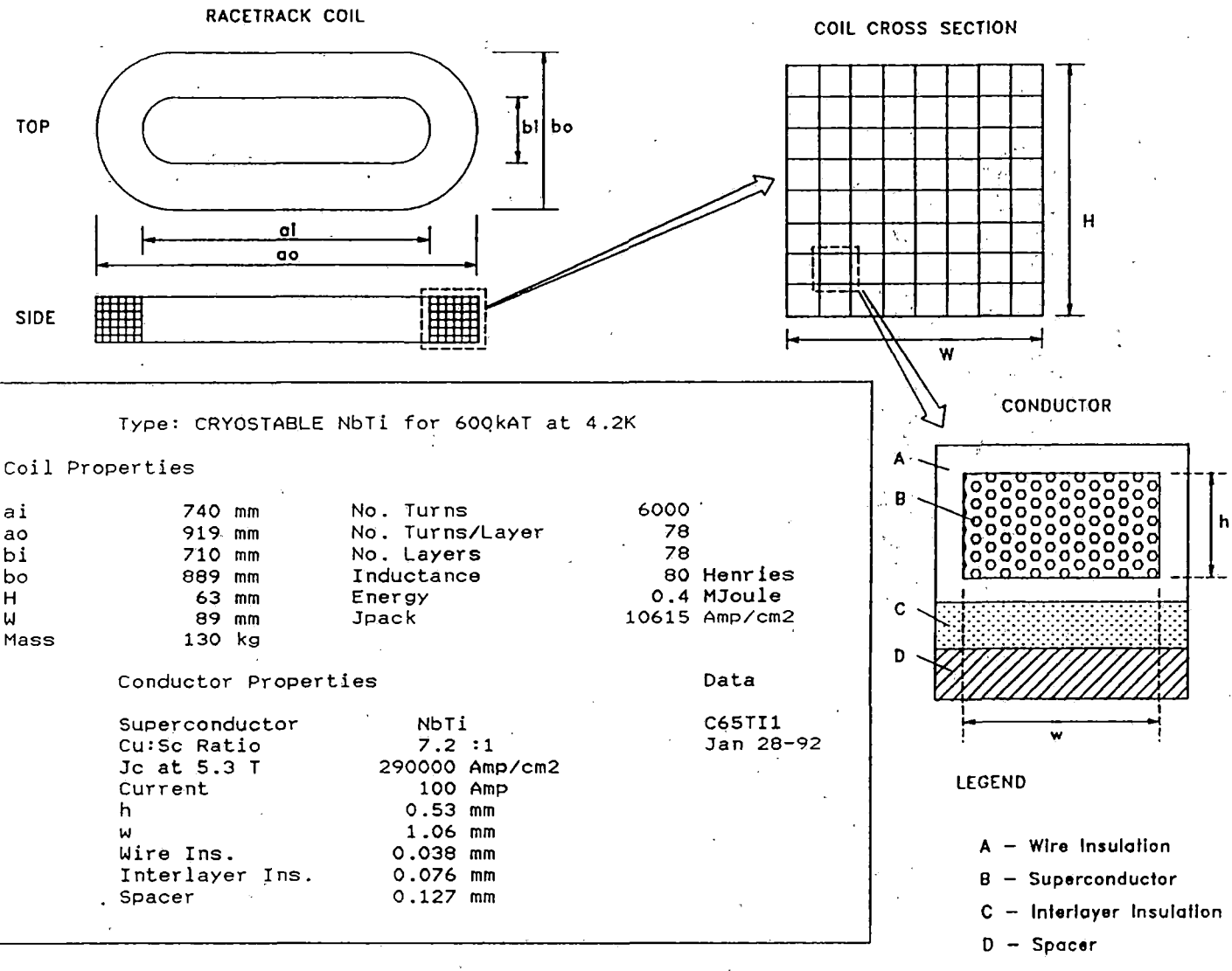

Type: CRYOSTABLE NbTi for 600kAT at 4.2K

Coil Properties

ai	740 mm	No. Turns	6000	
ao	919 mm	No. Turns/Layer	78	
bi	710 mm	No. Layers	78	
bo	889 mm	Inductance	80	Henries
H	63 mm	Energy	0.4	MJoule
W	89 mm	Jpack	10615	Amp/cm2
Mass	130 kg			

Conductor Properties		Data
Superconductor	NbTi	C65TI1
Cu:Sc Ratio	7.2 :1	Jan 28-92
Jc at 5.3 T	290000 Amp/cm2	
Current	100 Amp	
h	0.53 mm	
w	1.06 mm	
Wire Ins.	0.038 mm	
Interlayer Ins.	0.076 mm	
Spacer	0.127 mm	

Conductor and coil design parameters (NbTi – cryostable)

Figure 2-16-1

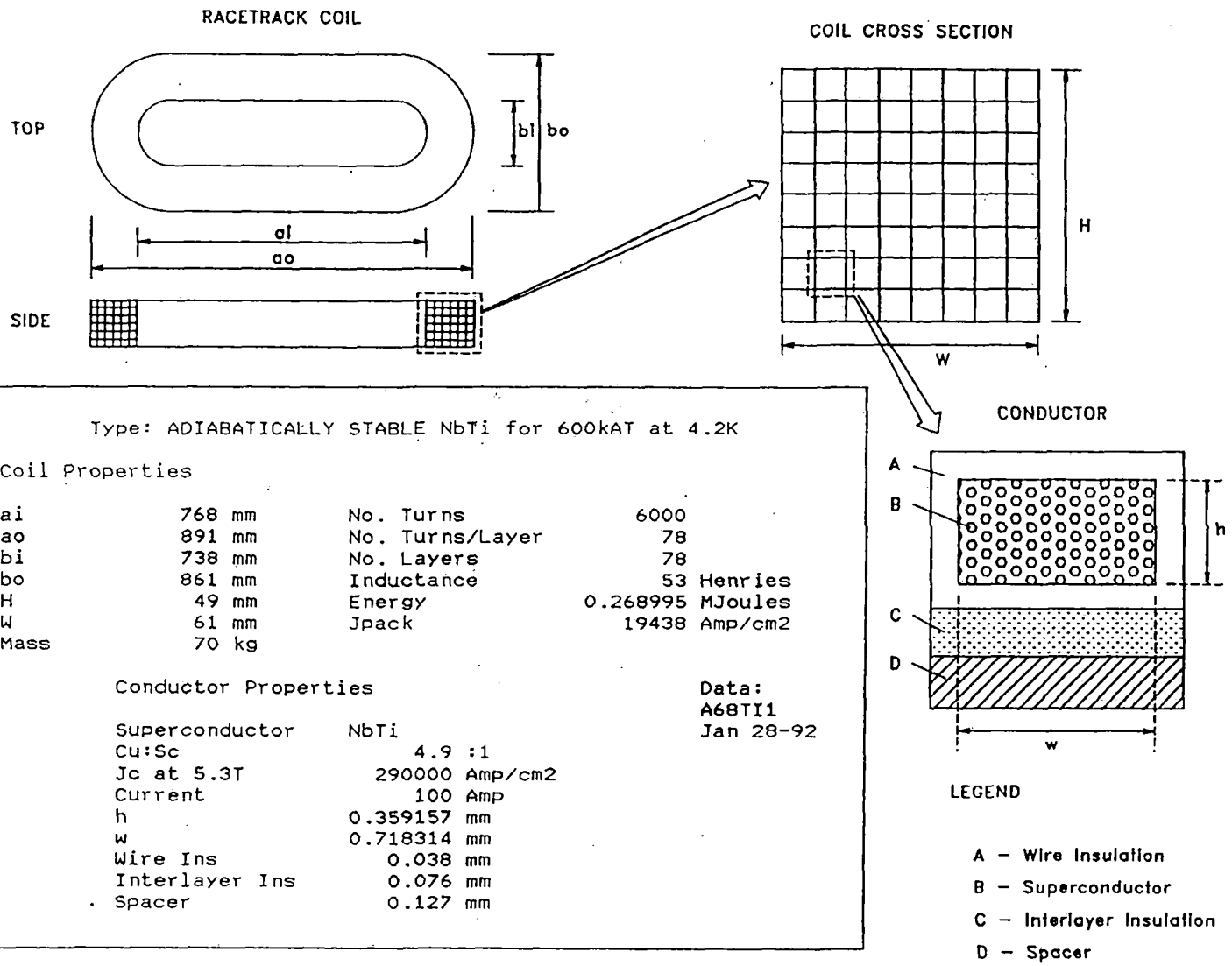

Type: ADIABATICALLY STABLE NbTi for 600kAT at 4.2K

Coil Properties

ai	768 mm	No. Turns	6000	
ao	891 mm	No. Turns/Layer	78	
bi	738 mm	No. Layers	78	
bo	861 mm	Inductance	53	Henries
H	49 mm	Energy	0.268995	MJoules
W	61 mm	Jpack	19438	Amp/cm2
Mass	70 kg			

Conductor Properties

Data: A68TI1 Jan 28-92

Superconductor	NbTi
Cu:Sc	4.9 :1
Jc at 5.3T	290000 Amp/cm2
Current	100 Amp
h	0.359157 mm
w	0.718314 mm
Wire Ins	0.038 mm
Interlayer Ins	0.076 mm
Spacer	0.127 mm

Conductor and coil design parameters (NbTi – adiabatic)

Figure 2-16-2

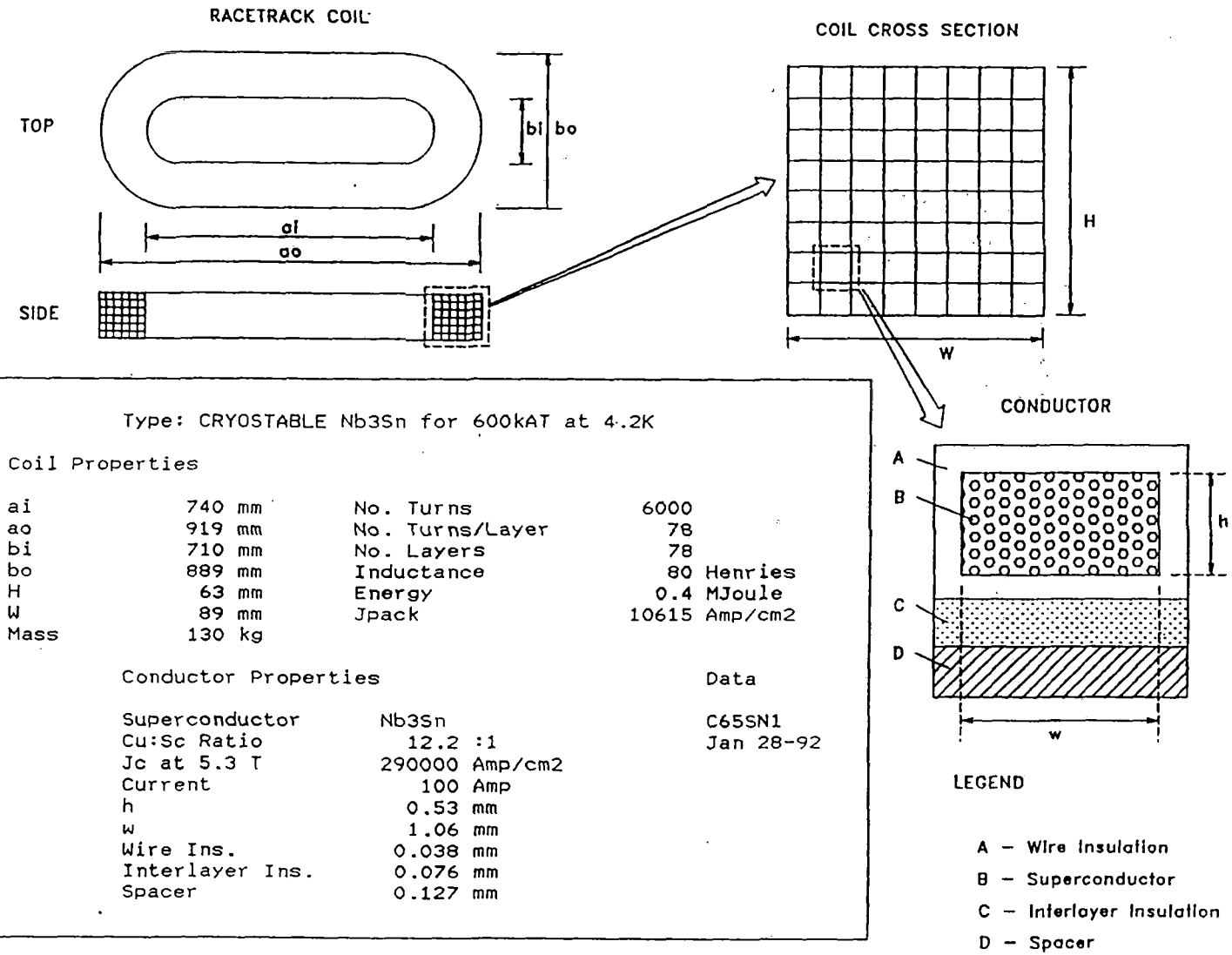

Type: CRYOSTABLE Nb3Sn for 600kAT at 4.2K

Coil Properties

ai	740 mm	No. Turns	6000
ao	919 mm	No. Turns/Layer	78
bi	710 mm	No. Layers	78
bo	889 mm	Inductance	80 Henries
H	63 mm	Energy	0.4 MJoule
W	89 mm	Jpack	10615 Amp/cm2
Mass	130 kg		

Conductor Properties		Data
Superconductor	Nb3Sn	C65SN1
Cu:Sc Ratio	12.2 :1	Jan 28-92
Jc at 5.3 T	290000 Amp/cm2	
Current	100 Amp	
h	0.53 mm	
w	1.06 mm	
Wire Ins.	0.038 mm	
Interlayer Ins.	0.076 mm	
Spacer	0.127 mm	

Conductor and coil design parameters (Nb_3Sn – cryostable)

Figure 2-16-3

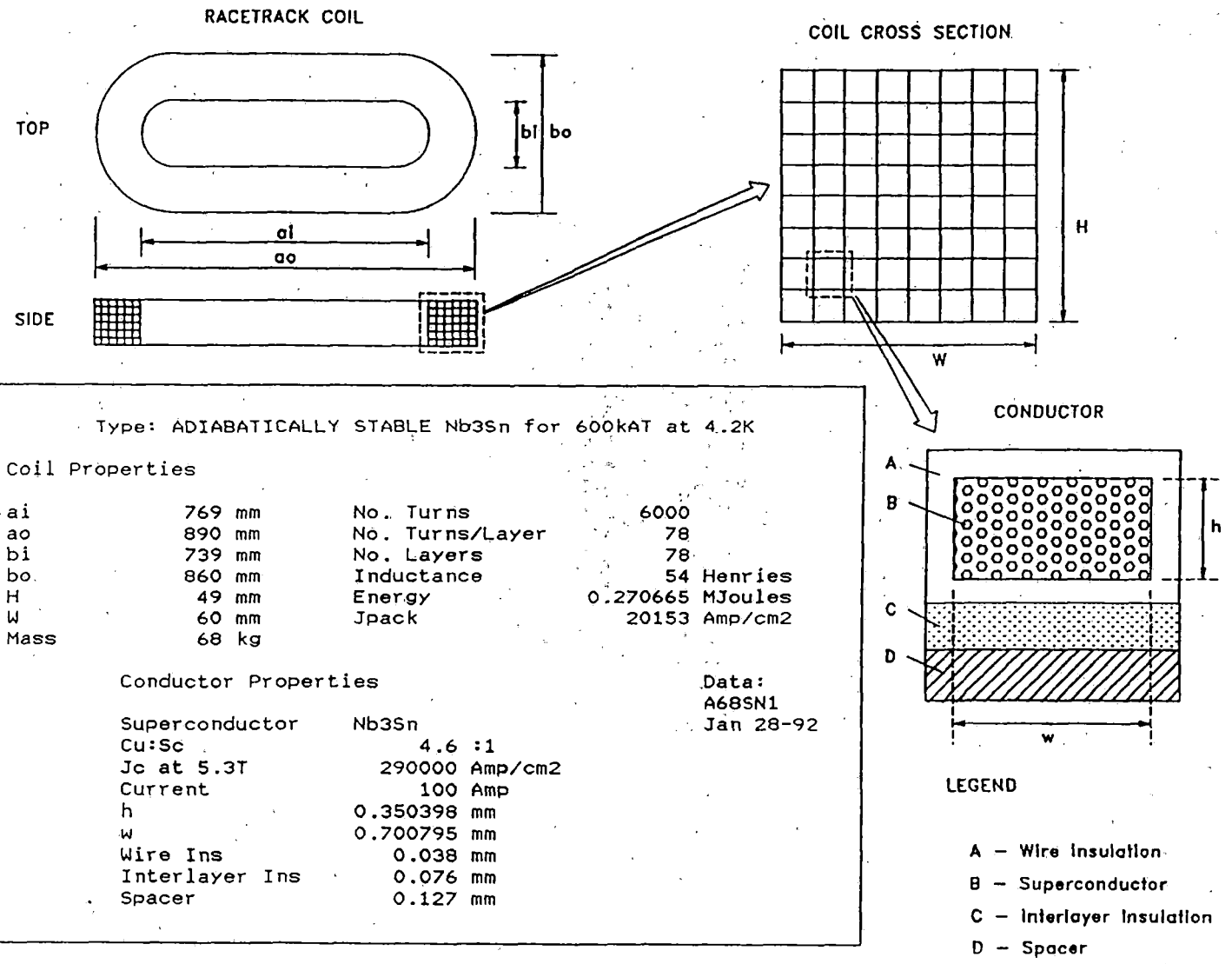

Type: ADIABATICALLY STABLE Nb3Sn for 600kAT at 4.2K

Coil Properties

ai	769 mm	No. Turns	6000
ao	890 mm	No. Turns/Layer	78
bi	739 mm	No. Layers	78
bo	860 mm	Inductance	54 Henries
H	49 mm	Energy	0.270665 MJoules
W	60 mm	Jpack	20153 Amp/cm2
Mass	68 kg		

Conductor Properties

Data: A68SN1 Jan 28-92

Superconductor	Nb3Sn
Cu:Sc	4.6 :1
Jc at 5.3T	290000 Amp/cm2
Current	100 Amp
h	0.350398 mm
w	0.700795 mm
Wire Ins	0.038 mm
Interlayer Ins	0.076 mm
Spacer	0.127 mm

Conductor and coil design parameters (Nb_3Sn – adiabatic)

Figure 2-16-4

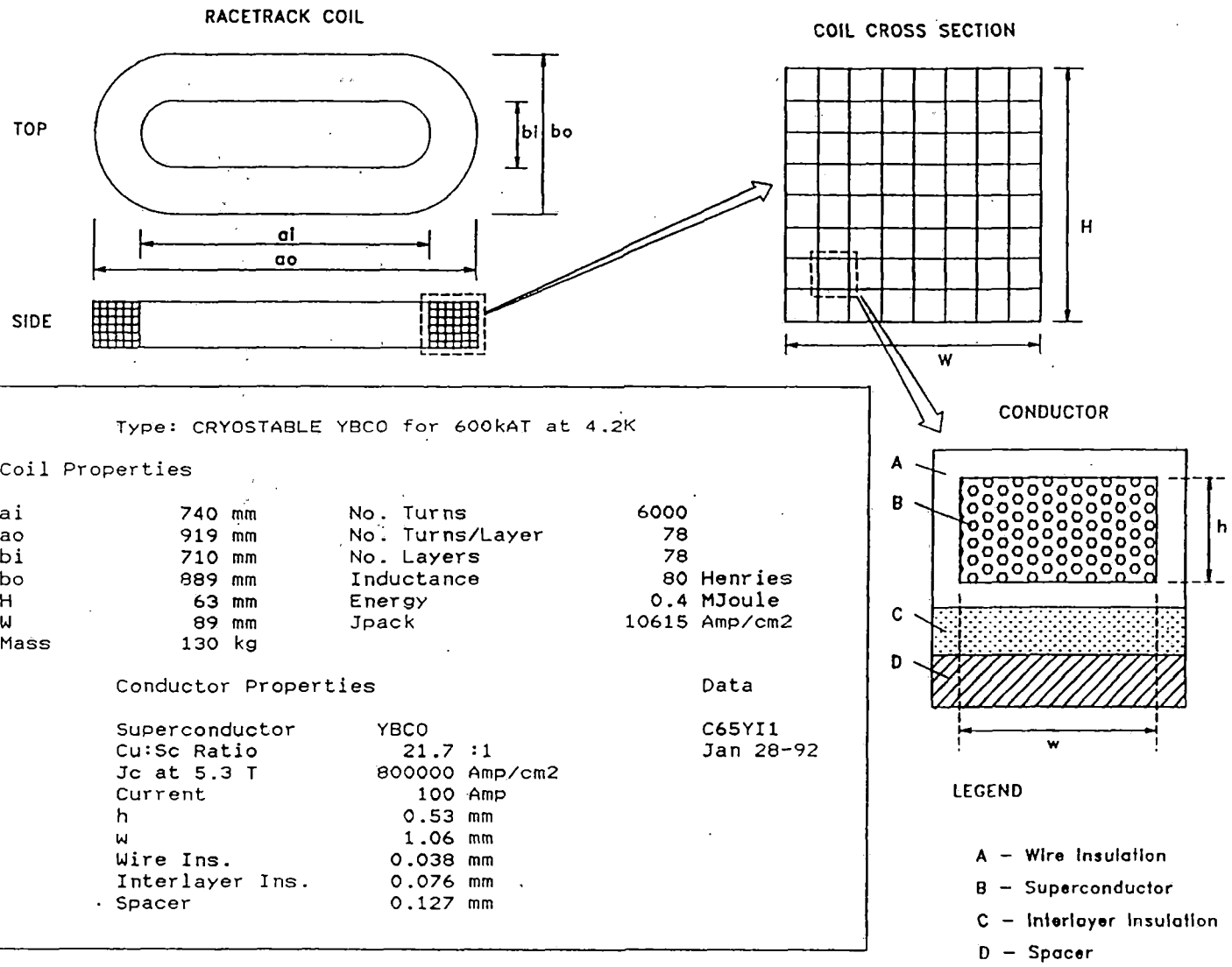

Type: CRYOSTABLE YBCO for 600kAT at 4.2K

Coil Properties

ai	740 mm	No. Turns	6000
ao	919 mm	No. Turns/Layer	78
bi	710 mm	No. Layers	78
bo	889 mm	Inductance	80 Henries
H	63 mm	Energy	0.4 MJoule
W	89 mm	Jpack	10615 Amp/cm2
Mass	130 kg		

Conductor Properties		Data
Superconductor	YBCO	C65YI1
Cu:Sc Ratio	21.7 :1	Jan 28-92
Jc at 5.3 T	800000 Amp/cm2	
Current	100 Amp	
h	0.53 mm	
w	1.06 mm	
Wire Ins.	0.038 mm	
Interlayer Ins.	0.076 mm	
Spacer	0.127 mm	

Conductor and coil design parameters (YBCO – cryostable)

Figure 2-16-5

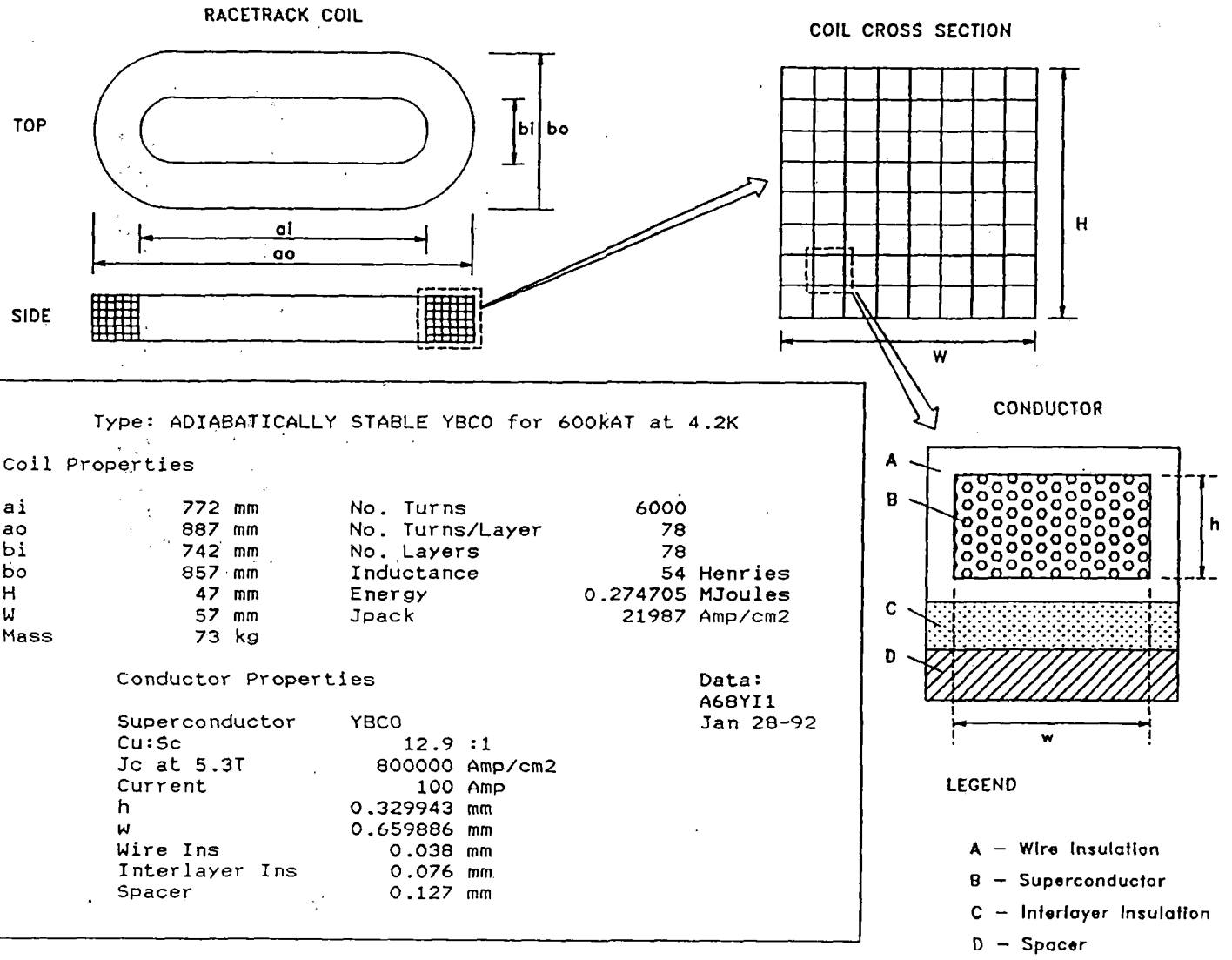

Type: ADIABATICALLY STABLE YBCO for 600kAT at 4.2K

Coil Properties

ai	772 mm	No. Turns	6000
ao	887 mm	No. Turns/Layer	78
bi	742 mm	No. Layers	78
bo	857 mm	Inductance	54 Henries
H	47 mm	Energy	0.274705 MJoules
W	57 mm	Jpack	21987 Amp/cm2
Mass	73 kg		

Conductor Properties

Data: A68YI1 Jan 28-92

Superconductor	YBCO
Cu:Sc	12.9 :1
Jc at 5.3T	800000 Amp/cm2
Current	100 Amp
h	0.329943 mm
w	0.659886 mm
Wire Ins	0.038 mm
Interlayer Ins	0.076 mm
Spacer	0.127 mm

Conductor and coil design parameters (YBCO – adiabatic)

Figure 2-16-6

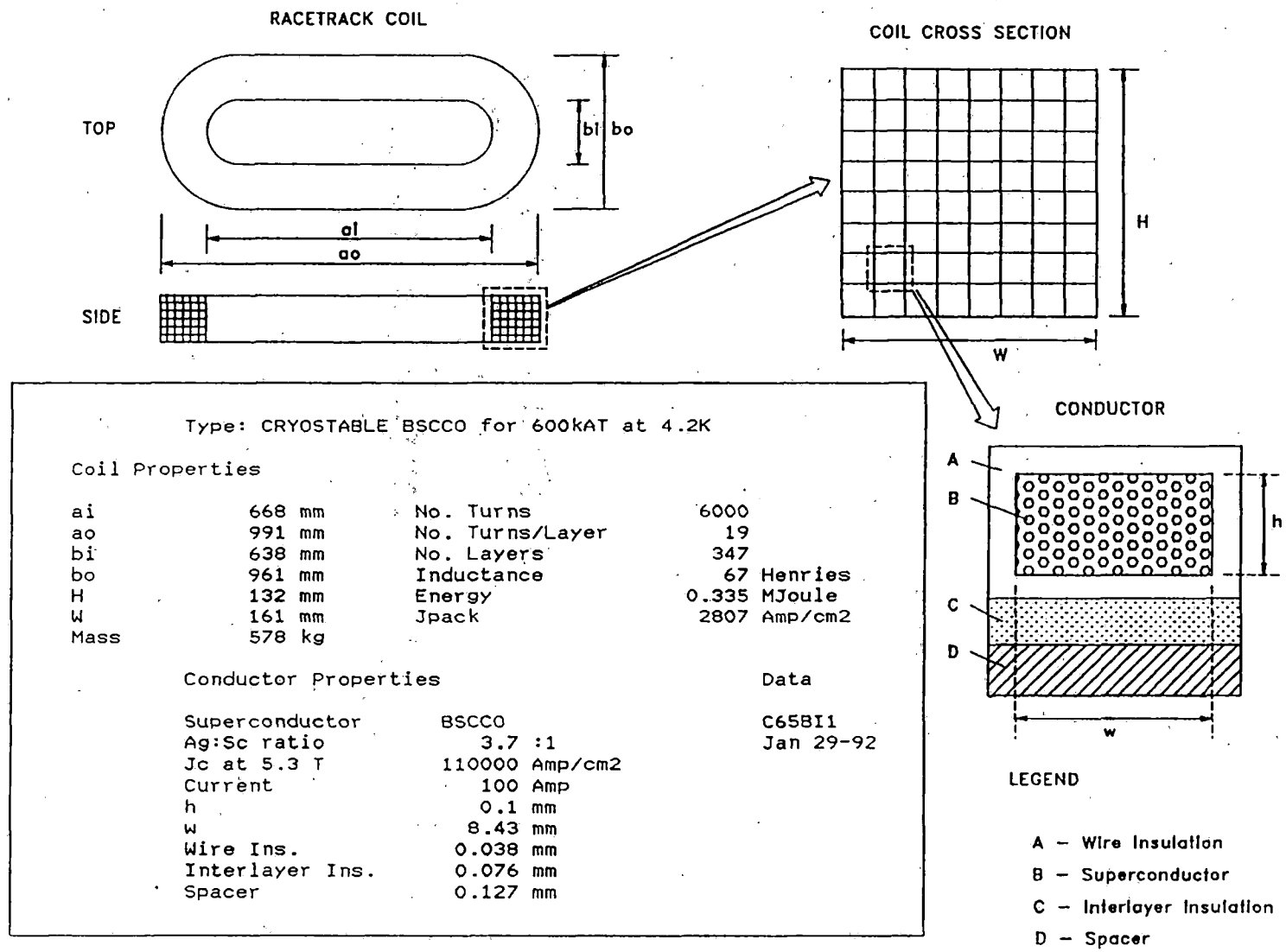

Type: CRYOSTABLE BSCCO for 600kAT at 4.2K

Coil Properties

ai	668 mm	No. Turns	6000	
ao	991 mm	No. Turns/Layer	19	
bi	638 mm	No. Layers	347	
bo	961 mm	Inductance	67	Henries
H	132 mm	Energy	0.335	MJoule
W	161 mm	Jpack	2807	Amp/cm2
Mass	578 kg			

Conductor Properties		Data
Superconductor	BSCCO	C65BI1
Ag:Sc ratio	3.7 :1	Jan 29-92
Jc at 5.3 T	110000 Amp/cm2	
Current	100 Amp	
h	0.1 mm	
w	8.43 mm	
Wire Ins.	0.038 mm	
Interlayer Ins.	0.076 mm	
Spacer	0.127 mm	

Conductor and coil design parameters (Bismuth 2223 – cryostable)

Figure 2-16-7

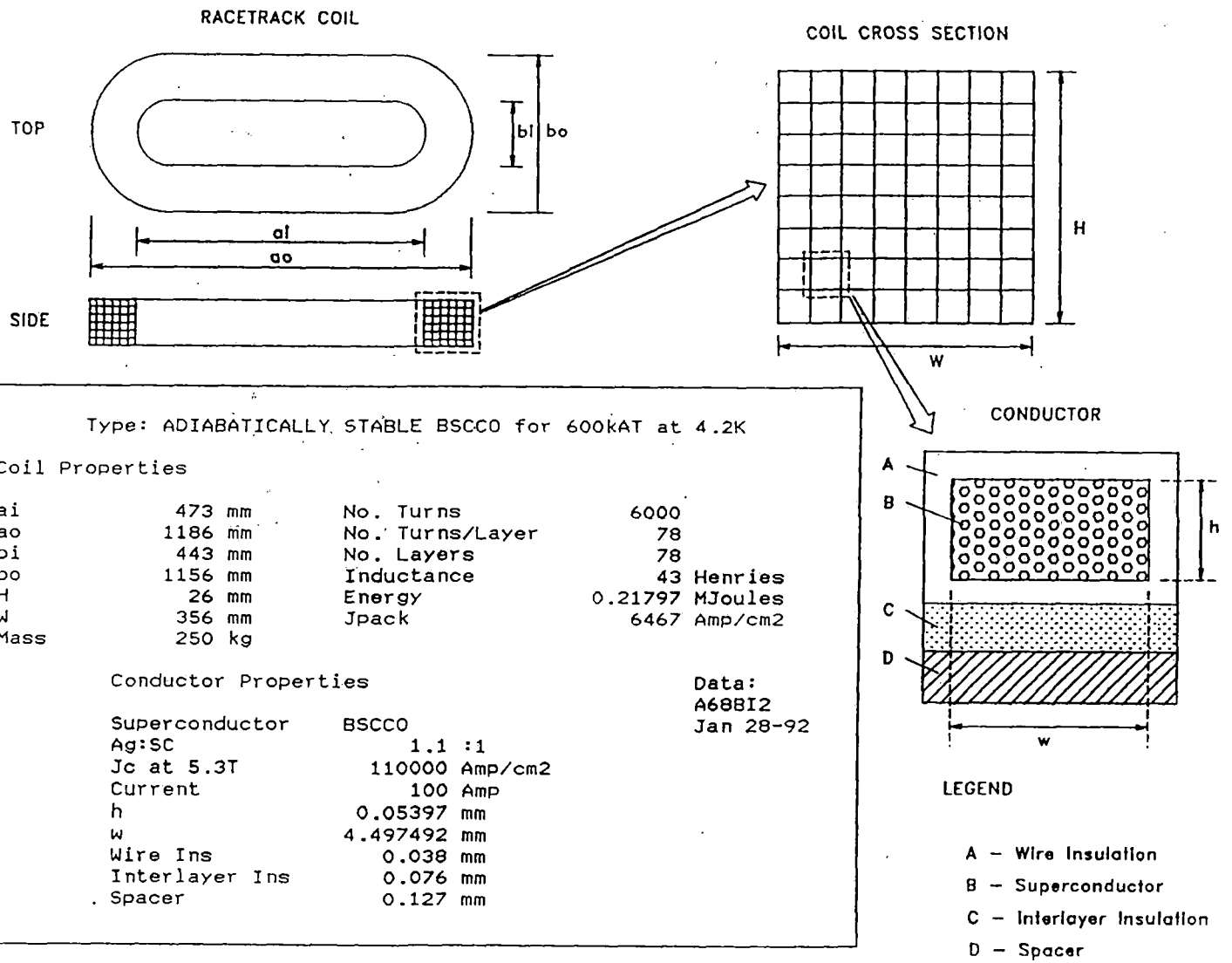

Type: ADIABATICALLY STABLE BSCCO for 600kAT at 4.2K

Coil Properties

ai	473 mm	No. Turns	6000
ao	1186 mm	No. Turns/Layer	78
bi	443 mm	No. Layers	78
bo	1156 mm	Inductance	43 Henries
H	26 mm	Energy	0.21797 MJoules
W	356 mm	Jpack	6467 Amp/cm2
Mass	250 kg		

Conductor Properties

Data: A68BI2 Jan 28-92

Superconductor	BSCCO
Ag:SC	1.1 :1
Jc at 5.3T	110000 Amp/cm2
Current	100 Amp
h	0.05397 mm
w	4.497492 mm
Wire Ins	0.038 mm
Interlayer Ins	0.076 mm
Spacer	0.127 mm

Conductor and coil design parameters (Bismuth 2223 – adiabatic)

Figure 2-16-8

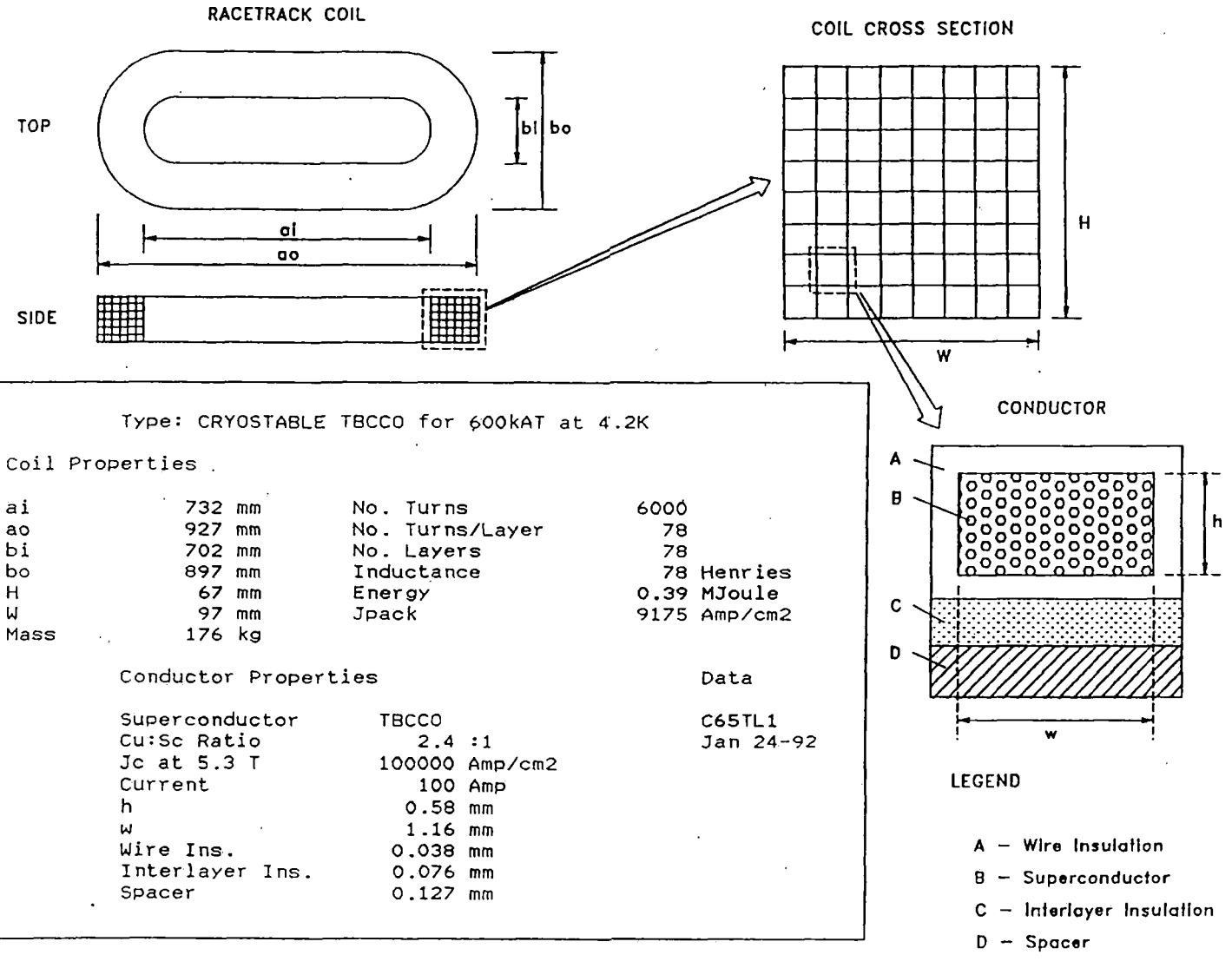

Type: CRYOSTABLE TBCCO for 600kAT at 4.2K

Coil Properties

ai	732 mm	No. Turns	6000	
ao	927 mm	No. Turns/Layer	78	
bi	702 mm	No. Layers	78	
bo	897 mm	Inductance	78	Henries
H	67 mm	Energy	0.39	MJoule
W	97 mm	Jpack	9175	Amp/cm2
Mass	176 kg			

Conductor Properties		Data
Superconductor	TBCCO	C65TL1
Cu:Sc Ratio	2.4 :1	Jan 24-92
Jc at 5.3 T	100000 Amp/cm2	
Current	100 Amp	
h	0.58 mm	
w	1.16 mm	
Wire Ins.	0.038 mm	
Interlayer Ins.	0.076 mm	
Spacer	0.127 mm	

Conductor and coil design parameters (TBCCO – cryostable)

Figure 2-16-9

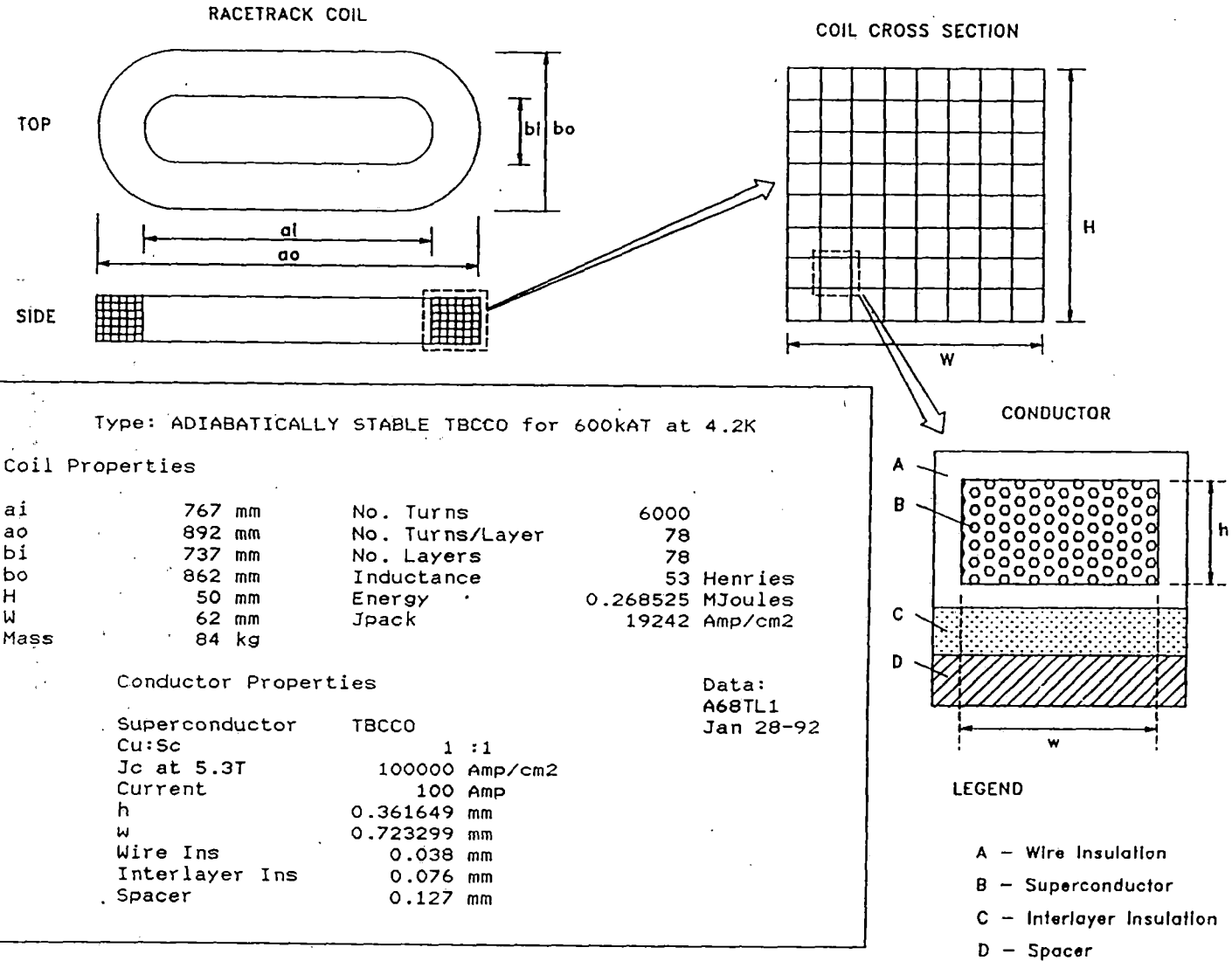

Type: ADIABATICALLY STABLE TBCCO for 600kAT at 4.2K

Coil Properties

ai	767 mm	No. Turns	6000
ao	892 mm	No. Turns/Layer	78
bi	737 mm	No. Layers	78
bo	862 mm	Inductance	53 Henries
H	50 mm	Energy	0.268525 MJoules
W	62 mm	Jpack	19242 Amp/cm2
Mass	84 kg		

Conductor Properties

Data: A68TL1 Jan 28-92

Superconductor	TBCCO
Cu:Sc	1 :1
Jc at 5.3T	100000 Amp/cm2
Current	100 Amp
h	0.361649 mm
w	0.723299 mm
Wire Ins	0.038 mm
Interlayer Ins	0.076 mm
Spacer	0.127 mm

Conductor and coil design parameters (TBCCO – adiabatic)

Figure 2-16-10

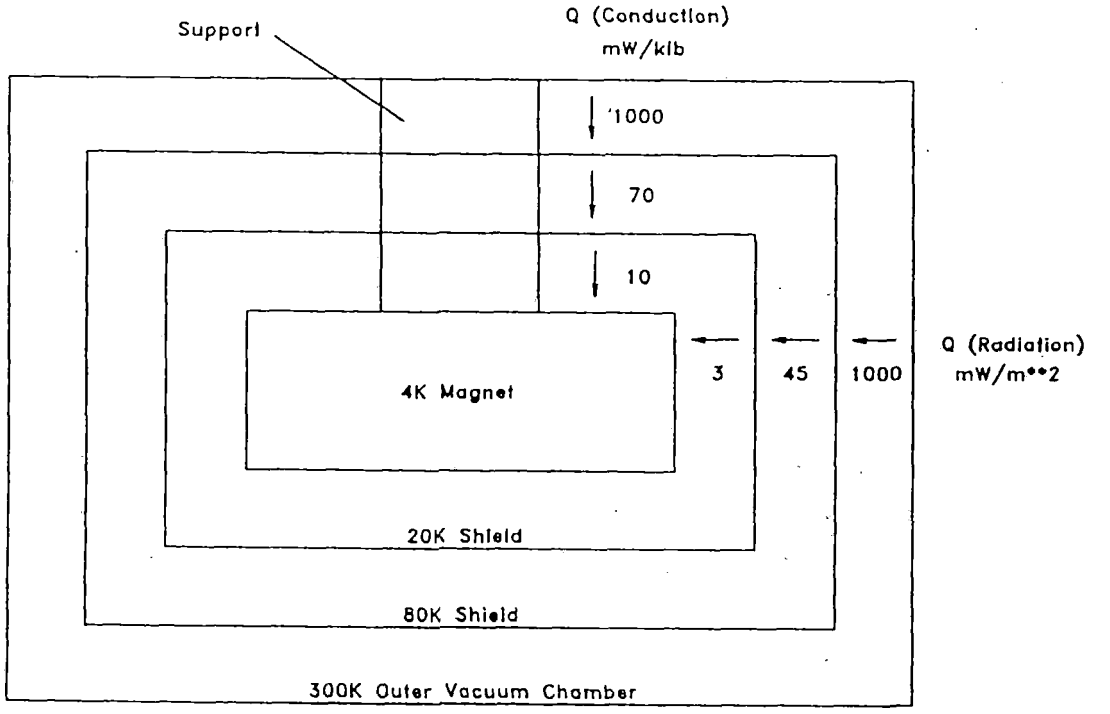

CRYOGENICS:

- 4K magnet cooled by pool boiling or 4K refrigerator.
- 20K shield and support intercept cooled by 20K refrigerator.
- 80K shield and support intercept and eddy current shield cooled by LN2 or 80K refrigerator.

Magnet/cryostat: cryogenic description (System 1 – refrigerated 20K heat shield)

Figure 2-17

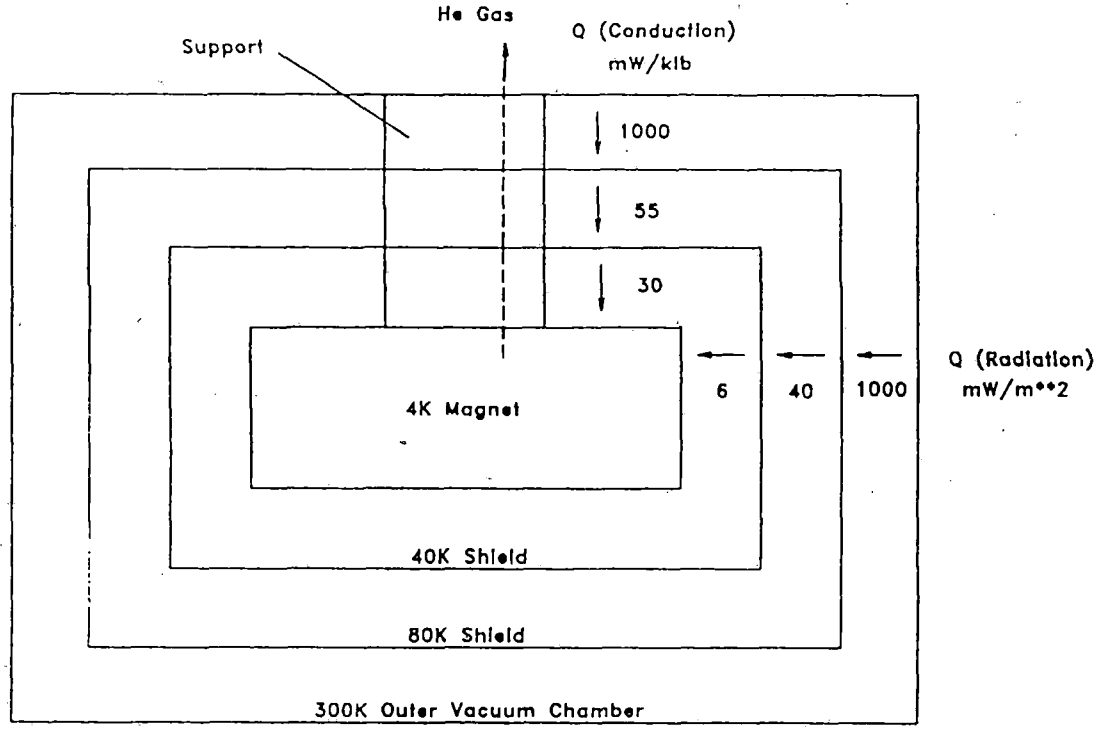

CRYOGENICS:

- 4K magnet must be cooled by pool boiling.
- 40K shield and support intercept cooled by vapor from pool boiling.
- 80K shield and support intercept and eddy currents shield cooled by LN2 or 80K refrigerator.

Magnet/cryostat: cryogenic description (System 2 – pool boiling, no refrigerators required)

Figure 2-18

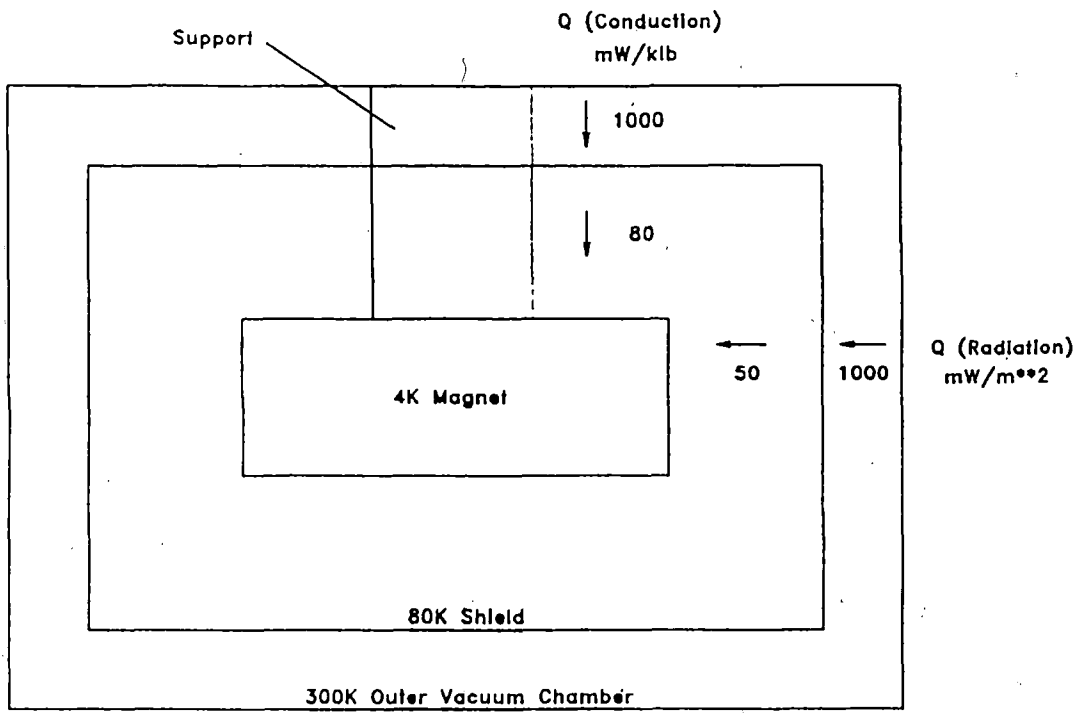

CRYOGENICS:

- 4K magnet cooled by pool boiling or 4K refrigerator.
- 80K shield and support intercept and eddy current shield cooled by LN2 or 80K refrigerator.

Magnet/cryostat: cryogenic description (System 3 – 80K shield only)

Figure 2-19

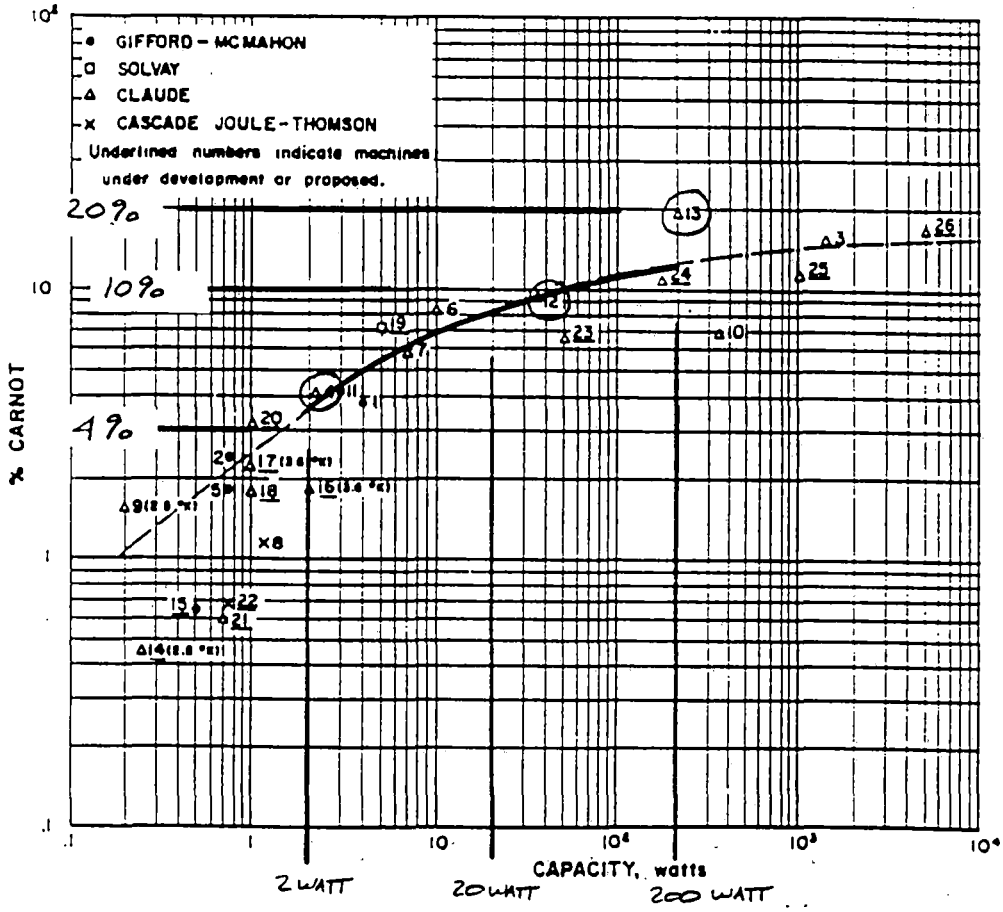

Efficiency of liquid helium temperature refrigerators
Figure 2-20

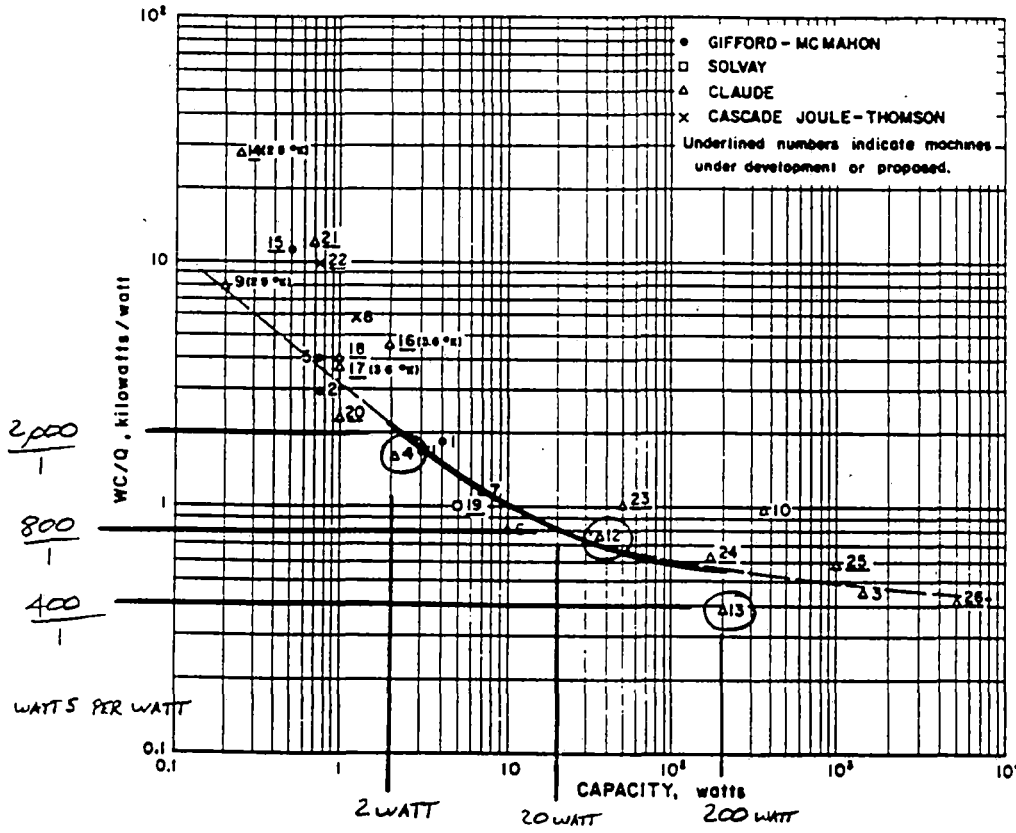

Specific work requirements of liquid helium temperature refrigerators
Figure 2-21

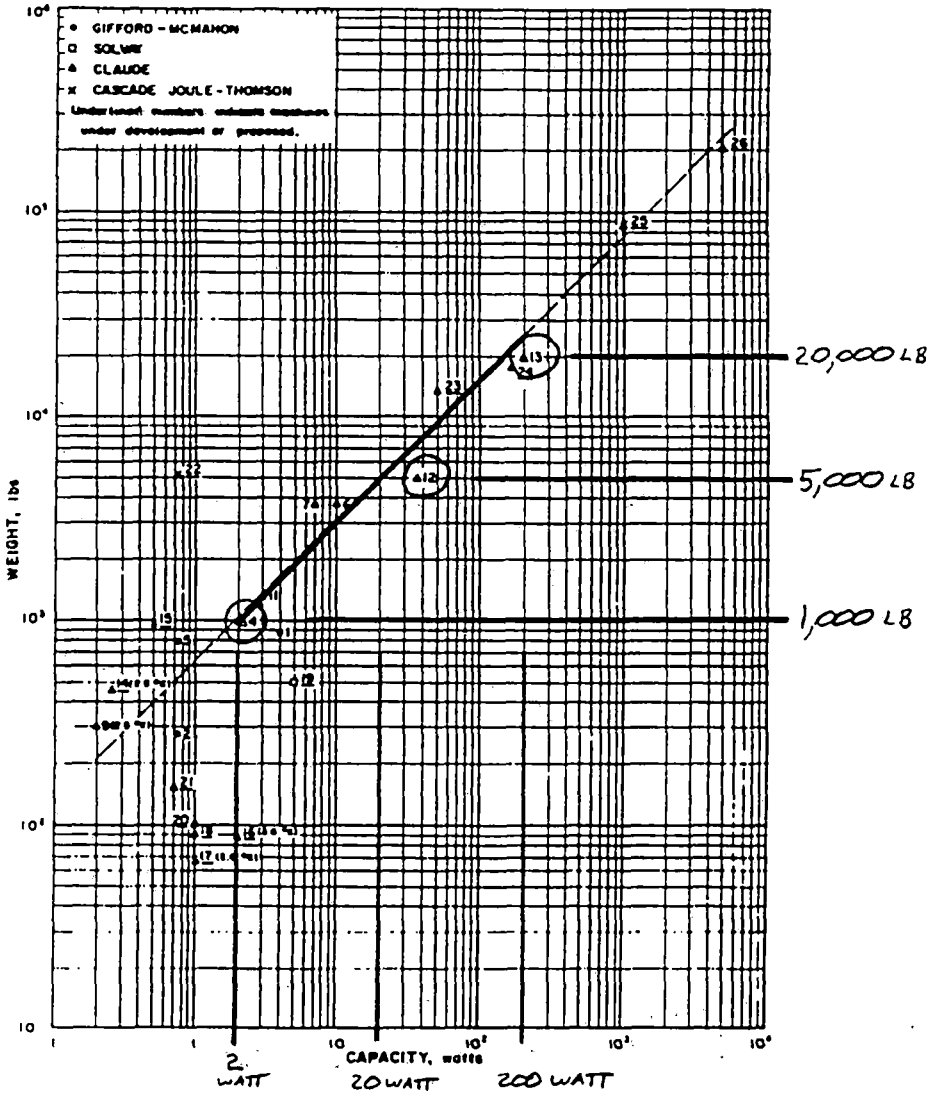

Weight of liquid helium temperature refrigerators
Figure 2-22

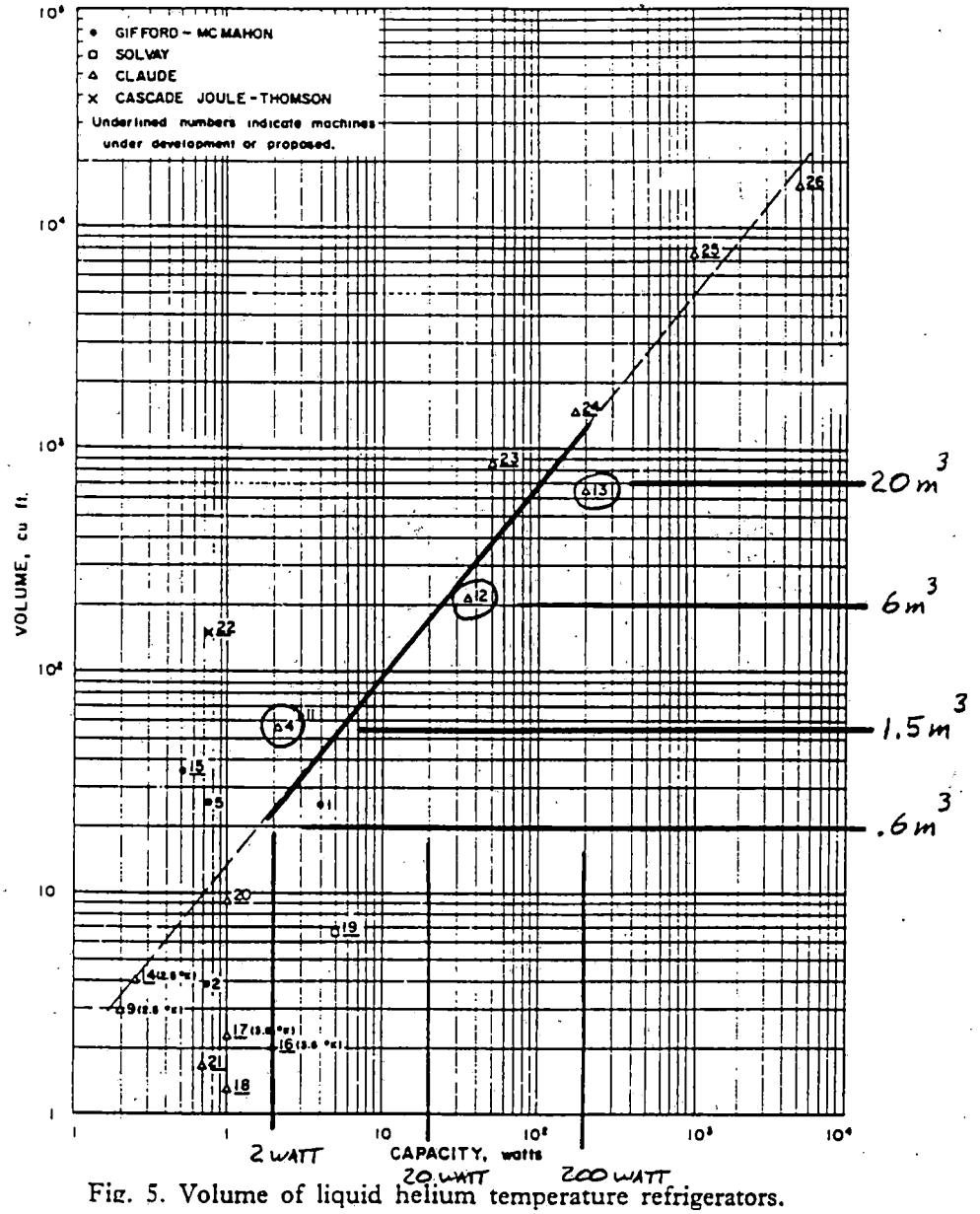

Fig. 5. Volume of liquid helium temperature refrigerators.

Volume of liquid helium temperature refrigerators
Figure 2-23

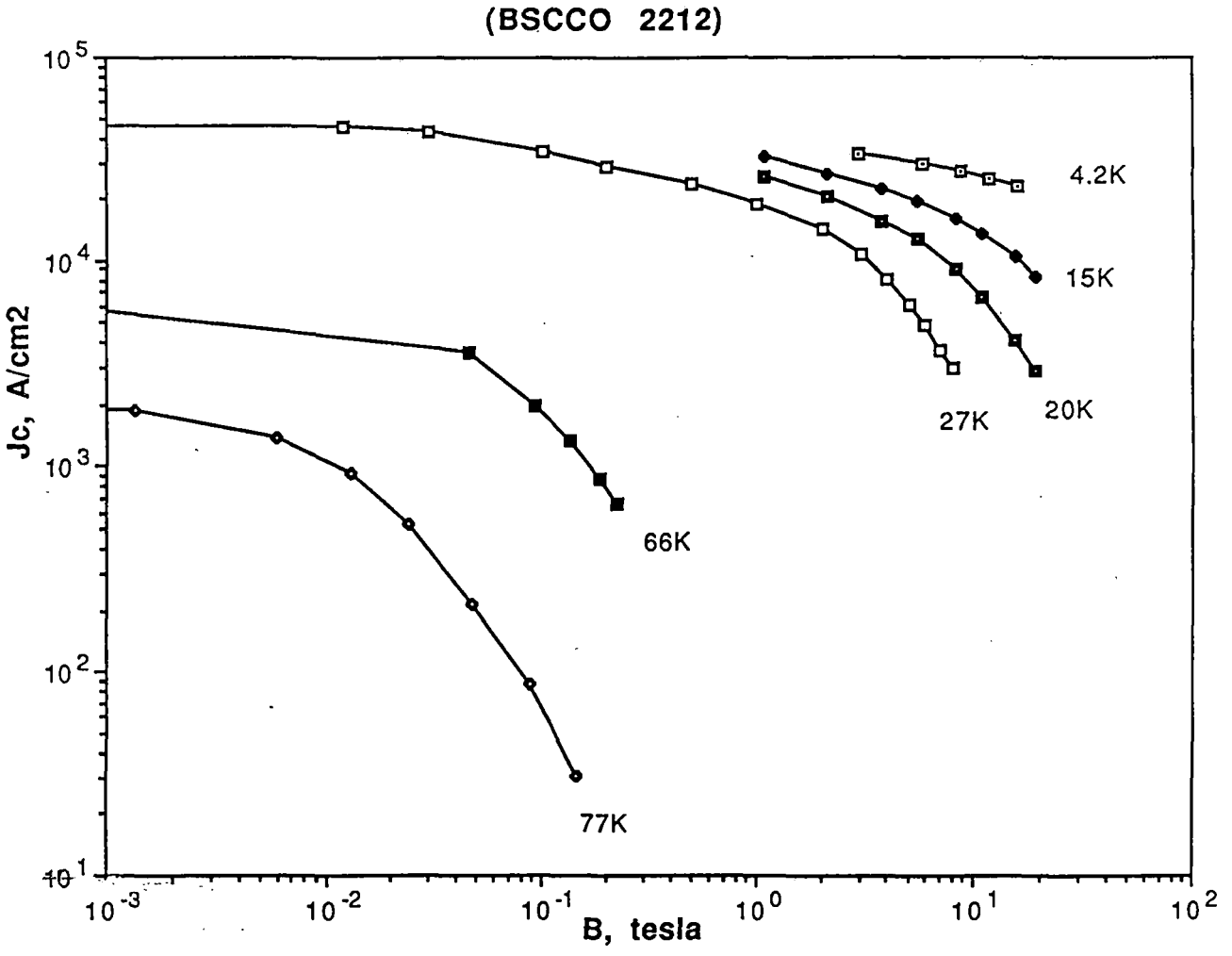

Typical Behavior of BSCCO as a Function of Field and Temperature

Figure 2-24

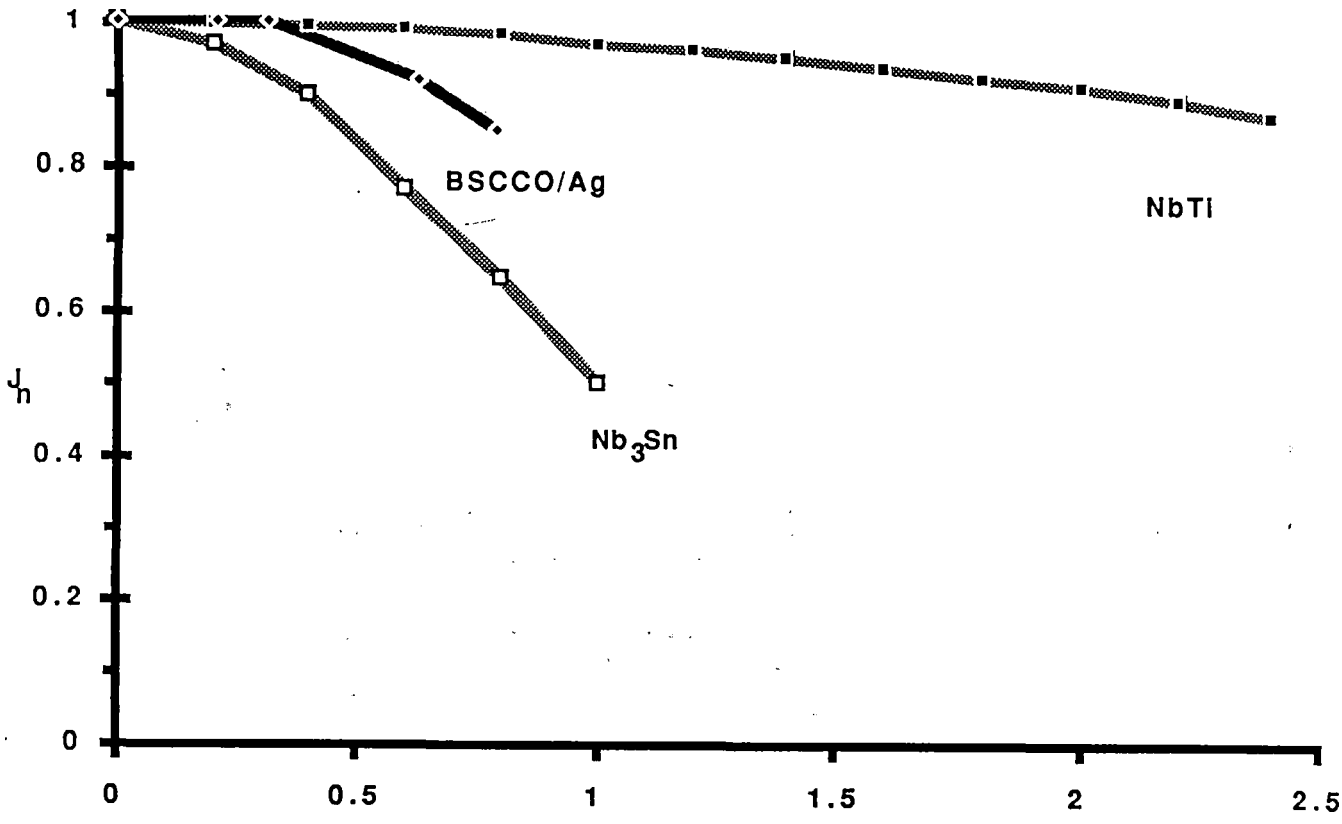

Normalized Critical Current vs. Strain for Low Temperature Superconductors and BSCCO

Figure 2-25

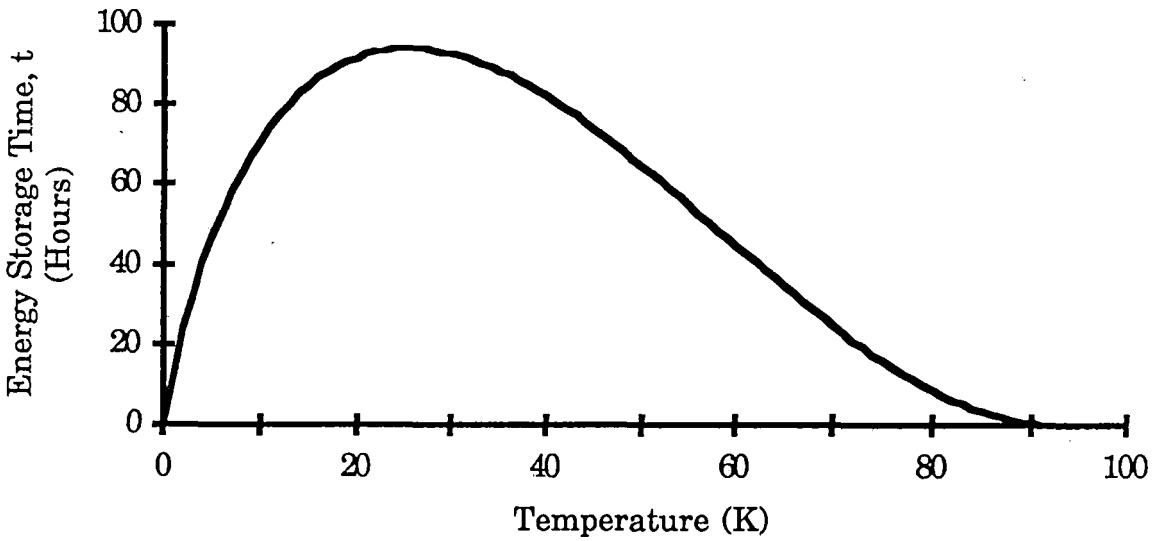

Energy-Storage Time for a 25.7 Henry Coil with a 20% of Carnot Efficient Refrigerator Attached
I = 100 A, Losses from Current Leads Included

Figure 2-26

GUIDEWAY EVALUATION

3.1 Existing Systems Integration

3.1.1 Description of Guideway Configurations

The five guideway configurations chosen for this evaluation are described in detail below and shown in Figures 3-1 thru 3-15. The five configurations are:

Type I	Flat-top Guideway
Type II	Wrap around or Clamp Type Guideway
Type III	Magnaplane Guideway
Type IV	Inverted "T" Guideway
Type V	U-shaped or Channel Guideway

The levitation and propulsion systems for each of these configurations has been designed and positioned on the guideway for optimum operation. The dimensions of the guideway are based on the requirements of these systems. Each of the guideways offers a unique solution for the future of Maglev transportation systems; and any of the five can be designed to provide a reliable means of mass transportation. The comparisons provided herein will demonstrate relative advantages and disadvantages of each of the configurations.

The five guideways have similar characteristics: materials of construction , construction technology required, installation techniques, and support systems. The base structural element for all five is a precast, prestressed concrete girder supplied by a vendor, pre-wired, control cables installed, aluminum levitation strips secured and grouted in position, linear synchronous motor (LSM) secured and grouted in position, assembly tested to ensure continuity for each girder, and the electronic/controls connections to the next girder prepared and ready for field installation. The entire assembly for a single girder is shipped as a unit for installation at the construction site.

All of the guideway configurations are designed as simply supported beams. A simply supported beam implies that there are no continous spans over column supports, that the maximum design moment occurs at the center of the span, and that the top of the girder is always in compression. Maintaining the top of the girder in compression minimizes the need for reinforcing in the top flange and permits the use of non-metal reinforcing. In order to limit the potential interaction between the superconducting levitation and propulsion systems and any metal reinforcing or anchor bolts, a minimum space of one meter is required between the superconducting systems and the reinforcing material and anchor bolts; therefore, fiber-reinforced plastic (FRP) reinforcing is used in the top flange and in the webs of the girder and fiber-reinforced plastic (FRP) bolts are used, to secure the aluminum levitation strips and the LSM in position.

The girders are designed to rest on two mechanically adjustable supports. Each of these items may be adjusted vertically to level the girder during installation and to maintain the girders level during operation. A sensor system, to alert operators that the guideway supports are not within level tolerances, will be utilized to aide the maintenance operations for the life of the guideway system. The sensors will also continuously monitor the girder to alert operators to the possibility that the girders are responding differently to the loads imposed during operation. The development of the sensor system and the mechanically adjustable supports are not a part of this study, but a cost has been included in the guideway costs provided later.

The girders are designed for expansion and contraction due to temperature variations. One end (fixed end) of the girder is secured by a steel pin that is cast-in-place in the concrete support and fits within a steel sleeve in the girder; the horizontal tolerance for movement laterally and longitudinally is five millimeters. The other end (sliding end) of the girder is secured by a steel pin that also is cast-in-place in the concrete support and fits within a steel channel in the girder; the lateral horizontal tolerance for movement is five millimeters and the longitudinal tolerance for movement is fifty millimeters. The longitudinal expansion and/or contraction of the girder is dependent on the change in temperature that the guideway will experience. For the purposes of this report a one hundred degree (F) differential has been chosen. The girders will be arranged such that both girders on a column support will have

either fixed or sliding ends. This will cause the forces created on the structural system at a particular column support to be in opposite directions and reduce the net effects of temperature variations. The effects of temperature variations from the top to the bottom of the girder have not been investigated at this time. However, a cost to paint the top surface of the guideway "white" in order to help minimize the temperature difference between the top and bottom flanges has been included in the guideway costs provided later.

The elevation criteria for each guideway requires a minimum clearance above roadways similar to bridge overpasses. Figure 3-16 defines the minimum vertical clearance from the ground or bridge deck to the underside of the guideway girder. The minimum clearances then vary from 4.5-meters (fifteen feet) near ground level to 10.7-meters (35-feet) above a bridge deck. The elevation of the top of the guideway will vary according to the depth of the cross-section required for the specific span.

The following describes each of the configurations in greater detail and provides additional information on the constructibility of each guideway.

TYPE I (Reference Figure 3-1)

The Type I guideway is a flat-top configuration and is the simplest of all the guideways to design, fabricate and install. The basic structural shape that provides support is a rectangular box beam with two rectangular voids separated by a central web. The girder will be cast with areas blocked out for the installation of the aluminum levitation ladders and the LSM assembly. The fabrication process will include casting the girder, drilling and setting the FRP anchor bolts in epoxy, setting the aluminum levitation ladders and filling the void area with non-shrink grout providing a smooth, level surface.

The level installation of the LSM assembly is critical to the optimum operation of the propulsion system. In order to set the LSM as level as possible, the area of the block-out is formed deeper than the aluminum tray. A non-shrink grout leveling pad is poured first and allowed to harden. This will account for any irregularities that may be

encountered for each individual girder. The motor assembly is placed on the level grout pad and secured using the FRP anchor bolts, which are located by the actual dimensions of the assembly. The area where the anchor bolts are located along each side of the assembly is grouted level with the top of the girder and the top of the LSM. The surface of the finished product is a level, plane surface without obstructions.

The guideway is elevated on either a single or a double column support. See Figures 3-2 and 3-3. The double column support is connected at the top with a precast concrete tie-beam that is designed as a pin connection at both ends. The two columns act together for lateral loads but are independent for vertical and longitudinal loads.

One of the objections to this guideway configuration is the perception that nothing "visible" is keeping the vehicle from sliding off the guideway.

TYPE II (Reference Figure 3-4)

The Type II guideway is a wrap-around or clamp type configuration. The basic structural shape providing support is an I-shape with flange top and bottom and a single center web. The girder will be cast with areas blocked out for the installation of the aluminum levitation ladders. The LSM is divided in half and is mounted below the flange on each side of the girder and levelled using the installation bolts and shims. Grouting will be required for the levitation strips only. All bolts will be FRP, as was the case for the Type I.

The aluminum levitation ladders are installed as in Type I. The sides of the top flange are deepened to allow the installation of an aluminum strip to be used in conjunction with magnets mounted of the vehicle to maintain the horizontal alignment of the vehicle. A minimum clearance of 500-millimeters is provided below the top flange to allow room for the vehicle magnet assembly and structure. The bottom flange was "filled" in to help

provide a better bearing area at the supports. The top surface of the guideway is a level, plane surface without obstructions.

The wrap-around effect offers greater confidence that the vehicle will stay with the guideway than any of the other guideway configurations.

The guideway is elevated the same as the Type I. See Figures 3-5 and 3-6.

TYPE III (Reference Figure 3-7)

The Type III guideway is a curved type configuration, referred to as magnaplane. The basic structural shape providing support is identical to the Type I having a rectangular box beam with two rectangular voids separated by a central web. The top of the girder will be cast with a central area blocked out for the installation of the LSM. The area between the LSM assembly and the side of the girder will be filled in continuously and a curved surface formed as the concrete reaches the proper elevations. A block out for the installation of the aluminum levitation ladders will be formed in the curved top surface. The forming of the curved surface will require both time and effort beyond the requirements of the other configurations. The fabricator must ensure that voids in the concrete surface are avoided and that the concrete surfaces are true and correct.

The top flange of the box section and the areas along the sides of the motor assembly that support the levitation ladders must be reinforced with FRP reinforcing rods. Similar to the Type I installation, the level installation of the LSM is critical to the optimum operation of the propulsion system. The motor assembly and the aluminum levitation ladders will be installed similar to the Type I installation.

Again, one potential objection is that there is nothing "visible" keeping the vehicle from sliding out of the trough.

The guideway is elevated the same as the Type I. See Figures 3-8 and 3-9.

TYPE IV (Reference Figure 3-10)

The Type IV guideway is an inverted "T" configuration. The basic structural shape providing support is identical to the Type I having a rectangular box beam with two rectangular voids separated by a central web. In this case the central web is extended above the box to form a vertical wall that is used to mount the LSM's. Similar to the Type II the LSM is divided in half and mounted on opposite sides of the central wall. The wall is formed such that the face of the wall at the top and the face of the LSM are in line. This will protect the LSM and provide a surface at the top of the wall for a guidance wheel mounted on the vehicle to impact the wall, rather than the LSM, in case the vehicle strays too far laterally. All the reinforcing in the wall must be FRP or other non-magnetic material.

The vehicle straddles the wall and is levitated by aluminum levitation ladders at either side of the guideway. The levitation ladders are installed as described in the Type I description. The motor assemblies are mounted on the center wall and are levelled using the FRP bolts and shims. The critical fabrication concern is the center wall above the main support girder. This wall may have to be cast after the box beam is completed. This will increase the fabrication time and cost for this guideway. The vehicle straddling the center wall offers greater confidence that the vehicle will stay with the guideway than the Type I or Type III configurations. Also the overall height of the the vehicle must be increased to account for the height of the wall.

The guideway is elevated the same as the Type I. See Figures 3-11 and 3-12.

TYPE V (Reference Figure 3-13)

The Type V guideway is an U-shaped configuration. The basic structural shape providing support is still the rectangular box beam. The overall width of the guideway is increased in order to position the vehicle within the U-shape or channel. The LSM is divided in half and mounted on the side walls similar to the Type IV. The shape of the interior face of the wall is formed similar to the Type IV to protect the LSM's and to provide a surface at the top of the wall for a guidance wheel mounted on the vehicle to impact the wall in case the vehicle strays too far laterally. All the reinforcing in the sidewalls must be FRP or other non-magnetic material.

The aluminum levitation ladders are mounted in the floor of the U-shaped channel. The levitation ladders are installed as described in the Type I description. As in the Type IV guideway, the sidewalls may have to be cast after the box beam is completed. This will increase fabrication time and cost of the guideway.

The vehicle operating within the confines of the U-shape offers increased confidence that the vehicle will stay with the guideway but adds the possiblity of a "bumper car" effect. The aerodynamics of this guideway is not clear at this time and will not be addressed in this study.

The guideway is elevated the same as the Type I. See Figures 3-14 and 3-15.

The guideway configurations described above and shown in Figures 3-1 thru 3-15 provide a general summary of the current research efforts for Maglev guideway support systems. However, no one has provided a complete design/construction estimate utilizing the same design criteria and parameters for all five configurations. The primary effort of this study is to design each of the configurations using the same design criteria and prepare a construction cost estimate for each. This will enable a rigorous comparison of each system and the advantages and limitations they present.

3.1.2 Guideway Design Criteria/Parameters

The design criteria, design allowables, and material properties and strengths used in the design effort are provided below:

DESIGN CRITERIA/PARAMETERS

ENVIRONMENTAL CRITERIA

Reference Standard:	ASCE 7-88 Minimum Design Loads for Buildings and Other Structures
Structure Classification:	Category III (ASCE 7-88 Table 1)
Wind Criteria:	Structure only; Basic Wind Speed 100 mph, Exposure C, at hurricane oceanline, 50-year recurrence interval
	Structure with vehicle operating; Basic Wind Speed 50 mph, Exposure C, at hurricane oceanline, 50-year recurrence interval
Seismic Criteria:	Zone 2 and/or Zone 4
Snow/Ice Criteria:	Ground Snow Loads (p_g) 20 psf, 2 inch ice accumulation
Frost Criteria:	Design Penetration 3 feet (establishes min. foundation depth)

FOUNDATION CRITERIA

Spread Footing:	Allowable gross bearing pressure of 4000 psf at 4.5 feet below finished grade
Pile Foundation:	Allowable vertical load of 50 tons with an allowable horizontal load of 5.0 tons for a pile with a 50 foot penetration depth

MATERIALS

Structural Steel:	ASTM A36,fy = 60000psi
Concrete:	Foundation (cast-in-place) - ACI 318, f'c = 4000 psi Column (cast-in-place) - ACI 318, f'c = 4000 psi T-beam (cast-in-place) - ACI 318, f'c = 4000psi Girder (precast) - ACI 318, f'c = 6000 psi
Concrete Reinf.:	Cast-in-place reinforcing - ASTM A615 Grade 60 Precast prestressing tendons - ASTM A615 (270 kips) Reinforcing near magnets - composite plastic materials
Anchor Bolts:	Clear of magnetic field - ASTM A36 In magnetic field - composite plastic materials
Connection Bolts:	Clear of magnetic field - ASTM A325 In magnetic field - composite plastic materials

DIMENSIONAL PARAMETERS

Guideway Height:	Varies from a ground clearance of 15-feet to 55-feet from grade to bottom of concrete girder; baseline design will be 35-feet.
Guideway Length:	Varies from 50-feet to 200-feet from centerline to centerline of supports; baseline design will 100-feet
Width:	Minimum two way traffic with minimum 16-feet clear between each vehicle
Vehicle support :	Reference sketches for the five systems under investigation

STRUCTURAL DESIGN CRITERIA

Deflection Criteria:	Column (lateral) - Height/250, Height/500* and Height/750
	Cantilever T-Beam (vertical) - Length/375, Length/500* and Length/750
	Girder (vertical) - Span/1000, Span/1500* and Span/2000 * - denotes baseline design
Foundation Stability Criteria:	Overturning - 2.0 Factor of Safety
	Sliding - 1.5 Factor of Safety

VEHICLE CRITERIA

Height	9 feet (from top of concrete guideway)

Width	10 feet (4 seats/row)
Length	75 feet per car (3 car typical train); 20 rows of seats per train (2.5' per seat) + 25' of space at end of vehicle
Weight	Empty - 850-plf
	Full - 850 + 200 #/person w/luggage X 4 seats/row X 20 rows / 75' = 1070 plf

The criteria and loads described above are combined to form the loadings that the guideway structure must be designed to resist. The load combinations that will be used to design the structure are outlined in the Load Combination Matrix Table.

3.1.3 Guideway Conceptual Designs

The descriptions and details in Section 4.3.1.1 are a result of an analysis of various structural systems using the criteria/parameters discussed in Section 4.3.1.2. The actual design of each item of the overall structure was an iteritive process based on economy of section and constructibilty. The girders are all precast, pre-assembled and pre-tested in a shop prior to shipment, the foundations, columns and T-beams are all cast-in-place using the same basic dimensions to ensure the use of pre-fabricated forming materials. The design dimensions provided on each of the Figures 3-1 thru 3-15 represent the results from the analysis and design using the criteria/parameters from Section 4.3.2 and the baseline deflection criteria, height requirement and width requirement, combined with a vehicle length equal to the span of the girder.

3.1.4 Cost Criteria

The items provided below are the basis for the development of construction costs for the guideway structure and associated systems:

- Engineering/Geotechnical Support
- Temporary Construction Facilities
- Site Preparation and Finishing
- Cast-in-place Foundation
- Cast-in-place Columns and T-beams
- Precast Concrete Girder (including Aluminum Levitation Ladders and LSM)
- Shop Installation of Levitation Strips, LSM, Sensor System, Cables and Wiring
- Precast Concrete Girder Installation and Hook-up
- Contractor contingency, overhead and profit

3.1.5 Guideway Cost Summary

The lowest estimated constucted cost of each of the guideway configurations is provided below for the base case which has been developed using the following criteria/parameters:

Single Column Spacing	30-meters (100')
Ground Clearance	10.7-meters (35')
Girder Vertical Deflection Limit	L/1500
Column Lateral Deflection Limit	L/500
T-beam Cantilever Vertical Deflection Limit	L/500
Foundation Gross Allowable Base Pressure	2.0-kg/cm^2 (4000-psf)

Guideway Cost Summary

Type I	$10,700,000/mile	$6,700,000/km
Type II	$13,700,000/mile	$8,500,000/km
Type III	$11,900,000/mile	$7,400,000/km
Type IV	$11,400,000/mile	$7,100,000/km
Type V	$15,200,000/mile	$9,500,000/km

The cost provided above reflect an estimate of the engineering, fabrication and construction costs associated with a large civil project. Only an order of magnitude cost for the levitation, propulsion, and sensor systems has been included. The guideway cross-section has not been studied to determine if a more economical shape can be used. This effort will be made after the Interim Report. The use of these numbers must be limited to only a comparison of the total cost between the different guideway configurations. The design of the guideways and the assimilation of cost data is an ongoing part of this study and the final assessment of each guideway and the associated cost will be presented in the Final Report. For example a review of the data presented above indicates that Type I has an overall constructed cost less than Type V and does not indicate an actual cost for the all in construction of the guideway.

3.1.6 Guideway Construction Problems

The fabrication problems concerning the guideways were previously discussed. A discussion of construction problems have not been included in the Interim Report.

3.2 Cost Relationships

The construction cost of the guideway is dependent on many variables including site location, congestion of other facilities, terrain, accessibility of construction materials, type of

soils supporting the structure, material strengths, length of span, number of supporting columns, height of structure, and the vehicle supported. The variables that have been estimated and a cost impact prepared are: number of supporting columns, span length, column lateral deflection criteria, girder vertical deflection criteria, height of the structure, and the seismic criteria.

The tables and charts which follow provide a summary of the design/estimating effort to date. They also provide a very detailed comparison of the guideways.

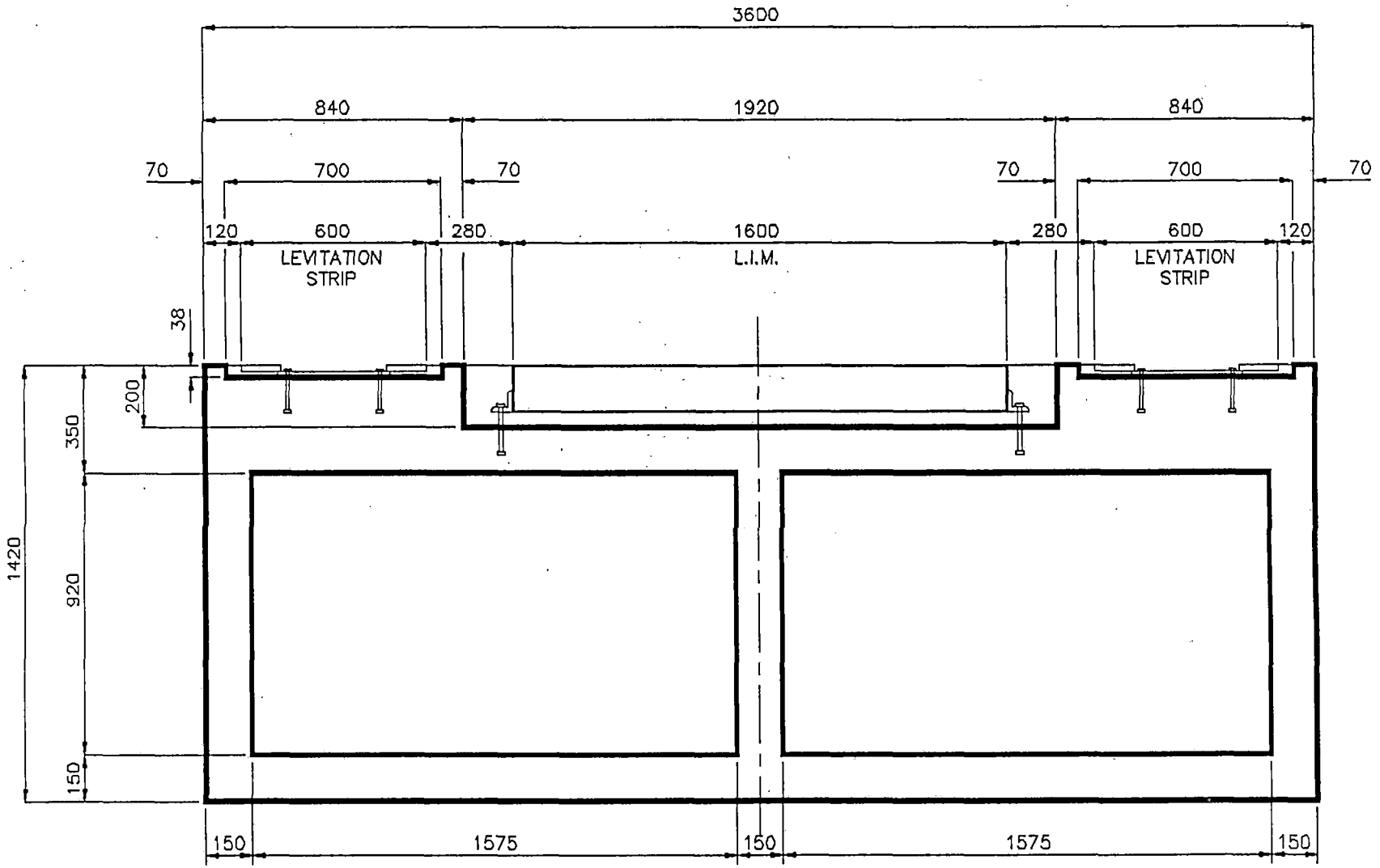

TYPE I – GUIDEWAY SECTION

FIGURE: 3–1

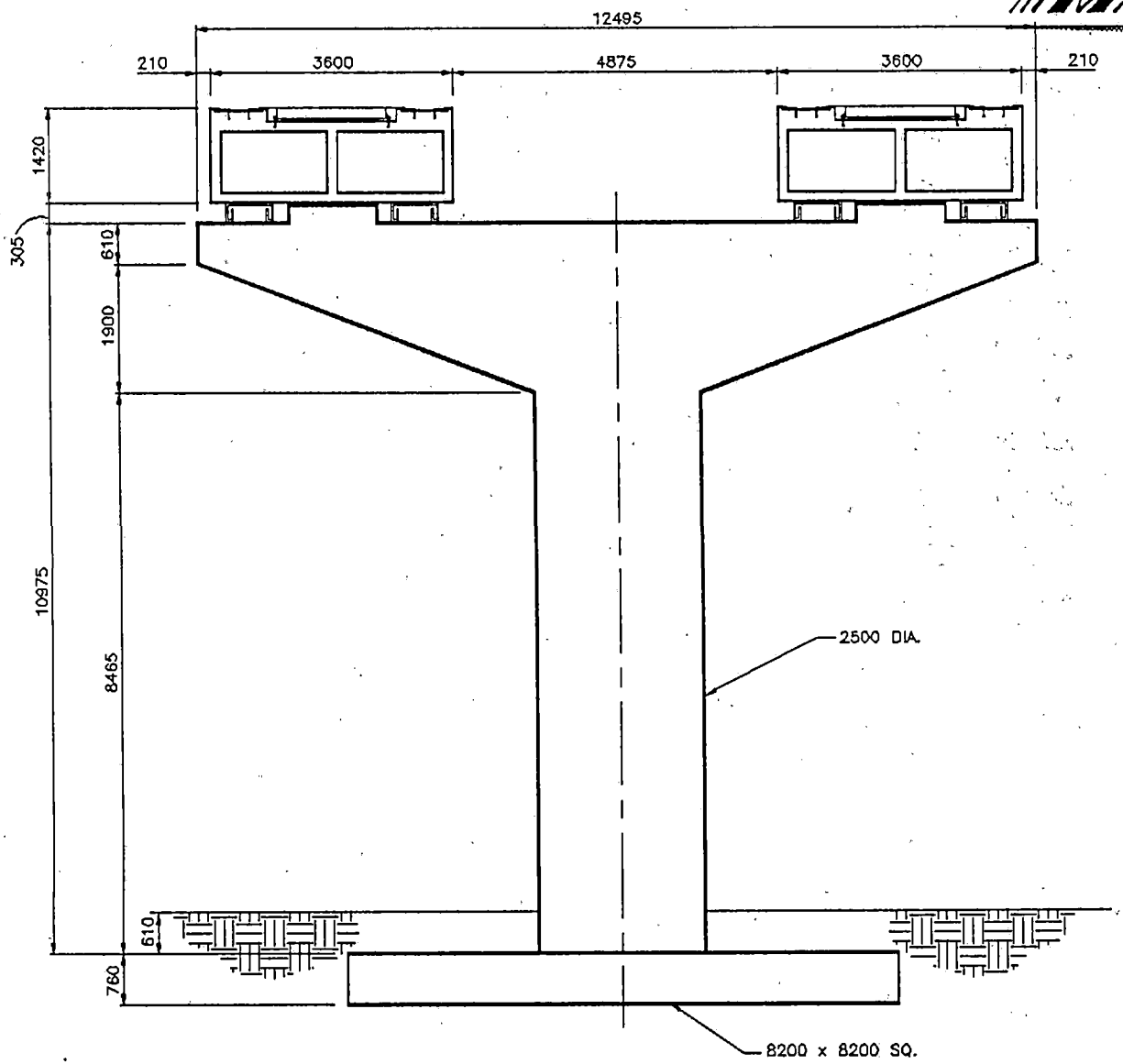

TYPE I – GUIDEWAY ELEVATION SINGLE COLUMN

FIGURE: 3–2

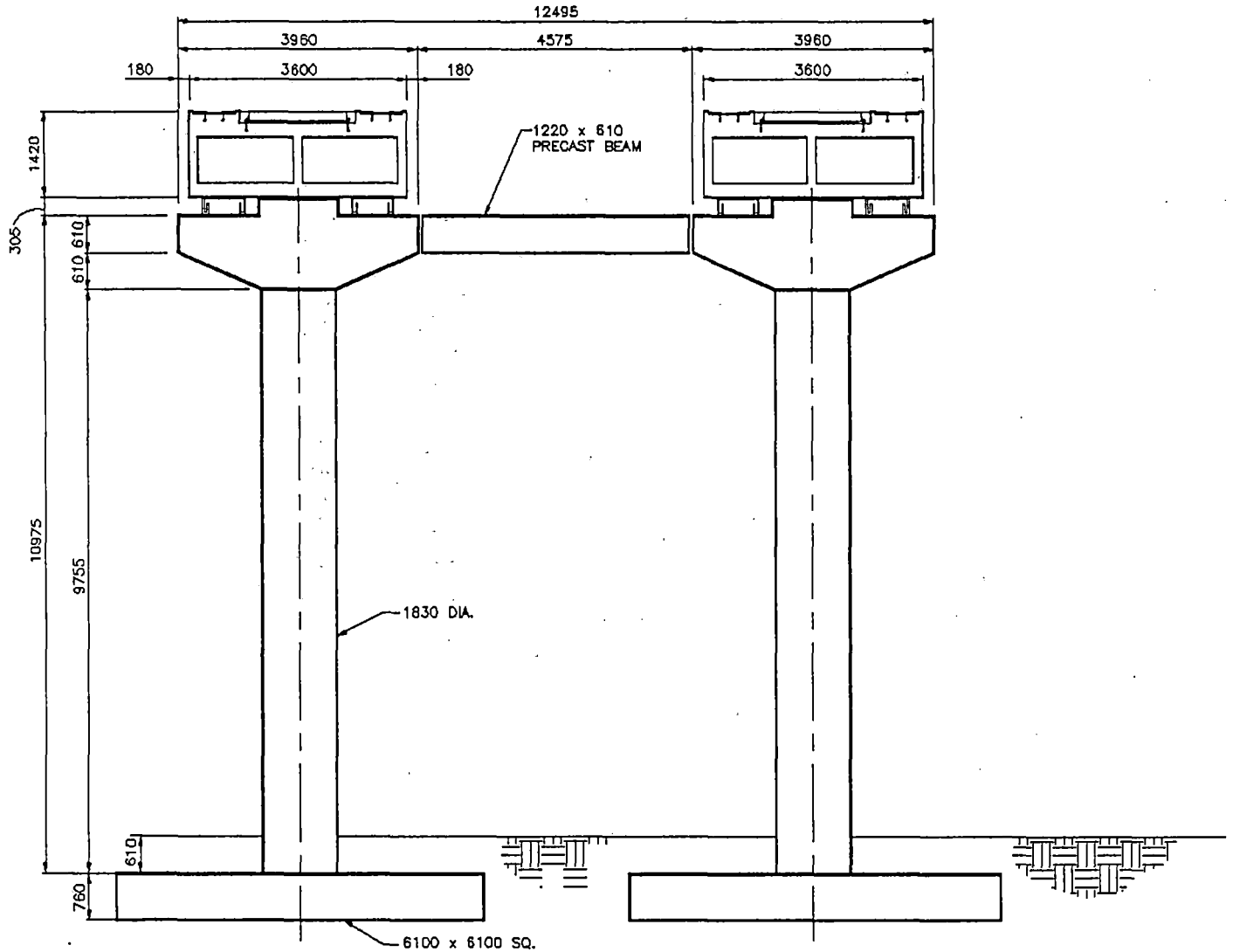

TYPE I – GUIDEWAY ELEVATION DOUBLE COLUMN

FIGURE: 3-3

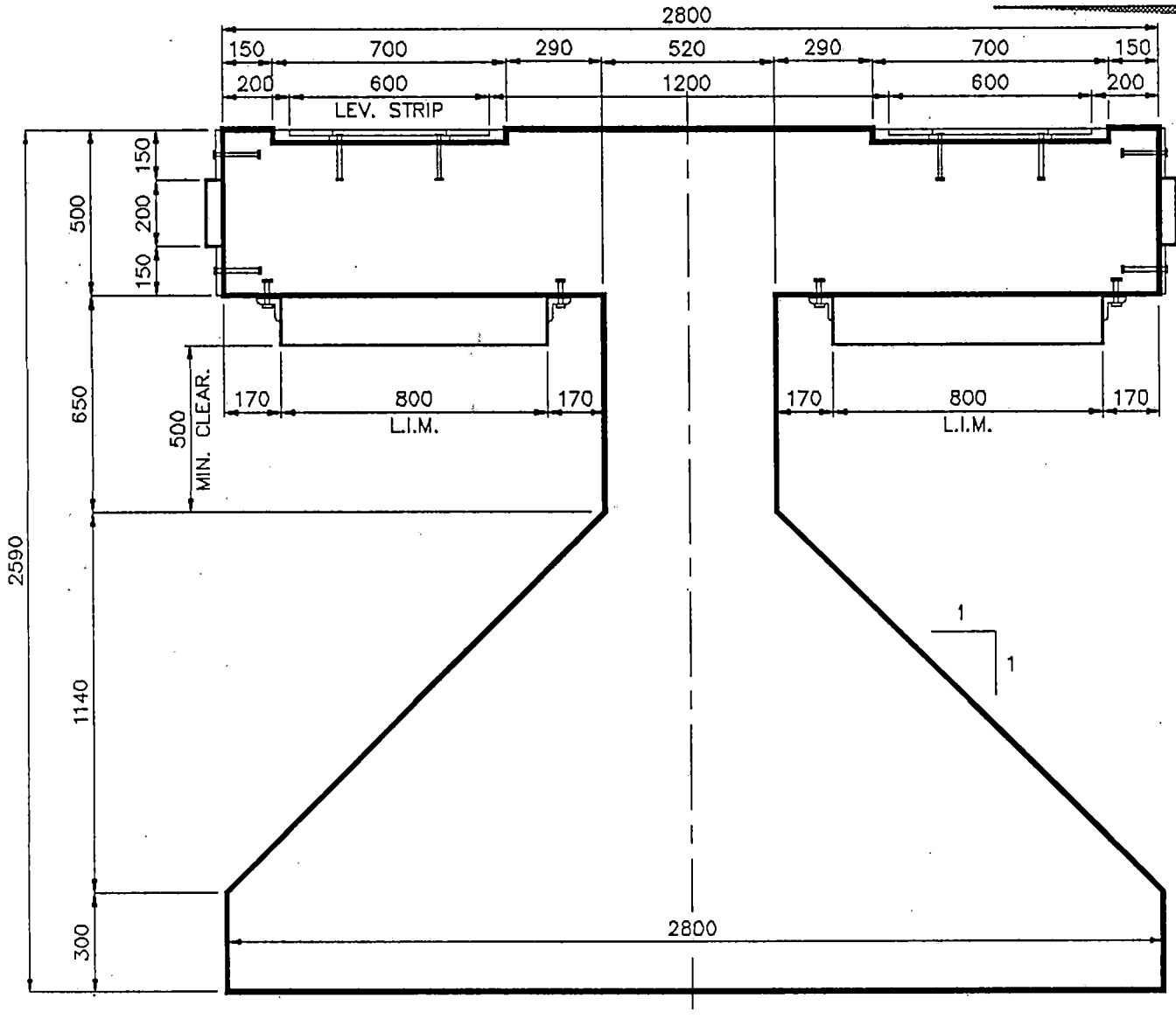

TYPE II – GUIDEWAY SECTION

FIGURE: 3–4

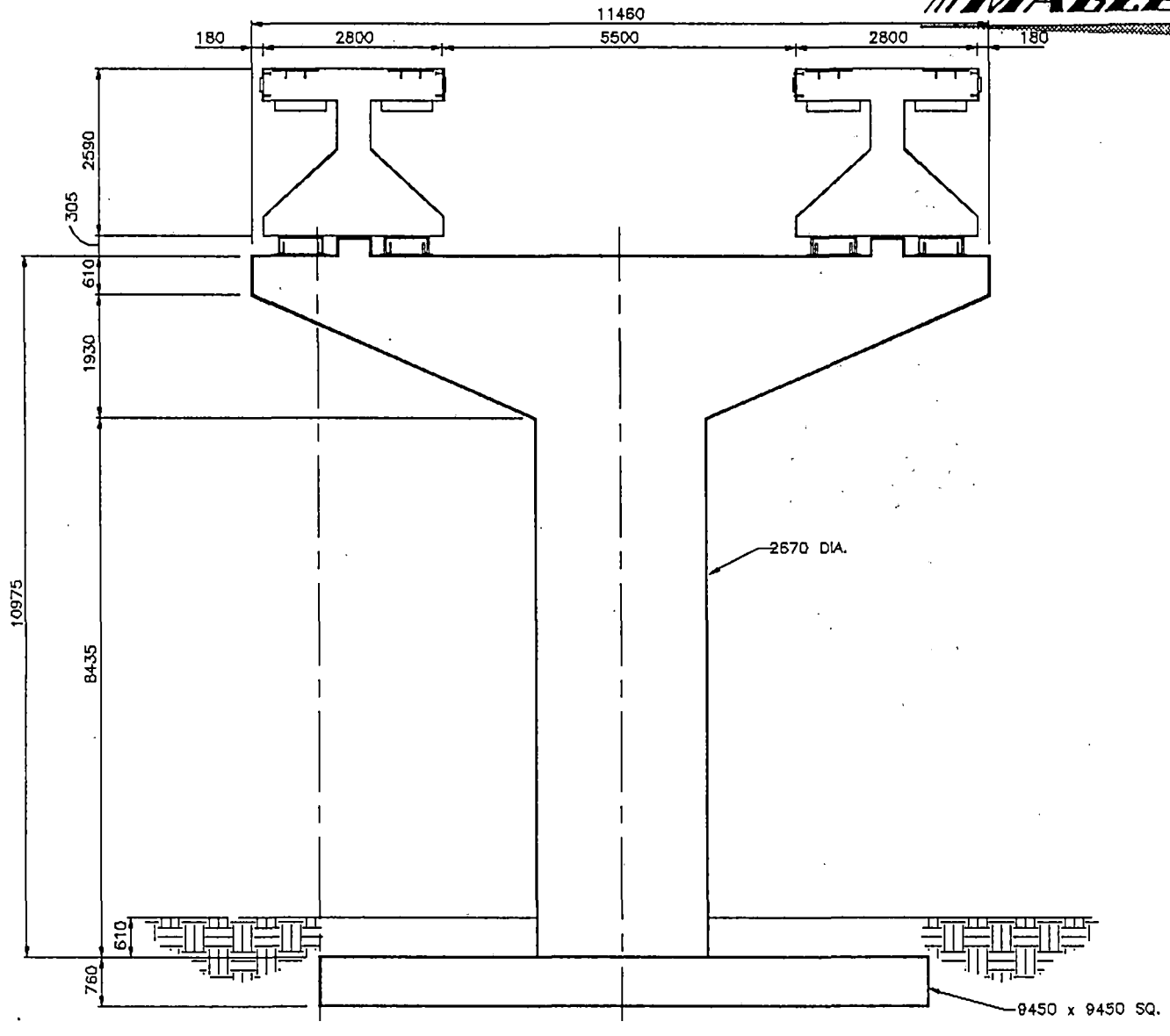

TYPE II – GUIDEWAY ELEVATION SINGLE COLUMN

FIGURE: 3-5

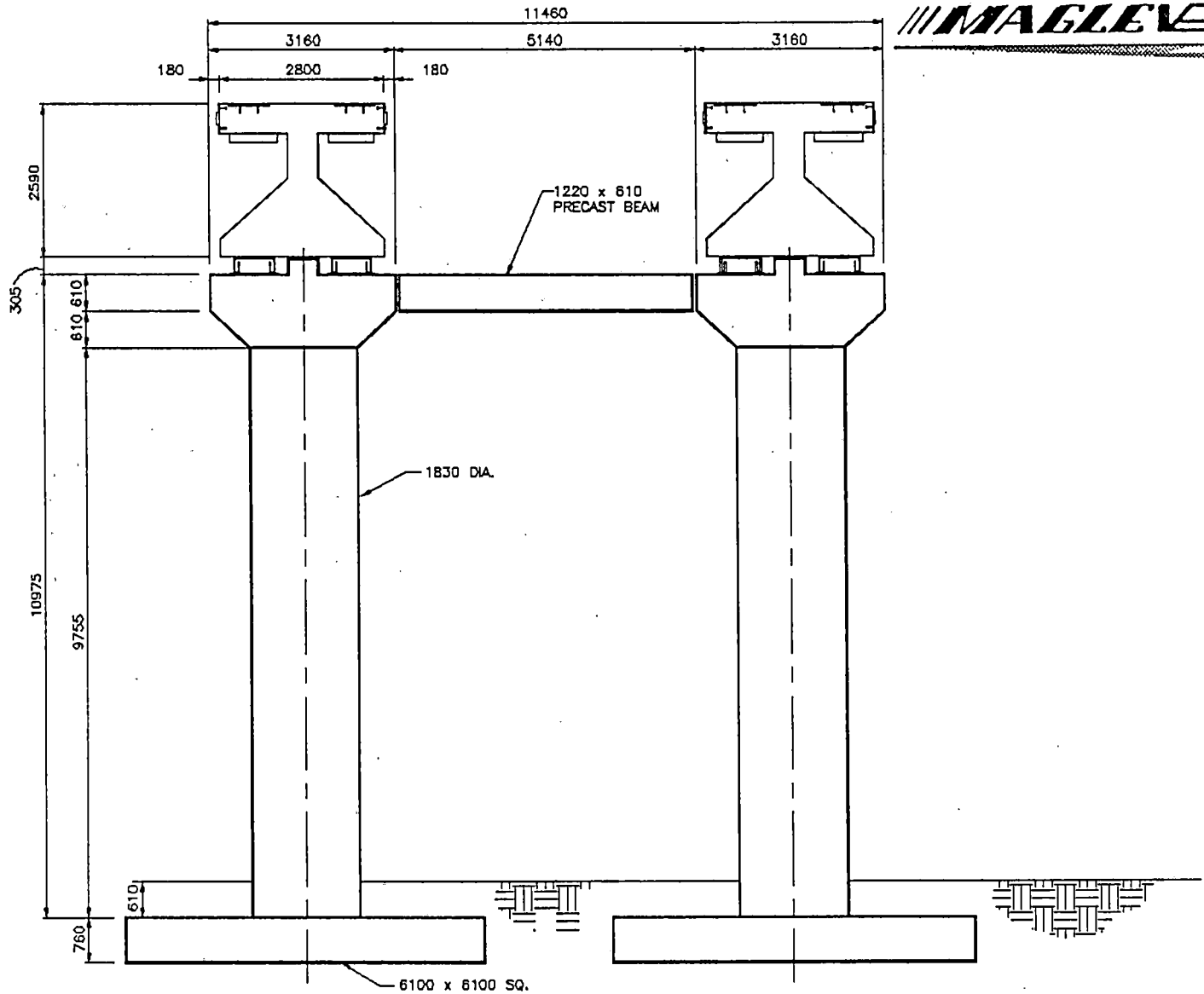

TYPE II – GUIDEWAY ELEVATION DOUBLE COLUMN

FIGURE: 3–6

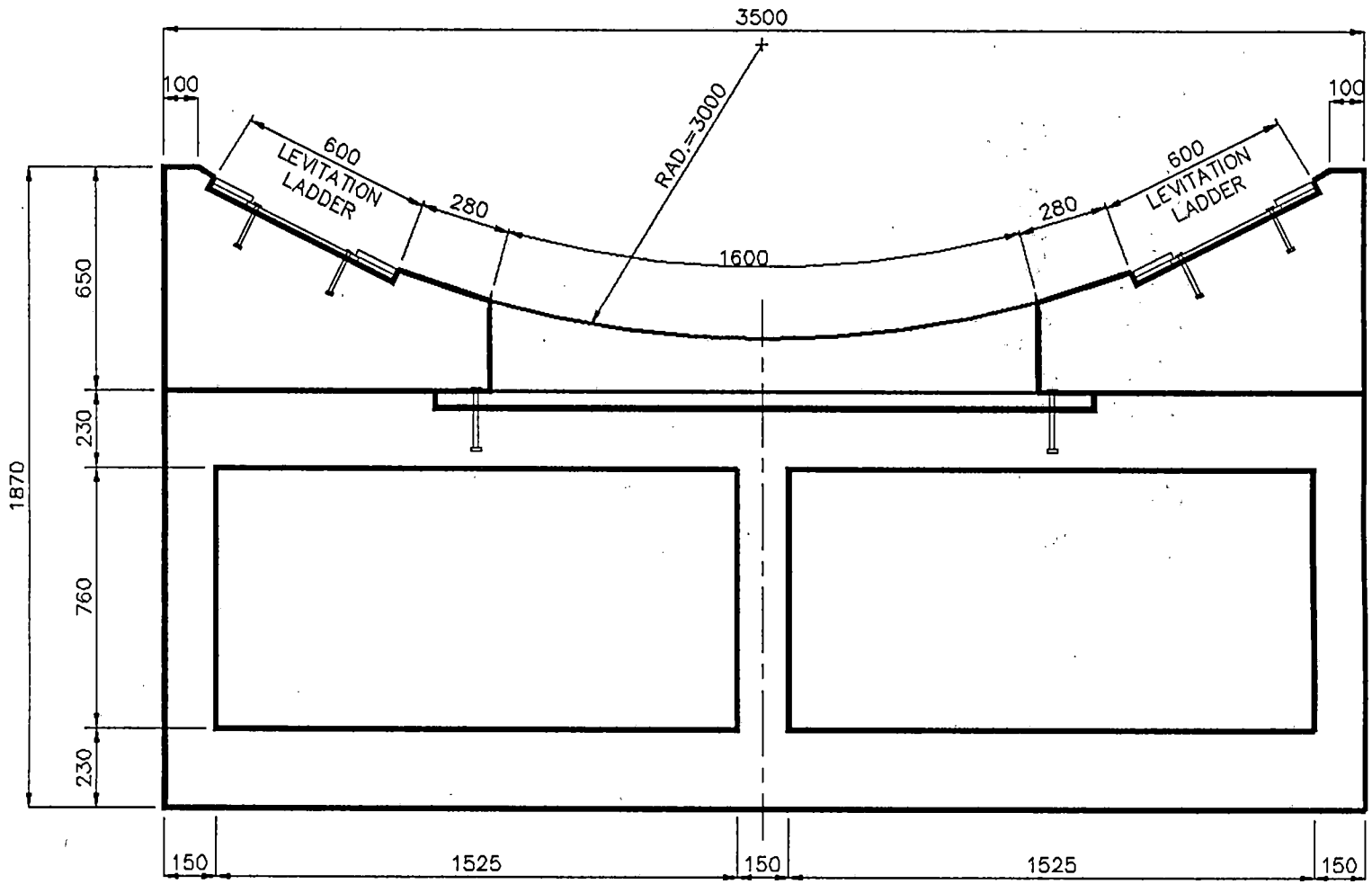

TYPE III – GUIDEWAY SECTION

FIGURE: 3–7

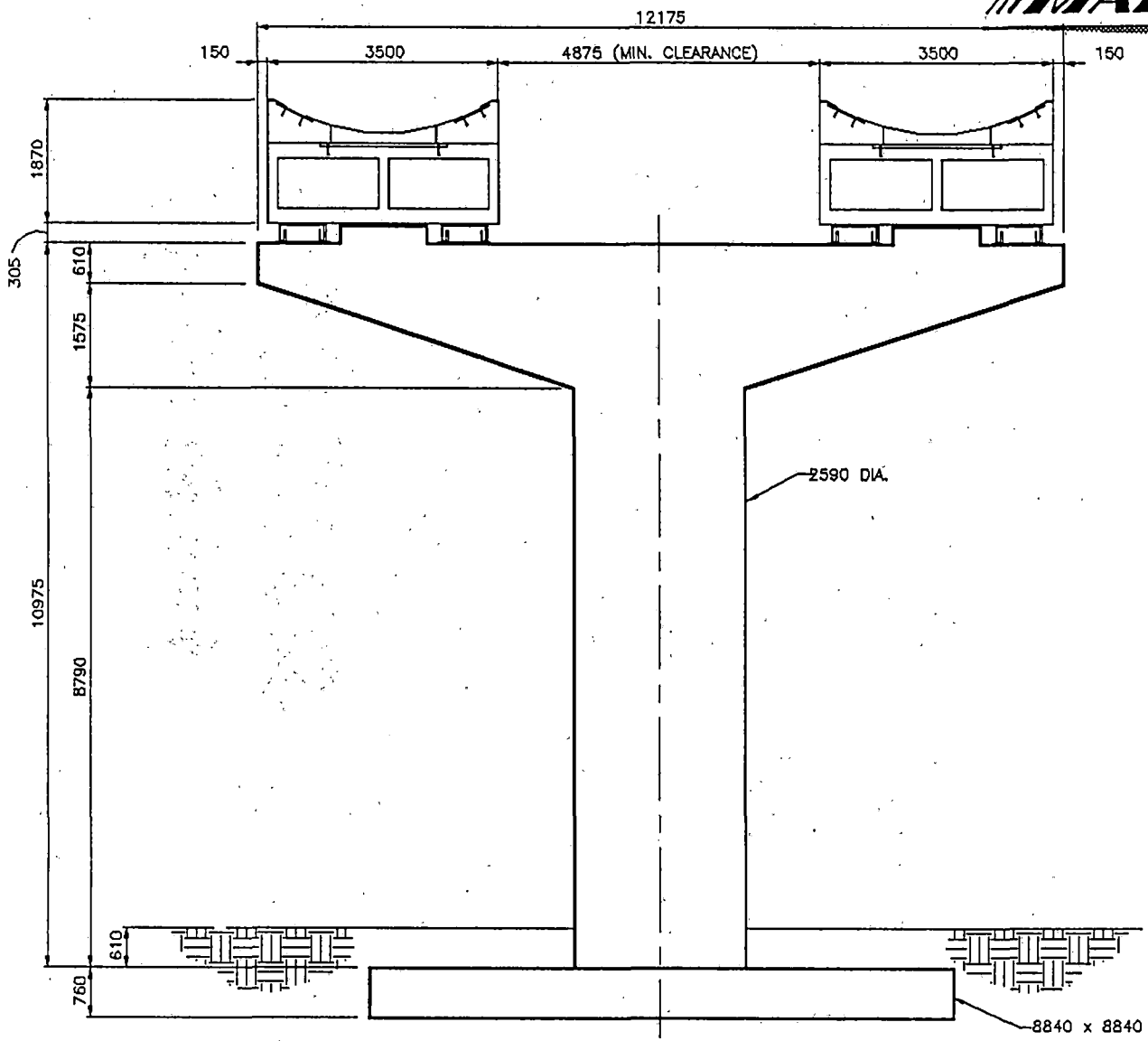

TYPE III – GUIDEWAY ELEVATION SINGLE COLUMN

FIGURE: 3-8

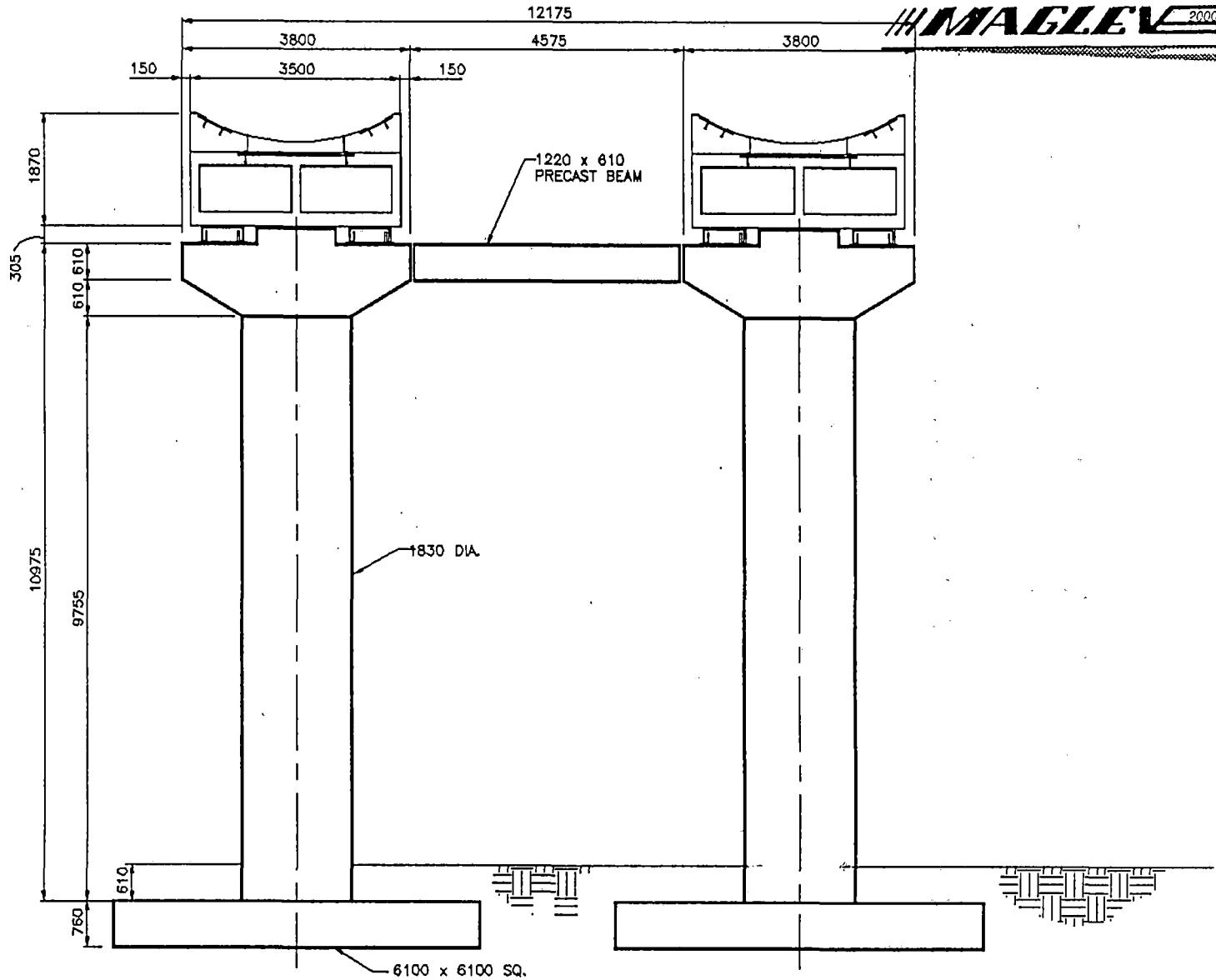

TYPE III – GUIDEWAY ELEVATION DOUBLE COLUMN

FIGURE: 3-9

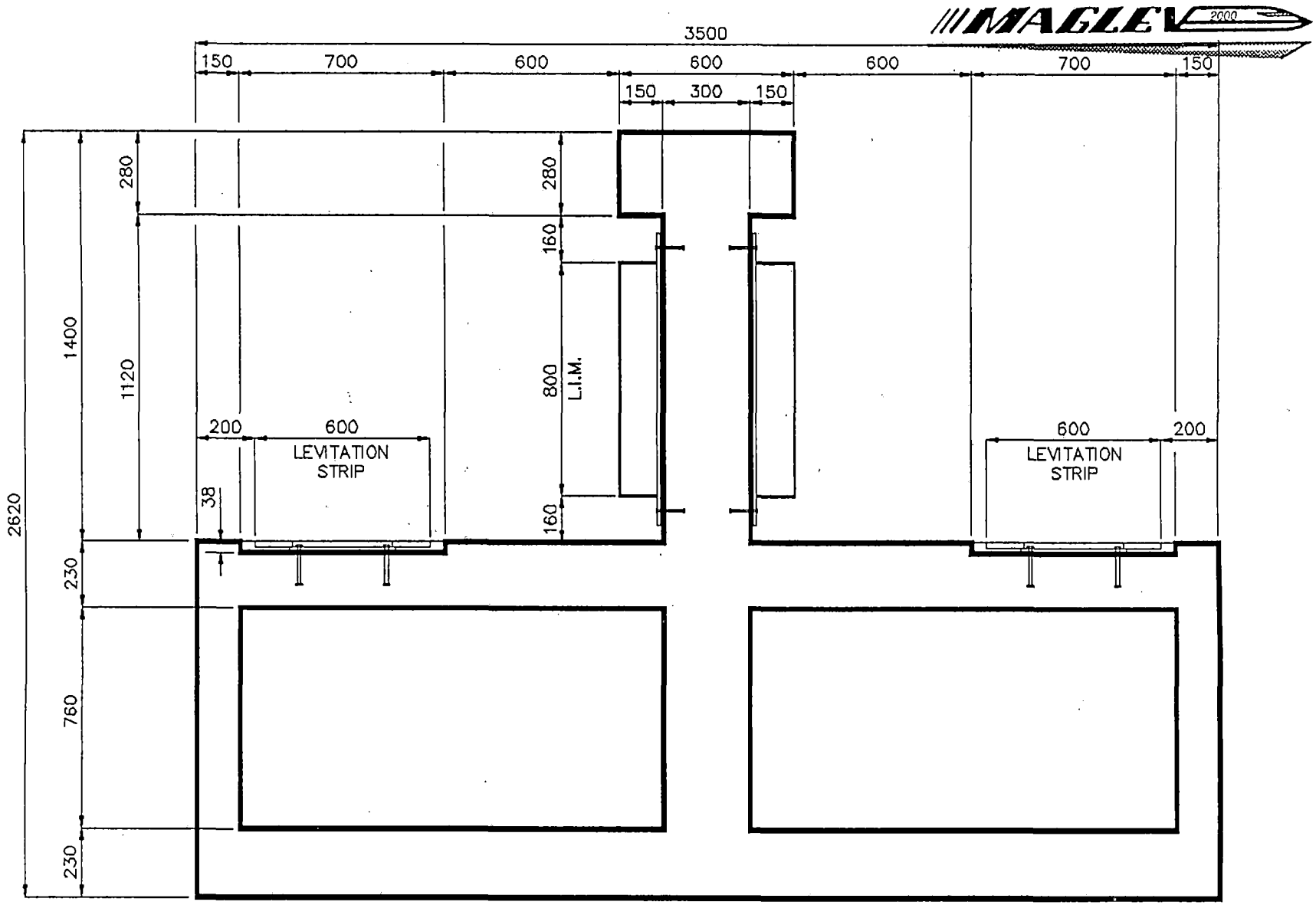

TYPE IV – GUIDEWAY SECTION

FIGURE: 3–10

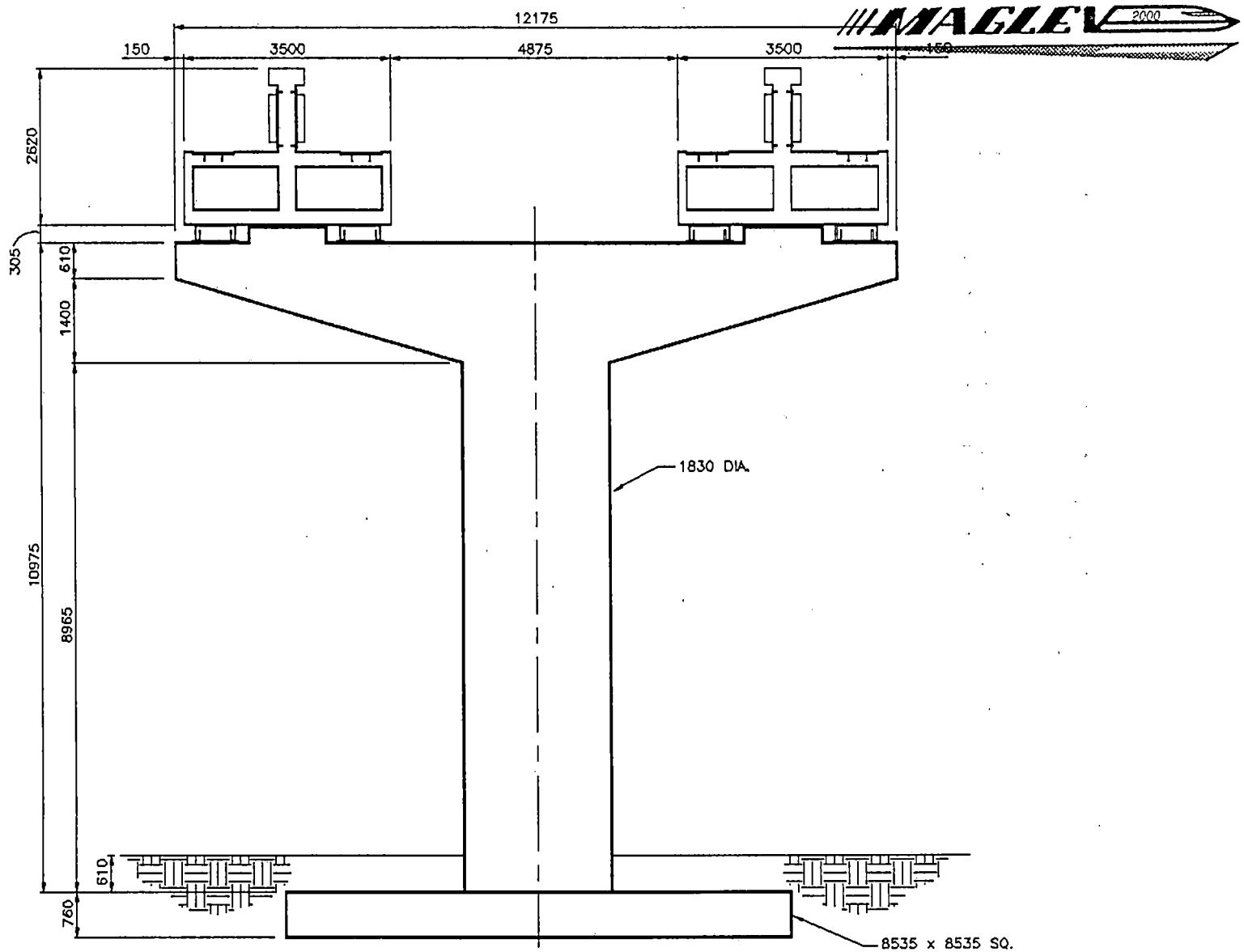

TYPE IV – GUIDEWAY ELEVATION SINGLE COLUMN

FIGURE: 3-11

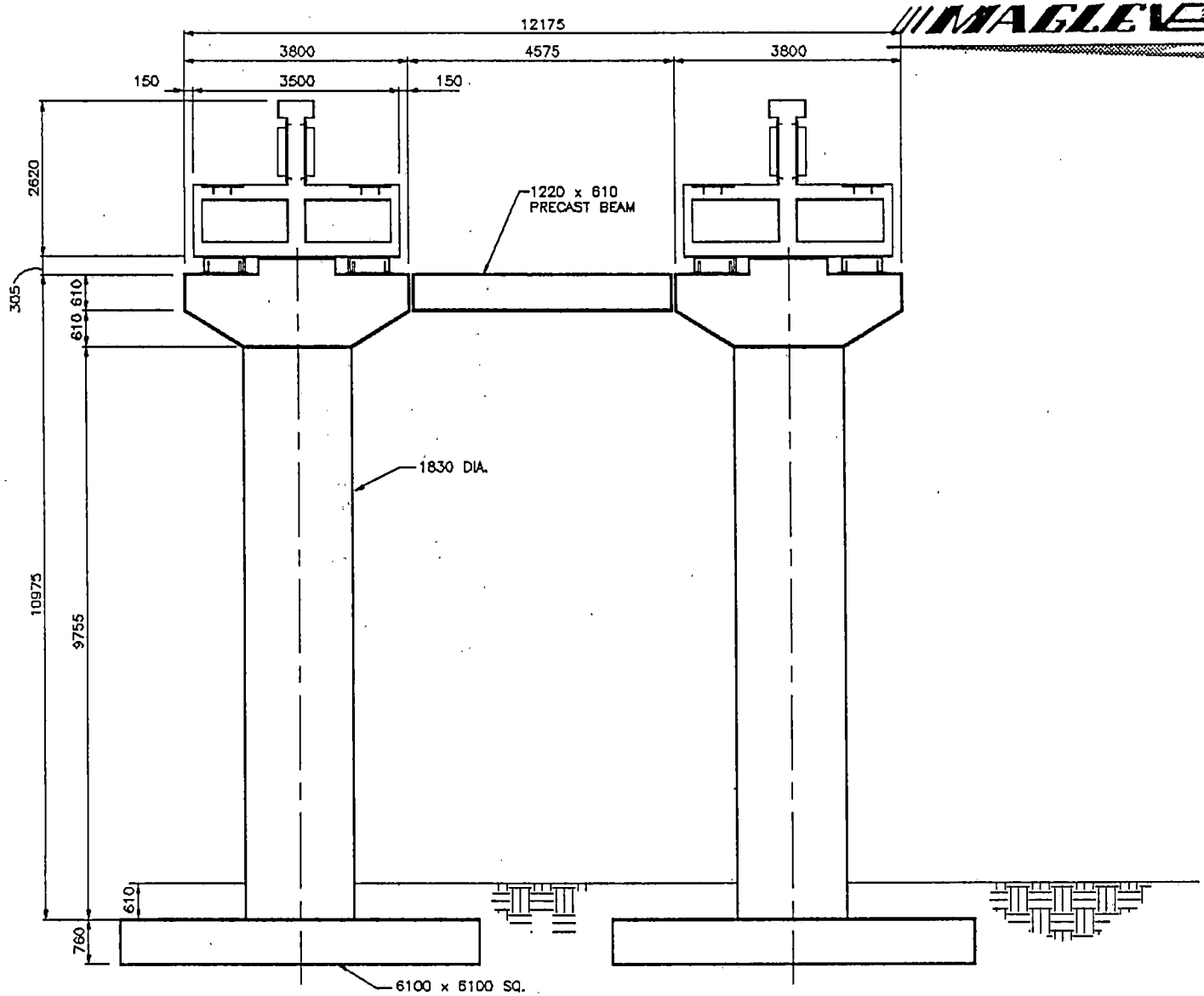

TYPE IV – GUIDEWAY ELEVATION DOUBLE COLUMN

FIGURE: 3-12

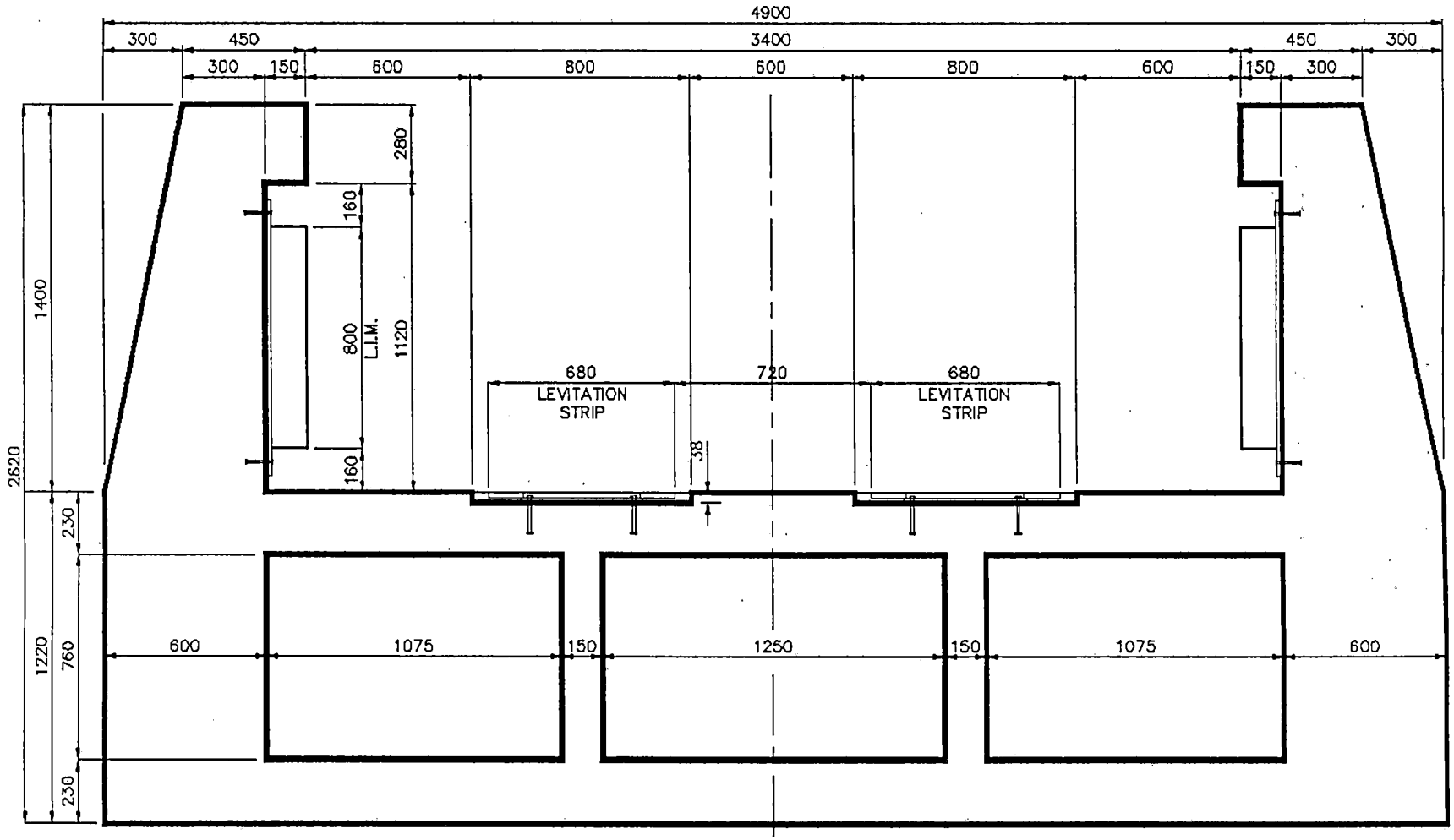

TYPE V – GUIDEWAY SECTION

FIGURE: 3–13

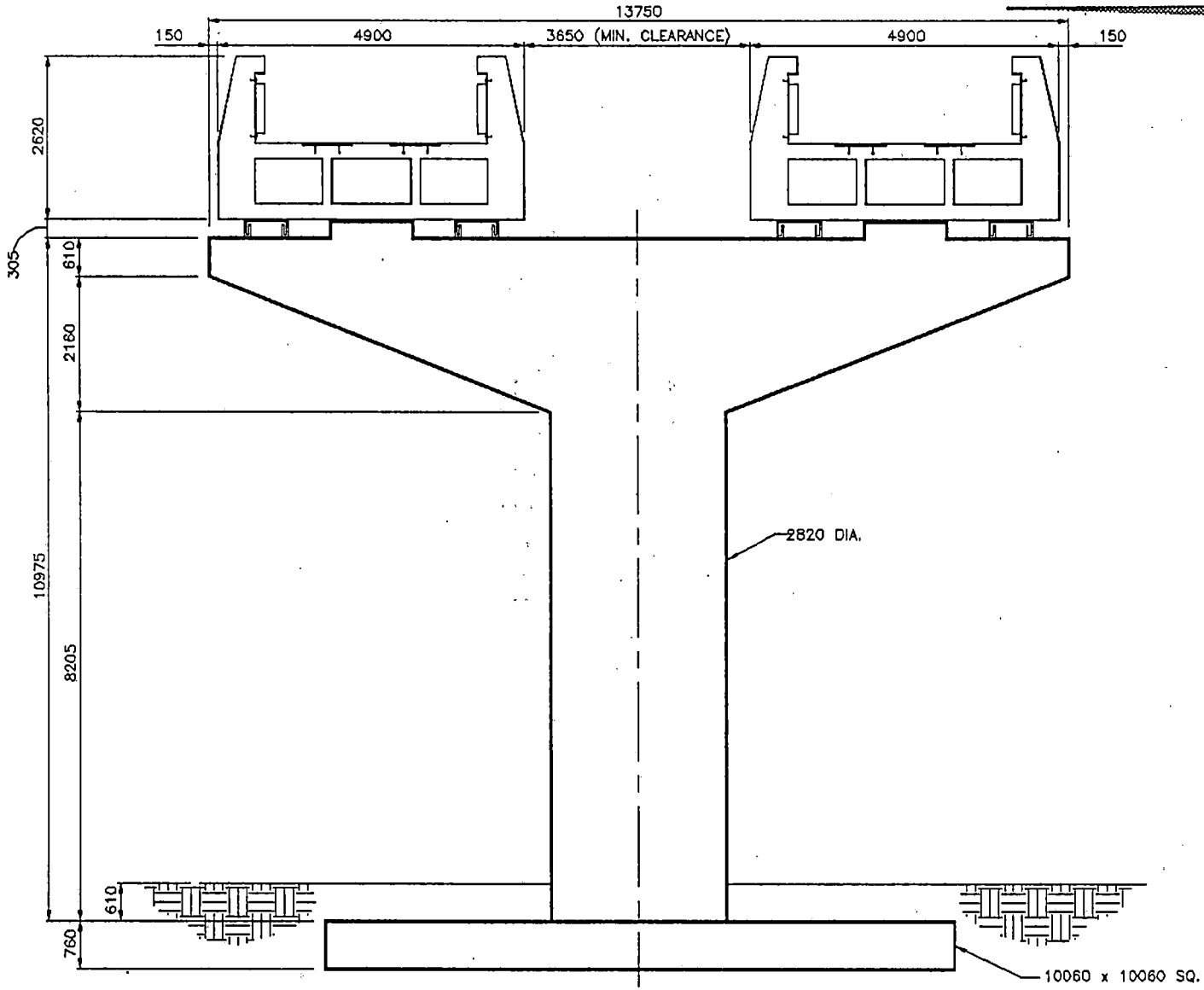

TYPE V – GUIDEWAY ELEVATION SINGLE COLUMN

FIGURE: 3–14

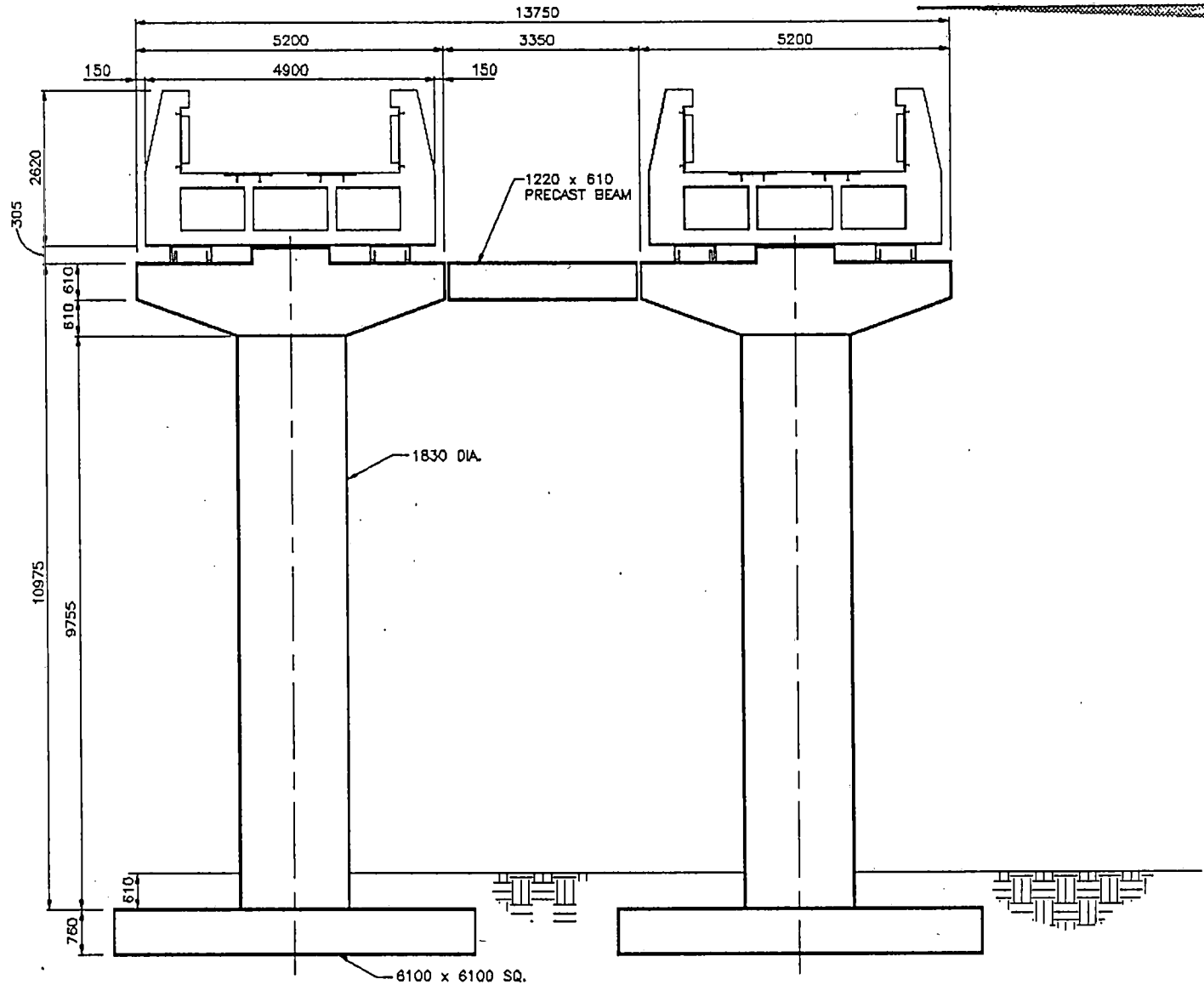

TYPE V – GUIDEWAY ELEVATION DOUBLE COLUMN

FIGURE: 3–15

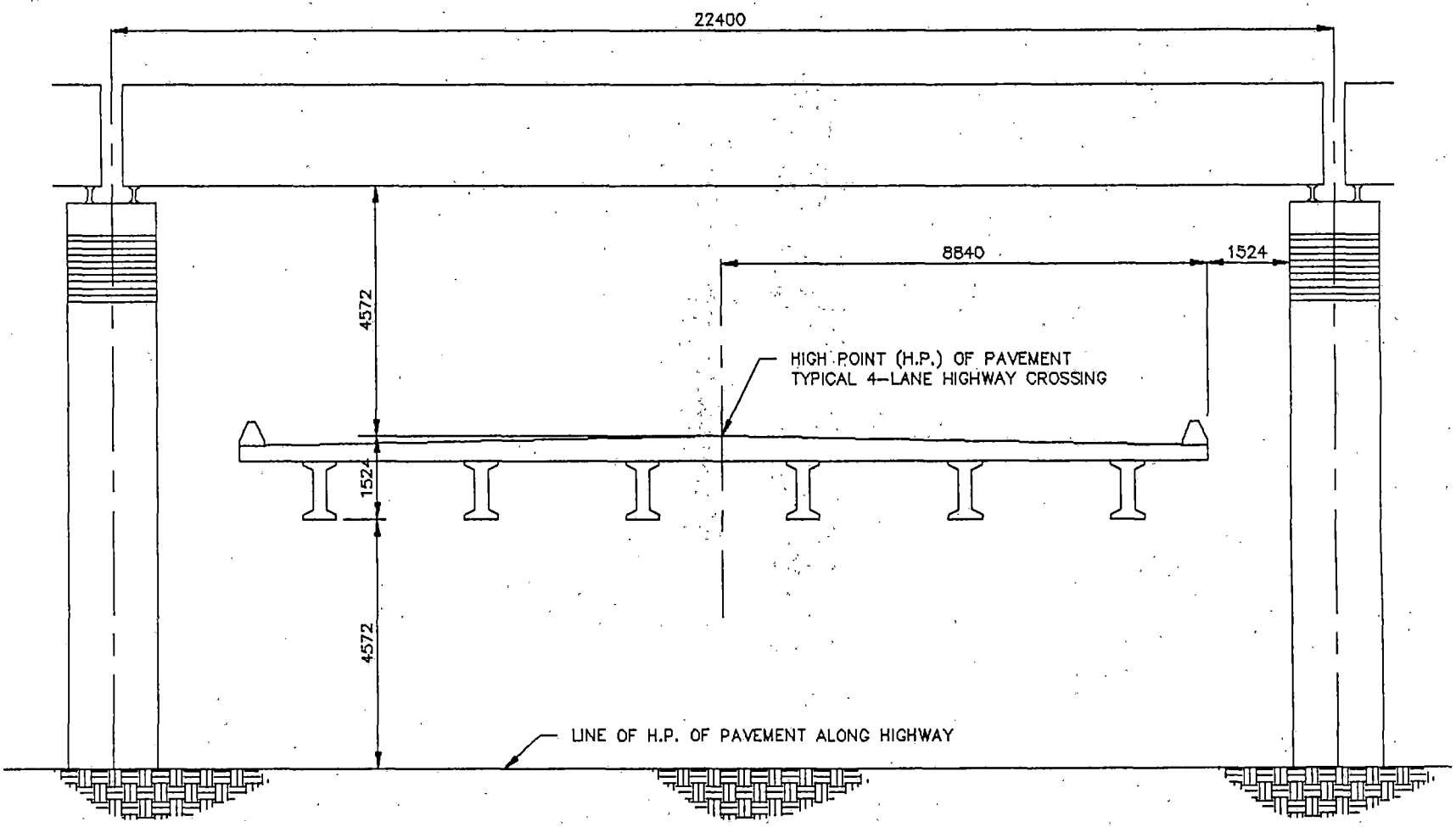

TYPICAL HIGHWAY CLEARANCE
FIGURE: 3-16

GUIDEWAY COST SUMMARY

Chart 3-1 and Tables 3-1 thru 3-5 provide a summary of the cost of each guideway configuration. The design criteria/parameters provided previously were used to analyze and design the structure. The material quantities and the labor requirements to construct the guideway including finish grading and painting have been estimated and are included in the overall cost of each guideway. The specific criteria for this Chart is provided below:

Ground Clearance	35'
Number of Columns	1
Section Type	Straight
Column Lateral Deflection	Height/500
Girder Vertical Deflection	Span/1500
Foundation Type	Spread Footing

Chart 3-1 summarizes the cost for all five configurations.

Table 3-1 provides the data used for the Type I guideway.
Table 3-2 provides the data used for the Type II guideway.
Table 3-3 provides the data used for the Type III guideway.
Table 3-4 provides the data used for the Type IV guideway.
Table 3-5 provides the data used for the Type V guideway.

GUIDEWAY COST SUMMARY

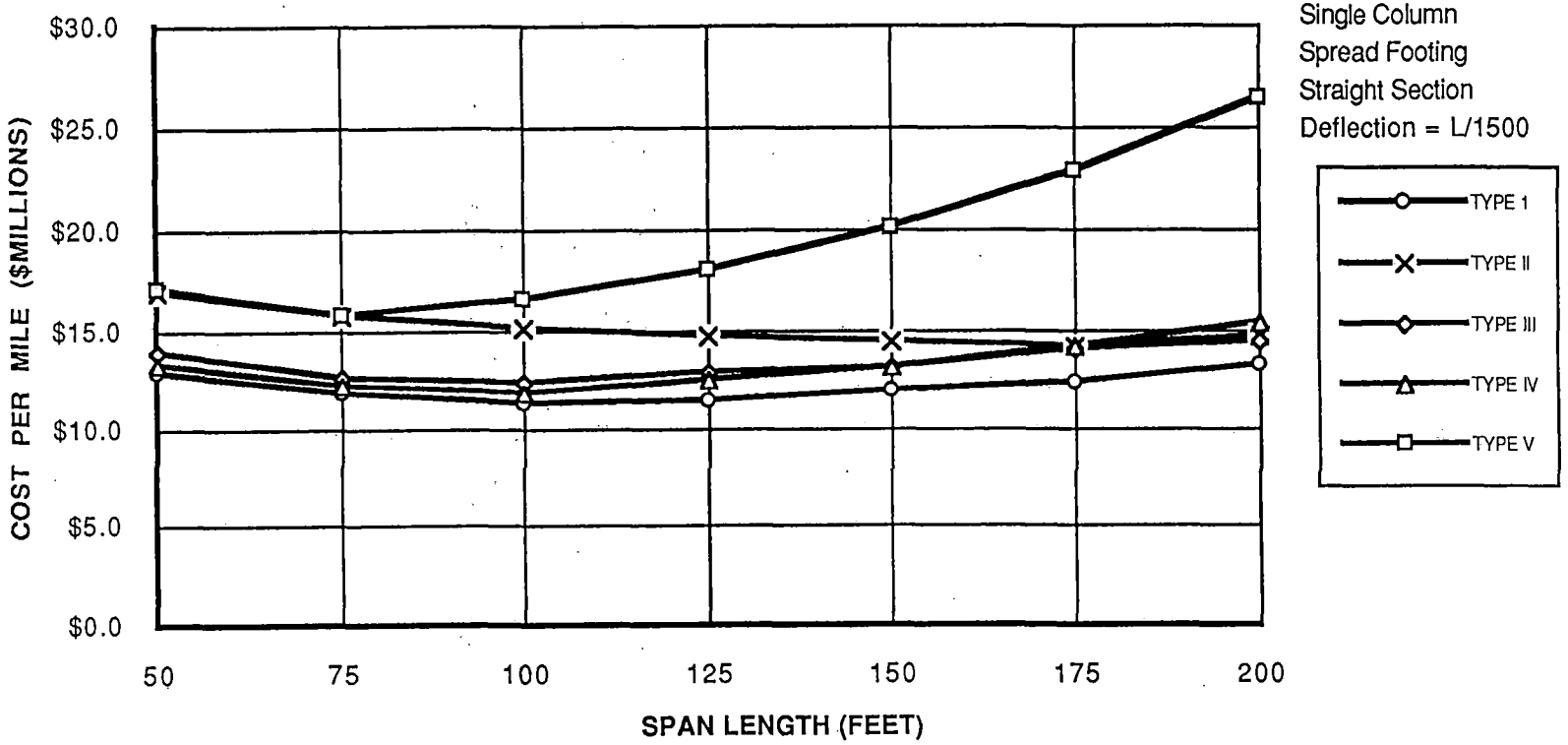

CHART 3-1

COST OF STRUCTURE PER MILE

SPAN (ft)	CONSTRUCTION FACILITIES	SITE PREPARATION & FINISHING	FOUNDATION	COLUMN	T-BEAM	GIRDER	GIRDER INSTALLLATION	COST/MILE	COST/KILOMETER
50.00	$50,000	$350,000	$1,370,000	$1,710,000	$1,090,000	$5,430,000	$2,810,000	$12,830,000	$7,980,000
75.00	$50,000	$310,000	$1,080,000	$1,360,000	$840,000	$5,260,000	$2,810,000	$11,730,000	$7,290,000
100.00	$50,000	$280,000	$1,030,000	$1,120,000	$710,000	$5,170,000	$2,810,000	$11,200,000	$6,960,000
125.00	$50,000	$270,000	$1,020,000	$970,000	$650,000	$5,570,000	$2,810,000	$11,360,000	$7,060,000
150.00	$50,000	$260,000	$1,020,000	$860,000	$630,000	$6,270,000	$2,810,000	$11,930,000	$7,410,000
175.00	$50,000	$260,000	$1,040,000	$780,000	$610,000	$6,690,000	$2,810,000	$12,270,000	$7,630,000
200.00	$50,000	$250,000	$1,130,000	$700,000	$620,000	$7,690,000	$2,810,000	$13,280,000	$8,250,000

SUMMARY OF CRITICAL DIMENSIONS

SPAN (ft)	GIRDER DIMENSIONS				T-BEAM DIMENSIONS		COLUMN DIAMETER (in)	GIRDER WEIGHT (tons)	GIRDER WEIGHT (kN)
	FLNG THK (in)	WB THK (in)	DEPTH (in)	WIDTH (in)	DEPTH (in)	WIDTH (ft)			
50.00	6.00	9.00	48.00	144.00	53.00	41.00	84.00	87.33	8.08
75.00	6.00	9.00	48.00	144.00	65.00	41.00	93.00	130.99	12.11
100.00	6.00	9.00	48.00	144.00	75.00	41.00	99.00	174.65	16.15
125.00	6.00	9.00	72.00	144.00	89.00	41.00	105.00	246.44	22.79
150.00	9.00	9.00	69.00	144.00	106.00	41.00	111.00	350.57	32.42
175.00	9.00	9.00	93.00	144.00	122.00	41.00	117.00	448.37	41.46
200.00	12.00	9.00	105.00	144.00	144.00	41.00	123.00	613.68	56.75

TYPE I - SINGLE COLUMN - BASE CASE COST COMPARISON CHART

TABLE 3-1

COST OF STRUCTURE PER MILE									
SPAN (ft)	CONSTRUCTION FACILITIES	SITE PREPARATION & FINISHING	FOUNDATION	COLUMN	T-BEAM	GIRDER	GIRDER INSTALLLATION	COST/MILE	COST/KILOMETER
50.00	$50,000	$350,000	$1,770,000	$1,890,000	$1,220,000	$8,790,000	$2,810,000	$16,900,000	$10,510,000
75.00	$50,000	$310,000	$1,580,000	$1,450,000	$970,000	$8,620,000	$2,810,000	$15,820,000	$9,830,000
100.00	$50,000	$280,000	$1,360,000	$1,170,000	$840,000	$8,530,000	$2,810,000	$15,070,000	$9,360,000
125.00	$50,000	$270,000	$1,310,000	$1,010,000	$740,000	$8,470,000	$2,810,000	$14,690,000	$9,130,000
150.00	$50,000	$260,000	$1,220,000	$900,000	$680,000	$8,440,000	$2,810,000	$14,380,000	$8,940,000
175.00	$50,000	$260,000	$1,230,000	$780,000	$630,000	$8,410,000	$2,810,000	$14,190,000	$8,820,000
200.00	$50,000	$250,000	$1,250,000	$700,000	$620,000	$9,020,000	$2,810,000	$14,730,000	$9,150,000

SUMMARY OF CRITICAL DIMENSIONS									
SPAN (ft)	GIRDER DIMENSIONS				T-BEAM DIMENSIONS		COLUMN DIAMETER (in)	GIRDER WEIGHT (tons)	GIRDER WEIGHT (kN)
	FLNG THK (in)	WB THK (in)	DEPTH (in)	WIDTH (in)	DEPTH (in)	WIDTH (ft)			
50.00	15.00	10.00	102.00	110.00	69.00	37.50	90.00	165.10	15.27
75.00	15.00	10.00	102.00	110.00	86.00	37.50	99.00	247.65	22.90
100.00	15.00	10.00	102.00	110.00	101.00	37.50	105.00	330.20	30.54
125.00	15.00	10.00	102.00	110.00	114.00	37.50	111.00	412.75	38.17
150.00	15.00	10.00	102.00	110.00	127.00	37.50	117.00	495.30	45.80
175.00	15.00	10.00	102.00	110.00	139.00	37.50	120.00	577.85	53.44
200.00	15.00	10.00	132.00	110.00	159.00	37.50	126.00	722.90	66.85

TYPE II - SINGLE COLUMN - BASE CASE
COST COMPARISON CHART

TABLE 3-2

COST OF STRUCTURE PER MILE									
SPAN (ft)	CONSTRUCTION FACILITIES	SITE PREPARATION & FINISHING	FOUNDATION	COLUMN	T-BEAM	GIRDER	GIRDER INSTALLLATION	COST/MILE	COST/KILOMETER
50.00	$50,000	$350,000	$1,500,000	$1,820,000	$1,100,000	$6,230,000	$2,810,000	$13,890,000	$8,630,000
75.00	$50,000	$310,000	$1,180,000	$1,340,000	$860,000	$6,050,000	$2,810,000	$12,630,000	$7,850,000
100.00	$50,000	$280,000	$1,110,000	$1,170,000	$740,000	$6,130,000	$2,810,000	$12,330,000	$7,660,000
125.00	$50,000	$270,000	$1,160,000	$990,000	$700,000	$6,890,000	$2,810,000	$12,900,000	$8,020,000
150.00	$50,000	$260,000	$1,150,000	$880,000	$670,000	$7,310,000	$2,810,000	$13,160,000	$8,180,000
175.00	$50,000	$260,000	$1,230,000	$780,000	$660,000	$8,260,000	$2,810,000	$14,070,000	$8,750,000
200.00	$50,000	$250,000	$1,250,000	$710,000	$640,000	$8,690,000	$2,810,000	$14,430,000	$8,970,000

SUMMARY OF CRITICAL DIMENSIONS									
SPAN	GIRDER DIMENSIONS				T-BEAM DIMENSIONS		COLUMN	GIRDER	GIRDER
(ft)	FLNG THK (in)	WB THK (in)	DEPTH (in)	WIDTH (in)	DEPTH (in)	WIDTH (ft)	DIAMETER (in)	WEIGHT (tons)	WEIGHT (kN)
50.00	6.00	9.00	48.00	138.00	56.00	40.00	87.00	101.29	9.37
75.00	6.00	9.00	48.00	138.00	69.00	40.00	93.00	151.93	14.05
100.00	6.00	9.00	57.00	138.00	82.00	40.00	102.00	208.20	19.25
125.00	9.00	9.00	60.00	138.00	100.00	40.00	108.00	310.64	28.73
150.00	9.00	9.00	84.00	138.00	116.00	40.00	114.00	410.74	37.98
175.00	12.00	9.00	96.00	138.00	137.00	40.00	120.00	564.51	52.20
200.00	12.00	9.00	120.00	138.00	155.00	40.00	126.00	690.15	63.82

TYPE III - SINGLE COLUMN - BASE CASE
COST COMPARISON CHART

TABLE 3-3

COST OF STRUCTURE PER MILE									
SPAN (ft)	CONSTRUCTION FACILITIES	SITE PREPARATION & FINISHING	FOUNDATION	COLUMN	T-BEAM	GIRDER	GIRDER INSTALLLATION	COST/MILE	COST/KILOMETER
50.00	$50,000	$350,000	$1,370,000	$1,710,000	$1,070,000	$5,850,000	$2,810,000	$13,240,000	$8,230,000
75.00	$50,000	$310,000	$1,180,000	$1,350,000	$830,000	$5,680,000	$2,810,000	$12,230,000	$7,600,000
100.00	$50,000	$280,000	$1,110,000	$1,110,000	$720,000	$5,740,000	$2,810,000	$11,850,000	$7,360,000
125.00	$50,000	$270,000	$1,080,000	$1,000,000	$690,000	$6,550,000	$2,810,000	$12,490,000	$7,760,000
150.00	$50,000	$260,000	$1,150,000	$880,000	$670,000	$7,270,000	$2,810,000	$13,120,000	$8,150,000
175.00	$50,000	$260,000	$1,230,000	$770,000	$670,000	$8,410,000	$2,810,000	$14,230,000	$8,840,000
200.00	$50,000	$250,000	$1,310,000	$680,000	$680,000	$9,560,000	$2,810,000	$15,370,000	$9,550,000

SUMMARY OF CRITICAL DIMENSIONS									
SPAN (ft)	GIRDER DIMENSIONS				T-BEAM DIMENSIONS		COLUMN DIAMETER (in)	GIRDER WEIGHT (tons)	GIRDER WEIGHT (kN)
	FLNG THK (in)	WB THK (in)	DEPTH (in)	WIDTH (in)	DEPTH (in)	WIDTH (ft)			
50.00	6.00	12.00	48.00	138.00	54.00	40.00	84.00	91.95	8.50
75.00	6.00	12.00	48.00	138.00	66.00	40.00	93.00	137.93	12.75
100.00	6.00	12.00	54.00	138.00	79.00	40.00	99.00	191.40	17.70
125.00	9.00	12.00	60.00	138.00	97.00	40.00	108.00	293.16	27.11
150.00	9.00	12.00	90.00	138.00	116.00	40.00	114.00	408.04	37.73
175.00	12.00	12.00	108.00	138.00	140.00	40.00	120.00	577.76	53.43
200.00	15.00	12.00	126.00	138.00	165.00	40.00	126.00	776.55	71.81

TYPE IV - SINGLE COLUMN - BASE CASE
COST COMPARISON CHART

TABLE 3-4

COST OF STRUCTURE PER MILE									
SPAN (ft)	CONSTRUCTION FACILITIES	SITE PREPARATION & FINISHING	FOUNDATION	COLUMN	T-BEAM	GIRDER	GIRDER INSTALLLATION	COST/MILE	COST/KILOMETER
50.00	$50,000	$350,000	$1,770,000	$2,010,000	$1,470,000	$8,600,000	$2,810,000	$17,080,000	$10,610,000
75.00	$50,000	$310,000	$1,480,000	$1,450,000	$1,160,000	$8,420,000	$2,810,000	$15,700,000	$9,760,000
100.00	$50,000	$280,000	$1,540,000	$1,280,000	$1,060,000	$9,520,000	$2,810,000	$16,570,000	$10,300,000
125.00	$50,000	$270,000	$1,630,000	$1,090,000	$1,040,000	$11,150,000	$2,810,000	$18,070,000	$11,230,000
150.00	$50,000	$260,000	$1,740,000	$930,000	$1,050,000	$13,290,000	$2,810,000	$20,170,000	$12,530,000
175.00	$50,000	$260,000	$2,020,000	$770,000	$1,100,000	$15,920,000	$2,810,000	$22,960,000	$14,270,000
200.00	$50,000	$250,000	$2,300,000	$590,000	$1,180,000	$19,220,000	$2,810,000	$26,430,000	$16,420,000

SUMMARY OF CRITICAL DIMENSIONS									
SPAN	GIRDER DIMENSIONS				T-BEAM DIMENSIONS		COLUMN	GIRDER	GIRDER
(ft)	FLNG THK (in)	WB THK (in)	DEPTH (in)	WIDTH (in)	DEPTH (in)	WIDTH (ft)	DIAMETER (in)	WEIGHT (tons)	WEIGHT (kN)
50.00	6.00	26.00	48.00	164.00	70.00	45.00	93.00	160.23	14.82
75.00	6.00	26.00	48.00	164.00	86.00	45.00	99.00	240.34	22.23
100.00	9.00	26.00	57.00	164.00	109.00	45.00	111.00	379.83	35.12
125.00	12.00	26.00	75.00	164.00	138.00	45.00	120.00	579.47	53.59
150.00	15.00	26.00	102.00	164.00	172.00	45.00	129.00	857.55	79.30
175.00	18.00	26.00	138.00	164.00	214.00	45.00	138.00	1232.35	113.96
200.00	21.00	26.00	186.00	164.00	266.00	45.00	147.00	1738.40	160.76

TYPE V - SINGLE COLUMN - BASE CASE COST COMPARISON CHART

TABLE 3-5

GUIDEWAY COST SUMMARY

Chart 3-2 and Tables 3-1, 3-5 and 3-6 provide a summary of the variation of the cost for the Type I guideway configuration when the column height varies. The design criteria/parameters provided previously were used to analyze and design the structure. The material quantities and the labor requirements to construct the guideway including finish grading and painting have been estimated and are included in the overall cost of the guideway. The specific criteria for this Chart is provided below:

Ground Clearance (Varies)	15', 35', and 55'
Number of Columns	1
Section Type	Straight
Column Lateral Deflection	Height/500
Girder Vertical Deflection	Span/1500
Foundation Type	Spread Footing

Chart 3-2 summarizes the cost for the Type I guideway configuration.

Table 3-6 provides the data used for the Type I guideway with 15' ground clearance.
Table 3-1 provides the data used for the Type I guideway with 35' ground clearance.
Table 3-7 provides the data used for the Type I guideway with 55' ground clearance.

COST VARIATION BY COLUMN HEIGHT

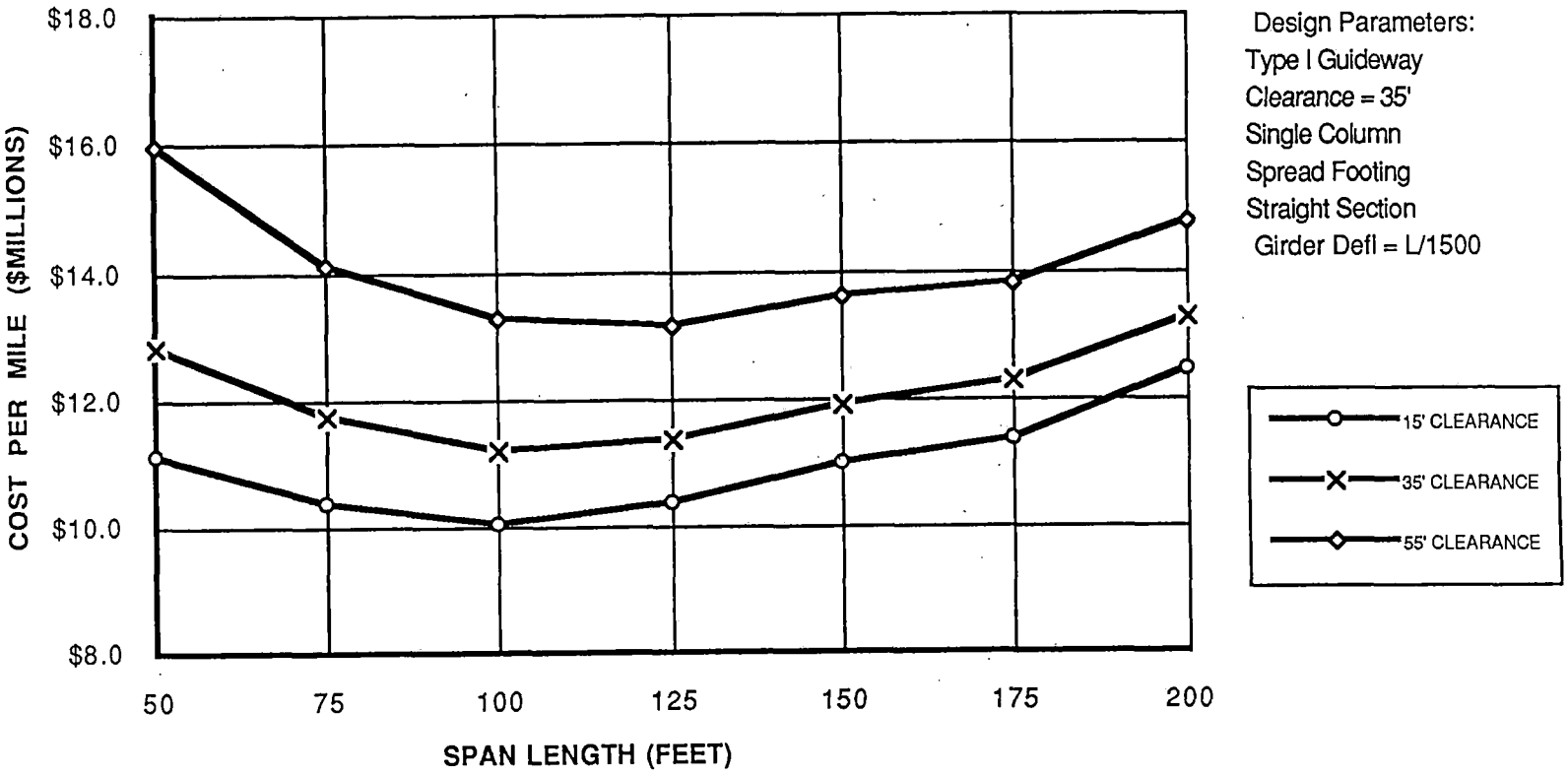

CHART 3-2

COST OF STRUCTURE PER MILE									
SPAN (ft)	CONSTRUCTION FACILITIES	SITE PREPARATION & FINISHING	FOUNDATION	COLUMN	T-BEAM	GIRDER	GIRDER INSTALLLATION	COST/MILE	COST/KILOMETER
50.00	$50,000	$350,000	$1,020,000	$330,000	$1,090,000	$5,430,000	$2,810,000	$11,110,000	$6,900,000
75.00	$50,000	$310,000	$830,000	$250,000	$840,000	$5,260,000	$2,810,000	$10,370,000	$6,440,000
100.00	$50,000	$280,000	$810,000	$190,000	$710,000	$5,170,000	$2,810,000	$10,050,000	$6,240,000
125.00	$50,000	$270,000	$820,000	$160,000	$650,000	$5,570,000	$2,810,000	$10,360,000	$6,440,000
150.00	$50,000	$260,000	$850,000	$120,000	$630,000	$6,270,000	$2,810,000	$11,010,000	$6,840,000
175.00	$50,000	$260,000	$820,000	$90,000	$610,000	$6,690,000	$2,810,000	$11,360,000	$7,060,000
200.00	$50,000	$250,000	$910,000	$70,000	$620,000	$7,690,000	$2,810,000	$12,430,000	$7,720,000

SUMMARY OF CRITICAL DIMENSIONS									
SPAN (ft)	*GIRDER DIMENSIONS*				*T-BEAM DIMENSIONS*		COLUMN	GIRDER	GIRDER
	FLNG THK (in)	WB THK (in)	DEPTH (in)	WIDTH (in)	DEPTH (in)	WIDTH (ft)	DIAMETER (in)	WEIGHT (tons)	WEIGHT (kN)
50.00	6.00	9.00	48.00	144.00	53.00	41.00	60.00	87.33	8.08
75.00	6.00	9.00	48.00	144.00	65.00	41.00	66.00	130.99	12.11
100.00	6.00	9.00	48.00	144.00	75.00	41.00	69.00	174.65	16.15
125.00	6.00	9.00	72.00	144.00	89.00	41.00	75.00	246.44	22.79
150.00	9.00	9.00	69.00	144.00	106.00	41.00	78.00	350.57	32.42
175.00	9.00	9.00	93.00	144.00	122.00	41.00	81.00	448.37	41.46
200.00	12.00	9.00	105.00	144.00	144.00	41.00	87.00	613.68	56.75

TYPE I - SINGLE COLUMN @ 15' CLEARANCE - BASE CASE COST COMPARISON CHART

TABLE 3-6

COST OF STRUCTURE PER MILE									
SPAN (ft)	CONSTRUCTION FACILITIES	SITE PREPARATION & FINISHING	FOUNDATION	COLUMN	T-BEAM	GIRDER	GIRDER INSTALLLATION	COST/MILE	COST/KILOMETER
50.00	$50,000	$350,000	$1,370,000	$1,710,000	$1,090,000	$5,430,000	$2,810,000	$12,830,000	$7,980,000
75.00	$50,000	$310,000	$1,080,000	$1,360,000	$840,000	$5,260,000	$2,810,000	$11,730,000	$7,290,000
100.00	$50,000	$280,000	$1,030,000	$1,120,000	$710,000	$5,170,000	$2,810,000	$11,200,000	$6,960,000
125.00	$50,000	$270,000	$1,020,000	$970,000	$650,000	$5,570,000	$2,810,000	$11,360,000	$7,060,000
150.00	$50,000	$260,000	$1,020,000	$860,000	$630,000	$6,270,000	$2,810,000	$11,930,000	$7,410,000
175.00	$50,000	$260,000	$1,040,000	$780,000	$610,000	$6,690,000	$2,810,000	$12,270,000	$7,630,000
200.00	$50,000	$250,000	$1,130,000	$700,000	$620,000	$7,690,000	$2,810,000	$13,280,000	$8,250,000

SUMMARY OF CRITICAL DIMENSIONS									
SPAN	GIRDER DIMENSIONS				T-BEAM DIMENSIONS		COLUMN	GIRDER	GIRDER
(ft)	FLNG THK (in)	WB THK (in)	DEPTH (in)	WIDTH (in)	DEPTH (in)	WIDTH (ft)	DIAMETER (in)	WEIGHT (tons)	WEIGHT (kN)
50.00	6.00	9.00	48.00	144.00	53.00	41.00	84.00	87.33	8.08
75.00	6.00	9.00	48.00	144.00	65.00	41.00	93.00	130.99	12.11
100.00	6.00	9.00	48.00	144.00	75.00	41.00	99.00	174.65	16.15
125.00	6.00	9.00	72.00	144.00	89.00	41.00	105.00	246.44	22.79
150.00	9.00	9.00	69.00	144.00	106.00	41.00	111.00	350.57	32.42
175.00	9.00	9.00	93.00	144.00	122.00	41.00	117.00	448.37	41.46
200.00	12.00	9.00	105.00	144.00	144.00	41.00	123.00	613.68	56.75

TYPE I - SINGLE COLUMN - BASE CASE
COST COMPARISON CHART

TABLE 3-1

COST OF STRUCTURE PER MILE									
SPAN (ft)	CONSTRUCTION FACILITIES	SITE PREPARATION & FINISHING	FOUNDATION	COLUMN	T-BEAM	GIRDER	GIRDER INSTALLLATION	COST/MILE	COST/KILOMETER
50.00	$50,000	$350,000	$1,910,000	$4,330,000	$1,090,000	$5,430,000	$2,810,000	$15,990,000	$9,940,000
75.00	$50,000	$310,000	$1,480,000	$3,330,000	$840,000	$5,260,000	$2,810,000	$14,100,000	$8,770,000
100.00	$50,000	$280,000	$1,360,000	$2,860,000	$710,000	$5,170,000	$2,810,000	$13,270,000	$8,250,000
125.00	$50,000	$270,000	$1,310,000	$2,460,000	$650,000	$5,570,000	$2,810,000	$13,140,000	$8,170,000
150.00	$50,000	$260,000	$1,290,000	$2,280,000	$630,000	$6,270,000	$2,810,000	$13,610,000	$8,460,000
175.00	$50,000	$260,000	$1,290,000	$2,070,000	$610,000	$6,690,000	$2,810,000	$13,800,000	$8,580,000
200.00	$50,000	$250,000	$1,370,000	$1,960,000	$620,000	$7,690,000	$2,810,000	$14,780,000	$9,180,000

SUMMARY OF CRITICAL DIMENSIONS									
SPAN	GIRDER DIMENSIONS				T-BEAM DIMENSIONS		COLUMN	GIRDER	GIRDER
(ft)	FLNG THK (in)	WB THK (in)	DEPTH (in)	WIDTH (in)	DEPTH (in)	WIDTH (ft)	DIAMETER (in)	WEIGHT (tons)	WEIGHT (kN)
50.00	6.00	9.00	48.00	144.00	53.00	41.00	84.00	87.33	8.08
75.00	6.00	9.00	48.00	144.00	65.00	41.00	93.00	130.99	12.11
100.00	6.00	9.00	48.00	144.00	75.00	41.00	99.00	174.65	16.15
125.00	6.00	9.00	72.00	144.00	89.00	41.00	105.00	246.44	22.79
150.00	9.00	9.00	69.00	144.00	106.00	41.00	111.00	350.57	32.42
175.00	9.00	9.00	93.00	144.00	122.00	41.00	117.00	448.37	41.46
200.00	12.00	9.00	105.00	144.00	144.00	41.00	123.00	613.68	56.75

TYPE I - SINGLE COLUMN @ 55' CLEARANCE - BASE CASE COST COMPARISON CHART

TABLE 3-7

GUIDEWAY COST SUMMARY

Chart 3-3 and Tables 3-1 and 3-8 provide a summary of the variation of the cost for the Type I guideway configuration when the girder vertical deflection criteria varies. For the criteria at Span/1000 the design of the guideway section did not change. The guideway cross-section was governed by strength criteria rather than deflection criteria. For this reason the Table 3-1 summarizes the data for both the Span/1000 and Span/1500. The design criteria/parameters provided previously were used to analyze and design the structure. The material quantities and the labor requirements to construct the guideway including finish grading and painting have been estimated and are included in the overall cost of the guideway. The specific criteria for this Chart is provided below:

Ground Clearance	35'
Number of Columns	1
Section Type	Straight
Column Lateral Deflection	Height/500
Girder Vertical Deflection (varies)	Span/1000, Span/1500 and Span/2000
Foundation Type	Spread Footing

Chart 3-3 summarizes the cost for the Type I guideway configuration.

Table 3-1 provides the data for the Type I guideway for deflections of Span/1000 and 1500.
Table 3-8 provides the data for the Type I guideway for deflection of Span/2000.

COST VARIATION BY GIRDER DEFLECTION

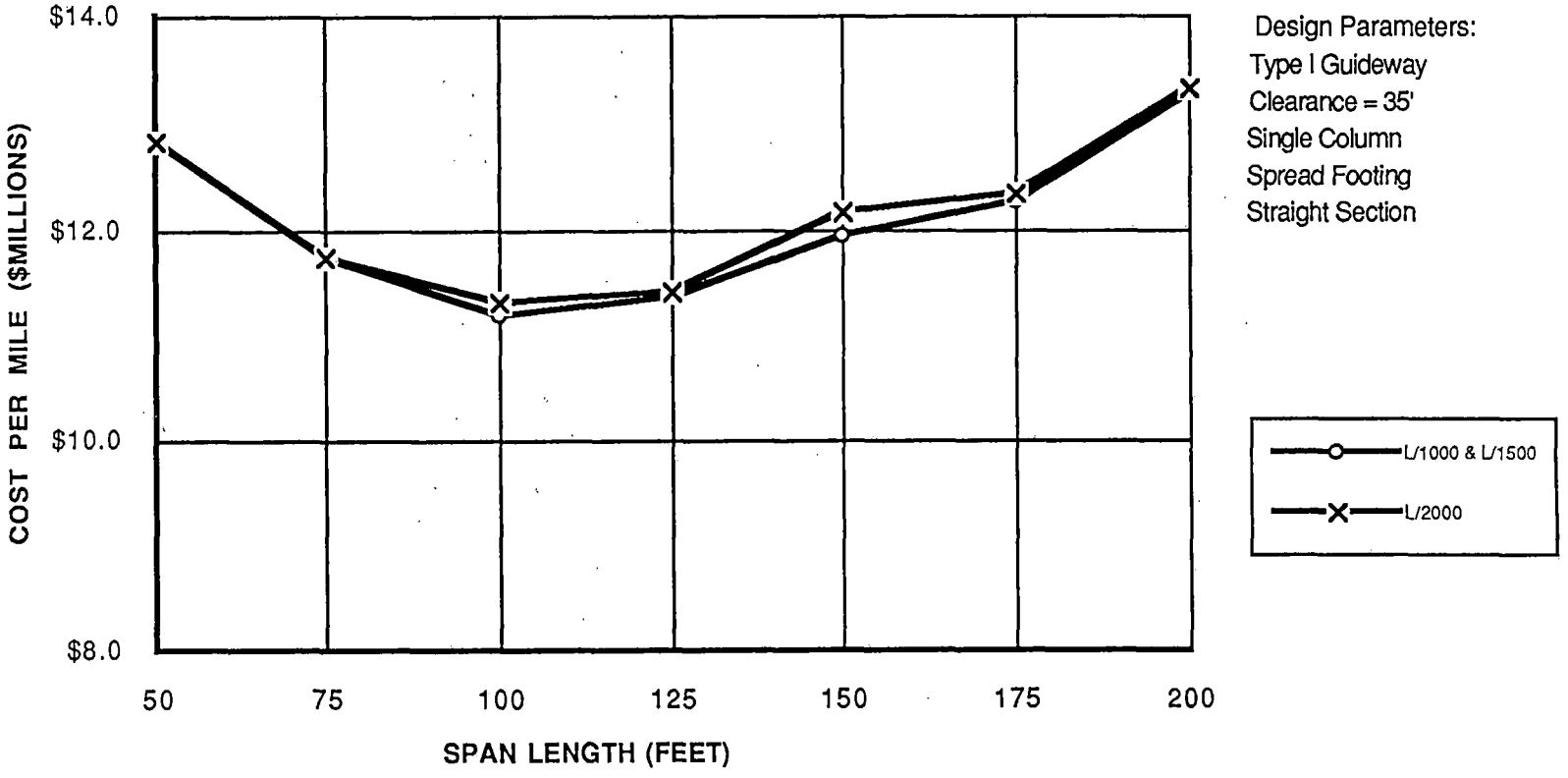

CHART 3-3

COST OF STRUCTURE PER MILE									
SPAN (ft)	CONSTRUCTION FACILITIES	SITE PREPARATION & FINISHING	FOUNDATION	COLUMN	T-BEAM	GIRDER	GIRDER INSTALLLATION	COST/MILE	COST/KILOMETER
50.00	$50,000	$350,000	$1,370,000	$1,710,000	$1,090,000	$5,430,000	$2,810,000	$12,830,000	$7,980,000
75.00	$50,000	$310,000	$1,080,000	$1,360,000	$840,000	$5,260,000	$2,810,000	$11,730,000	$7,290,000
100.00	$50,000	$280,000	$1,030,000	$1,120,000	$710,000	$5,170,000	$2,810,000	$11,200,000	$6,960,000
125.00	$50,000	$270,000	$1,020,000	$970,000	$650,000	$5,570,000	$2,810,000	$11,360,000	$7,060,000
150.00	$50,000	$260,000	$1,020,000	$860,000	$630,000	$6,270,000	$2,810,000	$11,930,000	$7,410,000
175.00	$50,000	$260,000	$1,040,000	$780,000	$610,000	$6,690,000	$2,810,000	$12,270,000	$7,630,000
200.00	$50,000	$250,000	$1,130,000	$700,000	$620,000	$7,690,000	$2,810,000	$13,280,000	$8,250,000

SUMMARY OF CRITICAL DIMENSIONS									
SPAN (ft)	GIRDER DIMENSIONS				T-BEAM DIMENSIONS		COLUMN DIAMETER (in)	GIRDER WEIGHT (tons)	GIRDER WEIGHT (kN)
	FLNG THK (in)	WB THK (in)	DEPTH (in)	WIDTH (in)	DEPTH (in)	WIDTH (ft)			
50.00	6.00	9.00	48.00	144.00	53.00	41.00	84.00	87.33	8.08
75.00	6.00	9.00	48.00	144.00	65.00	41.00	93.00	130.99	12.11
100.00	6.00	9.00	48.00	144.00	75.00	41.00	99.00	174.65	16.15
125.00	6.00	9.00	72.00	144.00	89.00	41.00	105.00	246.44	22.79
150.00	9.00	9.00	69.00	144.00	106.00	41.00	111.00	350.57	32.42
175.00	9.00	9.00	93.00	144.00	122.00	41.00	117.00	448.37	41.46
200.00	12.00	9.00	105.00	144.00	144.00	41.00	123.00	613.68	56.75

TYPE I - SINGLE COLUMN - BASE CASE
COST COMPARISON CHART

TABLE 3-1

COST OF STRUCTURE PER MILE									
SPAN (ft)	CONSTRUCTION FACILITIES	SITE PREPARATION & FINISHING	FOUNDATION	COLUMN	T-BEAM	GIRDER	GIRDER INSTALLLATION	COST/MILE	COST/KILOMETER
50.00	$50,000	$350,000	$1,370,000	$1,710,000	$1,090,000	$5,430,000	$2,810,000	$12,830,000	$7,980,000
75.00	$50,000	$310,000	$1,080,000	$1,360,000	$840,000	$5,260,000	$2,810,000	$11,730,000	$7,290,000
100.00	$50,000	$280,000	$1,030,000	$1,120,000	$720,000	$5,280,000	$2,810,000	$11,320,000	$7,030,000
125.00	$50,000	$270,000	$1,020,000	$970,000	$660,000	$5,620,000	$2,810,000	$11,420,000	$7,100,000
150.00	$50,000	$260,000	$1,020,000	$850,000	$640,000	$6,490,000	$2,810,000	$12,160,000	$7,560,000
175.00	$50,000	$260,000	$1,040,000	$780,000	$610,000	$6,750,000	$2,810,000	$12,330,000	$7,660,000
200.00	$50,000	$250,000	$1,130,000	$700,000	$620,000	$7,750,000	$2,810,000	$13,330,000	$8,290,000

SUMMARY OF CRITICAL DIMENSIONS									
SPAN (ft)	GIRDER DIMENSIONS				T-BEAM DIMENSIONS		COLUMN DIAMETER (in)	GIRDER WEIGHT (tons)	GIRDER WEIGHT (kN)
	FLNG THK (in)	WB THK (in)	DEPTH (in)	WIDTH (in)	DEPTH (in)	WIDTH (ft)			
50.00	6.00	9.00	48.00	144.00	53.00	41.00	84.00	87.33	8.08
75.00	6.00	9.00	48.00	144.00	65.00	41.00	93.00	130.99	12.11
100.00	6.00	9.00	54.00	144.00	76.00	41.00	99.00	180.28	16.67
125.00	6.00	9.00	75.00	144.00	90.00	41.00	105.00	249.95	23.11
150.00	9.00	9.00	81.00	144.00	109.00	41.00	111.00	367.44	33.98
175.00	9.00	9.00	96.00	144.00	123.00	41.00	117.00	453.29	41.92
200.00	12.00	9.00	108.00	144.00	145.00	41.00	123.00	619.30	57.27

TYPE I - SINGLE COLUMN - BASE CASE - GIRDER DEFL L/2000 COST COMPARISON CHART

TABLE 3-8

GUIDEWAY COST SUMMARY

Chart 3-4 and Tables 3-1, 3-9, and 3-10 provide a summary of the variation of the cost for the Type I guideway configuration when the lateral column deflection varies. The design criteria/parameters provided previously were used to analyze and design the structure. The material quantities and the labor requirements to construct the guideway including finish grading and painting have been estimated and are included in the overall cost of the guideway. The specific criteria for this Chart is provided below:

Ground Clearance	35'
Number of Columns	1
Section Type	Straight
Column Lateral Deflection	Height/250,Height/500 and Height/750
Girder Vertical Deflection	Span/1500
Foundation Type	Spread Footing

Chart 3-4 summarizes the cost for the Type I guideway configuration.

Table 3-9 provides the data used for the Type I guideway for the deflection of Height/250.
Table 3-1 provides the data used for the Type I guideway for the deflection of Height/500.
Table 3-10 provides the data used for the Type I I guideway for the deflection of Height/750.

COST VARIATION BY COLUMN DEFLECTION

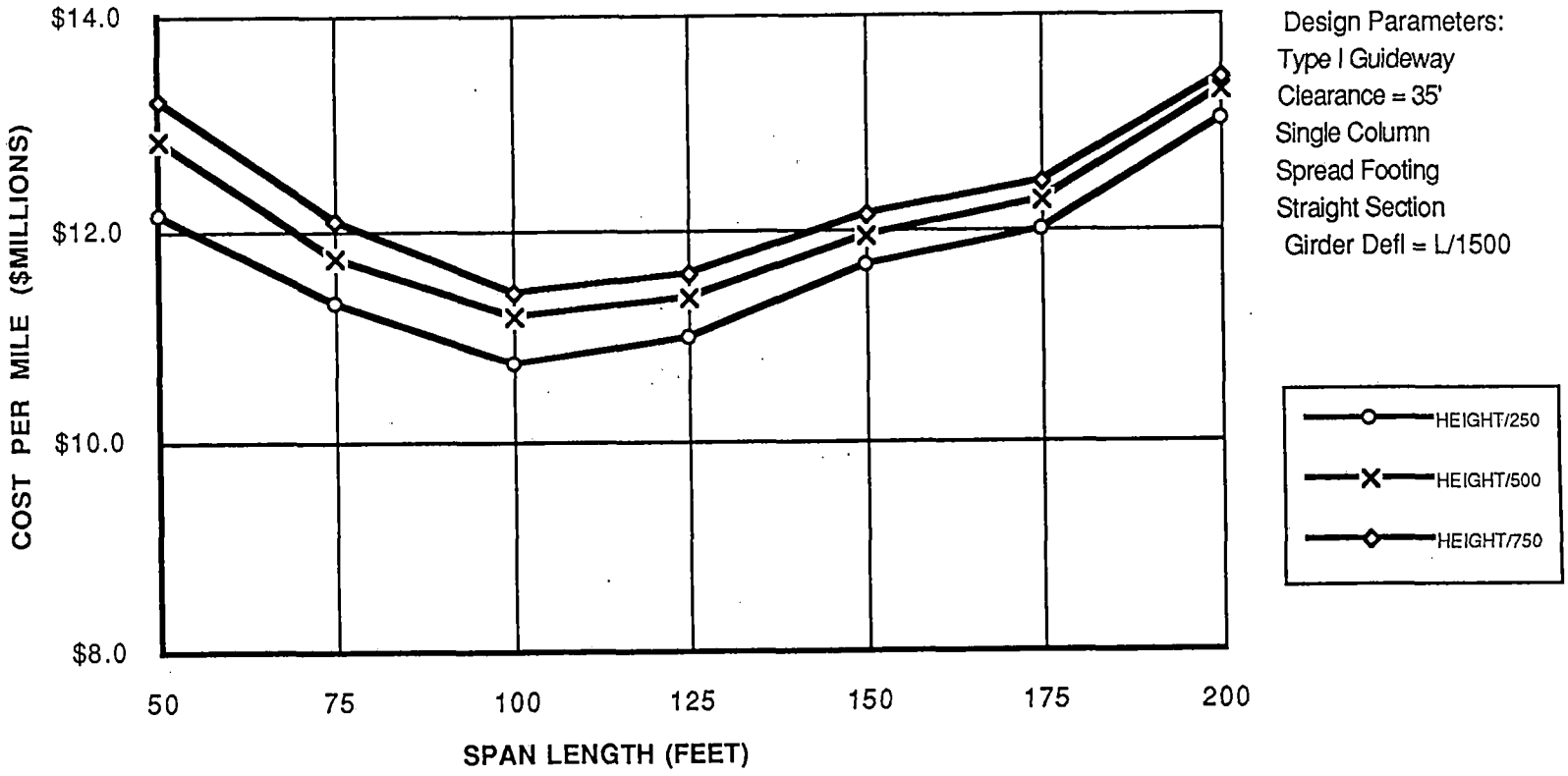

CHART 3-4

COST OF STRUCTURE PER MILE									
SPAN (ft)	CONSTRUCTION FACILITIES	SITE PREPARATION & FINISHING	FOUNDATION	COLUMN	T-BEAM	GIRDER	GIRDER INSTALLLATION	COST/MILE	COST/KILOMETER
50.00	$50,000	$350,000	$1,370,000	$1,710,000	$1,090,000	$5,430,000	$2,810,000	$12,830,000	$7,980,000
75.00	$50,000	$310,000	$1,080,000	$1,360,000	$840,000	$5,260,000	$2,810,000	$11,730,000	$7,290,000
100.00	$50,000	$280,000	$1,030,000	$1,120,000	$710,000	$5,170,000	$2,810,000	$11,200,000	$6,960,000
125.00	$50,000	$270,000	$1,020,000	$970,000	$650,000	$5,570,000	$2,810,000	$11,360,000	$7,060,000
150.00	$50,000	$260,000	$1,020,000	$860,000	$630,000	$6,270,000	$2,810,000	$11,930,000	$7,410,000
175.00	$50,000	$260,000	$1,040,000	$780,000	$610,000	$6,690,000	$2,810,000	$12,270,000	$7,630,000
200.00	$50,000	$250,000	$1,130,000	$700,000	$620,000	$7,690,000	$2,810,000	$13,280,000	$8,250,000

SUMMARY OF CRITICAL DIMENSIONS									
SPAN (ft)	GIRDER DIMENSIONS				T-BEAM DIMENSIONS		COLUMN DIAMETER (in)	GIRDER WEIGHT (tons)	GIRDER WEIGHT (kN)
	FLNG THK (in)	WB THK (in)	DEPTH (in)	WIDTH (in)	DEPTH (in)	WIDTH (ft)			
50.00	6.00	9.00	48.00	144.00	53.00	41.00	84.00	87.33	8.08
75.00	6.00	9.00	48.00	144.00	65.00	41.00	93.00	130.99	12.11
100.00	6.00	9.00	48.00	144.00	75.00	41.00	99.00	174.65	16.15
125.00	6.00	9.00	72.00	144.00	89.00	41.00	105.00	246.44	22.79
150.00	9.00	9.00	69.00	144.00	106.00	41.00	111.00	350.57	32.42
175.00	9.00	9.00	93.00	144.00	122.00	41.00	117.00	448.37	41.46
200.00	12.00	9.00	105.00	144.00	144.00	41.00	123.00	613.68	56.75

TYPE I - SINGLE COLUMN - BASE CASE
COST COMPARISON CHART

TABLE 3-1

COST OF STRUCTURE PER MILE									
SPAN (ft)	CONSTRUCTION FACILITIES	SITE PREPARATION & FINISHING	FOUNDATION	COLUMN	T-BEAM	GIRDER	GIRDER INSTALLLATION	COST/MILE	COST/KILOMETER
50.00	$50,000	$350,000	$1,250,000	$1,150,000	$1,090,000	$5,430,000	$2,810,000	$12,150,000	$7,550,000
75.00	$50,000	$310,000	$1,080,000	$950,000	$840,000	$5,260,000	$2,810,000	$11,330,000	$7,040,000
100.00	$50,000	$280,000	$950,000	$750,000	$710,000	$5,170,000	$2,810,000	$10,750,000	$6,680,000
125.00	$50,000	$270,000	$950,000	$660,000	$650,000	$5,570,000	$2,810,000	$10,990,000	$6,830,000
150.00	$50,000	$260,000	$1,020,000	$600,000	$630,000	$6,270,000	$2,810,000	$11,670,000	$7,250,000
175.00	$50,000	$260,000	$990,000	$560,000	$610,000	$6,690,000	$2,810,000	$11,990,000	$7,450,000
200.00	$50,000	$250,000	$1,070,000	$480,000	$620,000	$7,690,000	$2,810,000	$13,000,000	$8,080,000

SUMMARY OF CRITICAL DIMENSIONS									
SPAN (ft)	GIRDER DIMENSIONS				T-BEAM DIMENSIONS		COLUMN DIAMETER (in)	GIRDER WEIGHT (tons)	GIRDER WEIGHT (kN)
	FLNG THK (in)	WB THK (in)	DEPTH (in)	WIDTH (in)	DEPTH (in)	WIDTH (ft)			
50.00	6.00	9.00	48.00	144.00	53.00	41.00	69.00	87.33	8.08
75.00	6.00	9.00	48.00	144.00	65.00	41.00	78.00	130.99	12.11
100.00	6.00	9.00	48.00	144.00	75.00	41.00	81.00	174.65	16.15
125.00	6.00	9.00	72.00	144.00	89.00	41.00	87.00	246.44	22.79
150.00	9.00	9.00	69.00	144.00	106.00	41.00	93.00	350.57	32.42
175.00	9.00	9.00	93.00	144.00	122.00	41.00	99.00	448.37	41.46
200.00	12.00	9.00	105.00	144.00	144.00	41.00	102.00	613.68	56.75

TYPE I - SINGLE COLUMN - BASE CASE - COLUMN DEFL L/250 COST COMPARISON CHART

TABLE 3-9

COST OF STRUCTURE PER MILE

SPAN (ft)	CONSTRUCTION FACILITIES	SITE PREPARATION & FINISHING	FOUNDATION	COLUMN	T-BEAM	GIRDER	GIRDER INSTALLLATION	COST/MILE	COST/KILOMETER
50.00	$50,000	$350,000	$1,370,000	$2,100,000	$1,090,000	$5,430,000	$2,810,000	$13,220,000	$8,220,000
75.00	$50,000	$310,000	$1,180,000	$1,630,000	$840,000	$5,260,000	$2,810,000	$12,100,000	$7,520,000
100.00	$50,000	$280,000	$1,030,000	$1,330,000	$710,000	$5,170,000	$2,810,000	$11,410,000	$7,090,000
125.00	$50,000	$270,000	$1,020,000	$1,200,000	$650,000	$5,570,000	$2,810,000	$11,600,000	$7,210,000
150.00	$50,000	$260,000	$1,020,000	$1,060,000	$630,000	$6,270,000	$2,810,000	$12,130,000	$7,540,000
175.00	$50,000	$260,000	$1,040,000	$950,000	$610,000	$6,690,000	$2,810,000	$12,440,000	$7,730,000
200.00	$50,000	$250,000	$1,130,000	$850,000	$620,000	$7,690,000	$2,810,000	$13,420,000	$8,340,000

SUMMARY OF CRITICAL DIMENSIONS

SPAN (ft)	GIRDER DIMENSIONS				T-BEAM DIMENSIONS		COLUMN DIAMETER (in)	GIRDER WEIGHT (tons)	GIRDER WEIGHT (kN)
	FLNG THK (in)	WB THK (in)	DEPTH (in)	WIDTH (in)	DEPTH (in)	WIDTH (ft)			
50.00	6.00	9.00	48.00	144.00	53.00	41.00	84.00	87.33	8.08
75.00	6.00	9.00	48.00	144.00	65.00	41.00	93.00	130.99	12.11
100.00	6.00	9.00	48.00	144.00	75.00	41.00	99.00	174.65	16.15
125.00	6.00	9.00	72.00	144.00	89.00	41.00	105.00	246.44	22.79
150.00	9.00	9.00	69.00	144.00	106.00	41.00	111.00	350.57	32.42
175.00	9.00	9.00	93.00	144.00	122.00	41.00	117.00	448.37	41.46
200.00	12.00	9.00	105.00	144.00	144.00	41.00	123.00	613.68	56.75

TYPE I - SINGLE COLUMN - BASE CASE - COLUMN DEFL L/750
COST COMPARISON CHART

TABLE 3-10

GUIDEWAY COST SUMMARY

Chart 3-5 and Tables 3-1 and 3-11 provide a summary of the variation of the cost for the Type I guideway configuration when the seismic criteria varies between Zone 2 and Zone 4. The design criteria/parameters provided previously were used to analyze and design the structure. The material quantities and the labor requirements to construct the guideway including finish grading and painting have been estimated and are included in the overall cost of the guideway. The specific criteria for these Charts is provided below:

Ground Clearance	35'
Number of Columns	1
Section Type	Straight
Column Lateral Deflection	Height/500
Girder Vertical Deflection	Span/1500
Foundation Type	Spread Footing
Seismic Criteria	Zone 2 and Zone 4

Chart 3-5 summarizes the cost for the Type I five configurations.

Table 3-1 provides the data used for the Type I guideway for Zone 2 criteria.
Table 3-11 provides the data used for the Type I guideway for Zone 4 criteria.

COST VARIATION BY SEISMIC ZONE

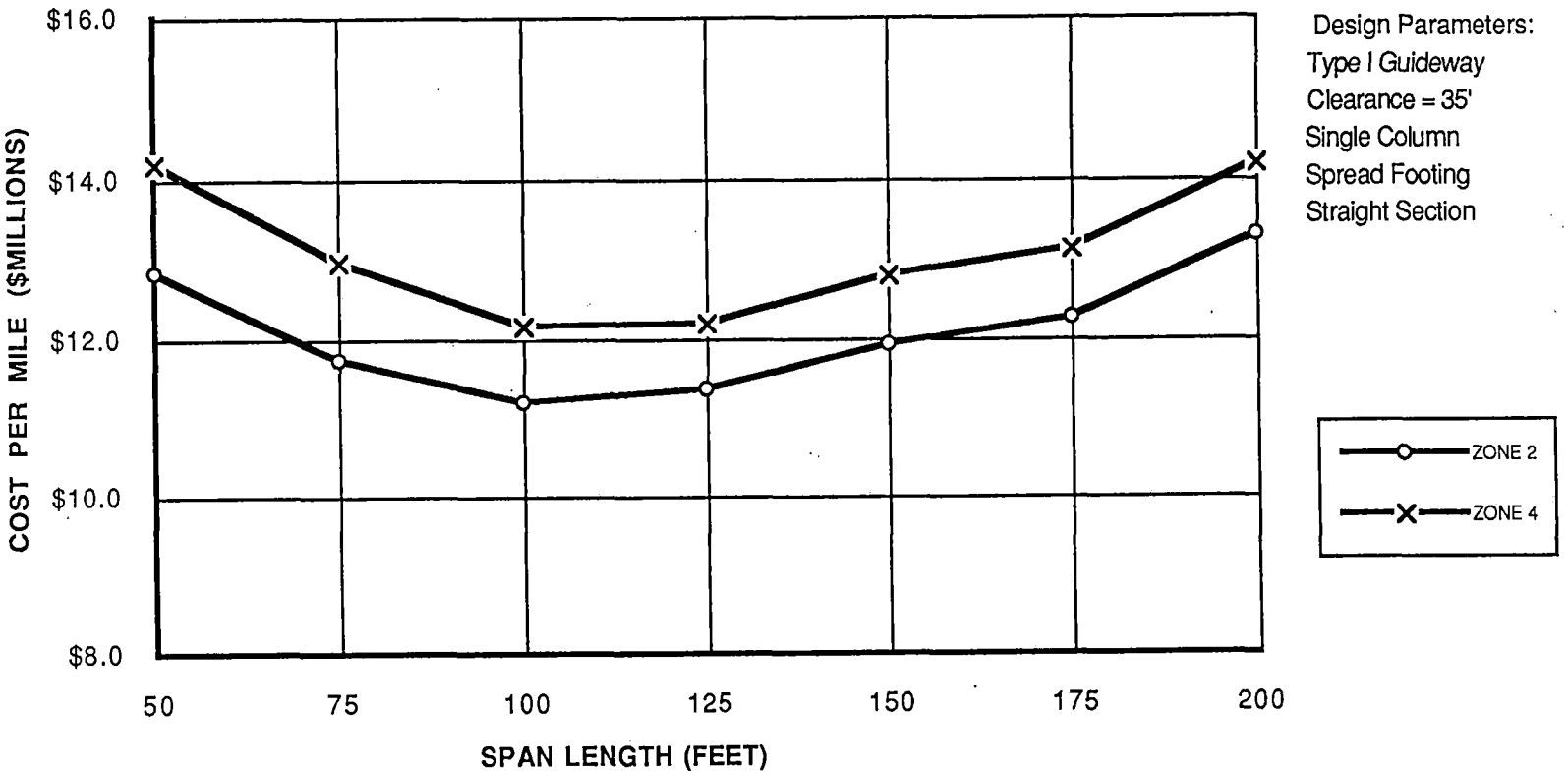

CHART 3-5

COST OF STRUCTURE PER MILE									
SPAN (ft)	CONSTRUCTION FACILITIES	SITE PREPARATION & FINISHING	FOUNDATION	COLUMN	T-BEAM	GIRDER	GIRDER INSTALLLATION	COST/MILE	COST/KILOMETER
50.00	$50,000	$350,000	$1,370,000	$1,710,000	$1,090,000	$5,430,000	$2,810,000	$12,830,000	$7,980,000
75.00	$50,000	$310,000	$1,080,000	$1,360,000	$840,000	$5,260,000	$2,810,000	$11,730,000	$7,290,000
100.00	$50,000	$280,000	$1,030,000	$1,120,000	$710,000	$5,170,000	$2,810,000	$11,200,000	$6,960,000
125.00	$50,000	$270,000	$1,020,000	$970,000	$650,000	$5,570,000	$2,810,000	$11,360,000	$7,060,000
150.00	$50,000	$260,000	$1,020,000	$860,000	$630,000	$6,270,000	$2,810,000	$11,930,000	$7,410,000
175.00	$50,000	$260,000	$1,040,000	$780,000	$610,000	$6,690,000	$2,810,000	$12,270,000	$7,630,000
200.00	$50,000	$250,000	$1,130,000	$700,000	$620,000	$7,690,000	$2,810,000	$13,280,000	$8,250,000

SUMMARY OF CRITICAL DIMENSIONS									
SPAN (ft)	GIRDER DIMENSIONS				T-BEAM DIMENSIONS		COLUMN DIAMETER (in)	GIRDER WEIGHT (tons)	GIRDER WEIGHT (kN)
	FLNG THK (in)	WB THK (in)	DEPTH (in)	WIDTH (in)	DEPTH (in)	WIDTH (ft)			
50.00	6.00	9.00	48.00	144.00	53.00	41.00	84.00	87.33	8.08
75.00	6.00	9.00	48.00	144.00	65.00	41.00	93.00	130.99	12.11
100.00	6.00	9.00	48.00	144.00	75.00	41.00	99.00	174.65	16.15
125.00	6.00	9.00	72.00	144.00	89.00	41.00	105.00	246.44	22.79
150.00	9.00	9.00	69.00	144.00	106.00	41.00	111.00	350.57	32.42
175.00	9.00	9.00	93.00	144.00	122.00	41.00	117.00	448.37	41.46
200.00	12.00	9.00	105.00	144.00	144.00	41.00	123.00	613.68	56.75

TYPE I - SINGLE COLUMN - BASE CASE
COST COMPARISON CHART

TABLE 3-1

COST OF STRUCTURE PER MILE									
SPAN (ft)	CONSTRUCTION FACILITIES	SITE PREPARATION & FINISHING	FOUNDATION	COLUMN	T-BEAM	GIRDER	GIRDER INSTALLLATION	COST/MILE	COST/KILOMETER
50.00	$50,000	$350,000	$2,060,000	$2,380,000	$1,090,000	$5,430,000	$2,810,000	$14,200,000	$8,820,000
75.00	$50,000	$310,000	$1,810,000	$1,830,000	$840,000	$5,260,000	$2,810,000	$12,940,000	$8,040,000
100.00	$50,000	$280,000	$1,630,000	$1,490,000	$710,000	$5,170,000	$2,810,000	$12,170,000	$7,560,000
125.00	$50,000	$270,000	$1,550,000	$1,270,000	$650,000	$5,570,000	$2,810,000	$12,190,000	$7,580,000
150.00	$50,000	$260,000	$1,580,000	$1,160,000	$630,000	$6,270,000	$2,810,000	$12,790,000	$7,950,000
175.00	$50,000	$260,000	$1,640,000	$1,040,000	$610,000	$6,690,000	$2,810,000	$13,120,000	$8,150,000
200.00	$50,000	$250,000	$1,770,000	$960,000	$620,000	$7,690,000	$2,810,000	$14,180,000	$8,810,000

SUMMARY OF CRITICAL DIMENSIONS									
SPAN (ft)	GIRDER DIMENSIONS				T-BEAM DIMENSIONS		COLUMN DIAMETER (in)	GIRDER WEIGHT (tons)	GIRDER WEIGHT (kN)
	FLNG THK (in)	WB THK (in)	DEPTH (in)	WIDTH (in)	DEPTH (in)	WIDTH (ft)			
50.00	6.00	9.00	48.00	144.00	53.00	41.00	84.00	87.33	8.08
75.00	6.00	9.00	48.00	144.00	65.00	41.00	93.00	130.99	12.11
100.00	6.00	9.00	48.00	144.00	75.00	41.00	99.00	174.65	16.15
125.00	6.00	9.00	72.00	144.00	89.00	41.00	105.00	246.44	22.79
150.00	9.00	9.00	69.00	144.00	106.00	41.00	111.00	350.57	32.42
175.00	9.00	9.00	93.00	144.00	122.00	41.00	117.00	448.37	41.46
200.00	12.00	9.00	105.00	144.00	144.00	41.00	123.00	613.68	56.75

TYPE I - SINGLE COLUMN - BASE CASE - ZONE 4 SEISMIC COST COMPARISON CHART

TABLE 3-11

GUIDEWAY COST SUMMARY

Chart 3-6 and Tables 3-12 thru 3-16 provide a summary of the cost of each guideway configuration supported on two columns. The design criteria/parameters provided previously were used to analyze and design the structure. The material quantities and the labor requirements to construct the guideway including finish grading and painting have been estimated and are included in the overall cost of each guideway. The specific criteria for this Chart is provided below:

Ground Clearance	35'
Number of Columns	2
Section Type	Straight
Column Lateral Deflection	Height/500
Girder Vertical Deflection	Span/1500
Foundation Type	Spread Footing

Chart 3-6 summarizes the cost for all five configurations.

Table 3-12 provides the data used for the Type I guideway.
Table 3-13 provides the data used for the Type II guideway.
Table 3-14 provides the data used for the Type III guideway.
Table 3-15 provides the data used for the Type IV guideway.
Table 3-16 provides the data used for the Type V guideway.

GUIDEWAY COST SUMMARY

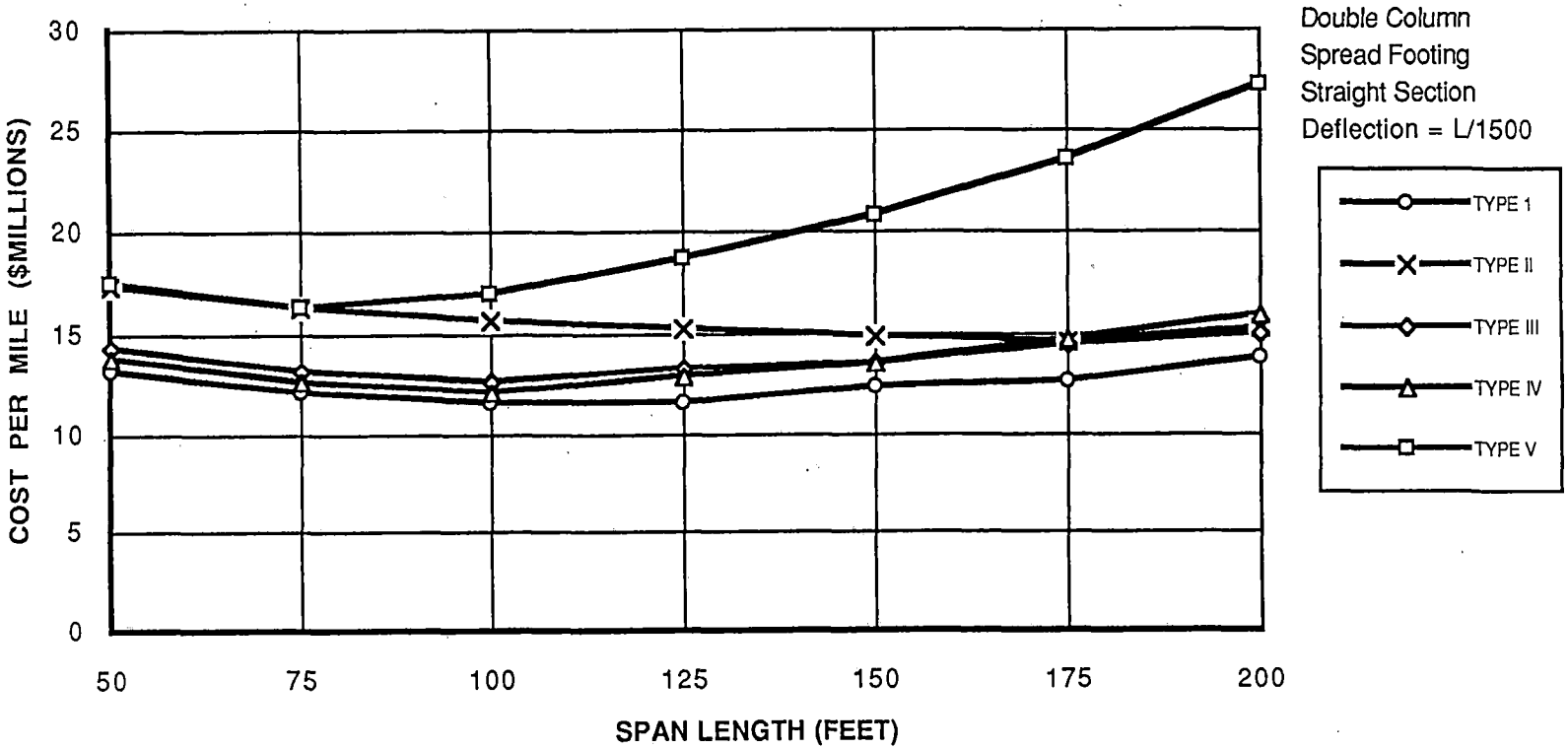

CHART 3-6

COST OF STRUCTURE PER MILE									
SPAN (ft)	CONSTRUCTION FACILITIES	SITE PREPARATION & FINISHING	FOUNDATION	COLUMN	T-BEAM	GIRDER	GIRDER INSTALLLATION	COST/MILE	COST/KILOMETER
50.00	$50,000	$350,000	$1,630,000	$2,140,000	$700,000	$5,430,000	$2,810,000	$13,140,000	$8,170,000
75.00	$50,000	$310,000	$1,510,000	$1,700,000	$460,000	$5,260,000	$2,810,000	$12,120,000	$7,530,000
100.00	$50,000	$280,000	$1,370,000	$1,490,000	$350,000	$5,170,000	$2,810,000	$11,550,000	$7,180,000
125.00	$50,000	$270,000	$1,300,000	$1,290,000	$280,000	$5,570,000	$2,810,000	$11,590,000	$7,210,000
150.00	$50,000	$260,000	$1,370,000	$1,240,000	$230,000	$6,270,000	$2,810,000	$12,260,000	$7,620,000
175.00	$50,000	$260,000	$1,360,000	$1,210,000	$200,000	$6,690,000	$2,810,000	$12,600,000	$7,830,000
200.00	$50,000	$250,000	$1,540,000	$1,200,000	$170,000	$7,690,000	$2,810,000	$13,740,000	$8,540,000

SUMMARY OF CRITICAL DIMENSIONS									
SPAN (ft)	GIRDER DIMENSIONS				T-BEAM DIMENSIONS		COLUMN DIAMETER (in)	GIRDER WEIGHT (tons)	GIRDER WEIGHT (kN)
	FLNG THK (in)	WB THK (in)	DEPTH (in)	WIDTH (in)	DEPTH (in)	WIDTH (ft)			
50.00	6.00	9.00	48.00	144.00	48.00	13.00	66.00	87.33	8.08
75.00	6.00	9.00	48.00	144.00	48.00	13.00	72.00	130.99	12.11
100.00	6.00	9.00	48.00	144.00	48.00	13.00	78.00	174.65	16.15
125.00	6.00	9.00	72.00	144.00	48.00	13.00	81.00	246.44	22.79
150.00	9.00	9.00	69.00	144.00	48.00	13.00	87.00	350.57	32.42
175.00	9.00	9.00	93.00	144.00	48.00	13.00	93.00	448.37	41.46
200.00	12.00	9.00	105.00	144.00	48.00	13.00	99.00	613.68	56.75

TYPE I - DOUBLE COLUMN - BASE CASE
COST COMPARISON CHART

TABLE 3-12

COST OF STRUCTURE PER MILE									
SPAN (ft)	CONSTRUCTION FACILITIES	SITE PREPARATION & FINISHING	FOUNDATION	COLUMN	T-BEAM	GIRDER	GIRDER INSTALLLATION	COST/MILE	COST/KILOMETER
50.00	$50,000	$350,000	$2,260,000	$2,550,000	$560,000	$8,790,000	$2,810,000	$17,400,000	$10,810,000
75.00	$50,000	$310,000	$2,000,000	$2,150,000	$370,000	$8,620,000	$2,810,000	$16,320,000	$10,150,000
100.00	$50,000	$280,000	$1,910,000	$1,730,000	$280,000	$8,530,000	$2,810,000	$15,620,000	$9,710,000
125.00	$50,000	$270,000	$1,770,000	$1,590,000	$220,000	$8,470,000	$2,810,000	$15,220,000	$9,460,000
150.00	$50,000	$260,000	$1,700,000	$1,420,000	$180,000	$8,440,000	$2,810,000	$14,880,000	$9,250,000
175.00	$50,000	$260,000	$1,550,000	$1,290,000	$160,000	$8,410,000	$2,810,000	$14,560,000	$9,050,000
200.00	$50,000	$250,000	$1,630,000	$1,280,000	$140,000	$9,020,000	$2,810,000	$15,210,000	$9,450,000

SUMMARY OF CRITICAL DIMENSIONS									
SPAN	GIRDER DIMENSIONS				T-BEAM DIMENSIONS		COLUMN	GIRDER	GIRDER
(ft)	FLNG THK (in)	WB THK (in)	DEPTH (in)	WIDTH (in)	DEPTH (in)	WIDTH (ft)	DIAMETER (in)	WEIGHT (tons)	WEIGHT (kN)
50.00	15.00	10.00	102.00	110.00	48.00	10.00	72.00	165.10	15.27
75.00	15.00	10.00	102.00	110.00	48.00	10.00	81.00	247.65	22.90
100.00	15.00	10.00	102.00	110.00	48.00	10.00	84.00	330.20	30.54
125.00	15.00	10.00	102.00	110.00	48.00	10.00	90.00	412.75	38.17
150.00	15.00	10.00	102.00	110.00	48.00	10.00	93.00	495.30	45.80
175.00	15.00	10.00	102.00	110.00	48.00	10.00	96.00	577.85	53.44
200.00	15.00	10.00	132.00	110.00	48.00	10.00	102.00	722.90	66.85

TYPE II - DOUBLE COLUMN - BASE CASE
COST COMPARISON CHART

TABLE 3-13

COST OF STRUCTURE PER MILE									
SPAN (ft)	CONSTRUCTION FACILITIES	SITE PREPARATION & FINISHING	FOUNDATION	COLUMN	T-BEAM	GIRDER	GIRDER INSTALLLATION	COST/MILE	COST/KILOMETER
50.00	$50,000	$350,000	$1,830,000	$2,340,000	$700,000	$6,230,000	$2,810,000	$14,340,000	$8,910,000
75.00	$50,000	$310,000	$1,510,000	$1,840,000	$460,000	$6,050,000	$2,810,000	$13,060,000	$8,120,000
100.00	$50,000	$280,000	$1,500,000	$1,490,000	$350,000	$6,080,000	$2,810,000	$12,590,000	$7,820,000
125.00	$50,000	$270,000	$1,530,000	$1,490,000	$280,000	$6,830,000	$2,810,000	$13,290,000	$8,260,000
150.00	$50,000	$260,000	$1,480,000	$1,330,000	$230,000	$7,310,000	$2,810,000	$13,490,000	$8,380,000
175.00	$50,000	$260,000	$1,550,000	$1,290,000	$200,000	$8,260,000	$2,810,000	$14,450,000	$8,980,000
200.00	$50,000	$250,000	$1,630,000	$1,280,000	$170,000	$8,690,000	$2,810,000	$14,920,000	$9,270,000

SUMMARY OF CRITICAL DIMENSIONS									
SPAN (ft)	GIRDER DIMENSIONS				T-BEAM DIMENSIONS		COLUMN DIAMETER (in)	GIRDER WEIGHT (tons)	GIRDER WEIGHT (kN)
	FLNG THK (in)	WB THK (in)	DEPTH (in)	WIDTH (in)	DEPTH (in)	WIDTH (ft)			
50.00	6.00	9.00	48.00	138.00	48.00	13.00	69.00	101.29	9.37
75.00	6.00	9.00	48.00	138.00	48.00	13.00	75.00	151.93	14.05
100.00	6.00	9.00	57.00	138.00	48.00	13.00	78.00	208.20	19.25
125.00	9.00	9.00	60.00	138.00	48.00	13.00	87.00	310.64	28.73
150.00	9.00	9.00	84.00	138.00	48.00	13.00	90.00	410.74	37.98
175.00	12.00	9.00	96.00	138.00	48.00	13.00	96.00	564.51	52.20
200.00	12.00	9.00	120.00	138.00	48.00	13.00	102.00	690.15	63.82

TYPE III - DOUBLE COLUMN - BASE CASE
COST COMPARISON CHART

TABLE 3-14

COST OF STRUCTURE PER MILE									
SPAN (ft)	CONSTRUCTION FACILITIES	SITE PREPARATION & FINISHING	FOUNDATION	COLUMN	T-BEAM	GIRDER	GIRDER INSTALLLATION	COST/MILE	COST/KILOMETER
50.00	$50,000	$350,000	$1,830,000	$2,140,000	$700,000	$5,850,000	$2,810,000	$13,760,000	$8,550,000
75.00	$50,000	$310,000	$1,510,000	$1,700,000	$460,000	$5,680,000	$2,810,000	$12,540,000	$7,790,000
100.00	$50,000	$280,000	$1,370,000	$1,490,000	$350,000	$5,740,000	$2,810,000	$12,120,000	$7,530,000
125.00	$50,000	$270,000	$1,410,000	$1,390,000	$280,000	$6,550,000	$2,810,000	$12,790,000	$7,950,000
150.00	$50,000	$260,000	$1,480,000	$1,330,000	$230,000	$7,270,000	$2,810,000	$13,450,000	$8,360,000
175.00	$50,000	$260,000	$1,650,000	$1,290,000	$200,000	$8,410,000	$2,810,000	$14,700,000	$9,140,000
200.00	$50,000	$250,000	$1,730,000	$1,280,000	$170,000	$9,560,000	$2,810,000	$15,880,000	$9,870,000

SUMMARY OF CRITICAL DIMENSIONS									
SPAN (ft)	GIRDER DIMENSIONS				T-BEAM DIMENSIONS		COLUMN DIAMETER (in)	GIRDER WEIGHT (tons)	GIRDER WEIGHT (kN)
	FLNG THK (in)	WB THK (in)	DEPTH (in)	WIDTH (in)	DEPTH (in)	WIDTH (ft)			
50.00	6.00	12.00	48.00	138.00	48.00	13.00	66.00	91.95	8.50
75.00	6.00	12.00	48.00	138.00	48.00	13.00	72.00	137.93	12.75
100.00	6.00	12.00	54.00	138.00	48.00	13.00	78.00	191.40	17.70
125.00	9.00	12.00	60.00	138.00	48.00	13.00	84.00	293.16	27.11
150.00	9.00	12.00	90.00	138.00	48.00	13.00	90.00	408.04	37.73
175.00	12.00	12.00	108.00	138.00	48.00	13.00	96.00	577.76	53.43
200.00	15.00	12.00	126.00	138.00	48.00	13.00	102.00	776.55	71.81

TYPE IV - DOUBLE COLUMN - BASE CASE
COST COMPARISON CHART

TABLE 3-15

COST OF STRUCTURE PER MILE									
SPAN (ft)	CONSTRUCTION FACILITIES	SITE PREPARATION & FINISHING	FOUNDATION	COLUMN	T-BEAM	GIRDER	GIRDER INSTALLLATION	COST/MILE	COST/KILOMETER
50.00	$50,000	$350,000	$2,260,000	$2,550,000	$790,000	$8,600,000	$2,810,000	$17,440,000	$10,840,000
75.00	$50,000	$310,000	$2,000,000	$2,150,000	$530,000	$8,420,000	$2,810,000	$16,290,000	$10,120,000
100.00	$50,000	$280,000	$2,060,000	$1,860,000	$390,000	$9,520,000	$2,810,000	$17,010,000	$10,570,000
125.00	$50,000	$270,000	$2,170,000	$1,810,000	$310,000	$11,150,000	$2,810,000	$18,610,000	$11,570,000
150.00	$50,000	$260,000	$2,310,000	$1,810,000	$260,000	$13,290,000	$2,810,000	$20,820,000	$12,940,000
175.00	$50,000	$260,000	$2,590,000	$1,730,000	$220,000	$15,920,000	$2,810,000	$23,610,000	$14,670,000
200.00	$50,000	$250,000	$3,000,000	$1,770,000	$190,000	$19,220,000	$2,810,000	$27,320,000	$16,980,000

SUMMARY OF CRITICAL DIMENSIONS									
SPAN (ft)	GIRDER DIMENSIONS				T-BEAM DIMENSIONS		COLUMN DIAMETER (in)	GIRDER WEIGHT (tons)	GIRDER WEIGHT (kN)
	FLNG THK (in)	WB THK (in)	DEPTH (in)	WIDTH (in)	DEPTH (in)	WIDTH (ft)			
50.00	6.00	26.00	48.00	164.00	48.00	15.00	72.00	160.23	14.82
75.00	6.00	26.00	48.00	164.00	48.00	15.00	81.00	240.34	22.23
100.00	9.00	26.00	57.00	164.00	48.00	15.00	87.00	379.83	35.12
125.00	12.00	26.00	75.00	164.00	48.00	15.00	96.00	579.47	53.59
150.00	15.00	26.00	102.00	164.00	48.00	15.00	105.00	857.55	79.30
175.00	18.00	26.00	138.00	164.00	48.00	15.00	111.00	1232.35	113.96
200.00	21.00	26.00	186.00	164.00	48.00	15.00	120.00	1738.40	160.76

TYPE V - DOUBLE COLUMN - BASE CASE COST COMPARISON CHART

TABLE 3-16

GUIDEWAY COST SUMMARY

Chart 3-7 and Tables 3-12, 3-17 and 3-18 provide a summary of the variation of the cost for the Type I guideway configuration supported on two columns when the column height varies. The design criteria/parameters provided previously were used to analyze and design the structure. The material quantities and the labor requirements to construct the guideway including finish grading and painting have been estimated and are included in the overall cost of the guideway. The specific criteria for this Chart is provided below:

Ground Clearance (Varies)	15', 35', and 55'
Number of Columns	2
Section Type	Straight
Column Lateral Deflection	Height/500
Girder Vertical Deflection	Span/1500
Foundation Type	Spread Footing

Chart 3-7 summarizes the cost for the Type I guideway configuration.

Table 3-17 provides the data used for the Type I guideway with 15' ground clearance.
Table 3-12 provides the data used for the Type I guideway with 35' ground clearance.
Table 3-18 provides the data used for the Type I guideway with 55' ground clearance.

COST VARIATION BY COLUMN HEIGHT

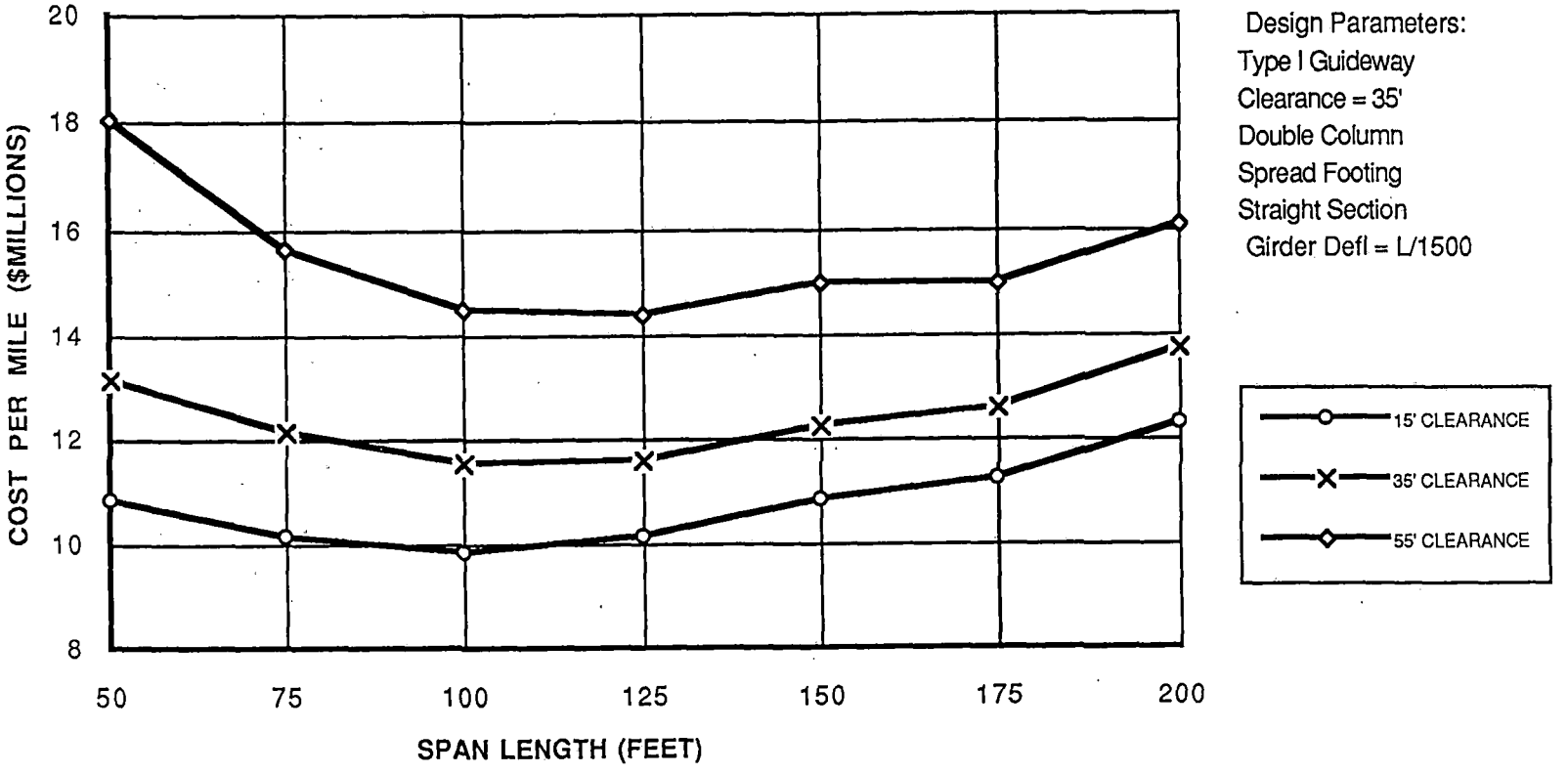

CHART 3-7

COST OF STRUCTURE PER MILE									
SPAN (ft)	CONSTRUCTION FACILITIES	SITE PREPARATION & FINISHING	FOUNDATION	COLUMN	T-BEAM	GIRDER	GIRDER INSTALLLATION	COST/MILE	COST/KILOMETER
50.00	$50,000	$350,000	$1,110,000	$390,000	$700,000	$5,430,000	$2,810,000	$10,860,000	$6,750,000
75.00	$50,000	$310,000	$960,000	$290,000	$460,000	$5,260,000	$2,810,000	$10,170,000	$6,320,000
100.00	$50,000	$280,000	$910,000	$250,000	$350,000	$5,170,000	$2,810,000	$9,850,000	$6,120,000
125.00	$50,000	$270,000	$900,000	$250,000	$280,000	$5,570,000	$2,810,000	$10,150,000	$6,310,000
150.00	$50,000	$260,000	$1,000,000	$230,000	$230,000	$6,270,000	$2,810,000	$10,870,000	$6,760,000
175.00	$50,000	$260,000	$1,010,000	$220,000	$200,000	$6,690,000	$2,810,000	$11,260,000	$7,000,000
200.00	$50,000	$250,000	$1,110,000	$210,000	$170,000	$7,690,000	$2,810,000	$12,310,000	$7,650,000

SUMMARY OF CRITICAL DIMENSIONS									
SPAN (ft)	GIRDER DIMENSIONS				T-BEAM DIMENSIONS		COLUMN	GIRDER	GIRDER
	FLNG THK (in)	WB THK (in)	DEPTH (in)	WIDTH (in)	DEPTH (in)	WIDTH (ft)	DIAMETER (in)	WEIGHT (tons)	WEIGHT (kN)
50.00	6.00	9.00	48.00	144.00	48.00	13.00	45.00	87.33	8.08
75.00	6.00	9.00	48.00	144.00	48.00	13.00	48.00	130.99	12.11
100.00	6.00	9.00	48.00	144.00	48.00	13.00	51.00	174.65	16.15
125.00	6.00	9.00	72.00	144.00	48.00	13.00	57.00	246.44	22.79
150.00	9.00	9.00	69.00	144.00	48.00	13.00	60.00	350.57	32.42
175.00	9.00	9.00	93.00	144.00	48.00	13.00	63.00	448.37	41.46
200.00	12.00	9.00	105.00	144.00	48.00	13.00	66.00	613.68	56.75

TYPE I - DOUBLE COLUMN @ 15' CLEARANCE - BASE CASE COST COMPARISON CHART

TABLE 3-17

COST OF STRUCTURE PER MILE									
SPAN (ft)	CONSTRUCTION FACILITIES	SITE PREPARATION & FINISHING	FOUNDATION	COLUMN	T-BEAM	GIRDER	GIRDER INSTALLLATION	COST/MILE	COST/KILOMETER
50.00	$50,000	$350,000	$1,630,000	$2,140,000	$700,000	$5,430,000	$2,810,000	$13,140,000	$8,170,000
75.00	$50,000	$310,000	$1,510,000	$1,700,000	$460,000	$5,260,000	$2,810,000	$12,120,000	$7,530,000
100.00	$50,000	$280,000	$1,370,000	$1,490,000	$350,000	$5,170,000	$2,810,000	$11,550,000	$7,180,000
125.00	$50,000	$270,000	$1,300,000	$1,290,000	$280,000	$5,570,000	$2,810,000	$11,590,000	$7,210,000
150.00	$50,000	$260,000	$1,370,000	$1,240,000	$230,000	$6,270,000	$2,810,000	$12,260,000	$7,620,000
175.00	$50,000	$260,000	$1,360,000	$1,210,000	$200,000	$6,690,000	$2,810,000	$12,600,000	$7,830,000
200.00	$50,000	$250,000	$1,540,000	$1,200,000	$170,000	$7,690,000	$2,810,000	$13,740,000	$8,540,000

SUMMARY OF CRITICAL DIMENSIONS									
SPAN (ft)	GIRDER DIMENSIONS				T-BEAM DIMENSIONS		COLUMN DIAMETER (in)	GIRDER WEIGHT (tons)	GIRDER WEIGHT (kN)
	FLNG THK (in)	WB THK (in)	DEPTH (in)	WIDTH (in)	DEPTH (in)	WIDTH (ft)			
50.00	6.00	9.00	48.00	144.00	48.00	13.00	66.00	87.33	8.08
75.00	6.00	9.00	48.00	144.00	48.00	13.00	72.00	130.99	12.11
100.00	6.00	9.00	48.00	144.00	48.00	13.00	78.00	174.65	16.15
125.00	6.00	9.00	72.00	144.00	48.00	13.00	81.00	246.44	22.79
150.00	9.00	9.00	69.00	144.00	48.00	13.00	87.00	350.57	32.42
175.00	9.00	9.00	93.00	144.00	48.00	13.00	93.00	448.37	41.46
200.00	12.00	9.00	105.00	144.00	48.00	13.00	99.00	613.68	56.75

TYPE I - DOUBLE COLUMN - BASE CASE
COST COMPARISON CHART

TABLE 3-12

COST OF STRUCTURE PER MILE									
SPAN (ft)	CONSTRUCTION FACILITIES	SITE PREPARATION & FINISHING	FOUNDATION	COLUMN	T-BEAM	GIRDER	GIRDER INSTALLLATION	COST/MILE	COST/KILOMETER
50.00	$50,000	$350,000	$2,740,000	$5,990,000	$700,000	$5,430,000	$2,810,000	$18,090,000	$11,240,000
75.00	$50,000	$310,000	$2,170,000	$4,560,000	$460,000	$5,260,000	$2,810,000	$15,650,000	$9,720,000
100.00	$50,000	$280,000	$1,910,000	$3,870,000	$350,000	$5,170,000	$2,810,000	$14,470,000	$8,990,000
125.00	$50,000	$270,000	$1,900,000	$3,490,000	$280,000	$5,570,000	$2,810,000	$14,390,000	$8,940,000
150.00	$50,000	$260,000	$1,930,000	$3,420,000	$230,000	$6,270,000	$2,810,000	$15,000,000	$9,320,000
175.00	$50,000	$260,000	$1,870,000	$3,090,000	$200,000	$6,690,000	$2,810,000	$14,990,000	$9,320,000
200.00	$50,000	$250,000	$1,940,000	$3,140,000	$170,000	$7,690,000	$2,810,000	$16,070,000	$9,990,000

SUMMARY OF CRITICAL DIMENSIONS									
SPAN (ft)	GIRDER DIMENSIONS				T-BEAM DIMENSIONS		COLUMN DIAMETER (in)	GIRDER WEIGHT (tons)	GIRDER WEIGHT (kN)
	FLNG THK (in)	WB THK (in)	DEPTH (in)	WIDTH (in)	DEPTH (in)	WIDTH (ft)			
50.00	6.00	9.00	48.00	144.00	48.00	13.00	87.00	87.33	8.08
75.00	6.00	9.00	48.00	144.00	48.00	13.00	93.00	130.99	12.11
100.00	6.00	9.00	48.00	144.00	48.00	13.00	99.00	174.65	16.15
125.00	6.00	9.00	72.00	144.00	48.00	13.00	105.00	246.44	22.79
150.00	9.00	9.00	69.00	144.00	48.00	13.00	114.00	350.57	32.42
175.00	9.00	9.00	93.00	144.00	48.00	13.00	117.00	448.37	41.46
200.00	12.00	9.00	105.00	144.00	48.00	13.00	126.00	613.68	56.75

TYPE I - DOUBLE COLUMN @ 55' CLEARANCE - BASE CASE COST COMPARISON CHART

TABLE 3-18

GUIDEWAY COST SUMMARY

Chart 3-8 and Tables 3-12 and 3-19 provide a summary of the variation of the cost for the Type I guideway configuration supported on two columns when the girder vertical deflection criteria varies. For the criteria at Span/1000 the design of the guideway section did not change. The guideway cross-section was governed by strength criteria rather than deflection criteria. For this reason the Table 3-12 summarizes the data for both the Span/1000 and Span/1500. The design criteria/parameters provided previously were used to analyze and design the structure. The material quantities and the labor requirements to construct the guideway including finish grading and painting have been estimated and are included in the overall cost of the guideway. The specific criteria for this Chart is provided below:

Ground Clearance	35'
Number of Columns	2
Section Type	Straight
Column Lateral Deflection	Height/500
Girder Vertical Deflection (varies)	Span/1000, Span/1500 and Span/2000
Foundation Type	Spread Footing

Chart 3-8 summarizes the cost for the Type I guideway configuration.

Table 3-12 provides the data for the Type I guideway for deflections of Span/1000 and 1500. Table 3-19provides the data for the Type I guideway for deflection of Span/2000.

COST VARIATION BY GIRDER DEFLECTION

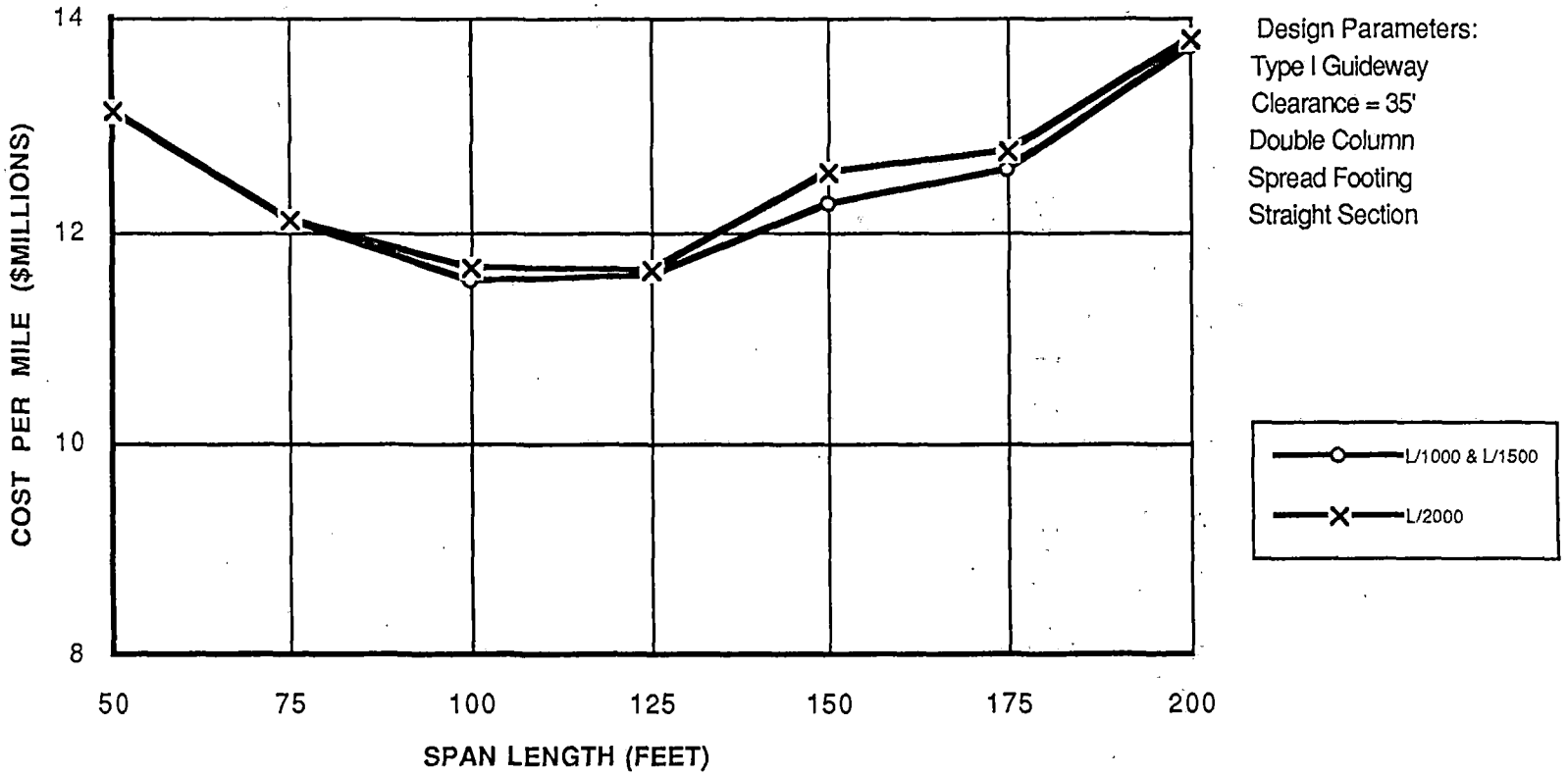

CHART 3-8

COST OF STRUCTURE PER MILE									
SPAN (ft)	CONSTRUCTION FACILITIES	SITE PREPARATION & FINISHING	FOUNDATION	COLUMN	T-BEAM	GIRDER	GIRDER INSTALLLATION	COST/MILE	COST/KILOMETER
50.00	$50,000	$350,000	$1,630,000	$2,140,000	$700,000	$5,430,000	$2,810,000	$13,140,000	$8,170,000
75.00	$50,000	$310,000	$1,510,000	$1,700,000	$460,000	$5,260,000	$2,810,000	$12,120,000	$7,530,000
100.00	$50,000	$280,000	$1,370,000	$1,490,000	$350,000	$5,170,000	$2,810,000	$11,550,000	$7,180,000
125.00	$50,000	$270,000	$1,300,000	$1,290,000	$280,000	$5,570,000	$2,810,000	$11,590,000	$7,210,000
150.00	$50,000	$260,000	$1,370,000	$1,240,000	$230,000	$6,270,000	$2,810,000	$12,260,000	$7,620,000
175.00	$50,000	$260,000	$1,360,000	$1,210,000	$200,000	$6,690,000	$2,810,000	$12,600,000	$7,830,000
200.00	$50,000	$250,000	$1,540,000	$1,200,000	$170,000	$7,690,000	$2,810,000	$13,740,000	$8,540,000

SUMMARY OF CRITICAL DIMENSIONS									
SPAN (ft)	GIRDER DIMENSIONS				T-BEAM DIMENSIONS		COLUMN DIAMETER (in)	GIRDER WEIGHT (tons)	GIRDER WEIGHT (kN)
	FLNG THK (in)	WB THK (in)	DEPTH (in)	WIDTH (in)	DEPTH (in)	WIDTH (ft)			
50.00	6.00	9.00	48.00	144.00	48.00	13.00	66.00	87.33	8.08
75.00	6.00	9.00	48.00	144.00	48.00	13.00	72.00	130.99	12.11
100.00	6.00	9.00	48.00	144.00	48.00	13.00	78.00	174.65	16.15
125.00	6.00	9.00	72.00	144.00	48.00	13.00	81.00	246.44	22.79
150.00	9.00	9.00	69.00	144.00	48.00	13.00	87.00	350.57	32.42
175.00	9.00	9.00	93.00	144.00	48.00	13.00	93.00	448.37	41.46
200.00	12.00	9.00	105.00	144.00	48.00	13.00	99.00	613.68	56.75

TYPE I - DOUBLE COLUMN - BASE CASE COST COMPARISON CHART

TABLE 3-12

COST OF STRUCTURE PER MILE									
SPAN (ft)	CONSTRUCTION FACILITIES	SITE PREPARATION & FINISHING	FOUNDATION	COLUMN	T-BEAM	GIRDER	GIRDER INSTALLLATION	COST/MILE	COST/KILOMETER
50.00	$50,000	$350,000	$1,630,000	$2,140,000	$700,000	$5,430,000	$2,810,000	$13,140,000	$8,170,000
75.00	$50,000	$310,000	$1,510,000	$1,700,000	$460,000	$5,260,000	$2,810,000	$12,120,000	$7,530,000
100.00	$50,000	$280,000	$1,370,000	$1,490,000	$350,000	$5,280,000	$2,810,000	$11,660,000	$7,250,000
125.00	$50,000	$270,000	$1,300,000	$1,290,000	$280,000	$5,620,000	$2,810,000	$11,650,000	$7,240,000
150.00	$50,000	$260,000	$1,370,000	$1,330,000	$230,000	$6,490,000	$2,810,000	$12,570,000	$7,810,000
175.00	$50,000	$260,000	$1,450,000	$1,210,000	$200,000	$6,750,000	$2,810,000	$12,760,000	$7,930,000
200.00	$50,000	$250,000	$1,540,000	$1,200,000	$170,000	$7,750,000	$2,810,000	$13,800,000	$8,580,000

SUMMARY OF CRITICAL DIMENSIONS									
SPAN	GIRDER DIMENSIONS				T-BEAM DIMENSIONS		COLUMN	GIRDER	GIRDER
(ft)	FLNG THK (in)	WB THK (in)	DEPTH (in)	WIDTH (in)	DEPTH (in)	WIDTH (ft)	DIAMETER (in)	WEIGHT (tons)	WEIGHT (kN)
50.00	6.00	9.00	48.00	144.00	48.00	13.00	66.00	87.33	8.08
75.00	6.00	9.00	48.00	144.00	48.00	13.00	72.00	130.99	12.11
100.00	6.00	9.00	54.00	144.00	48.00	13.00	78.00	180.28	16.67
125.00	6.00	9.00	75.00	144.00	48.00	13.00	81.00	249.95	23.11
150.00	9.00	9.00	81.00	144.00	48.00	13.00	90.00	367.44	33.98
175.00	9.00	9.00	96.00	144.00	48.00	13.00	93.00	453.29	41.92
200.00	12.00	9.00	108.00	144.00	48.00	13.00	99.00	619.30	57.27

TYPE I - DOUBLE COLUMN - BASE CASE - GIRDER DEFL L/2000
COST COMPARISON CHART

TABLE 3-19

GUIDEWAY COST SUMMARY

Chart 3-9 and Tables 3-12, 3-20, and 3-21 provide a summary of the variation of the cost for the Type I guideway configuration supported on two columns when the lateral column deflection varies. The design criteria/parameters provided previously were used to analyze and design the structure. The material quantities and the labor requirements to construct the guideway including finish grading and painting have been estimated and are included in the overall cost of the guideway. The specific criteria for this Chart is provided below:

Ground Clearance	35'
Number of Columns	2
Section Type	Straight
Column Lateral Deflection	Height/250,Height/500 and Height/750
Girder Vertical Deflection	Span/1500
Foundation Type	Spread Footing

Chart 3-9 summarizes the cost for the Type I guideway configuration.

Table 3-20 provides the data used for the Type I guideway for the deflection of Height/250.
Table 3-12 provides the data used for the Type I guideway for the deflection of Height/500.
Table 3-21 provides the data used for the Type I I guideway for the deflection of Height/750.

COST VARIATION BY COLUMN DEFLECTION

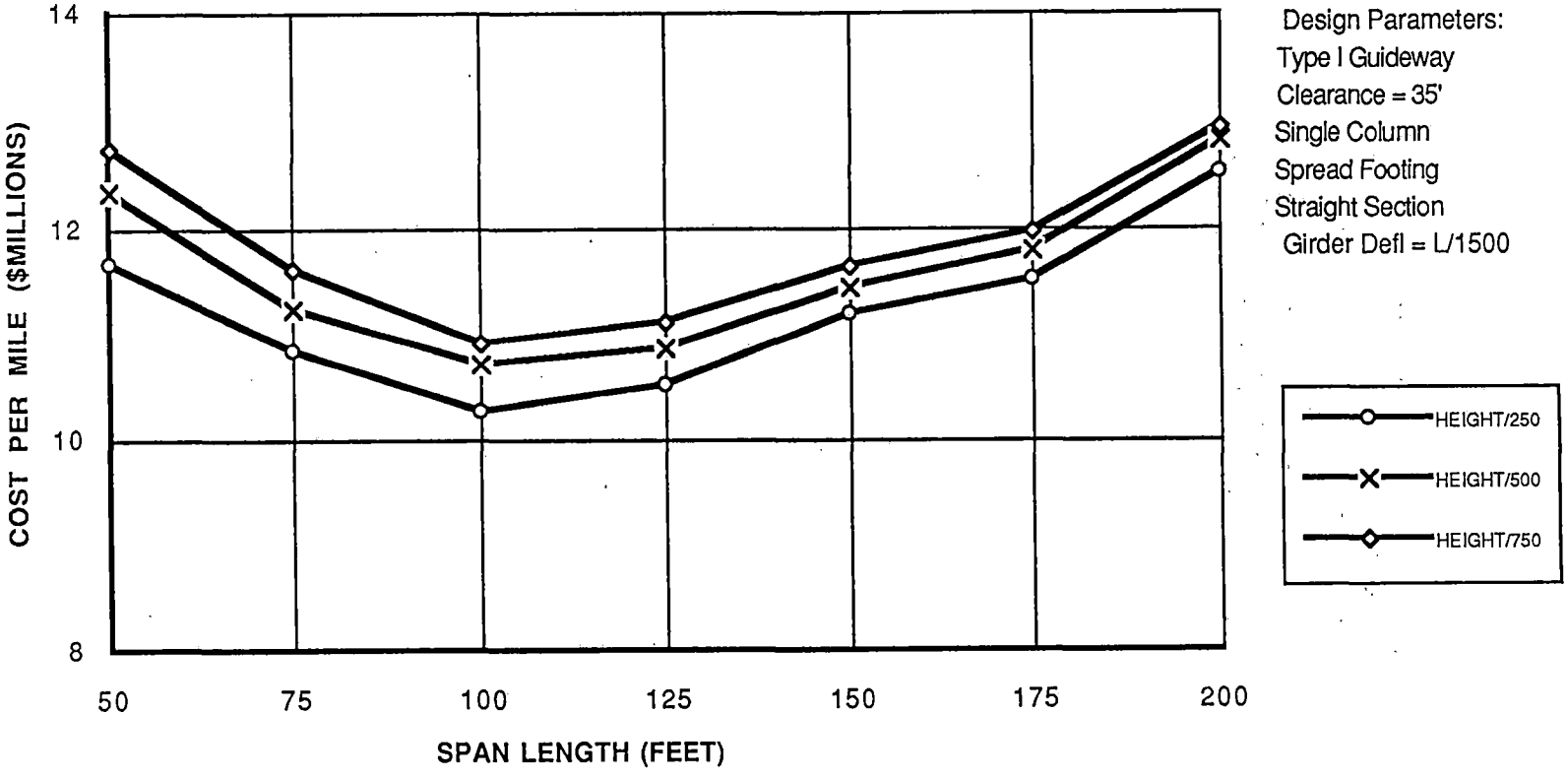

CHART 3-9

COST OF STRUCTURE PER MILE									
SPAN (ft)	CONSTRUCTION FACILITIES	SITE PREPARATION & FINISHING	FOUNDATION	COLUMN	T-BEAM	GIRDER	GIRDER INSTALLLATION	COST/MILE	COST/KILOMETER
50.00	$50,000	$350,000	$1,630,000	$1,430,000	$700,000	$5,430,000	$2,810,000	$12,430,000	$7,730,000
75.00	$50,000	$310,000	$1,360,000	$1,180,000	$460,000	$5,260,000	$2,810,000	$11,450,000	$7,120,000
100.00	$50,000	$280,000	$1,250,000	$970,000	$350,000	$5,170,000	$2,810,000	$10,910,000	$6,780,000
125.00	$50,000	$270,000	$1,300,000	$930,000	$280,000	$5,570,000	$2,810,000	$11,240,000	$6,980,000
150.00	$50,000	$260,000	$1,370,000	$920,000	$230,000	$6,270,000	$2,810,000	$11,940,000	$7,420,000
175.00	$50,000	$260,000	$1,360,000	$850,000	$200,000	$6,690,000	$2,810,000	$12,240,000	$7,610,000
200.00	$50,000	$250,000	$1,450,000	$860,000	$170,000	$7,690,000	$2,810,000	$13,310,000	$8,270,000

SUMMARY OF CRITICAL DIMENSIONS									
SPAN (ft)	GIRDER DIMENSIONS				T-BEAM DIMENSIONS		COLUMN DIAMETER (in)	GIRDER WEIGHT (tons)	GIRDER WEIGHT (kN)
	FLNG THK (in)	WB THK (in)	DEPTH (in)	WIDTH (in)	DEPTH (in)	WIDTH (ft)			
50.00	6.00	9.00	48.00	144.00	48.00	13.00	54.00	87.33	8.08
75.00	6.00	9.00	48.00	144.00	48.00	13.00	60.00	130.99	12.11
100.00	6.00	9.00	48.00	144.00	48.00	13.00	63.00	174.65	16.15
125.00	6.00	9.00	72.00	144.00	48.00	13.00	69.00	246.44	22.79
150.00	9.00	9.00	69.00	144.00	48.00	13.00	75.00	350.57	32.42
175.00	9.00	9.00	93.00	144.00	48.00	13.00	78.00	448.37	41.46
200.00	12.00	9.00	105.00	144.00	48.00	13.00	84.00	613.68	56.75

TYPE I - DOUBLE COLUMN - BASE CASE - COLUMN DEFL L/250
COST COMPARISON CHART

TABLE 3-20

COST OF STRUCTURE PER MILE									
SPAN (ft)	CONSTRUCTION FACILITIES	SITE PREPARATION & FINISHING	FOUNDATION	COLUMN	T-BEAM	GIRDER	GIRDER INSTALLLATION	COST/MILE	COST/KILOMETER
50.00	$50,000	$350,000	$1,630,000	$2,140,000	$700,000	$5,430,000	$2,810,000	$13,140,000	$8,170,000
75.00	$50,000	$310,000	$1,510,000	$1,700,000	$460,000	$5,260,000	$2,810,000	$12,120,000	$7,530,000
100.00	$50,000	$280,000	$1,370,000	$1,490,000	$350,000	$5,170,000	$2,810,000	$11,550,000	$7,180,000
125.00	$50,000	$270,000	$1,300,000	$1,290,000	$280,000	$5,570,000	$2,810,000	$11,590,000	$7,210,000
150.00	$50,000	$260,000	$1,370,000	$1,240,000	$230,000	$6,270,000	$2,810,000	$12,260,000	$7,620,000
175.00	$50,000	$260,000	$1,360,000	$1,210,000	$200,000	$6,690,000	$2,810,000	$12,600,000	$7,830,000
200.00	$50,000	$250,000	$1,540,000	$1,200,000	$170,000	$7,690,000	$2,810,000	$13,740,000	$8,540,000

SUMMARY OF CRITICAL DIMENSIONS									
SPAN	GIRDER DIMENSIONS				T-BEAM DIMENSIONS		COLUMN	GIRDER	GIRDER
(ft)	FLNG THK (in)	WB THK (in)	DEPTH (in)	WIDTH (in)	DEPTH (in)	WIDTH (ft)	DIAMETER (in)	WEIGHT (tons)	WEIGHT (kN)
50.00	6.00	9.00	48.00	144.00	48.00	13.00	66.00	87.33	8.08
75.00	6.00	9.00	48.00	144.00	48.00	13.00	72.00	130.99	12.11
100.00	6.00	9.00	48.00	144.00	48.00	13.00	78.00	174.65	16.15
125.00	6.00	9.00	72.00	144.00	48.00	13.00	81.00	246.44	22.79
150.00	9.00	9.00	69.00	144.00	48.00	13.00	87.00	350.57	32.42
175.00	9.00	9.00	93.00	144.00	48.00	13.00	93.00	448.37	41.46
200.00	12.00	9.00	105.00	144.00	48.00	13.00	99.00	613.68	56.75

TYPE I - DOUBLE COLUMN - BASE CASE
COST COMPARISON CHART

TABLE 3-12

COST OF STRUCTURE PER MILE									
SPAN (ft)	CONSTRUCTION FACILITIES	SITE PREPARATION & FINISHING	FOUNDATION	COLUMN	T-BEAM	GIRDER	GIRDER INSTALLLATION	COST/MILE	COST/KILOMETER
50.00	$50,000	$350,000	$1,830,000	$2,770,000	$700,000	$5,430,000	$2,810,000	$13,970,000	$8,680,000
75.00	$50,000	$310,000	$1,510,000	$2,150,000	$460,000	$5,260,000	$2,810,000	$12,570,000	$7,810,000
100.00	$50,000	$280,000	$1,370,000	$1,730,000	$350,000	$5,170,000	$2,810,000	$11,790,000	$7,330,000
125.00	$50,000	$270,000	$1,410,000	$1,590,000	$280,000	$5,570,000	$2,810,000	$12,010,000	$7,460,000
150.00	$50,000	$260,000	$1,370,000	$1,600,000	$230,000	$6,270,000	$2,810,000	$12,620,000	$7,850,000
175.00	$50,000	$260,000	$1,450,000	$1,460,000	$200,000	$6,690,000	$2,810,000	$12,950,000	$8,050,000
200.00	$50,000	$250,000	$1,540,000	$1,510,000	$170,000	$7,690,000	$2,810,000	$14,050,000	$8,730,000

SUMMARY OF CRITICAL DIMENSIONS									
SPAN (ft)	GIRDER DIMENSIONS				T-BEAM DIMENSIONS		COLUMN DIAMETER (in)	GIRDER WEIGHT (tons)	GIRDER WEIGHT (kN)
	FLNG THK (in)	WB THK (in)	DEPTH (in)	WIDTH (in)	DEPTH (in)	WIDTH (ft)			
50.00	6.00	9.00	48.00	144.00	48.00	13.00	75.00	87.33	8.08
75.00	6.00	9.00	48.00	144.00	48.00	13.00	81.00	130.99	12.11
100.00	6.00	9.00	48.00	144.00	48.00	13.00	84.00	174.65	16.15
125.00	6.00	9.00	72.00	144.00	48.00	13.00	90.00	246.44	22.79
150.00	9.00	9.00	69.00	144.00	48.00	13.00	99.00	350.57	32.42
175.00	9.00	9.00	93.00	144.00	48.00	13.00	102.00	448.37	41.46
200.00	12.00	9.00	105.00	144.00	48.00	13.00	111.00	613.68	56.75

TYPE I - DOUBLE COLUMN - BASE CASE - COLUMN DEFL L/750
COST COMPARISON CHART

TABLE 3-21

GUIDEWAY COST SUMMARY

Chart 3-10 and Tables 3-12 and 3-22 provide a summary of the variation of the cost for the Type I guideway configuration supported on two columns when the seismic criteria varies between Zone 2 and Zone 4. The design criteria/parameters provided previously were used to analyze and design the structure. The material quantities and the labor requirements to construct the guideway including finish grading and painting have been estimated and are included in the overall cost of the guideway. The specific criteria for these Charts is provided below:

Ground Clearance	35'
Number of Columns	2
Section Type	Straight
Column Lateral Deflection	Height/500
Girder Vertical Deflection	Span/1500
Foundation Type	Spread Footing
Seismic Criteria	Zone 2 and Zone 4

Chart 3-10 summarizes the cost for the Type I five configurations.

Table 3-12 provides the data used for the Type I guideway for Zone 2 criteria.
Table 3-22 provides the data used for the Type I guideway for Zone 4 criteria.

COST VARIATION BY SEISMIC ZONE

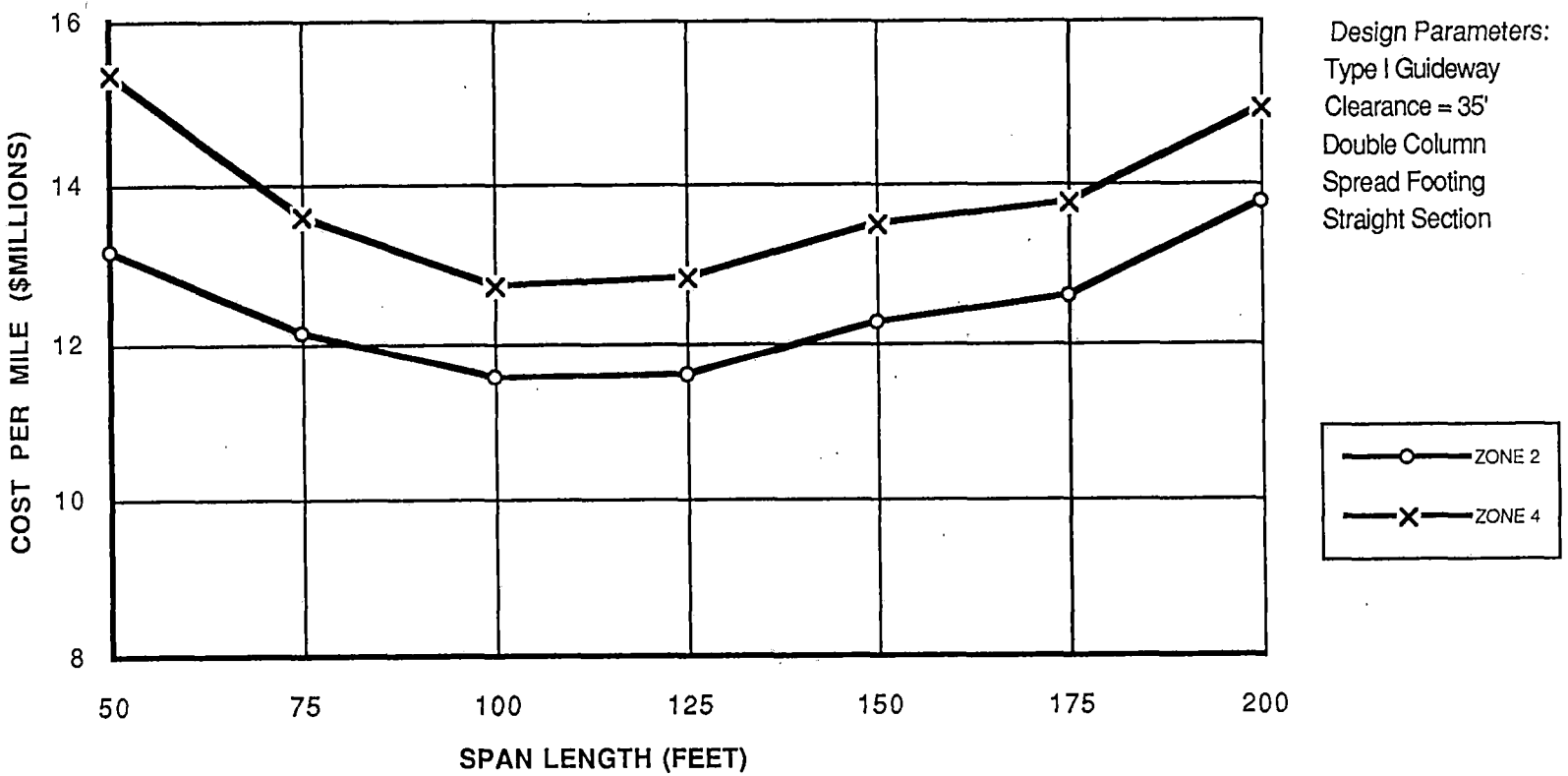

CHART 3-10

COST OF STRUCTURE PER MILE									
SPAN (ft)	CONSTRUCTION FACILITIES	SITE PREPARATION & FINISHING	FOUNDATION	COLUMN	T-BEAM	GIRDER	GIRDER INSTALLLATION	COST/MILE	COST/KILOMETER
50.00	$50,000	$350,000	$1,630,000	$2,140,000	$700,000	$5,430,000	$2,810,000	$13,140,000	$8,170,000
75.00	$50,000	$310,000	$1,510,000	$1,700,000	$460,000	$5,260,000	$2,810,000	$12,120,000	$7,530,000
100.00	$50,000	$280,000	$1,370,000	$1,490,000	$350,000	$5,170,000	$2,810,000	$11,550,000	$7,180,000
125.00	$50,000	$270,000	$1,300,000	$1,290,000	$280,000	$5,570,000	$2,810,000	$11,590,000	$7,210,000
150.00	$50,000	$260,000	$1,370,000	$1,240,000	$230,000	$6,270,000	$2,810,000	$12,260,000	$7,620,000
175.00	$50,000	$260,000	$1,360,000	$1,210,000	$200,000	$6,690,000	$2,810,000	$12,600,000	$7,830,000
200.00	$50,000	$250,000	$1,540,000	$1,200,000	$170,000	$7,690,000	$2,810,000	$13,740,000	$8,540,000

SUMMARY OF CRITICAL DIMENSIONS									
SPAN (ft)	GIRDER DIMENSIONS				T-BEAM DIMENSIONS		COLUMN DIAMETER (in)	GIRDER WEIGHT (tons)	GIRDER WEIGHT (kN)
	FLNG THK (in)	WB THK (in)	DEPTH (in)	WIDTH (in)	DEPTH (in)	WIDTH (ft)			
50.00	6.00	9.00	48.00	144.00	48.00	13.00	66.00	87.33	8.08
75.00	6.00	9.00	48.00	144.00	48.00	13.00	72.00	130.99	12.11
100.00	6.00	9.00	48.00	144.00	48.00	13.00	78.00	174.65	16.15
125.00	6.00	9.00	72.00	144.00	48.00	13.00	81.00	246.44	22.79
150.00	9.00	9.00	69.00	144.00	48.00	13.00	87.00	350.57	32.42
175.00	9.00	9.00	93.00	144.00	48.00	13.00	93.00	448.37	41.46
200.00	12.00	9.00	105.00	144.00	48.00	13.00	99.00	613.68	56.75

TYPE I - DOUBLE COLUMN - BASE CASE COST COMPARISON CHART

TABLE 3-12

COST OF STRUCTURE PER MILE									
SPAN (ft)	CONSTRUCTION FACILITIES	SITE PREPARATION & FINISHING	FOUNDATION	COLUMN	T-BEAM	GIRDER	GIRDER INSTALLLATION	COST/MILE	COST/KILOMETER
50.00	$50,000	$350,000	$2,740,000	$3,230,000	$700,000	$5,430,000	$2,810,000	$15,340,000	$9,530,000
75.00	$50,000	$310,000	$2,170,000	$2,480,000	$460,000	$5,260,000	$2,810,000	$13,570,000	$8,430,000
100.00	$50,000	$280,000	$1,910,000	$2,130,000	$350,000	$5,170,000	$2,810,000	$12,730,000	$7,910,000
125.00	$50,000	$270,000	$1,900,000	$1,930,000	$280,000	$5,570,000	$2,810,000	$12,830,000	$7,980,000
150.00	$50,000	$260,000	$1,930,000	$1,910,000	$230,000	$6,270,000	$2,810,000	$13,490,000	$8,380,000
175.00	$50,000	$260,000	$1,980,000	$1,730,000	$200,000	$6,690,000	$2,810,000	$13,740,000	$8,540,000
200.00	$50,000	$250,000	$2,150,000	$1,770,000	$170,000	$7,690,000	$2,810,000	$14,920,000	$9,270,000

SUMMARY OF CRITICAL DIMENSIONS									
SPAN (ft)	GIRDER DIMENSIONS				T-BEAM DIMENSIONS		COLUMN DIAMETER (in)	GIRDER WEIGHT (tons)	GIRDER WEIGHT (kN)
	FLNG THK (in)	WB THK (in)	DEPTH (in)	WIDTH (in)	DEPTH (in)	WIDTH (ft)			
50.00	6.00	9.00	48.00	144.00	48.00	13.00	81.00	87.33	8.08
75.00	6.00	9.00	48.00	144.00	48.00	13.00	87.00	130.99	12.11
100.00	6.00	9.00	48.00	144.00	48.00	13.00	93.00	174.65	16.15
125.00	6.00	9.00	72.00	144.00	48.00	13.00	99.00	246.44	22.79
150.00	9.00	9.00	69.00	144.00	48.00	13.00	108.00	350.57	32.42
175.00	9.00	9.00	93.00	144.00	48.00	13.00	111.00	448.37	41.46
200.00	12.00	9.00	105.00	144.00	48.00	13.00	120.00	613.68	56.75

TYPE I - DOUBLE COLUMN - BASE CASE - ZONE 4 SEISMIC COST COMPARISON CHART

TABLE 3-22

Guideway Structural Design and Power/Propulsion/Braking in Relation to Guideways, Interim Study Report, Babcock & Wilcox, 1992 -11-Advanced Systems